2018

Estuarine geomorphodynamic assessment of environmental change and stressor impacts: a geographic information systems and remote sensing (geoinformatic) modelling approach for sustainable management of southeast Australian coastal ecosystems

Ali K. M. AL-Nasrawi
University of Wollongong

UNIVERSITY
OF WOLLONGONG
AUSTRALIA

GeoQuEST Research Centre

School of Earth and Environmental Sciences

Estuarine geomorphodynamic assessment of environmental change and stressor impacts: a geographic information systems and remote sensing (geoinformatics) modelling approach for sustainable management of southeast Australian coastal ecosystems

---

Ali K. M. AL-Nasrawi, MSc

This thesis is presented as part of the requirements for
the conferral of the degree: Doctor of Philosophy

The University of Wollongong
Faculty of Science,
Medicine and
Health

Supervisors:
A/Prof. Brian G. Jones
Dr Sarah M. Hamylton

June, 2018

ABSTRACT

Increased habitation and global warming is posing growing threats to the coastal zone and estuarine settings through direct and indirect environmental and anthropogenic modification of sensitive coastal systems and their relevant catchments. It is essential to understand the impact of the different stressors on the coastal environment under current conditions and within the historical record in order to predict future responses of estuaries and coastal wetlands.

Short-term remote sensing and GIS modelling and field assessment have made a significant contribution to our knowledge on estuarine and coastal wetland dynamism within the last few decades. This thesis assesses the potential impacts of anthropogenic modifications, climatic factors and sea level rise on estuarine eco-geomorphic intertidal sedimentary landforms and their associated coastal wetlands in southeastern Australia based on three estuarine systems on the south coast of NSW: the estuarine Comerong Island, Wandandian deltaic estuary, and Towamba estuary.

The thesis' short-term evaluation approach shows that the degradation levels on estuarine platforms are dependent on catchment development, sediment characteristics, ecosystem stability and sea level rise inundation. During anticipated climate change and rising sea level conditions, estuaries depend on their sediment source areas, especially on modifications to their river catchment. Catchments with high anthropogenic modification levels, like the dam infrastructure in the Shoalhaven River catchment, influence sediment availability and transportation with clear impacts on eco-geomorphic coastal platform losses. In contrast, mostly unmodified but high-sloped catchments, such as the Towamba example, may have other negative effects on the estuary since the sediments are poorly sorted and coarser non-cohesive quartz-dominated particles cause the geomorphic landforms and associated ecosystems to be more vulnerable to erosion and lead to less stable vegetation. Regions with small moderately modified catchments, such as the Wandandian site, allow ideal geomorphic processes to occur. Here, sediment is weathered slowly and moved downstream naturally to a secure inner estuarine deltaic setting where fine sandy/silty particles accumulate and provide more geomorphic stability. Associated vegetation assemblages ensure the progradation and steady growth of the deltaic eco-geomorphic system.

The thesis assessment shows the eco-geomorphic-dynamism of the Towamba estuary, which has a mostly unmodified catchment surface (only 14% anthropogenic modifications), has grown a total of 0.17 km^2 since 1949. This growth rate indicates that the Towamba estuary future scenarios will mostly be filled at the completion of the 21st Century. In comparison, the

partially modified (22.1%) catchment has prograded the Wandandian deltaic shorelines resulting in the total growth of 0.24 km^2 during the study period (1949-2016). However, results on Comerong Island show significant changes in the spatial extent, elevation, and shorelines with total net losses of 0.3 km^2 over the investigated timespan (1949-2014). Changes included northern accretion (0.4 km^2), and western, middle and southern erosion (0.7 km^2) of the island.

The thesis emphasises the dynamic character of the estuarine eco-geomorphic system, particularly using Normalised Difference Vegetation Index (NDVI) as a vegetation canopy assessment approach. This approach illustrates the significant correlations between vegetation and climatic and geomorphic influences at the study sites, indicating that these factors are the main drivers of vegetation canopy disturbance on intertidal sedimentary landforms during the 21st Century. Locally, map-algebra expression shows the spatial distribution of the NDVI identifies areas that need to be managed in relation to the causes and drivers. This modelling confirms the LiDAR-DEMs-driven character of the existing situations to their influencing factors, which also control the estimated future-scenarios and illustrate clear inundatable landform zones at the study sites by 2100. Results indicate that the rise of sea level will have tremendous effects on the coastal eco-geomorphic systems, particularly wetlands, throughout southeastern Australia and equivalent systems overseas by the end of this century.

This thesis develops possible mitigation and adaptation strategies and sustainable solutions that might be utilized to minimize the indirect devastating consequences of climate change and anthropogenic modifications, particularly damming rivers, which cause direct sedimentation problems as implied by the Tallowa Dam case study.

The thesis shows that intertidal sedimentary landforms will have a future negative or positive vegetarian response according to their evolving morphological character. Within a short-term timescale, the whole eco-geomorphic system will interact with many environmental and anthropogenic variables (particularly sedimentation rates) to evolve its own character over a longer timescale. Therefore, the long term assessment approach can be directed by having a better understanding of the existing situation and accurately identifying the past drivers.

Future projections indicate that indirect anthropogenic-induced global warming will have a great effect on estuaries and coastal wetlands in the 21st Century. This research helps to provide an important framework for quantifying the current situation, future stressors and vulnerability responses during any intensification of natural and artificial coastal hazards, which may be of concern to the general public and environmental scientists who are currently focusing their attention on the best way to preserve estuaries and their wetland ecosystems at the current stage of global warming and human settlement.

ACKNOWLEDGMENTS

I thank my supervisors Associate Professor Brian Jones and Dr Sarah Hamilton for their constant support during the ups and downs of this project. It has not only been a rugged road, as Dr L. Devriendt stated from the Molière *"un long fleuve tranquille, un doctorat n'est pas"*, but it faced me with a solid wall several times along the PhD-journey that I've had to dig through with no step-back option!. Without Brian, this thesis won't exist and particularly sampling soft sediments along a mangrove shore during fieldwork at Comerong Island and Eden sites would have been impossible. Sarah has great RS and GIS processing skills, and without Sarah's assistance I would still be stuck within my GIS-machine and trying to get the extra bits of information. I am also grateful for the constructive criticism I received from Brian and Sarah, the thorough reviews and for the wise advice. Thank you, Brian and Sarah, for your commitment; I have learnt a lot from you.

Some of the new ideas presented in this thesis greatly benefited from discussions with Professor Colin D. Woodroffe, Associate Professor Laurie Chisholm, Dr Kerrylee Rogers, Dr Alexandru Codilean and Dr Tim Cohen (University of Wollongong). I also would extend my thanks to the valuable RS and GIS modelling advice from Dr Thomas Oliver, Dr Rafael C. Carvalho, Chris Owers, Thomas Doyle and Farrah Adnan (UOW), which served as a foundation work for this thesis. Their enthusiasm and scientific inputs certainly brought new light to the project. Colin Murray-Wallace, Penny Williamson (UOW) and Craig Sloss (Queensland University of Technology) are thanked for reviewing and proofreading some of my thesis chapters and for useful discussions on modelling estuarine dynamism, which contributed to some of the findings in this thesis. I also would like to thank A/Prof Helen McGregor for her smart climatic hints along the way. Exchange of ideas with Martin Struck, Dr Brent Koppel, Dr Laurent Devriendt (UOW), Dr Duncan Rayner (University of New South Wales) and Ameen Kadhim (Michigan State University) also helped to connect the dots during this project.

I wish to thank Valda Corrigan (Nowra area, Office of Environment and Heritage) for some data providing, Heidi Brown (Geospatial Systems Analyst, UOW), Alexandra Ullrich and Alex Pescud (Spatial Data Officers, UOW) for their continued support and patience, as well as Dr Ben Marwick for his R analysis support (UOW). Special thanks to Associate Professor Paul Carr, Dr Yasir Alyazichi, Mr José Abrantes for sample preparation and analysis (including XRD and XRF). Mr Brent Peterson, Mr Josef Stocker (fieldwork technical engineers and driller) and Dr Lili Yu (Geochemistry Laboratory support) are also thanked for their wise supports on how to use the equipment during the fieldwork to gain and analyse the data accurately. Administrative and publishing consultations and support along the cliffs by Professor Hadi Alfaraji, Mrs Denise

Alsop, Ms Stephanie Toole (UOW) and Dr Farzin Shabani (UNE) are highly appreciated. Many thanks to A/Prof Mohammad Hadi and Dr Thong M. Pham (Civil-CME-UOW) for inspiring the thesis structure in a smart Civil-engineering way. Thanks are extended to all my research' co-authors for their appreciated collaborations as well as Dr Ahmad K. O. Al-bdoor (MMMB-UOW) for his mathematic involvement within chapter three. God blessed the unevaluable family and friends support including Endewa, Hamoodi, Sarah, Hasony, and Heydory as well as my siblings and parents.

Carl A Hopley (Sustainability Planner, Wollongong City Council) is thanked for sharing and explaining his useful datasets and publication involvement, as well as his highly appreciated tutorial on using the bathymetric Ceeducer and the assistance during a field trip to Eden (Towamba estuary).

Highly appreciated efforts were provided by all employees of Ministry of Higher Education and Scientific Research, and the HCED-Iraq scholarships program, in particular to Dr. Zuhair Humadi (HCED-General Director), who was the founder of this program that provides such invaluable opportunity for the excellent and outstanding students.

Finally, god of gods has gathered all of the above and everything to be accrued by his majesty and kindness, so thanks mighty god forever.

DECLARATION

This thesis submitted in partial fulfillment of the requirements for the conferral of the degree *Doctor of Philosophy*, from the University of Wollongong, is wholly my own work unless otherwise referenced or acknowledged. This document has not been submitted for qualifications at any other academic institution.

Ali K. M. AL-Nasrawi
June, 2018

LIST OF PUBLICATIONS INCLUDED IN THIS THESIS

Last updated version of Chapters 2-7 are published and recommended online:

Peer-reviewed publications (included in the Appendices):

1. Al-Nasrawi, A. K., Jones, B. G. & Hamylton, S. M., 2016. GIS-based modelling of vulnerability of coastal wetland ecosystems to environmental changes: Comerong Island, southeastern Australia. *Journal of Coastal Research*, 75, 33-37. https://doi.org/10.2112/SI75-007.1.

*This paper is presented in **Chapter 2**: Al-Nasrawi has 85% contributed to this paper. Jones and Hamylton gave 7.5% contribution each.*

2. Al-Nasrawi, A. K. M., Jones, B. G., Alyazichi, Y. M., Hamylton, S. M., Jameel, M. T., & Hammadi, A. F., 2016b. Civil-GIS incorporated approach for water resource management in a developed catchment for urban-geomorphic sustainability: Tallowa Dam, southeastern Australia. *International Soil and Water Conservation Research,* 4, 304-313. https://doi.org/10.1016/j.iswcr.2016.11.001.

*This paper is presented in **Chapter 3**: Al-Nasrawi has 80% contributed to this paper. Jones, Alyazichi, Hamylton, Jameel, and Hammadi have contributed 4% each.*

3. Al-Nasrawi, A., Hopley, C., Hamylton, S. & Jones, B. 2017. A spatio-temporal assessment of landcover and coastal changes at Wandandian delta system, southeastern Australia. *J. Mar. Sci. Eng.* 2017, *5*(4), 55; doi:10.3390/jmse5040055.

*This paper is presented in **Chapter 4**: Al-Nasrawi has 80% contributed to this paper. Hopley have 10% contributed, Hamylton and Jones have the contribution of 5% each.*

4. Al-Nasrawi, A. K. M., Hamylton, S. M., & Jones, B. G., 2018a. An assessment of anthropogenic and climate stressors on estuaries using a spatio-temporal GIS-modelling approach for sustainability: Towamba estuary, southeastern Australia. *Environmental Monitoring and Assessment*, (in press). DOI: 10.1007/s10661-018-6720-5.

.

*This paper is presented in **Chapter 5**: Al-Nasrawi has contributed 90% to this paper. Jones and Hamylton gave a contribution of 5% each.*

5. Al-Nasrawi, A. K., Hamylton, S. M., Jones, B. G. & Kadhim, A., 2018b. Geoinformatic analysis of vegetation and climate change on intertidal sedimentary landforms in southeastern Australian estuaries from 1975–2015, *AIMS Geosciences*, 4(1): 36-65. doi: 10.3934/geosci.2018.1.36.

*This paper is presented in **Chapter 6**: Al-Nasrawi has contributed 85% to this paper. Jones, Hamylton, and Kadhim have contributed 5% each.*

6. Al-Nasrawi, A. K., Sarah M. Hamylton, Brian G. Jones, Carl A. Hopley, Yasir M. Al Yazichi. (2017). Geoinformatics vulnerability predictions of coastal ecosystems to sea level rise in southeastern Australia. *Geomatics, Natural Hazards and Risk Journal* (in press). https://doi.org/10.1080/19475705.2018.1470112.

*This paper is presented in **Chapter 7**: Al-Nasrawi has contributed 80% to this paper. Hamylton, Jones, Hopley, and Alyazichi have contributed 4% each.*

Conference proceedings, papers, and abstracts

1. Al-Nasrawi, A. K., Jones, B. G. & Hamylton, S. (2015). Modelling changes of coastal wetlands responding to disturbance regimes (Eastern Australia) Using GIS. Conference: Australian Mangrove and Saltmarsh Network - Working with Mangrove and Saltmarsh for Sustainable Outcomes, At the University of Wollongong. https://smah.uow.edu.au/content/groups/public/@web/@smah/@sees/documents/doc/uow188074.pdf

*This paper is used in parts of **Chapters 1 and 2**: Al-Nasrawi has contributed 80% to this paper. Hamylton, Jones, have contributed 10% each.*

2. Al-Nasrawi, A. K. M., Al-Hamdany, U. A., Hamylton, S. M., Jones, B. G. & Alyazichi, Y. M. 2017a. Surface Elevation Dynamics Assessment Using Digital Elevation Models, Light Detection and Ranging, GPS and Geospatial Information Science Analysis: Ecosystem Modelling Approach. *International Journal of Environmental, Chemical, Ecological, Geological and Geophysical Engineering*, Vol: 11, No: 11, 2017, 918 - 923. Digital Article Identifier (DAI): urn:dai:10.1999/1307-6892/10008196. Available at: http://waset.org/publications/10008196.

This paper is used in parts of Chapters 1, 7 and 8: authors have contributed equally to this paper.

3. Al-Nasrawi, A. K., Sarah M. Hamylton, Brian G. Jones, Qassim Al-Aesawi, 2017. Using GIS-modelling to determine the hydrological factors that affect a catchment area: a practical experiment. In: program and abstract, 6th Australian Universities Geoscience Educators Network Conference, Sydney, Australia. *Geological Society of Australia Abstracts* 123, p11-13.

*This paper is used in parts of **Chapters 1 and 5**: Al-Nasrawi has contributed 80% to this paper. Al-Aesawi contributed 10%, Hamylton and Jones have contributed 5% each.*

4. Alyazichi, Y. M., Jones, B. G., McLean, E., Altalyan, H. N. & Al-Nasrawi, A. K. M. (2015). Risk assessment of trace element pollution in Gymea Bay, NSW, Australia. World Academy of Science, Engineering and Technology. Proceedings, 9 (12), 1286-1292. Melbourne, Australia. *International Journal of Environmental, Chemical, Ecological, Geological and Geophysical Engineering*. ICEWRE 2015: 17th International Conference on Environmental and Water Resources Engineering. http://ro.uow.edu.au/smhpapers/3336/.

*This paper is used in part of **Chapter 3**: Al-Nasrawi has contributed 10% to this paper. Alyazichi has contributed 75%, Jones, McLean, Altalyan have contributed 5% each.*

5. Al-Nasrawi, A. K., Jones, B. G., Al Yazichi, Y. M. & Hamylton, S. 2015. Modelling the future eco-geomorphological change scenarios of coastal ecosystems in southeastern Australia for sustainability assessment using GIS. ACSUS 2015 Proceedings: The Second Asian Conference on the Social Sciences and Sustainability (ACSUS- INTESDA), Fukuoka, Japan ISSN: 2188-6857. 0196. http://ro.uow.edu.au/smhpapers/3402/

*This paper is used in part of **Chapter 7**: Al-Nasrawi has contributed 85% to this paper. Jones, Alyazichi, and Hamylton have contributed 5% each.*

CONTENTS

List of Figures

List of Tables

Chapter I: INTRODUCTION

1.1 The general introduction and background

Coastal environments around the globe contain a variety of landforms that have been constructed by the dynamic interaction of rivers, waves and tides on the rock and sediment at their disposal (Fischlin *et al.*, 2007). Intertidal estuarine landforms represent one of the most geomorphically dynamic systems formed through continued sediment movement above and below current sea level, as sediment from the catchment is reworked by the river and tidal interactions and partially stabilized by vegetation communities (Fischlin *et al.*, 2007; Woodroffe, 2002; Murray-Wallace and Woodroffe, 2014).

The ecosystems on Earth, particularly in the coastal zones, have become balanced and stabilized since the mid-Holocene sea level stabilization (Troedson *et al.*, 2004; Murray-Wallace & Woodroffe, 2014). Ever since, estuaries form a dynamic, transitional zone between rivers and the sea and allow people to achieve many economic, social and environmental benefits worldwide (Dalrymple *et al.*, 1992; Crossland *et al.*, 2005). Early Sumerians (Mesopotamia 4500 BC) and most other ancient civilizations were attracted to these coastal and estuarine environments, which provided people with many ecologically valuable services, especially food, transport and access within a specific ecosystem (Postgate, 1992). Since then, habitation in the coastal zone has increased for economic and environmental reasons, impacting estuarine settings directly and/or indirectly through modifying their relevant catchments (Cherfas, 1990; Crossland *et al.*, 2005; Pendleton, 2010; Neumann *et al.*, 2015). Nowadays, 70% of the global population and 86% of Australians live in coastal environments (Cherfas, 1990; Lee *et al.*, 2006; Australian Bureau of Statistics (ABS), 2011). As a result, coastal ecosystems are threatened by (i) population concentration and growth stressing the ecological and geomorphological (eco-geomorphic) systems of many estuaries (Deeley & Marine, 1999; Kennish, 2002; Crosset *et al.*, 2004), (ii) related anthropogenic modification of their catchments (Davenport and Davenport, 2006; Lee *et al.*, 2006; Hopley, 2013; Al-Nasrawi *et al.*, 2016a), and more recently, (iii) global warming, its consequential climate change and sea level rise, which has become another factor stressing estuarine intertidal landforms and their associated habitats (Woodroffe, 1990; Nicholls, 2004; Day *et al.*, 2008; Nielsen & Brock, 2009; Lovelock *et al.*, 2011; Bonetti *et al.*, 2012).

The formation of an estuary depends on the position of sea-level compared to the amount and level of fresh water flow from the catchment through the river (Wright, 1970; Woodroffe *et al.*, 2000). Sloss *et al.* (2005) have stated that estuarine systems along the southern NSW coast can

provide many examples of such eco-geomorphologically disturbed regimes. NSW estuaries were partly infilled late Quaternary low-stand incised valley systems (Roy *et al.*, 2001; Sloss *et al.*, Sloss *et al.*, 2006b, Sloss *et al.*, 2010). At the time of the Last Glacial Maximum (LGM) low-stand riverine sediment accumulated within the continental-shelf. Over the subsequent transgression, this sediment was moved landward forming the Holocene coastal sandy barrier estuaries (Roy & Crawford, 1977; Sloss *et al.*, 2010). The high-stand Holocene sea-level caused estuarine systems to simultaneously infill with marine sediment and sediment derived from the river catchment (Hopley & Jones, 2006; Carlson *et al.*, 2008). NSW estuaries vary greatly in their rate of infilling depending on their sediment supply and the geomorphic ability to keep the sediment within the estuary, i.e. a balance between the river and nearshore ocean energies (Roy *et al.*, 2001; Sloss *et al.*, 2005, 2006a, 2006b). The southeast Australian coast is influenced by two oceanic-water masses; the southern end of the warm Eastern Australian Current and the cold waters of the Southern-Ocean (Yassini & Jones, 1995). Additionally to being wave-dominated (Woodroffe, 2002; Sloss *et al.*, 2006b; Roper *et al.*, 2011), the NSW south coast is also a popular place for many anthropogenic activities, including large boat traffic, commercial and recreational fishing, personal recreation, mussel farming, whaling, timber export and Australian Navy activities, putting even more pressure on the coastal environments (Dean & De Deckker, 2013).

Successive erosion and deposition cycles in estuaries of NSW have resulted in ecological and morphological (eco-geomorphic) changes over time (Roy *et al.*, 2001; Roper *et al.*, 2011). Furthermore, there has been a clear increase in the possible effects of changes in natural environmental aspects, such as the dynamics of coastal sand bodies. This has been caused by: i) global warming, such as the rising temperature and mean sea level, as well as increasing high-energy event frequencies (e.g. tornados and floods); and ii) anthropogenic influences including farming, industrial development and urbanisation within the catchment, together with the dredging of channels, embankment modification and sand-mining in estuaries (Roy *et al.*, 2001). These geomorphic changes have also led to ecological responses, particularly within the estuaries and their associated coastal wetlands, because of their sensitivity and relatively rapid responses (Roper *et al.*, 2011; Semeniuk & Semeniuk, 2013; Al-Nasrawi *et al.*, 2016b; Al-Nasrawi *et al.*, 2017a). Responses include the development of shorelines, levees, sandspits and vegetation canopy (mainly mangrove, *Casuarina* and some *Juncus* spp.) particularly within the shoreline zones, but also in saltmarsh areas, which offer suitable accommodation and habitat for other ecological and biological communities to develop.

The focus of this thesis is on monitoring and assessing environmentally sensitive areas, such as intertidal estuarine landforms and their associated coastal wetlands, which is an essential

factor for government agencies and for the broader research and local communities. Comprehensive understanding of the dynamic processes in these zones will provide considerable help to manage such areas globally. The thesis provides detailed insights about the three chosen representative sites on the southeast Australian coast, focusing on geomorphic and resulting vegetation dynamics (as a conservation indicator) for historical and current eco-geomorphic evaluation and probable future response to environmental changes.

1.1.1 Background

Riverine estuary studies have mainly focused on sedimentological characteristics, shoreline responses, the formation processes and subsequent eco-geomorphic responses. They covered different estuarine research scopes, including: (i) weathering and transport processes (Goodbred, 2003; Wei *et al.*, 2007); (ii) fluvial geomorphic and sediment aspects (Jones *et al.*, 1993) (iii) characteristics of particle size and load dynamics of river sedimentation (Yang *et al.*, 2009; Hoque *et al.*, 2013); (iv) hydrological processes (Li and Heap, 2008); (v) mineralogical sediment analysis (Sondi *et al.*, 2008); (vi) geochemistry studies (Jones *et al.*, 2003a; Zhou *et al.*, 2005); (vii) delta characteristics, such as elevation change (Jones *et al.*, 2003b; Li *et al.*, 2004); (viii) general environment dynamics (Harji *et al.*, 2008; Hu *et al.*, 2009); (ix) climatic record investigations of the late Quaternary (Hudson, 1991; Troedson *et al.*, 2004; Zhou *et al.*, 2005); (x) sea level change responses (Fairbanks, 1989; Sloss *et al.*, 2007; Gabler *et al.*, 2017); and (xi) annual sediment delivery to the oceans, which is estimated between 15 to 16 × 10^9 tons under current climatic conditions (Singh *et al.*, 2007).

The form of estuaries is largely governed by the movement of sediments into and out of the accommodation space defined by the estuary (Roy *et al.*, 2001; Sloss *et al.*, 2006a, 2006b). Figure 1.1 shows the general morphology and stratigraphy of estuarine dynamics and a sequence of development stages during which the estuary is filled with sediment derived from the catchment and/or the continental shelf. The accumulated sediment offers new shallow water space and gradually converts the lagoonal basin to a swamp, allowing the development of intertidal/coastal wetland vegetation canopies, saltmarsh species and mangroves and thus building its ecosystem habitats (Kelleway *et al.*, 2017). At a more mature stage, the estuary starts to build seawards over transgressive sediment accumulations (Fig. 1.1c), confirming the process of estuary filling as a geologically-inherited river characteristic that combines with stabilisation of ecosystem habitats.

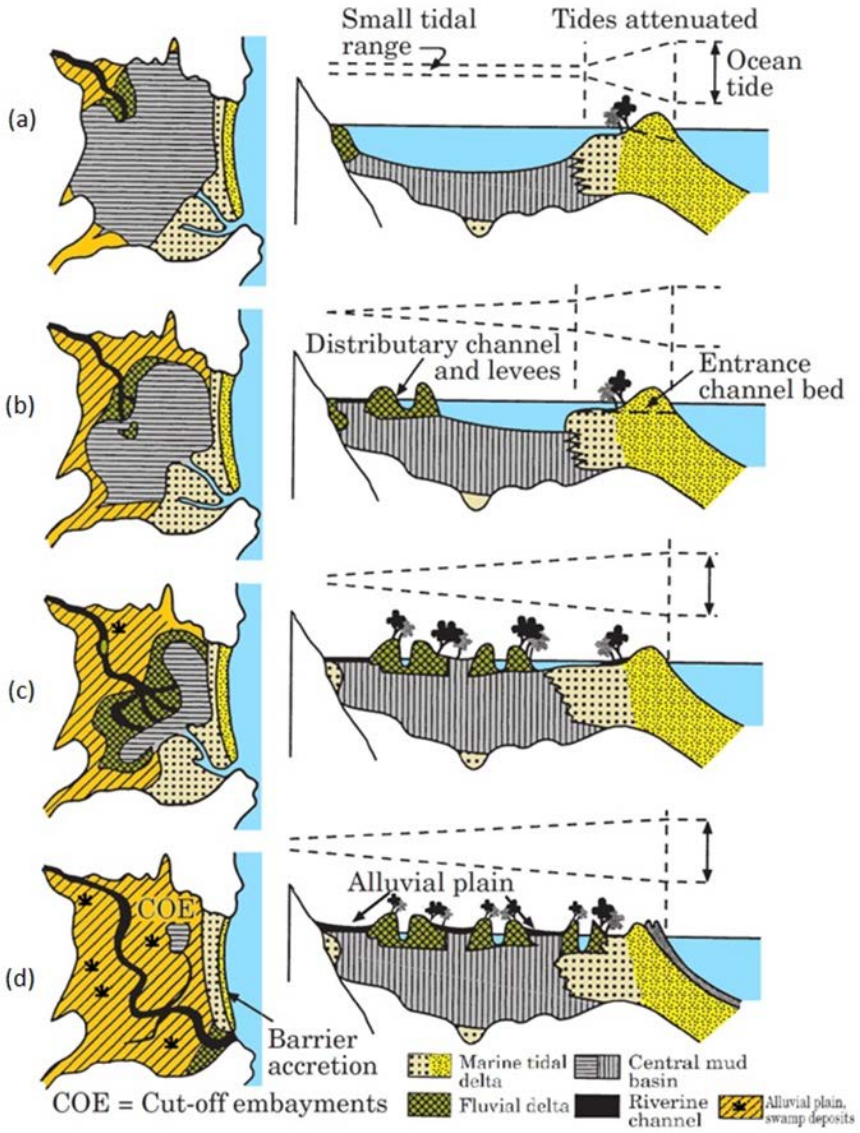

Figure 1-1. The ideal four estuarine infilling stages Illustrate the morphodynamic changes to shorelines and vegetation development on a standard barrier estuary: (a) youthful stage, (b) intermediate stage, (c) semi-mature estuary, and (d) mature stage, of the estuarine developments (after Roy *et al.*, 2001; Sloss *et al.*, 2006a).

Estuarine morphodynamics have been recognised through chronological changes of shoreline positions and elevations, and have been used in coastal evaluation studies (Firth *et al.*, 1996; Hopley, 2013; Oliver *et al.*, 2017). Historically, estuarine development was first reconstructed morphologically, chronologically and stratigraphically based on drilling and radiocarbon dating of many Holocene estuaries both locally (Nott and Price, 1991; Umitsu *et al.*, 2001; Hopley, 2004; Hopley & Jones, 2006; Carlson *et al.*, 2008; Oliver *et al.*, 2017b), regionally (Al-Nasrawi *et al.*, 2016b; Al-Nasrawi *et al.*, 2017b) and globally (Rohling and Palike, 2005; Zhou *et al.*, 2005). These studies established a long-term assessment of permanent sediment accumulation over the Holocene period and demonstrated the complexity of coastal evolution, which also involves the deposition of lagoonal or estuarine mud prior to the integrated geomorphic growth of the estuarine delta.

Short-term assessment commonly incorporates a coastal compartment, including coastal sensitivity to dynamic coastal (Håkanson *et al.*, 2004), and estuarine dynamic approach to understand estuarine morphological growth (Wright, 1970; Ball, 1994; Malczewski, 2004). Where a surplus of sand is supplied to a compartment or 'store', it results in geomorphic progradation of the coastal sets causing a dynamic shoreline position over a short timescale, which fundamentally needs to be addressed (Davies, 1974; Malczewski, 2004). This approach guides many examples worldwide using modern remote sensing and GIS assessment (Chen & Gong, 1998; Rogers *et al.*, 2017). Several datasets/tools have been utilised in this field including shoreline detection and digital shoreline analysis systems (DSAS) to track the estuarine morphodynamics (Thieler *et al.*, 2009). More recently, an increasing focus has been on vegetation assessment of the associated estuarine wetlands as they play important roles in the estuary development stages (Mitsch & Gosselink, 1993; Cronk & Fennessy, 2001; Gedan *et al.*, 2011) and on assessing the effects of global warming (Wall, 1998; Nicholls, 2004; Day *et al.*, 2008). One of the most successful vegetation assessment tools is the normalised difference vegetation index (NDVI) that is used to identify the vegetation dynamics over time (Weier & Herring, 2000; Pettorelli *et al.*, 2005; Tian *et al.*, 2015).

In southeastern Australia, stratigraphic reconstruction from radiocarbon and amino acid racemisation dating of prograded estuaries deposits has been used in numerous sites and a cohesive picture of late Holocene sea levels and depositional history was established (Thom, 1967; Thom *et al.*, 1981; Roy & Cowell, 1994; Kench, 1999; Skilbeck *et al.*, 2017). Such work has been fundamental in understanding the historic sediment accumulation with sea level interactions on the southeastern Australian coastline where estuarine growth has proceeded at various rates following Holocene sea level rise to be almost equivalent to the contemporary level (Carlson *et al.*, 2008). These compartment-scale investigations of estuarine dynamic deposits in southeastern Australia have resulted in the modelling of long-term sea level impacts on this coastline and its associated low-lying landforms/ecosystems (Woodroffe, 1990; Siddall *et al.*, 2003; Deconto & Pollard, 2016).

Short-term impact evaluations have used other models of coastal change to understand coastal behaviour on the decadal to interdecadal time scale relevant to coastal managers (Cowell *et al.* 1999; Li &d Heap, 2008; Deng *et al.* 2014; Hamylton *et al.*, 2016; Hamylton, 2017; Kassakian *et al.*, 2017; Kelleway *et al.*, 2017; Oliver *et al.*, 2017a; Rogers *et al.*, 2017). Such models attempt to quantify the critical factors for estuarine development such as the dynamics of shoreline positions, sea level, sediment supply and accommodation space, as well as their associated vegetation canopies/wetlands.

Another approach to understanding estuarine deposition and prograded landform

development considers sediment supply interactions between the estuary and its catchment (Wright, 1970; Davies, 1974; Koltun *et al.*, 1997; Borrell, 2013; Kamwi *et al.*, 2017). Such an approach involves the quantification of sediment budgets and catchment land cover dynamics for various components of the estuarine system in an attempt to understand how interactions of these components may control estuarine morphodynamics (Anthony 1995; Garrido *et al.*, 2013; Carvalho & Woodroffe, 2014).

With the development of remote sensing techniques, including satellite and airborne imagery and light detection and ranging (LiDAR) datasets, estuarine morphodynamics and coastal wetlands around the world have been subject to spatio-temporal evaluations using geographic information system (GIS) investigations (Pijanowski *et al.*, 2002; Beluru & Hegde, 2016). These remote sensing investigations have been supplemented by fieldwork and laboratory analysis, sediment sampling, water quality analysis, bathymetric and land surface surveys to determine the causes of changes to estuarine conditions (Murray *et al.*, 2005; Dittmer, 2010; OEH, 2013; Al-Nasrawi *et al.*, 2017a). The use of new technologies offers the potential to reinvigorate the study of estuaries and their associated vegetation cover/coastal wetlands, and provides further opportunities to continue to unravel the trends of such unique coastal morphodynamic and environmental records (Priestas & Fagherazzi, 2010; Tamura, 2012; Kench *et al.*, 2014; Oliver *et al.*, 2017a).

1.1.1.1 Estuarine ecosystems

Estuarine platforms are ecologically very diverse, but therefore also very vulnerable to anthropogenic changes (Hopley, 2013) and climate change/tidal dynamism (Van Den Bergh, 2004; Day *et al.*, 2008; Rogers *et al.*, 2017). This indicates that coastal eco-geomorphic stability is a transitional status that will evolve in response to alteration threats (Dall'osso *et al.*, 2014). Changes may be neither restorable nor stabilisable in the long term to act as a permanent geomorphic platform suitable for wetland habitation (Zedler & Kercher, 2005).

A wetland ecosystem is an ecological area whose soil is dominated by anoxic conditions caused by water replacing air in the soil. Associated plants are usually physiologically adapted to an excess of water and anaerobic conditions in the soil (Haslam, 2004; Keddy, 2010). Wetlands are considered important natural resources that define biological diversity in a typical functioning ecosystem. Mitsch & Gosselink (1993) refer to them as “kidneys of the landscape” because of their systematic role in the natural purification of the hydrological cycle and their natural pollutant removal mechanisms, as well as attenuating wave roles. The USEPA (2001) identified that “Wetlands occupy are the transitional sector between the permanently wetted area and generally dried conditions, and between anthropogenic and biodiversity environments”

(Shepard, 2011).

The functional goods and services provided by wetland ecosystems are important and valued as precious in economic terms (Van Den Bergh, 2004; Fischlin *et al.*, 2007; Pendleton, 2010). Regionally and globally, estuarine ecosystems have high estimated economic values (in US$/year) per hectare as follows: “lakes/rivers 8,498, mangrove/saltmarsh 9,990, coastal sea grass/algae beds = 19,004, swamps/floodplains = 19,580, estuaries = 22,832” (Batzer & Sharitz, 2014). Hence protecting wetland systems is very important both ecologically and economically. They contain a diversity of both aquatic and terrestrial flora and fauna and form the most productive and diverse biological systems on Earth (Zedler & Kercher, 2005; Fischlin *et al.*, 2007). Wetlands fulfil an important role in maintaining the hydrological stability of a region (Bullock & Acreman, 2003) by acting like sponges, storing rainfall, reducing the volume and speed of runoff, slowly releasing water through drier periods (Bullock & Acreman, 2003), and acting as ‘sinks’ for nutrients and pollutants, and they are also valued for recreational activities (Zedler & Kercher, 2005; Davenport & Davenport, 2006). In addition, they are significantly important for flood protection (Costanza *et al.*, 2008), erosion control (Carter, 1999), wildlife food and habitat (U.S. Fish and Wild Life Service, 2014), water quality (Carter, 1999) and carbon sequestration (Twilley *et al.*, 1992). Moreover, many commercial fishing operations are found within coastal zones (Meynecke *et al.*, 2008). Wetlands could also be used to investigate evidence of past human settlement, and their activities (Hopley, 2004; Lee *et al.*, 2006; Hopley & Jones, 2006). Wetland vegetation can modify shorelines (biotic and abiotic accumulations) in ways that increase shoreline integrity and thus provide a lasting coastal adaptation measure that can protect shorelines against sudden sea level rise and more frequent storm inundation (Fischlin *et al.*, 2007). This represents a shoreline protection paradigm for coastal wetlands that should be monitored and conserved (Gedan *et al.*, 2011).

Although there are several ways to classify wetlands, the Ramsar classification proposed by UNESCO (1971) is the most accurate and exhaustive one that has been adopted worldwide, including Australia (Matthews, 1993). It subdivides wetlands into coastal, inland and artificial wetlands (Matthews, 1993; Department of Sustainability and Environment, 2007). Moreover, five main types of wetlands can be found in each of these three major classes which are swamps, bogs, fens, marshes and mangroves (Haslam, 2004; Keddy, 2010). Coastal wetlands are among the most sensitive and productive natural ecosystems (Bullock & Acreman, 2003; Al-Nasrawi *et al.*, 2016b). They have a longer succession of sequential eco-geomorphological stages and could continue forever, compared with inland and artificial wetlands which can be more rapidly filled (Murray *et al.*, 2013; Phillips, 2017). Coastal wetland ecosystems are found

within an elevation gradient that ranges between sub-tidal depths, where light penetrates to support photosynthesis of benthic plants, and the shoreline where the sea passes its hydrologic influence to groundwater and atmospheric processes, and they occur in estuaries and deltas, which indicate that they have a high morphodynamic signature (Thom, 1967; Thom *et al.*, 1975; Perillo *et al.*, 2009; Ganju & Schoellhamer, 2010; Skilbeck *et al.*, 2017; Al-Nasrawi *et al.*, 2018a, b).

Changes to the Earth's surface in coastal areas and estuarine wetlands may lead to complicated outcomes (Al-Nasrawi *et al.*, 2017a; Al-Nasrawi *et al.*, 2018c) for the biota that are not intuitive due to biological interactions (Day *et al.*, 2008). Feedbacks between the biotic and abiotic components of ecosystems will affect the response of coastal wetland systems to climate change, which is the essence of eco-geomorphic sustainability that should be considered (USEPA, 2001).

Approximately one-third to half of the major coastal environments on Earth have been degraded, including eastern Australian estuarine/coastal wetlands, during the past decades (Valiela & Fox, 2008; Saintilan & Williams, 2010; BOM, 2017b). Threats are at multi-levels and aspects, with most of them being shown in Figures 1.2a and b.

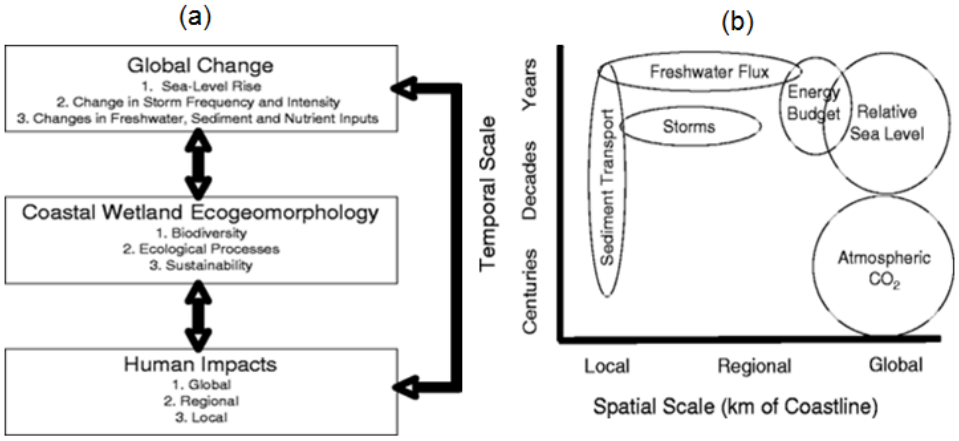

Figure 1-2. Coastal eco-geomorphic change interactions, showing: (a) Coastal wetland eco-geomorphology: a global climate change and bio-complexity relationship, (b) Estuarine geomorphology: impacts of processes controlled by global climate (directly/indirectly). Source: after Day *et al.*, 2008.

There are four changes to eco-geomorphic reactions of coastal and estuarine wetlands due to climate related factors such as elevation, boundary or edge distribution, canopy extent (such as shorelines and vegetation cover), and the composition of soil or sediment (Roper *et al.*, 2011; Skilbeck *et al.*, 2017). Increasing sea level, floods, sediment delivery, and changes to the input of fresh water can dominate coastal and estuarine wetlands (Christiansen *et al.*, 2000; Kelleway *et al.*, 2017).

Globally, it has been predicted that the world will lose 6-22 % of its estuarine and coastal

wetland areas by 2080 under different natural impact scenarios resulting from global warming (Nicholls *et al.*, 1999; Nicholls, 2004). However, direct and indirect anthropogenic modifications will probably have more impact than the magnitude surge of sea level on the future of estuaries and their associated wetlands during the current century (Nicholls *et al.*, 1999). Losses of 36-70% by 2080 are expected by scenarios of combined natural and human effects, suggesting that most estuarine habitats/wetlands are likely to have higher levels of degradation than other parts of the coastline and that estuarine/coastal wetlands will present clear monitoring challenges to the coastal managers to achieve their sustainable conservation targets (Michener *et al.*, 1997; Wall, 1998; Nicholls *et al.*, 1999; Morris *et al.*, 2002; Nicholls, 2004). Within Australia, more than 1000 estuaries are distributed along 34000 kilometres of coastline, with about 50% of the population and their infrastructure concentrated within 7 kilometres of the coast (Geoscience Australia, 2017). This has resulted in increasing pressure levels on the coastal environments, particularly estuarine bodies, in response to global climate change. Along the southeastern coastline of New South Wales, some of the best representative examples of such stressed estuaries have been found and contain the most eco-geomorphically sensitive and responsive estuarine/coastal wetland systems that need to be investigated (Blay, 1944; Wright, 1970; Yassini & Jones, 1995; Kench, 1999; Sloss *et al.*, 2004, 2006a, 2006b, 2010; Hopley, 2013; OEH, 2013).

1.2 Gaps in the current knowledge of estuaries and coastal wetlands

Potential impacts of climatic and rising sea level factors on estuarine and associated coastal wetland sensitivity are not yet understood well enough to provide appropriate remediation. Therefore, more research is needed on the dynamics of geomorphic and vegetation interactions (the eco-geomorphic trends) and on global warming impacts on such dynamic intertidal sedimentary landforms. In this regard, and because comprehensive research is rare on estuaries in the region, temperate southeastern NSW is a great setting to investigate effects on eco-geomorphic facies in estuaries and associated wetlands (Roper *et al.*, 2011). Furthermore, short-term potential consequences of climate change (including the rise in sea-level and temperature and the concurrent precipitation decline) on the catchment area require more research using spatial analysis approaches at both local and national levels. This research could provide important details for the potential influences, strategies of adaptation and extenuation, which can be considered and adopted by the relevant conservation agencies in terms of planning and managements to curb the devastating climate change influences.

The causes of environmental change in estuarine systems have been strongly debated for many years, with sometimes opposing opinions as to whether they result from inherited or contemporary stressors (Meng & Liu, 2010; Rose *et al.*, 2012). For a long time researchers have considered that the main determining factor is erosion combined with rising sea level (Vail *et al.*, 1977; Woodroffe, 1990; Nicholls *et al.*, 1999; Morris *et al.*, 2002), yet anthropogenic impacts have also been suggested (Kingsford, 1990; Vörösmarty *et al.*, 2010; Venter *et al.*, 2016). Coastal residents and tourists congregate within coastal zones for a range of recreation reasons and the existence of significant levels of alteration and stress involved within such low-lying zones has been recognised (Edington & Edington, 1986; Crosset *et al.*, 2004). Unstable geomorphic patterns around sandspits, saltmarshes, mangroves and associated unvegetated intertidal areas are facing a strong pressure from sediment supply sources and intensive use activities worldwide (Thom, 1967; Thom *et al.*, 1975; Hosier & Cleary, 1977; Short & Hesp, 1982; Rose *et al.*, 2012; Phillips, 2017).

Most estuarine studies indicate that the 21st Century will see high sea level rise stresses on such communities (Nicholls, 2004; Mcivor *et al.*, 2013; IPCC, 2014; Phillips, 2017). However, anthropogenic modification of catchments could have a higher impact on estuaries, as it will be the main control on the sedimentary process (amount and characteristics of the sediment) that in turn control the shorelines and their relevant elevation dynamics, as well as their associated habitats. In fact, the sedimentary process can benefit from sea level rise by having wider and longer shorelines with low-lying shallow platforms providing stable accommodation space (Vail *et al.*, 1977; Walters *et al.*, 2014; Woodroffe *et al.*, 2016). Sediment accumulation will provide a more habitable area for vegetation to become established. Thus the estuary may develop/grow, keep-pace with, or erode/drown depending on the balance between the sediment supply and sea level rise factors (Woodroffe *et al.*, 2016).

1.3 The research problem

Preservation and sustainability of estuaries and their coastal wetlands has become the main focus of numerous coastal ecosystem management strategies (Aarts & Nienhuis, 1999; Day *et al.*, 2008) on: (i) local (Oliver *et al.*, 2012), (ii) regional (Kench, 1999; Department of Environment, 2010; Zuo *et al.*, 2013) and (iii) global scales (Morris *et al.*, 2002; Kirkpatrick, 2012; Gabler *et al.*, 2017; Phillips, 2017), regarding their particular functional ecosystem characteristics (Costanza *et al.*, 2008). However, estuaries are situated in sensitive areas where climate change, oceanic and anthropogenic stressors are combined (Ehrenfeld, 2000; Morris *et al.*, 2002; Lee *et al.*, 2006). Therefore, it is vital to get thorough knowledge about the

environmental reactions of estuaries to climatic and anthropogenic influences during the recent and past centuries, with a consideration of the geoinformatic dataset limits, that would allow a better more efficient future understanding and management of such areas.

1.4 Research scope, aims and objectives

This thesis is designed to test the susceptibility and adaptability of estuaries to increased anthropogenic modification levels, including the impact of sediment load (its character and amount) from the catchment and the environmental stresses (change in climate and sea level surge). Such changes affect the geomorphic facies distribution, shoreline positions and associated wetlands in estuarine environments. The goals of this thesis are to evaluate the impact of the anthropogenic and environmental pressures on the intertidal sedimentary platforms and their associated vegetation canopies, particularly coastal wetlands (Figure 1.3).

Figure 1-3. Aims and objectives using a geoinformatics and coastal sustainability approach.

The aims include:

- determining the spatial ecological and geomorphological (eco-geomorphic) changes in estuarine systems within the past few decades, to provide an overview of morphodynamic coastal and estuarine platforms and wetlands on the southeastern Australian coast (Fig. 1.4);
- investigating the direct and indirect interactions between the environmental trends on the catchment runoff and sedimentation factors and the anthropogenic modifications;
- determining some implications of the ecological and geomorphic trends for the future estuarine-ecosystem health, including vegetation and geomorphic dynamic assessments; and
- indicating the possibility of applying these findings to coastal/estuarine wetlands, including deltaic systems, around the world. To find and suggest some solutions for management,

mitigation and adaptation strategies, which can be used to minimise the influence of global warming and the anthropogenic modification on sensitive intertidal platforms and wetlands.

These aims are achieved through the following objectives:

- monitoring, mapping, measuring, and comparing changes of estuarine shoreline and vegetation extent and trends from past and present information using RS and GIS analysis approaches, with a focus on three riverine estuaries that illustrate such responses – the Towamba estuary, Wandandian delta, and Comerong Island (southeastern NSW, Australia; see Figure 1.4);
- modelling and investigating current anthropogenic and environmental influences on the study sites and their relevant catchments to detect and observe the reasons for any trends and changes. This included field sampling and laboratory analysis of sediment characteristics and sedimentation rates, as well as catchment and estuarine land-cover analysis;
- building a model for future responses and changes by detecting inundated areas using DEMs in ArcGIS. This links the response of estuarine morphodynamics (using LiDAR datasets) to global warming and its consequence of rising sea level that is stated in the Intergovernmental Panel on Climate Change (IPCC)/Fifth Assessment Report (AR5);
- evaluating the temporal relationship between the coastal wetland vegetation canopies and climatic, sea level and geomorphic factors, using the NDVI index in ERDAS IMAGINE and RStudio; and
- examining various models in the context of sustaining eco-geomorphic sets, and devising the most suitable modelling approach for different estuaries and coastal wetlands by comparing the results from the applying the proposed methods to the study sites that represent different estuaries/wetland and disturbance regimes.

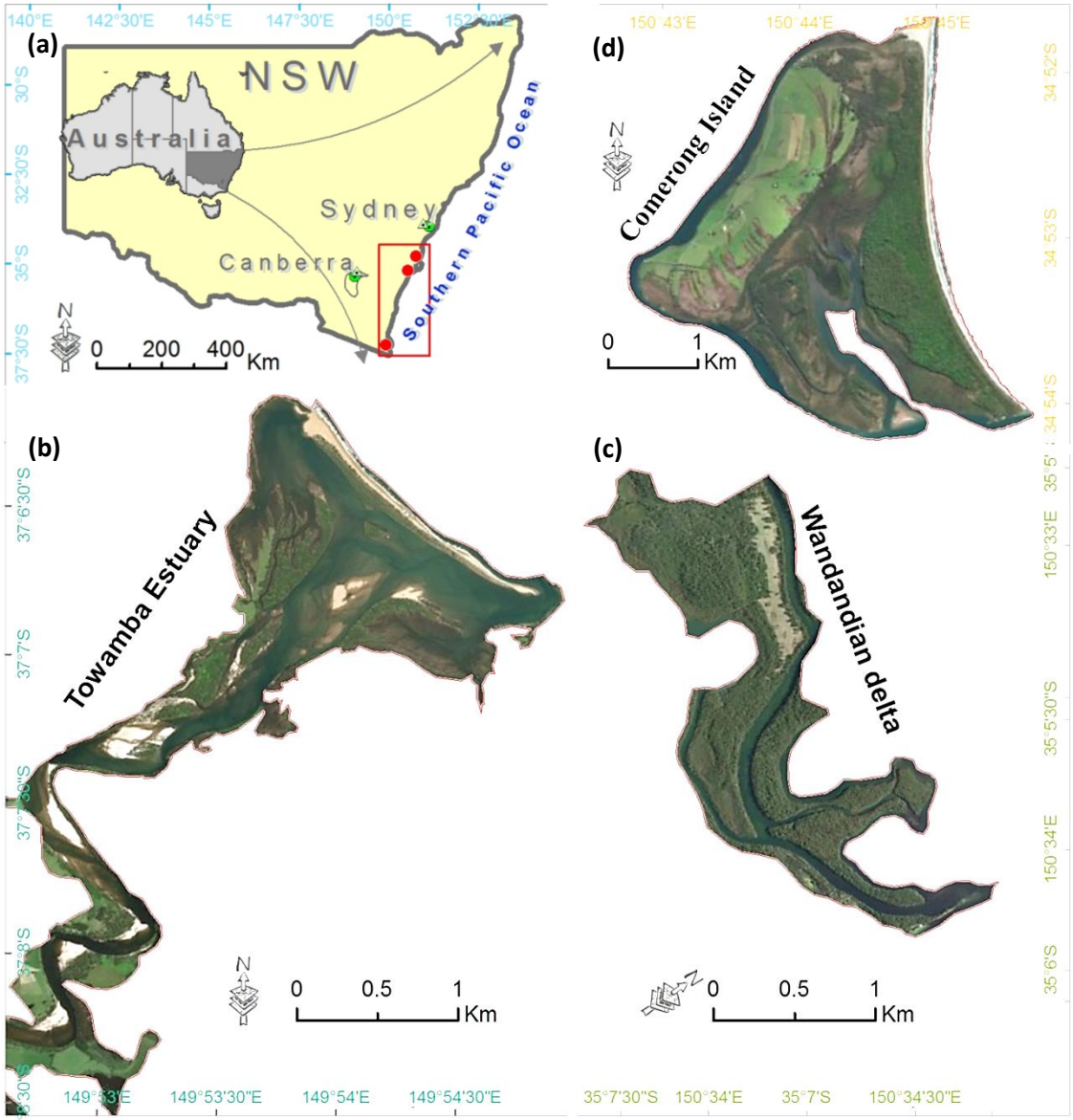

Figure 1-4. (a) Study site locations along the NSW coast in southeastern Australia. From south to north they include the (b) Towamba estuarine ecosystem, (c) Wandandian estuarine delta and (d) estuarine portions of Comerong Island.

1.5 Importance and significance of the proposed research

This research provides the potential for estuarine and coastal managers to isolate the risks of individual stressors on estuaries and their ecosystems, particularly coastal wetlands, to make more informed conservation and restoration decisions (Miller *et al.*, 2016). Three key measurable and observable parameters (variables) are defined in this research: sedimentation rates combined with climatic factors and rising sea interactions; consequent estuarine shoreline changes; and land cover and vegetation canopy dynamics. This study establishes a continuous potential for remote sensing and GIS assessment of multi-temporal eco-geomorphic changes to assess alteration threats that are associated with increasing

anthropogenic modifications and global warming. It will benefit future studies by investigating the impacts of interaction between eco-geomorphic dynamics and particular communities, such as species of vegetation and/or birds.

The relevance of this work to environmental management is that it shows the sensitivity of an estuary to shoreline shrinking or expansion, which would result in significant changes to the estuarine ecosystem platforms as a function of sediment movement from the catchment and its accumulation/erosion downstream.

1.6 Methods

This research evaluates the potential eco-geomorphological degradation of three representative estuarine platforms. Analysis of estuarine eco-geomorphology is complex since individual stressors can interact to cause significant alterations to various aspects of the eco-geomorphic system. This thesis focuses on the short term assessment of changes to estuarine environments that cannot be obtained by more traditional methods like radiocarbon dating or stratigraphic studies. Thus, a GIS and RS modelling approach is the most appropriate method to monitor such short-term changes in estuarine morphodynamics.

This thesis focuses on the dynamics of shoreline position, land cover, vegetation changes and sedimentation rates on three intertidal sedimentary estuarine platforms, which gives a historical coastal perspective that can be used to predict future response to anthropogenic and natural stressors on the southeastern Australian coast.

Utilising remote sensing datasets, including satellite imagery, aerial photography, airborne LiDAR and GIS analysis, the characteristics of estuarine shoreline, vegetation dynamics, and the associated catchment modification levels are combined with fieldwork sampling/surveys and laboratory analysis to determine the most important parameters for this research assessment. Morphology, land cover analysis and sedimentology are formative process indicators, the estuarine shoreline position is a morphodynamic indicator, whereas, ecologically, the vegetation canopy dynamics acts as an ecosystem indicator.

The thesis establishes a spatio-temporal intertidal landform dynamic evaluation, utilising a morphodynamic assessment guided by fieldwork-sampling and the geoinformatic analytic tools, to investigate the dynamism of estuaries eco-geomorphically (e.g. vegetation canopy dynamic and rates of shoreline accretion-erosion.

To obtain the best accuracy, the GIS modelling approach uses the Geocentric Datum of Australia (GDA94-MGA/Zone 55 and 56; for the local latitude and longitude (x and y) distributions), which is the latest coordinate system adopted in Australia, and it is part of the

global coordinate reference frame that utilising the Universal Transverse Mercator (UTM) according to the ellipsoid-GRS80 and the 1994-Australian Map Grid. At the same time, the vertical (z) and elevational control on the mapping processes depends on the assigned value (0.000 m) of the Australian Height Datum (AHD) for the mean sea level. AHD was adopted by the National Mapping Council in 1971 when it was termed the Australian Height Datum.

Project targets are achieved on several levels. Much of the work is based on the RS and GIS analysis, in identifying and classifying the vegetation canopy and shoreline dynamics, at the study sites according to existing and inherited imagery and LiDAR datasets. The vegetation edge-line on the seaward side of an estuary is a common proxy used to assess the dynamics of shoreline position, but using the high water level line on the beach is also a safe approach and more accurate for coastal evaluation (Adnan *et al.*, 2016; Hamylton, 2016, 2017; Kelleway *et al.*, 2017; Rogers *et al.*, 2017). This identifies deposits within the embayments that can be related to human modification of the catchment. For instance, RS data classification for the land-cover of the catchments presents the proportion of human activities that control the natural processes in this area and have affected many aspects of recent wetlands such as sediment deposition/erosion. This is combined with field sampling of soil and sediment to assess the architecture of sedimentary deposits along the shorelines, and to identify which factors (e.g. sea level rise or anthropogenic modifications) have had the greatest effect on sediment availability. The resulting data pool is statistically checked using SPSS and correlation coefficients to determine the relationships between the study sites and their parameters, and between each pair of parameters.

Soil and sediment samples were collected for laboratory analysis at the University of Wollongong. Samples from study sites were collected from 50 mm below the surface to minimise the short-term changes in clay proportions. Grain size, loss on ignition (LOI) and X-ray diffraction (XRD) are then used to identify sediment composition and provenance. This allows an assessment to be made about the amount and rates of sedimentation or erosion, mineralogy and organic matter.

This research utilises the Normalized Difference Vegetation Index (NDVI) to investigate vegetation canopy changes using ERDAS IMAGINE. NDVI grids were obtained from satellite imagery. The derived datasets allow observation of the vegetation dynamic status across study sites over the study period. NDVIs reflect the vegetation-live-greenness amount which is, for example, expressed by declining NDVI trends due to stressor scenarios such as water shortage, and plant disease or death (Weier & Herring, 2000; BOM, 2017b). Moreover, this research uses ArcGIS mapping methods for classification and shorelines digitising to ensure the results are precise. Image classifications are applied, using ERDAS IMAGINE, to validate and monitor the

changes of shoreline positions at the study sites. Both supervised and unsupervised classifications are used to identify the best method for the study sites to obtain accurate results of landcover dynamics (Hegarat-Mascle *et al.*, 1997; Hamylton, 2016, 2017).

Historical and current satellite imagery (1973-2016) and aerial photos (1949-2014) provide evidence of changing wetlands. Using GIS analytic software (ArcGIS) on the images then allows the prediction of modification trends to estuaries/wetlands. The results are evaluated and compared to establish a classification based on land-use by applying digital super-classification and visual classification. Then, combinations of the two classification methods can determine the changes, and categorize the risk level. All the changes that have been determined within the last 68 years are then considered and checked in combination with field observations, sampling, and GPS-surface and bathymetric surveys (Al-Nasrawi *et al.*, 2018a, 2018c).

Solutions for each category are proposed and comparisons between them are made to identify changes. Furthermore, the future shoreline distributions of global warming-affected wetlands are examined using Arc Scene software to model the distribution of geomorphological and vegetation scenarios of the estuarine eco-geomorphic units.

1.7 Thesis structure

This thesis is based on six publications investigating the shoreline, land cover and resulting sedimentation characteristics of three intertidal estuarine platforms and their associated eco-geomorphic sets on the southeastern Australian coast using a combination of GIS analysis and remote sensing, as geoinformatic tools along with fieldwork/surveys.

Chapter 1 provides a general introduction and background on short-term estuarine morphodynamics and the associated wetland ecosystems.

Chapters 2, 4, and 5 apply a comprehensive modelling approach on three different intertidal landforms, each with different catchment sizes, extents of catchment modification, geomorphic settings (broad versus confined valleys), and tidal influences, to evaluate and compare the controlling eco-geomorphic dynamics and predict the likely consequences of environmental changes in the 21st Century, by focusing on the shorelines and land cover dynamics.

Chapter 2 applies the modelling approach to the estuarine Comerong Island (southeastern NSW, Australia) at the Shoalhaven River mouth. This estuary depends on the sixth largest catchment in NSW with high anthropogenic modification levels and provides an example (as a case study) to determine the essential of modelling adjustments to environmental abilities/efforts.

Chapter 3 illustrates that changes observed on Comerong Island are mainly due to sedimentation readjustments caused by damming the Shoalhaven River. This detailed investigation proposes sustainable solutions for some of the resulting sedimentation changes (as a geomorphic problem) on Comerong Island that results from the increased anthropogenic modification of the catchment. This is in addition to increasing human activities that limit the amount and character of the sediment supply from the Shoalhaven catchment. At the same time, declining precipitation caused by global warming affects runoff amounts and transport capacities of the rivers which, in turn, reduce sediment transport downstream. Thus, limited sediment is available to build or maintain the estuarine platforms and develop and stabilise the vegetated ecosystems to benefit the whole estuarine environment.

Chapter 4 applies the same modelling approach as Chapter 2 to present the historical and current situation of eco-geomorphological dynamics on the sensitive estuarine section of the Wandandian Creek delta (30 km south of Comerong Island), which has a very small intermediately modified catchment and discharges into a large lagoon with limited tidal activity.

Chapter 5 continues to use the same modelling methodology to investigate Towamba estuary further south on the NSW coast with a mostly unmodified and high-sloped catchment. Chapters 2, 4 and 5 conclude that the main factors controlling the eco-geomorphic bodies at these three study sites are the sedimentary character and the consequential dynamics of growth rates. This is confirmed in chapter 6.

Chapter 6 compares vegetation changes (as an ecosystem indicator) over time to climatic and geomorphic factors. This results in a significant dependency of vegetation changes on sedimentation rates rather than on climatic factors or sea level rise. Chapter 6 captures the overall trends of the vegetation canopy dynamics based on a new assessment method using NDVI with a focus on the greenness side of the NDVI scale (0.0 to +1.0), and then regressing it to the related causative factors. Datasets used include satellite imagery, climatic variables, sea level and geomorphic representors from the three study sites, with calculations conducted in ERDAS IMAGINE, SPSS, and RStudio. The vegetation extent represents the main ecosystem indicator. Analysis of these indicators shows that sediment delivery/deposition is the most influential factor controlling intertidal platform dynamics and/or vegetation stability. This geomorphological control influences habitable opportunities and allows ecosystem developments that reduce the estuary's vulnerability to erosive action.

Chapter 7 focuses on geomorphic attributes of the three sedimentary landforms by modelling the vulnerability and responses of the study sites to any future environmental stressors (mainly surge in sea level) based on the historical/existing situations, by utilising LiDAR-DEMs,

and based on the estimated scenarios of sea levels by the Fifth Assessment Report (AR5) of the Intergovernmental Panel on Climate Change (IPCC).

Chapter 8 draws the main conclusions from this research (Figure 1.5).

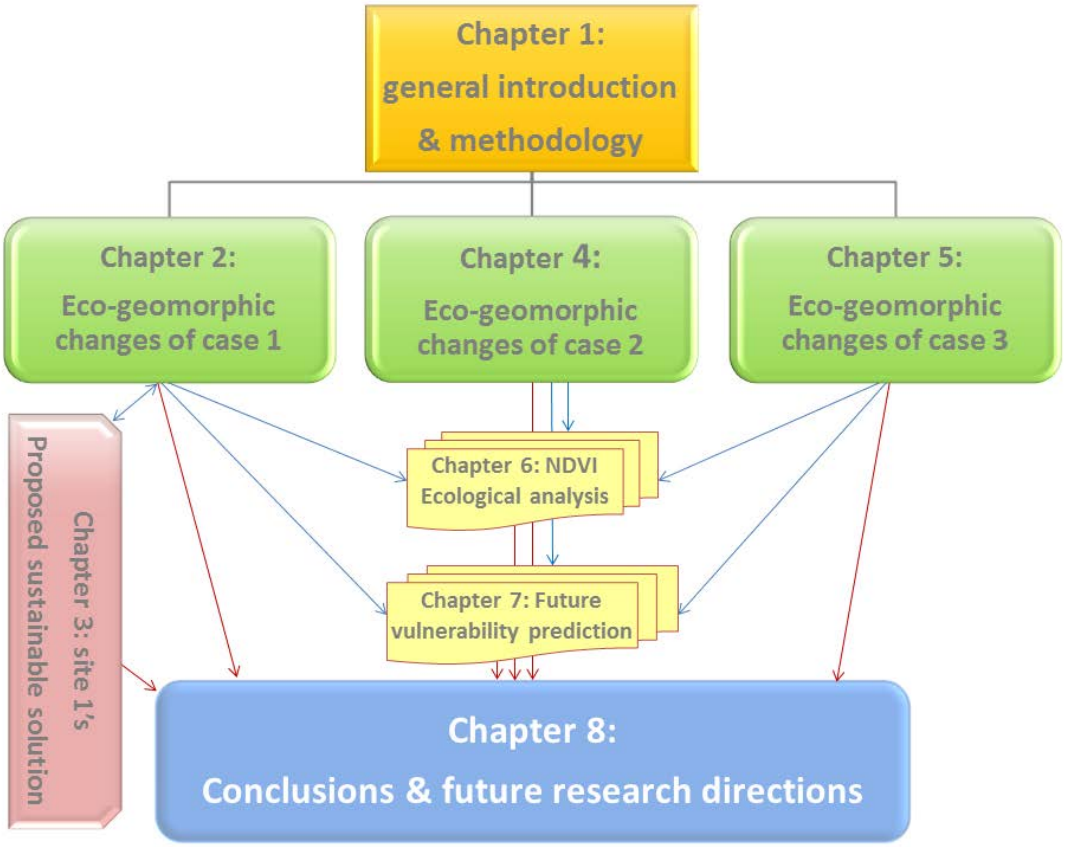

Figure 1-5. Thesis methodology and linked strictures.

Chapter II: Vulnerability of coastal wetland ecosystems to environmental changes on Comerong Island

2.1 Abstract

Sustainably managing coastal zones is increasingly complicated. Most human populations live along the coast, where their activities, together with a range of environmental changes, alter the natural ecosystem processes and caused changes in coastal wetlands. To ensure sustainable use of coastal resources, a comprehensive set of modelling tools can help managers to make decisions. This study uses Comerong Island (southeastern NSW, Australia) as a case study to demonstrate the importance of modelling modifications to environmental change. Several data-based modelling approaches are employed to explore how human activities have altered this estuarine island setting over the last 60 years (1949–2014). Multi-temporal changes in land cover, shorelines and sediment delivery are estimated from remote sensing data, GIS analysis, and laboratory tests on water and sediment samples (grain size, X-ray diffraction and loss on ignition and water analysis). Results show there are significant changes to the areal extents and elevation of mangroves, saltmarshes and shorelines on Comerong Island over the period of analysis, including northern accretion (0.4 km^2), eastern, middle and southern erosion (0.7 km^2) of the island. By implementing modelling using GIS tools, water and sediment samples to monitor ecosystem processes, such as sediment transport and erosion/deposition, resource managers will be able to make informed decisions by evaluating the potential consequences of the existing situation.

ADDITIONAL INDEX WORDS: *eco-geomorphology, sediment transport, erosion, human modifications.*

2.2 Introduction

Coastal wetlands are among the most productive, sensitive and responsive ecosystems in the world. However, they are affected by climate change and human influences (DSE, 2007). Particularly within New South Wales (NSW), coasts and their hinterlands have been substantially modified since European settlement. Thus, human and natural dangers that affect coastal wetlands need to be monitored, to catch the direct threats of loss to the wetlands itself or to observe indirect loss to its catchment.

Early civilisations inhabited coastal areas (e.g. Mesopotamia; Postgate, 1992) and nowadays 70% of the human population and 86% of Australians live along the coasts for ecological and

economic reasons (Cherfas, 1990; Neumann *et al.*, 2015). Human-induced stressors have increased since last century and caused loss of coastal ecosystems, particularly within coastal wetlands (DSE, 2007). Wetland studies across the globe have indicated the negative effects of human activities on wetlands (Ehrenfeld, 2000).

In addition, modifying the catchment and its water usage has caused many problems. For example, 60% of fresh water has been diverted from coastal NSW, Australia, since the start of European settlement (Saintilan & Imgraben, 2012). Kingsford (1990) revealed that direct and indirect human influences could change estuarine habitats, which can then affect the conservation of shorebirds.

2.2.1 Background

The NSW coastal areas are a great natural asset, making an enormous contribution to the economy. Although Australian governments apply conservation rules strictly, many studies estimate than human activities have caused significant indirect destruction to Australian wetlands. Thus, examining the existing situation and modelling the current modifications to natural processes is important for any applicable study site. Comerong Island (Fig. 2.1) represents an ideal example of disturbed regimes.

The island is a nature reserve situated about 170 km south of Sydney and 11 km east of Nowra, between the current southern Shoalhaven River mouth (at Greenwell Point and Orient Point) and the northern river mouth (the old entrance; see Fig. 2.1). The nature reserve comprises many coastal platforms including the island and the dune barrier sands, and has stabilised to flourish coastal wetland habitats, including mangroves, salt marshes and *Casuarina* (Fig. 2.2).

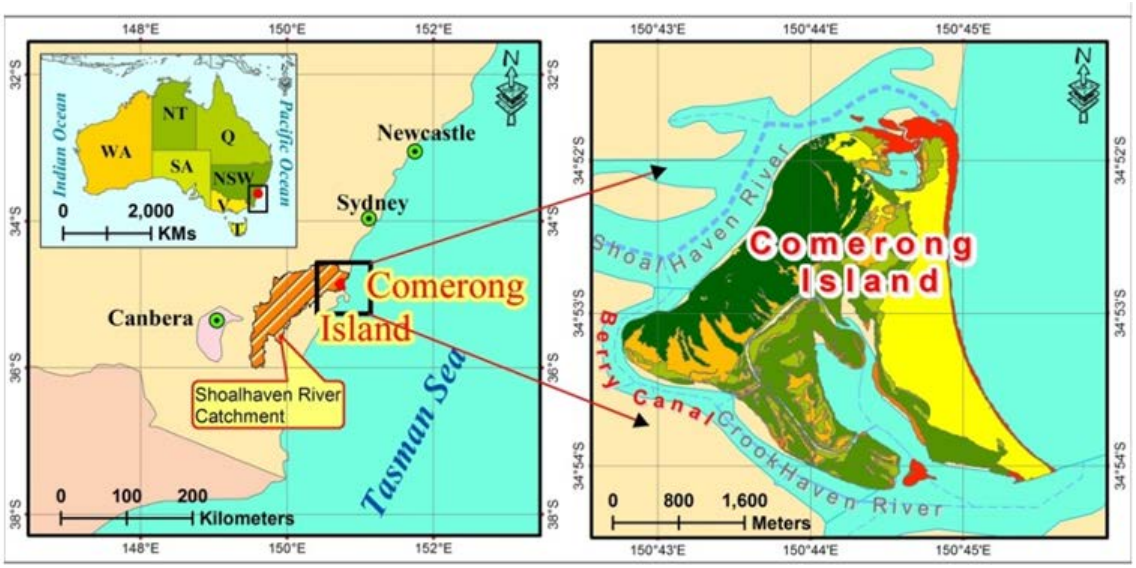

Figure 2-1. Location of the Comerong Island (study site), southeast NSW, Australia.

Comerong Island is part of an infilled coastal deltaic estuary and is mostly made of sediments derived from the Shoalhaven River catchment associated with its ocean sandy barrier built up from marine sand during the Holocene transgression (Woodroffe *et al.*, 2000; Wright, 1970).

The Shoalhaven River has a 7177 km^2 of catchment area, which is the sixth largest catchment in NSW (OWA, 2010). This large catchment provides abundant sediment during high flood flows which move down to the delta and have infilled the estuary during the last 7000 yrs (Umitsu *et al.*, 2001; Woodroffe *et al.*, 2000). In 1822, Alexander Berry built a canal that linked the Shoalhaven and Crookhaven Rivers (Fig. 2.1) as an alternative entrance since the Shoalhaven Heads. This entrance had become shallow causing higher water levels that threatened the estuary and all associated human settlements (Thompson, 2012). The area encompassed by the two rivers and the canal became Comerong Island (Umitsu *et al.*, 2001). After the construction of the Berry Canal both the Shoalhaven and Crookhaven (5 km south) entrances act as discharge points to the sea. Berry Canal was originally only 190 m long and 5.5 m wide, but erosion pressure on the banks and bed of the canal has increased its width to 250 m (Thompson, 2012; Umitsu *et al.*, 2001).

The study site on Comerong Island has been heavily modified since European settlement and these changes have caused a series of sediment availability and transport problems and negatively affected natural processes. Water flow and sediment transport were further modified after the Tallowa Dam was constructed in 1976, shown in Figure 2.2 (SCA, 2015). The dam has blocked most of the water and its sediment derived from the upper catchment making it effectively inactive (Fig. 2.2). Moreover, 35% of the catchment has been used for farming and a further 11% for forestry (OWA, 2010; Fig. 2.2).

Human activities are placing unprecedented pressure on these coastal resources. Studies conducted on the effects of human activities on wetlands indicate the many different requirements to use wetlands for multiple objectives, such as human development, recreation, tourism, agriculture and conservation (Shahbaz *et al.*, 2009). The Shoalhaven River floodplain, which covers approximately 5% of the catchment, has a reputable history of being one of the richest dairy areas in NSW (NPWS, 1998). Other significant industries include commercial fishing, oyster growing and vegetable farming (Shahbaz *et al.*, 2009). Additionally, the tourism industry is one of the main human activities, with recreational fishing, surfing and boating (NPWS, 1998). The floodplain is also experiencing considerable urban and industrial growth, particularly in and around Comerong Island (OWA, 2010). This has resulted in increasing the erosion rates in the estuarine area. This is particularly apparent at Comerong Island where strong tidal movements combine with the Shoalhaven River flow and heavy boating and fishing activities (Fig. 2.3).

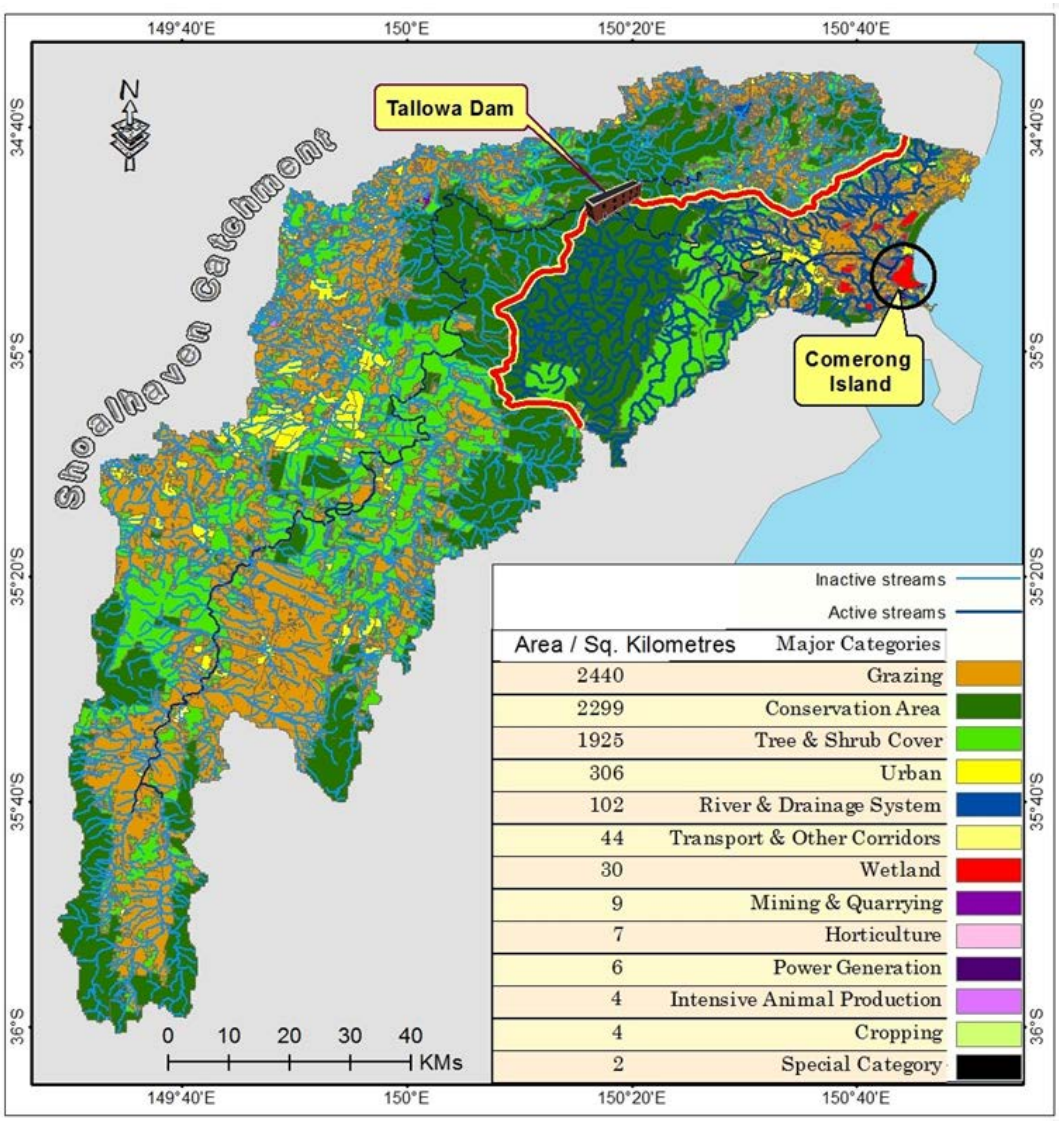

Figure 2-2. Shoalhaven Catchment showing; land use classes and Tallowa Dam that separates the upper and lower catchments.

To protect the marine and coastal ecosystems, this exploratory study has investigated the human activity influences on the eco-geomorphic systems of Comerong Island. The study is based on a literature review combined with fieldwork-sampling and consequent GIS-based-modelling that will offer a qualitative outcome, which can be utilised to suggest an adaptable and sustainable coastal management solution.

2.3 Methods

This research is based on continuous assessments of multi-temporal transformation, elevation and shoreline stabilities/dynamics at the landscape levels. The reduced or increased areas of wetlands have been assessed by measuring the land cover on aerial photographs and satellite images over time. Shoreline evaluation has specified the changes in erosion/accretion rates

around Comerong Island. Changes to the mangrove and saltmarsh areas (as a land cover function) illustrate the shoreline position and elevation stability in the Comerong coastal wetlands. This project entails assessing potential threats, such as shoreline erosion and sediment delivery problems. In addition, the effects of artificial modification in the catchment are the principle element addressed.

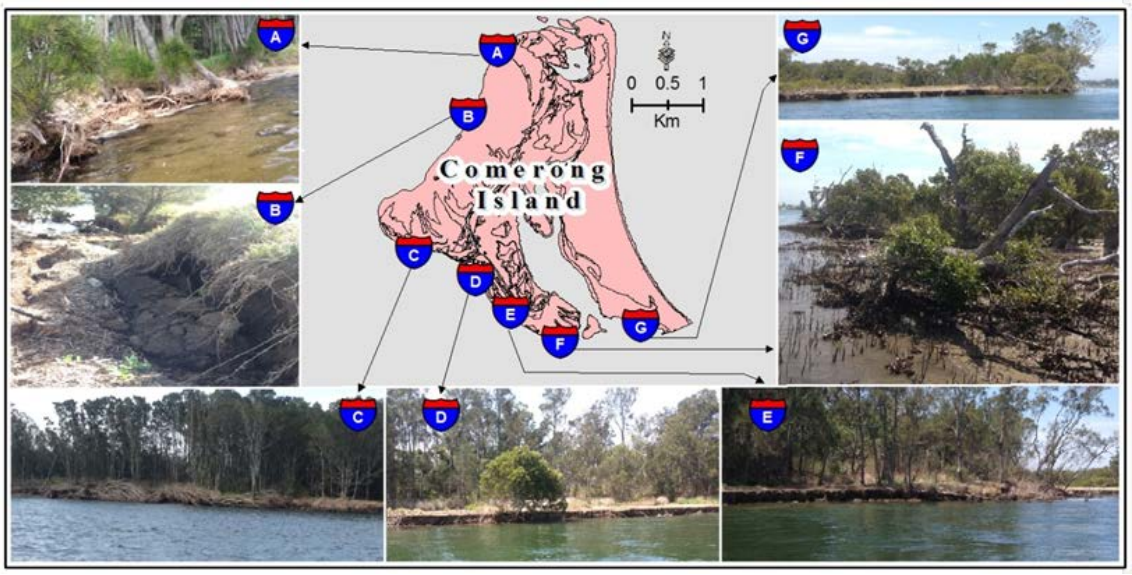

Figure 2-3. Chosen photos of Comerong Island showing clear eroding within shorelines and mangroves at western and southern sides.

The project targets were achieved at several levels, starting with GIS and RS-based analysis to identify and classify the land cover and shoreline changes at specific study sites depending on recent and historical records of aerial photography, satellite and LiDAR data. This was combined with sampling the water, soil and sediment.

The prime goals are to monitor and detect the shoreline dynamics, land cover and elevation changes/trends of coastal wetlands to simulate possible modifications for the wetland rehabilitation.

To gain accurate results, the most recent GIS analytic modelling tools (including ArcGIS and ERDAS IMAGINE) have been used to simulate, monitor and model the environmental changes by utilising the available and reliable remote sensing datasets. High resolution remote sensing datasets ranged from historical mapped sheets plus aerial photographic records of the chosen site (provided by the UOW, SEES-GIS Unit). Meanwhile, broader satellite imagery have been obtained from several sources including LPI (Land and Property Information – NSW), Landsat, and LiDAR point cloud dataset (from Shoalhaven City Council).

To achieve these aims, this study divided the methodology into three parts, as seen in Figure 2.4.

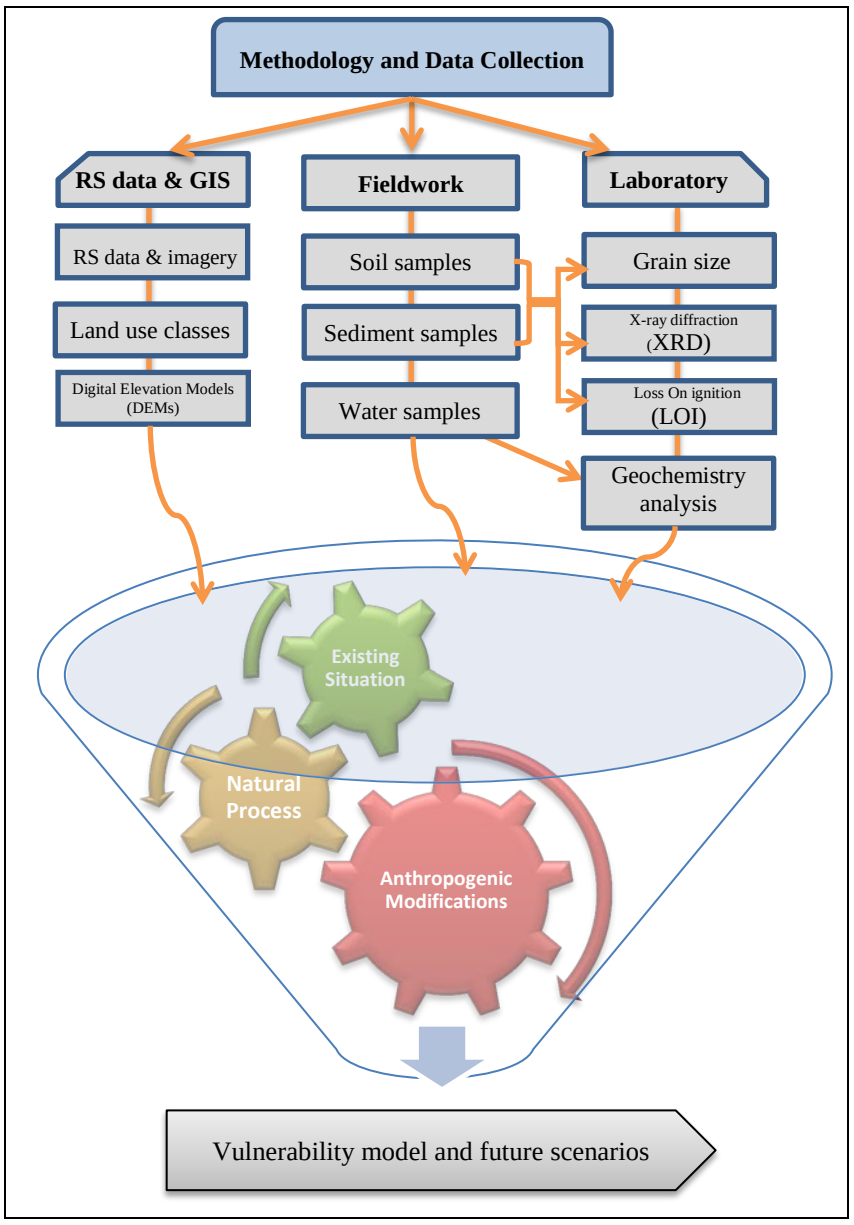

Figure 2-4. Methodology; data collection and analysis sequences.

2.3.1 Data Collection

Various data have been collected to achieve the study aims. Remote sensing and GIS data were used to classify land use classes. LiDAR (2004 and 2010) and SRTM (2011) data have been used in ArcGIS10.2 to create DEMs. LiDAR and SRTM data sets have also been used to extract various DEMs using TIN and surface analytic GIS tools for elevation analysis and validations (Al-Nasrawi *et al.*, 2018a).

Field work collected 113 sediment/soil samples from Comerong Island. Grain size analyses, X-ray diffraction (XRD) and loss on ignition (LOI) tests on these samples yielded the grain size and proportions of minerals and organic matter. A Yeo-Kal 615 multi-parameter water quality

analyser was used in the field to measure water samples in real time to test it for turbidity, salinity, conductivity, pH and dissolved oxygen (DO).

2.4 Results

Results showed significant coastal wetland degradation and change, causing wetland loss. The geoinformatic analysis of remote sensing datasets using GIS indicates that the island and its associated ecosystems have suffered from a huge loss of wetlands (approximately 0.3 km^2). Additionally, it indicated that some of the saltmarsh areas were converted for agricultural use, and the mangrove cover lost ground because of shoreline erosion (Fig. 2.5). This study also determined the effects of human modification within the wetland's catchment and assessed the extent of the human activities' impact during sea-level rise stresses.

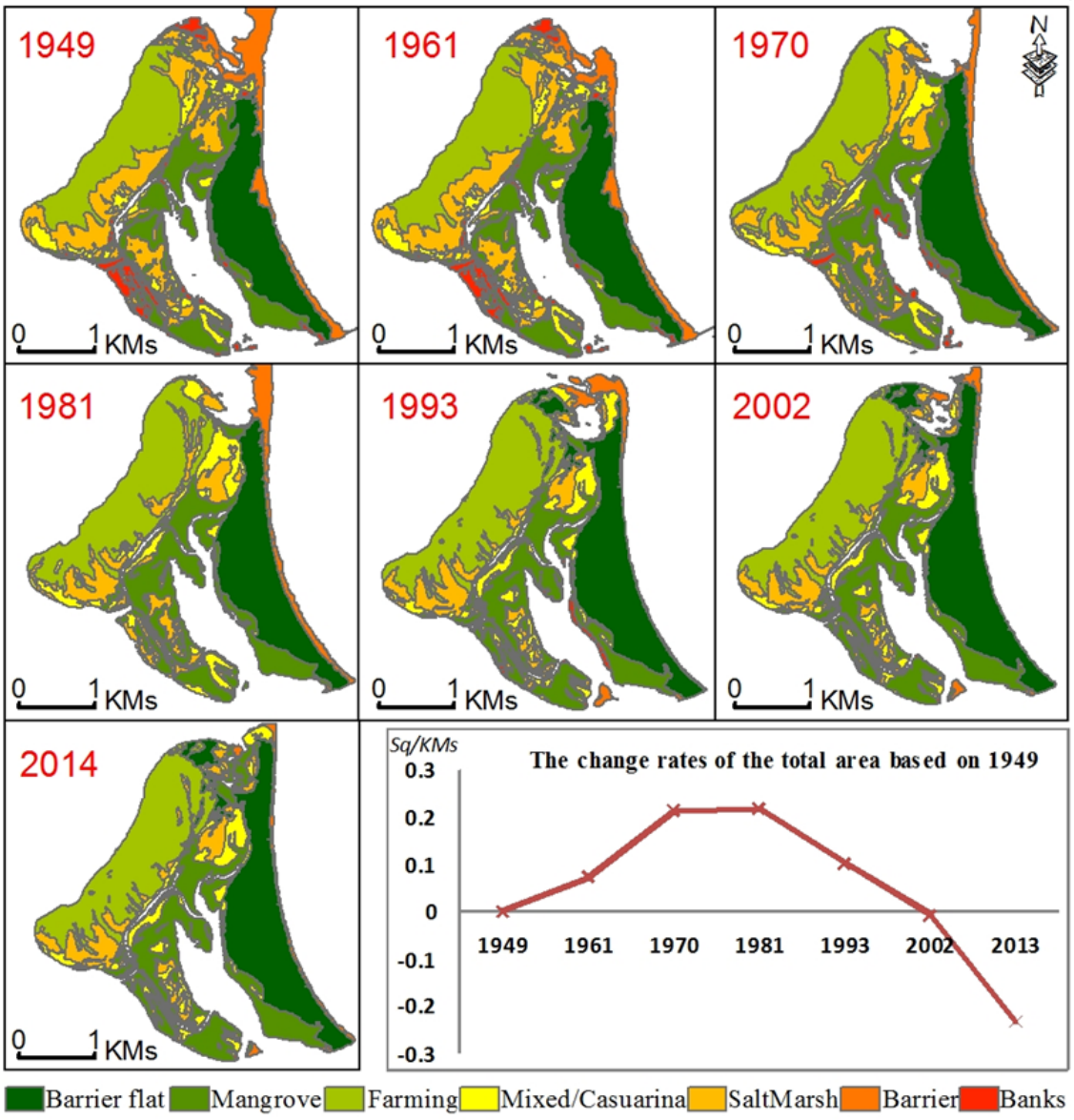

Figure 2-5. Multi-temporal imagery (1949–2014) showing significant changes of land cover, shorelines and total area.

DEMs have shown significant elevation changes over time on Comerong Island as shown in Figure 2.6. So far, the western, mid and southern sides of the island have eroded as mapped in red on Figure 2.6a and b. Meanwhile, accretion has expanded the northern region with minor erosion in the middle of that area.

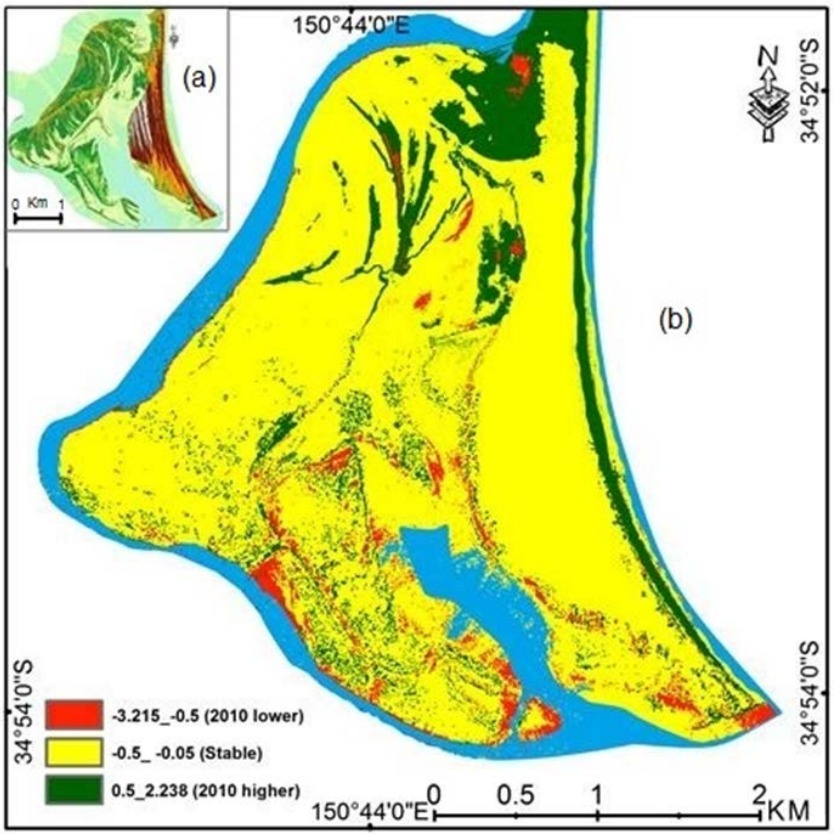

Figure 2-6. DEMs analysis showing: (a) elevation distribution on Comerong Island, (b) overtime elevation comparison show significant change-loss in red and accretion in green while stable areas are shown in yellow (LPI, 2004 & 2010).

Soil and sediment samples have been checked for their grain size using a Mastersizer 2000 laser diffraction particle size analyzer, which generated results shown in Figure 2.7a-c.

Most of the island is made of sand, especially along the north, east and south sides, where wave energy has built those parts of the island (Fig. 2.7). The silt and clay present along the western side of Comerong Island have been derived from the Shoalhaven River catchment. The rates of sedimentation and types of sedimentary sequences could then be related to high energy events such as the flood history records.

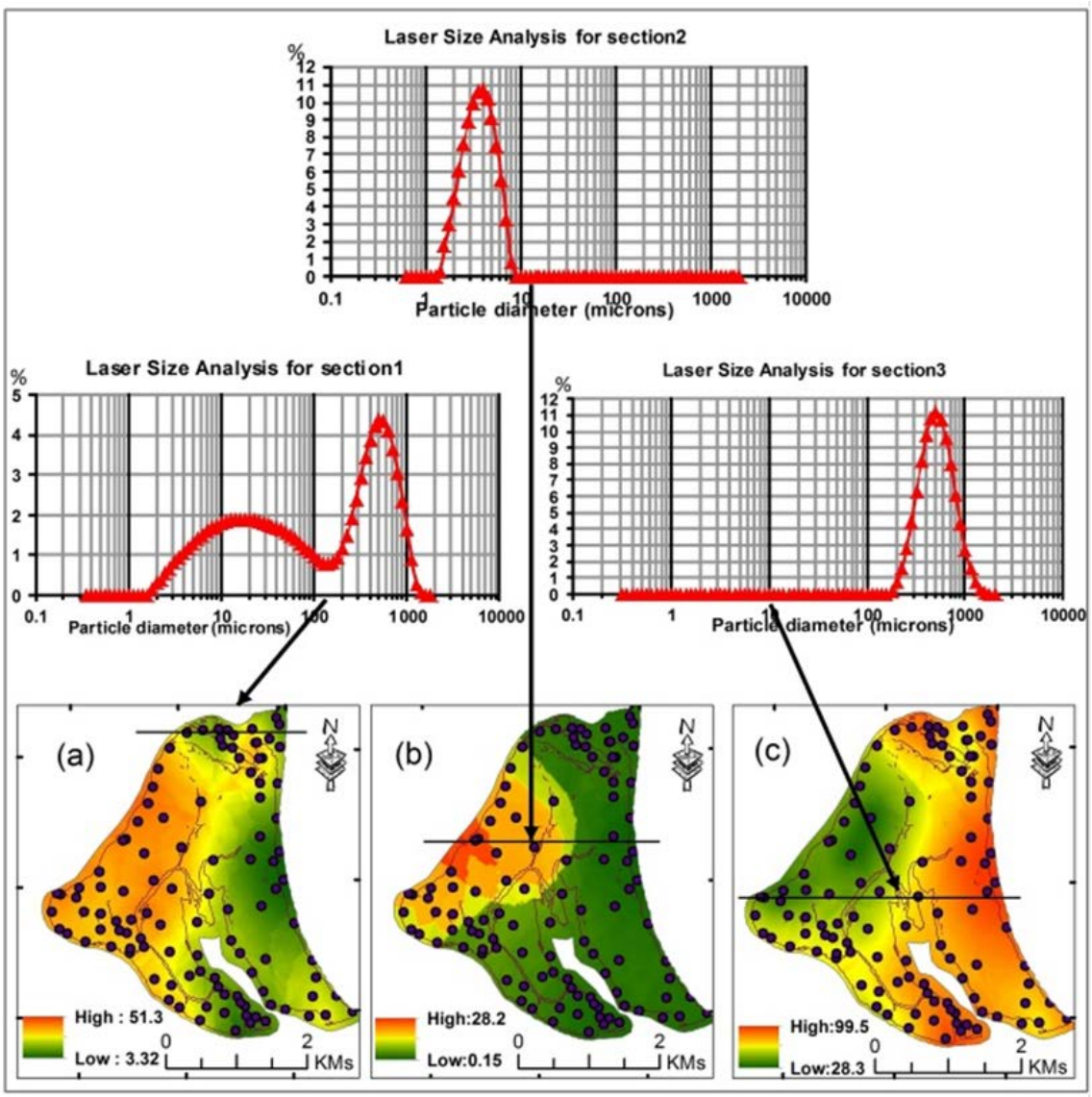

Figure 2-7. Soil, sediment samples and grain size analysis from Comerong Island; (a) clay proportion, (b) silt proportion and (c) sand proportion.

Twenty-four samples tested with X-ray diffraction (XRD) showed that all samples are dominated by quartz, especially along the eastern beach and barrier where wave action has eliminated most of the softer minerals and clays (Fig. 2.8). Along the western and southern sides of Comerong Island and in the active channel areas, feldspar and lithic sand grains form a prominent component representing fluvial sands derived from volcanic, volcaniclastic and mudstone rocks in the source area. Clay content in the samples is highest in the low-energy environments around the island, but also occurs in the fluvial lithic sands through the diagenetic alteration of feldspar and lithic sand grains.

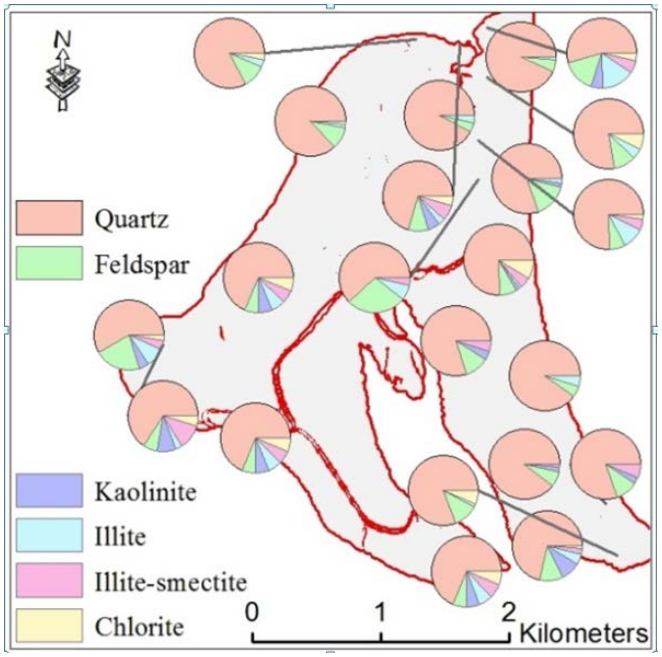

Figure 2-8. Mineral content of sediment samples of Comerong Island.

Utilising a loss on ignition (LOI) test, twenty samples chosen from an east-west cross-section were analysed for proportion of organic matter (OM %) in the samples. This has checked how much the biotic and abiotic components played roles in changing the elevation. LOI data show two main areas with the highest proportion of organic matter; one positioned in the very muddy section in the middle of the island represented by mangrove area, and the other occurring in the area with the highest density of native plants in the eastern part of the island. LOI data was also used to evaluate changes in elevation with respect to the water table, see Figure 2.9.

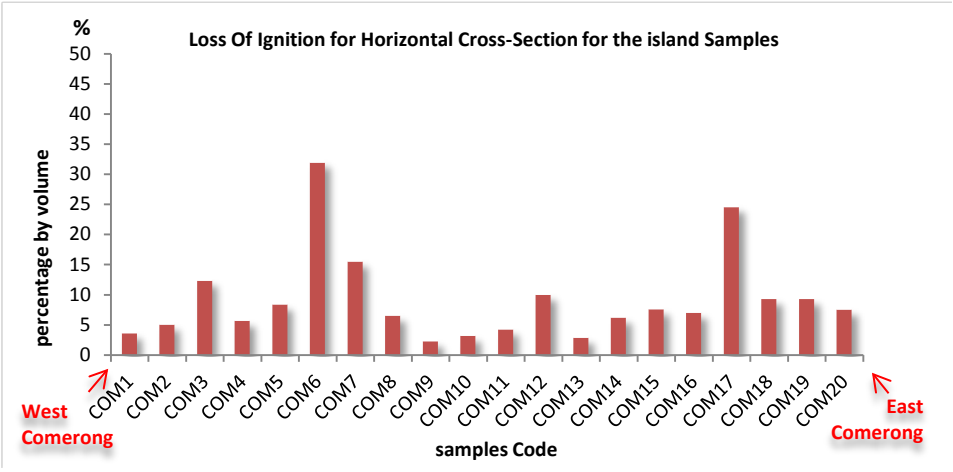

Figure 2-9. Loss on ignition of the analysed sediment samples of Comerong Island.

The average discharge of the Shoalhaven River is below five megalitres per day from 1914-

2014 with the exception of flood-related events. However, since these gauging stations are located in the up-stream/riverine-systems, they do not reflect the situation downstream, thus eight samples from below Tallowa Dam have been collected and tested. Water samples from the Shoalhaven River show very low amounts of suspended sediment downstream from Tallowa Dam (Fig. 2.10).

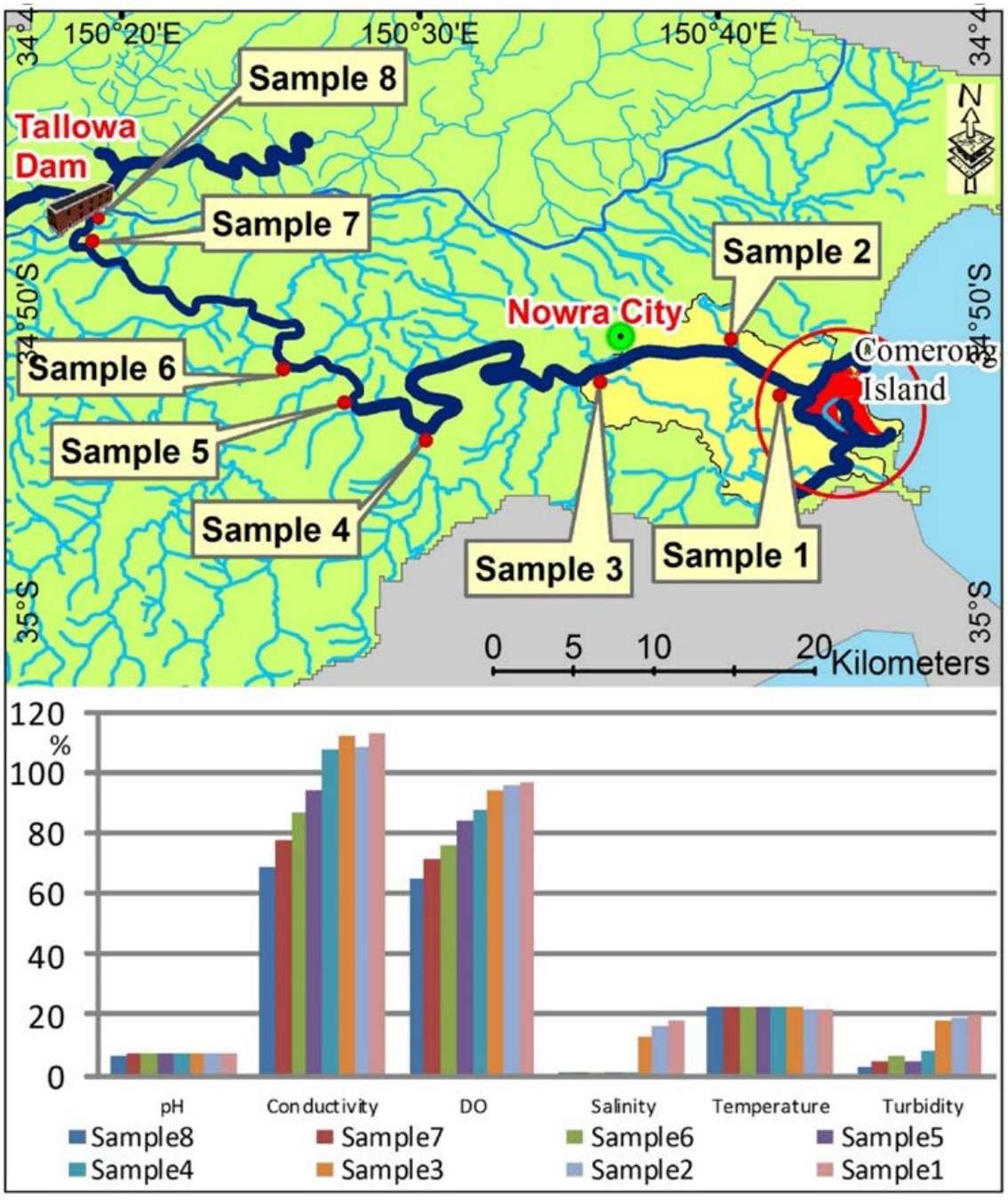

Figure 2-10. Analyses of water samples show significant spatial changes in pH, salinity, temperature, turbidity, dissolved oxygen (DO) and conductivity.

The water samples show a significant increase in turbidity, conductivity and dissolved oxygen downstream from the dam reflecting an increase in suspended sediment and salinity. These

results clearly prove there is less sediment delivery and high rates of bank erosion in the downstream areas, which leads to increasing turbidity and siltation in the adjacent wetlands.

2.5 Discussion

This multi-temporal study of the Comerong Island wetland shows a significant loss of coastal wetland in southeastern Australia. The main losses were changes in landcover, shoreline and elevation that resulted from the negative effects of human activities on the wetland's catchment. This comprehensive monitoring, plus other studies conducted by multiple researchers, has revealed the serious negative anthropogenic influences in and around the Comerong Island wetlands. A number of spatial and temporal monitoring solutions should be considered for effective coastal wetland management. Significant results include:

a) Mapping processes for monitoring and modelling aerial photographs and RS data (1949-2014) of the shorelines show the northern part of the island has expanded by 0.41 km^2, whereas, the western and southern portions have been eroded by 0.73 km^2. This situation has resulted from the sediment delivery and erosion/deposition processes, that are mostly controlled by human infrastructure up stream such as Tallowa Dam, combined with the ocean tidal affected by sea level rise. Together these have caused a reduction in sediment delivery, which cannot balance the erosion/deposition caused by natural processes.

b) Grain size tests show most of the island is composed of sand, with clay in the west and uniform silt contents. Comerong Island is therefore made of soft materials, which are more easily eroded and lost than in other coastal ecosystems and therefore the Comerong may be more sensitive to rising sea level.

c) XRD test shows the minerals make up the sediment in Comerong Island originate from both the catchment and the ocean. Northern accretion on the island has been caused by adding ocean sediment via the open mouth of the Shoalhaven River.

d) LOI shows high plant density in the east and middle parts of the island. The high proportion of organic matter included biotic components such as leaf litter, mangrove debris and roots. This organic matter plays an important role on elevation changes and surface accretion.

e) Construction of the Berry Canal appears to have dropped water levels and reduced the wetland area, especially saltmarshes, on Comerong Island.

This modelling framework could be applied to study coastal wetlands all over the world. This project proved significant, detailed and accurate results of changing coastal wetlands in an eco-geomorphological context for risk assessment, using modern modelling methods. Such information will be essential for government agencies to issue and revise their policies. It will

also be important for the public and scientists who currently focus their attention on the best way to preserve wetland ecosystems to achieve conservation targets.

2.6 Conclusions

Both natural and anthropogenic processes control the balance between sediment deposition and erosion rates. Historically, the Shoalhaven River has provided high sedimentation rates and these high sedimentation rates and lower erosion rates have controlled the natural accretion processes around Comerong Island. The aerial photographs and RS analysis (1949, 1961, 1973 and 1982) have shown that the island has grown constantly. After 1982, however, the island has eroded and its size has declined as shown in the aerial photographs and RS data (1993, 2002 and 2014). The reason behind this change was the building of Tallowa Dam, which blocked most of the sediments collected from the catchment. Thus 80.1% of the catchment (5750 km^2 of 7177.5 km^2) was converted to geomorphologically inactive catchment. That caused serious sediment transport and availability problems, which changed the positive sedimentation rates to negative values, and favoured erosion.

After the Tallowa Dam was constructed in 1976, the sediment rates initially remained high and the island continued to grow. This was due to the new water level within the Shoalhaven River that dropped below the dam (for 58.8 km until it reached Comerong Island) that caused erosion of the riverbed and edges providing sediment to the Comerong Island area. However, this only occurred for a few years, after which the natural processes failed to erode additional sediment resulting in less sediment availability and deposition in the lower reaches. This is reflected in higher erosion rates that now control the site. This study has shown that the shoreline eroded by 0.73 km^2 since 1982 (0.02 km^2 annually), while the northern part of the island grew significantly (about 20% between 1949 and 2014). This can be related to barrier deposition by natural tidal processes that have affected the northern area during periods when the river mouth was open.

To restore the coastal wetland ecosystems fully, its extent needs to be monitored carefully. One can choose a natural mechanism that will offer a self-sustaining approach or self-management. By considering the findings from scientific studies, resource managers can implement relevant policies need to repair the damage from human activities in such wetlands.

Chapter III: A developed catchment assessment for urban-geomorphic sustainability: Tallowa Dam

3.1 Abstract

Damming rivers causes two main problems affecting a river's geomorphic ecosystem and its water quality. The Tallowa Dam on the Shoalhaven River in southeastern NSW, Australia, provides a case study to find the best sustainable solutions to avoid these problems. The project uses a civil-infrastructure idea to design a grid of collector pipes from the reservoir bottom surface. Spatial data analysis using ArcGIS 10.2 is used to determine the best grid location for the pipes in the reservoir. Water and sediment samples have been analysed for grain size, heavy metal and organic matter contents. The dam has led to a significant decline in sediment transport and water discharge to the lower reaches of the river which has resulted in greater erosion of sediment and higher salinity rates within the lower reaches and coastal streams. Water quality in the reservoir has been affected by increased sediment accumulation, particularly mud, which has increased the amount of heavy metal and nutrient pollution that could eventually affect the water users. A proposed solution is to use over-storage water to remove accumulated sediment from the base of the dam through a net of collector pipes controlled by auto-mechanical gates, instead of flowing over the top of the dam. This would maximize the volume of upstream sediment and contained pollutants that can be released from the reservoir into the downstream river ecosystems as well as providing better water quality and a longer water storage time.

Keywords: *Water quality, geomorphology, pollutants, civil-infrastructure, GIS-detection.*

3.2 Introduction

As urbanisation of the world is growing, an adequate fresh water supply is required. Damming and storing river water during seasonally and annually variable rainfall is one of the solutions to meet the demand of the growing population in urban areas. (Saeijs & Van Berkel, 1995; Newton *et al.*, 1998; Duda, 2002; Nielsen & Brock, 2009). Dam construction for the regulation and impounding of river systems has played an important role in human life by regulating floods, generating electricity and providing water for commercial, agriculture and domestic use (Michener *et al.*, 1997; Newton *et al.*, 1998; Costanza, 1999; Hughes, 2003; Fensham *et al.*, 2005; Liu, 2012; IPCC, 2013).

At the close of the 20th Century, the application of dams and weirs to control fresh water bodies had become so extensive that over 850,000 dams had been set up globally, leading to the regulation of over 65% of the global freshwater discharges (Lynch *et al.*, 2011). Apart from storing water and altering flow regimes, dams also lead to reduced downstream sedimentation and nutrient transportation to coastal regions (Growns *et al.*, 2009; Dao, 2011). The acceptance that dams have a multitude of direct and indirect impacts on freshwater systems implies that their construction in developed and developing nations has become controversial. Sediment transport and damaging water quality are some problems caused by dams (Koltun *et al.*, 1997), leading to huge erosion and salinity intrusion rates within downstream and coastal reaches. Meanwhile, the quality of the water within the dam is impacted by increasing sediment deposition, particularly the accumulation of fine and very fine particles. This has increased the amount of chemical pollution, such as heavy metals, which could include arsenic, copper, nickel, zinc chromium and lead), nutrients and organic matter, which have entered the reservoir from the streams through developed catchment areas. In the long term, heavy metals and nutrients can be released from the muddy particles into the water by changes in pH and the oxidation-reduction potential (Eh), which may eventually affect the water quality (Alyazichi *et al.*, 2015).

Despite there being several integrative reviews of environmental impacts downstream from concrete dams (Magilligan *et al.*, 2003; Braatne *et al.*, 2008) there have been few attempts to integrate sediment transportation through dammed reservoir systems. This highlights the need to conduct prospective research given that, contrary to the wider understanding of ecosystem functions, it is apparent that dammed river systems can still be dynamic. As Magilligan *et al.* (2003) indicated, this presents conceptual problems in understanding the impacts of human influences that are overlain on regular spatial and sequential river attributes. Again, contrary to the typical perception of primary river process, every dam represents a critical perturbation to the extent that investigating the physical and biological impacts can offer insights into aquatic and riparian ecosystems (Boyes, 2006). However, the process of river damming commonly impacts downstream ecosystems over longer river reaches compared to the inundated segments (Braatne *et al.*, 2008; State of the Catchments [SOC], 2010; Lynch *et al.*, 2011). Downstream ecological effects mostly follow three environmental factors: variations in the volume of downstream water flow; constrained passage of unconsolidated sedimentary constituents; sometimes coupled with fragmentation of the river corridor (Cukic & Venter, 2012). A dam can also cause interruptions in the downstream or upstream passage of biota (Lynch *et al.*, 2011).

Damming rivers has proved to be an ideal fresh water management approach to meet the needs of humanity (Rood & Mahoney, 1993; Postel *et al.*, 1996; Zhang *et al.*, 1999; Gleick, 2003) by smoothing out the variable seasonal and annual precipitation and runoff (Rood & Mahoney, 1993; March *et al.*, 2003), and maximising the benefit from this invaluable fresh water before it goes back to the ocean (Duda, 2002). However, some issues have been raised concerning the quality of the stored water (Day *et al.*, 2008; Nielsen & Brock, 2009), ecological aspects (Ligon *et al.*, 1995; Costanza, 1999; Petts & Gurnell, 2005), geomorphological effects (Petts & Gurnell, 2005), problems caused by changing groundwater levels (Kingsford, 2000; Petts & Gurnell, 2005) as well as pollution problems of sedimentation and trace element accumulation (Alyazichi *et al.*, 2015). Scientists have reported on a range of sustainable solutions for most of these issues (Gleick, 2003; Hadadin *et al.*, 2010) however reservoir sediment and water storage optimisations have not been reported in an eco-geomorphically sustainable manner.

Ultimately, there arises a necessity to champion robust study proposals for ecological assessment of new reservoirs being established, particularly in NSW. Dao (2011) indicated that previous dams were mostly commissioned without comprehensive environmental assessment and a study such as this will provide a scope for analysing and even mitigating some environmental impacts of dammed rivers.

This cross-discipline research aims to assess the problems associated with current dam design, in terms of sediment accumulation in the dam and sediment starvation below the dam, and to proposed and designed a specific sustainable solution that could be applied worldwide.

3.2.1 Study site (specification and background)

A case study has been investigated, using the Tallowa Dam as an example on the Shoalhaven River in southeastern Australia (Fig. 3.1a-e). The reservoir behind the dam has formed Lake Yarrunga that covers 9.3 km^2 with an averaged depth of 15 m and has 7500 ML total operating capacity of water supply for the southern Sydney region (Sydney Catchment Authority [SCA], 2015, 2016). This research has shown that by taking water and sediment flow from the base of the reservoir, it is possible to maximize the volume of sediment transported past the dam and hence foster sustainability of the coastal ecosystem. Based on this argument, the study presents a brief appraisal of the relevant literature as it pertains to dam construction and the nurturing of sustainability through modern day dam practices (SCA, 2015, 2016).

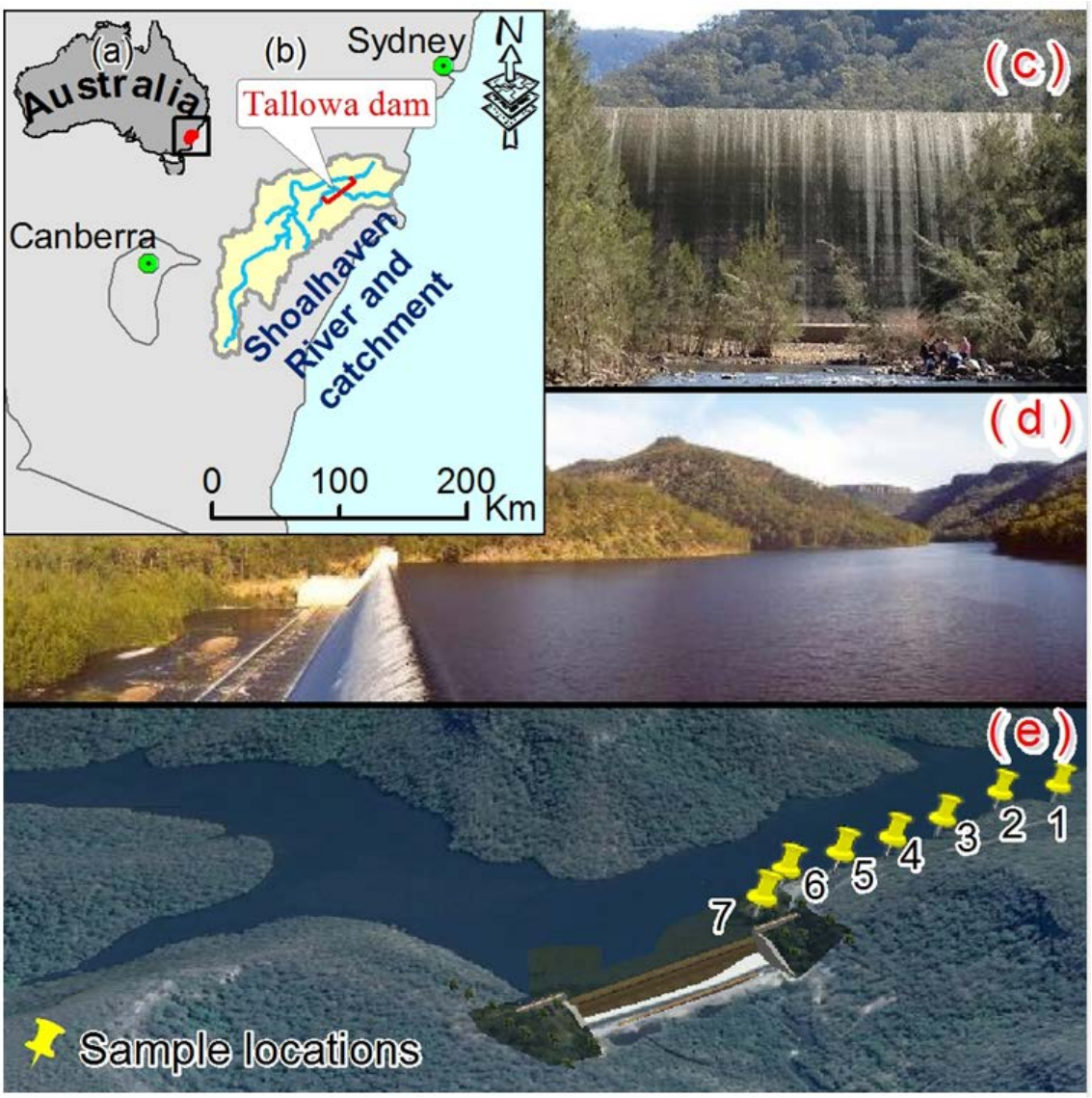

Figure 3-1. Study site, (a and b) Tallowa Dam in southeastern NSW, Australia, showing the (c) dam wall, (d) reservoir and (e) aerial view showing sample locations (images from Google Earth).

The Shoalhaven River catchment is the sixth largest catchment (7177.5 km^2) in NSW (OceanWatch Australia [OWA], 2010). This large catchment with its high terrain and complex surface (Fig. 3.2a) has impacted the weathering processes resulting in high erosion rates that have resulted in variations in soil distribution within the catchment (Fig. 3.2b). The erosion has provided abundant sediment which has moved down to the delta during high flood flow periods. This resulted in the Shoalhaven River estuary becoming infilled during the past 7000 years (Umitsu *et al.*, 2001; Woodroffe *et al.*, 2000).

A ground digital elevation model (GDEM) of the upper catchment (Fig. 3.2a) shows an elevated and high-sloped terrain that mostly consists of steep valleys surrounded by hills and plateaus, which have played an important role in sediment generation with high erosion and sediment transport rates within the Shoalhaven River. In contrast, the northeastern coastal area consists

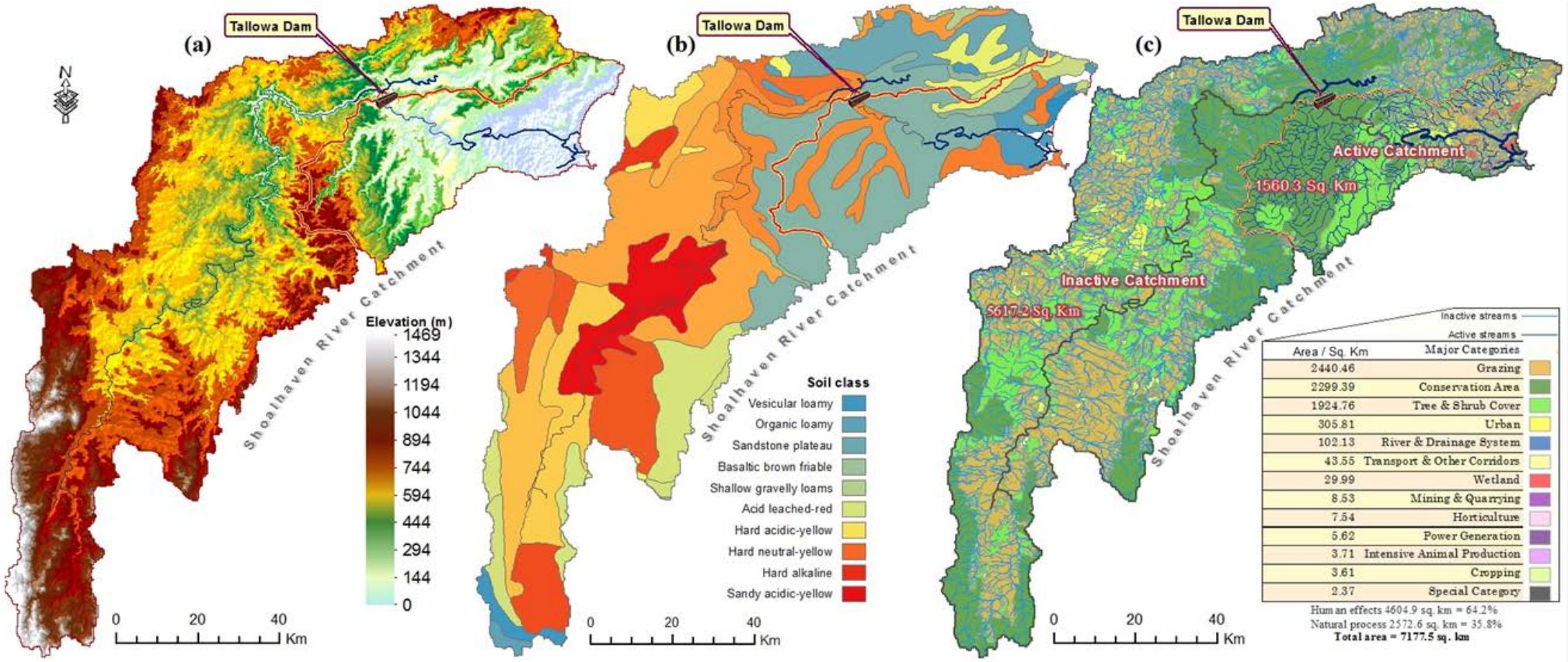

Figure 3-2. The Shoalhaven River catchment; (a) Terrain and DEM of the surface (b) Soil classification (c) Landcover classes (plus area size /km^2) of, active/inactive catchment areas and the active/inactive streams (Australian Land Use and Management [ALUM], 2010; ASTER GDEM, 2016).

of a low-lying subhorizontal floodplain. Since the Tallowa Dam was constructed less sediment has been delivered from the upper streams causing periodic interruptions or even losses of some unique ecosystems, like downstream wetlands.

The higher/upper slopes, hills and plateaus are covered by shallow Uc1.11 and Uc2.22 soil, that are mottled brown-yellow or brown-red with a thin pale subsoil consisting of quartz and/or buckshot. In comparison, the lower slopes and valleys in the catchment are mainly characterised by duplex soils, including Dy2.41, Dy3.41, Gn2 and Db3.21, with yellow-brown or mottled topsoil over red subsoil that has high quartz, buckshot and mud contents (Fig. 3.2b).

The land-cover patterns reported in Fig. 3.2c show that the catchment area has faced strong human modifications since European settlement that have influenced about 64.2% of the catchment (4604.9 km^2). This land clearing has increased sediment supply leaving only 35.8% (2672.6 km^2) of the area under natural eco-geomorphic processes. This change has caused a series of sediment availability and transport problems and has negatively affected natural processes (Al-Nasrawi *et al.*, 2015b, 2016b). Water flow and sediment transport have been further modified since the construction of Tallowa Dam in 1976, (Fig. 3.2; SCA, 2016). The dam has blocked most of the water and its sediment derived from the upper catchment making it effectively inactive (Fig. 3.2c), which may affect the stored water quality as well. Also of significance, the landuse patterns have effectively increased the nutrient availability into the drainage system (Boto & Wellington, 1984; Koltun *et al.*, 1997). For example, 35% of the catchment has been used for farming and a further 11% for forestry (OWA, 2010; Fig. 3.2c). Although the nutrient availability is an ecosystem enrichment, the increase in nutrients and associated trace elements in the water bodies the later deposition in the reservoirs would cause a decrease in the dissolved oxygen and more acidity. The anoxic conditions result in black or dark grey sediment that trap more pollution (Essington & Carpenter, 2000; Alyazichi *et al.*, 2015).

Climate factors should also be considered (Aziz & Scott, 1989; Fernandes *et al.*, 2011). The climate along the Australian eastern coast includes a wide range of environmental conditions across a huge spatial scale, varied topography, local air/ocean currents and coastal ecosystems, making generalisations difficult based on the Köppen system. Thus, the Australian Bureau of Meteorology (Bureau of Meteorology [BOM], 2016) has modified Köppen classification system to meet local specific needs. The BOM (2016) has classified the Shoalhaven River catchment to be part of a southeastern temperate climate area, with no dry season and a warm summer. However, the northeastern part of the catchment (on and around

Comerong Island) has been classified as a temperate climate that has a hot summer but lacks a dry season.

In the elevated parts of the catchment, the two main climatic factors that would influence sediment production and transportation rates are increasing temperature and declining precipitation. The interaction between regional and global climatic trends plus the local conditions cause fluctuations in the records (Fig. 3.3). The catchment has a temperate oceanic climate (Cfb) with mean temperatures between 15.33°C - 17.43°C while the northeastern floodplain region has a warm oceanic to humid subtropical climate (Cfa). Over the study site, a clear increase in air temperature has occurred during the last four decades, with some fluctuations (Fig. 3.3a). The average/overall temperature has increased by 0.48°C (from 16.25°C to 16.73°C; Fig. 3.3a). This increasing temperature would slowly increase sediment production and sedimentation rates (Mkpenie *et al.*, 2007). These climatic variations would also affect the soil salinity and its nutrients.

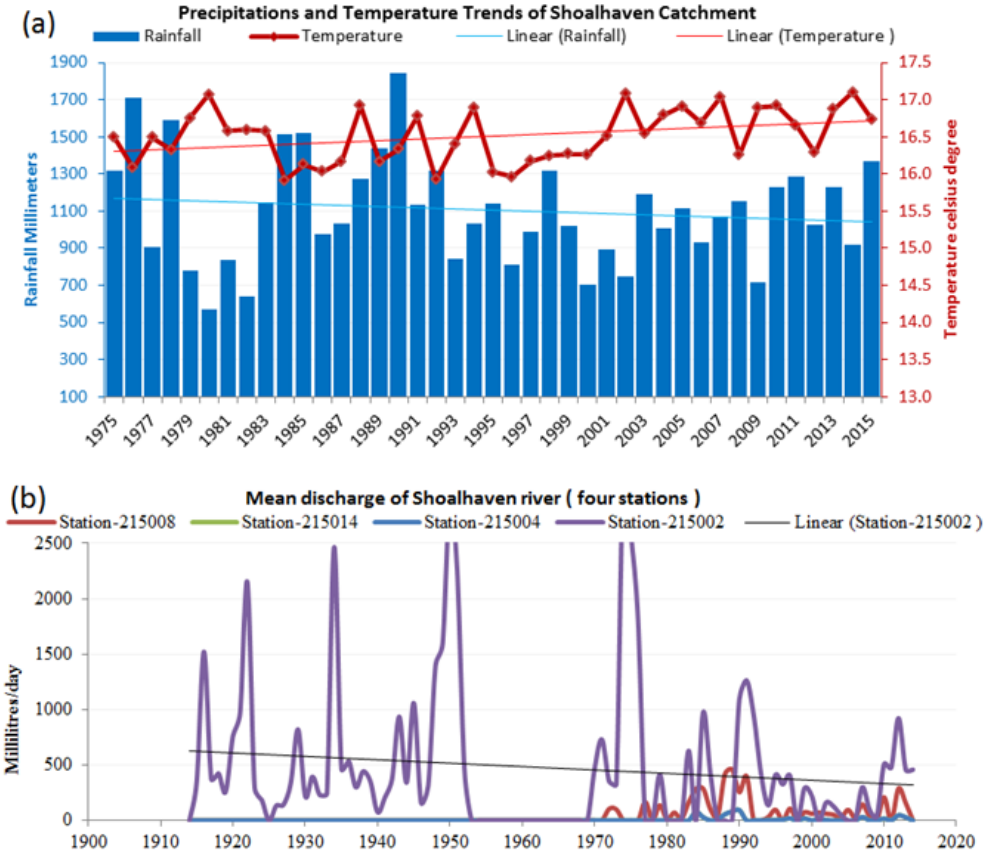

Figure 3-3. Physical parameter of the Shoalhaven River catchment; (a) precipitation (millimetres/annually) and temperature (°C) between 1975 and 2015, (b) the Shoalhaven River water flow discharge (of four upper catchment gauging stations) from 1914 to 2015. Sources; (BOM, 2016; KINMI climate explore at https://climexp.knmi.nl/).

The geomorphological setting of Tallowa Dam has divided the Shoalhaven River catchment leaving an essentially inactive catchment (78.3%, 5617.2 km^2) above the dam (see Fig. 3.2) and

an active catchment (21.7%, 1560.3 km^2) below the dam. Below the dam the river is divided into a bedrock river style, a floodplain river style and a tidal river style (Growns *et al.*, 2009). However Growns *et al.* (2009) posited that the tidal river style covers both the bedrock controlled river reach that extends 20 km upstream from Nowra, NSW, coupled with the coastal plain river reach downstream from Nowra. This implies that the Tallowa Dam has only two distinct reaches below it. The deficiency of adequate sediment cover over the steeply sloping continental landscape in the bedrock river reach has led to a relatively low rate of sediment supply downstream from the dam, such that Comerong Island is facing clear shoreline erosion problems (Boyes, 2006; Al-Nasrawi *et al.*, 2015b, 2016b).

This research includes a literature review, augmented by sampling and subsequent modelling, to provide some qualitative results that can be utilized to offer possible sustainable management solutions. The study uses a civil-infrastructure idea to design a method of flushing sediment and pollutants from a dam reservoir during periods of excess water flow. This could be achieved using a net of collector pipes controlled by auto-mechanical gates in the base of the dam whenever over-storage water is present. Spatial data analysis using ArcGIS 10.2 has been used to determine the best grid location for the pipes in the reservoir. This proposal would provide better water quality and a longer water storage time within the reservoir as well as increasing sediment supply to the lower reaches of the river which would alleviate the greater erosion of sediment and higher salinity rates within the lower river.

3.3 Methodology

A proposed method to solve both accumulation of sediment in the reservoir and the shortage of sediment supply to the downstream river reaches is to make the over-storage water flow through the dam's base as an alternative of flowing over the top. This would be the best sustainable way to maximize the volume of upstream sediment that could be transported and released into the downstream river ecosystems. At the same time it would clear sediment and pollutants from the bottom surface of the reservoir to get better water quality and a longer storage time.

Organizing a reservoir bottom flow system needs to start by designing a net of collector pipes that spread across the sub-surface reservoir area. Discharge channels should be constructed through the dam wall to connect to the collector pipes. The collector pipes extend various distances back into the reservoir to collect the sediment from areas of maximum deposition according to GIS-based surface models (Lim *et al.*, 2005) that can estimate sedimentation grid positions. The grid positions would be chosen within the lowest zones that would act as

sediment traps and could be defined via echosounding from the surface of the reservoir. In order to collect and transport the optimum amount of sediment from the basal surface of the reservoir in front of the dam, a specific slope with specific aspect ratio and alignment for both the pipes and channels should be designed to achieve sufficient flow velocity for efficient transport of water and sediments and to avoid blockages inside the channels and pipes. Pipe flows could also be affected by the compatibility of flow of both the transported sediment and the transporting water from the catchment area during floods. An excess generated/ outstanding payload of sediment during floods or an excessive sediment grain size could cause agglomeration and blockage of the pipes and channels. Thus the distance and slope of the pipe inlets from the dam would be important, as well as, considering the problem of suspended woody debris that would be avoided by placing the pipes on the bottom of the lake. Moreover, flow discharge would be controlled by auto-mechanical gates, installed on the exit side of the channels, according to the height of the water head.

The sediment sampling methodology at the study site was limited to the publically accessible margin of the reservoir by the Sydney Catchment Authority. Hence the sediment samples were collected from the reservoir to the northeast of Tallowa dam (where the public picnic area is located). A Yeo-Kal 615 multi-parameter water quality analyzer was used in the field area to measure water sample qualities in real time to test for pH, salinity and turbidity. In the laboratory each sample is tested for particle size by utilising the laser-diffractions Mastersizer 2000 particle size analyser. Part of each sample was dried and crushed in an agate mortar and pestle and analysed for heavy metal components using X-ray fluorescence (XRF; SPECTRO-analytical XEPOS instrument energy dispersive spectrometer fitted with a Si-docile detector; following the established standard procedure by Norrish & Chappel, 1977). Sediment and water sample sites are shown in Fig. 1c.

3.4 Results and discussion

3.4.1 Water quality analyses

Seven water samples were collected from the accessible margin of the reservoir (Fig. 3.1) and as the distance from the dam wall increased a gradual decrease occurred in pH, salinity and turbidity. This reflects the presence of more suspended sediment within the reservoir adjacent to the dam (Fig. 3.4).

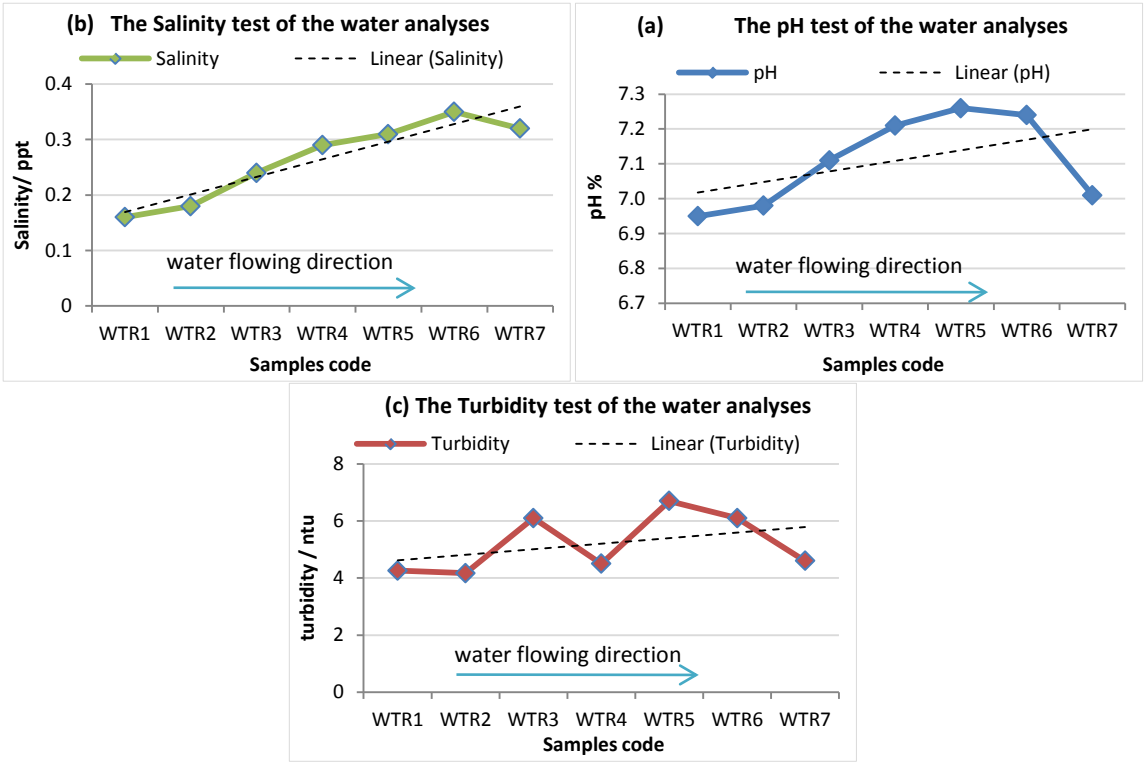

Figure 3-4. Water quality analyses of the seven water samples have shown an increase in; (a) pH, (b) salinity and (c) turbidity towards the dam.

3.4.2 Sedimentary analyses

Sediment samples have been collected at the same locations as the water quality tests, and they have been checked for their grain size. Figure 3.5 and Table 3.1 show that, the reservoir adjacent to Tallowa dam has a highly muddy basal surface. The average mud component is 58.5 % for all seven sediment samples, whereas, the sand comprises 41.5 % at an average depth of 1.30 m. This results in an average grain size of 121 µm (Table 3.1) with a medium-grained sand mode (400 µm) and a dominant silt mode (40 µm). However, difficulties of obtaining permission to access the reservoir site and the depth of the reservoir, has led to limited sampling work, so getting more accurate results need more field work and equipment.

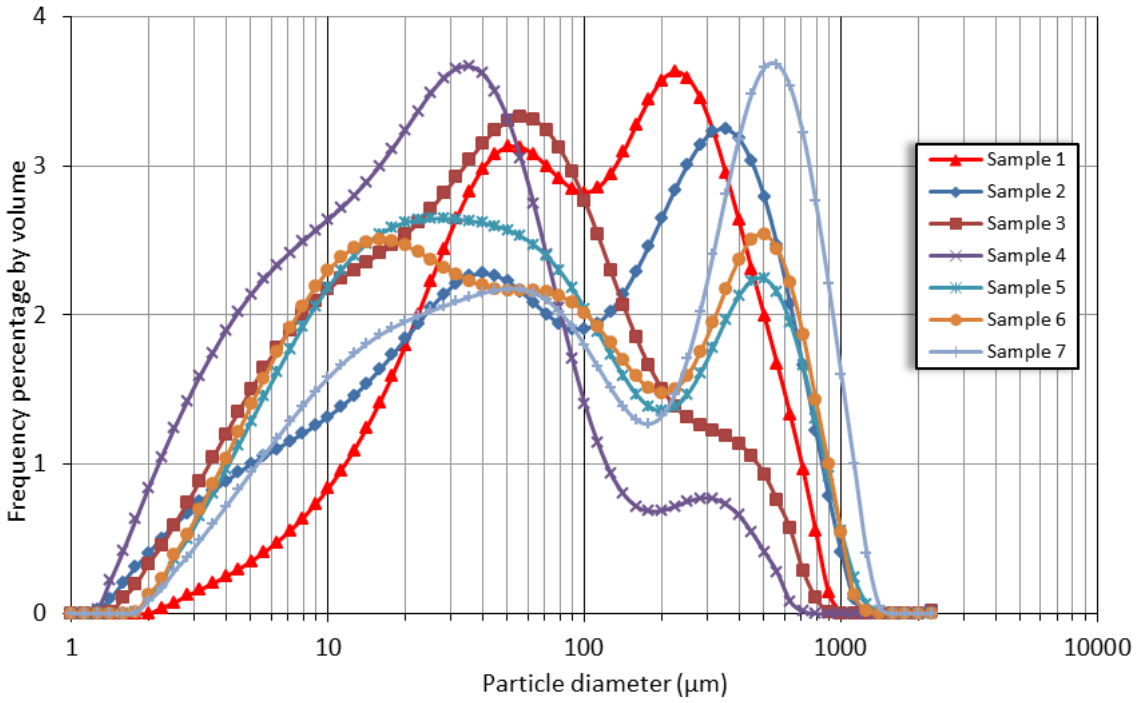

Figure 3-5. Grain size analyses of the seven sediment samples have shown that the accumulated sediment contains a large proportion of mud. The sediment samples have been taken from the northeastern bank near Tallowa Dam.

Table 3-1. Mean and modal grain size analyses and Loss on Ignition (LOI %) of the seven sediment samples from Tallowa dam showing the proportion of sand, silt and clay, and depth of the taken samples in metres.

Sample number	Water depth (m)	Vol. wt. mean grain size (µm)	Sand mode (µm)	Silt mode (µm)	Sand (%)	Silt (%)	Clay (%)	LOI (%)
1	0.83	121.2	225	50.2	53.4	45.1	1.5	8.4
2	1.41	174.1	356	38.01	54.5	40.2	5.3	15.5
3	1.80	81.7	-	56.4	35.4	59.1	5.6	9.6
4	1.36	48.6	281	35.6	18.4	70.5	11.1	12.3
5	1.27	115.1	502	28.3	37.4	56.5	6.1	24.5
6	1.31	122	495	15.9	40.2	53.2	6.5	31.9
7	1.13	186.3	544	51.8	51.4	44.1	4.5	5.0
Average	**1.30**	**121.3**	**401**	**39.5**	**41.5**	**52.7**	**5.8**	**15.3**

3.4.3 Assessment of trace elements

High mud components may lead to some water quality considerations for urban supplements, thus trace element XRF analysis was done on the seven sediment samples (Fig. 3.1). The concentrations of the trace elements Cr, Ni, Cu, Zn, As and Pb are directly related to the mud content in the sediment (Table 3.2) with the highest concentrations of these elements found in the samples 4, 5 and 6. These sites have the highest percentages of mud and organic matter, which are indicated by the proxies rubidium (Rb) and bromine (Br), respectively (Table 3.2).

Table 3-2. Comparison of trace elements (mg/kg) in the study area with Interim Sediment Quality Guideline values (Australian and New Zealand Environment Conservation Council [ANZECC] & National Health and Medical Research Council [NHMRC], 2000).*

Sample	Cr	Ni	Cu	Zn	As	Pb	Br	Rb
1	94	42	22	79	10	39	54	135
2	61	31	26	67	11	29	210	68
3	79	26	24	80	16	25	80	133
4	89	27	27	85	16	28	166	141
5	86	28	27	88	18	31	203	147
6	88	39	28	130	10	31	431	82
7	70	19	20	68	7	19	16	99
Mean±SD.	82±14	30±7	25±3	85±21	12±4	32±12	166±139	115±31
LSQG/Low	80	21	65	200	20	50	NA*	NA*
LSQG/High	370	52	270	410	70	220	NA*	NA*

*NA = not available.

Both muddy particles and organic matter commonly play significant roles in absorbing and accumulating trace elements (Fernandes *et al.*, 2011; Alyazichi *et al.*, 2015). The trace element concentrations were compared with the ANZECC & NHMRC (2000) sediment and water quality guidelines as shown in Table 3.2. This revealed whether the trace elements were at acceptable levels below the low trigger values or whether they exceeded that limit and needed more examination according to the national guidelines. Harmful biological effects or trace elements are periodically detected between the low and high values in the ANZECC & NHMRC (2008) guidelines (Alyazichi, 2015). According to Australian and New Zealand protocols (ANZECC & NHMRC), the mean concentrations of the analysed elements are below the LSQG/Low except for Cr and Ni where several samples are higher than LSQG/Low but well below LSQG/High. For example, sample 1 was taken from the shallow edge (83 cm depth) in a highly vegetated area with discharge points as well as recreational activities, which means more biotic and abiotic influences at this site that raised the contents of Cr, Ni, Zn and Pb.

3.4.4 Surface analyses and pipe grid placing

Analysing the contour map and digital elevation model (DEM) created using ArcGIS10.2 detected the location of the primary sediment pool areas, which represent the best locations for the pipe mouth grid (Fig. 3.6). This result could be confirmed using an echosound technique

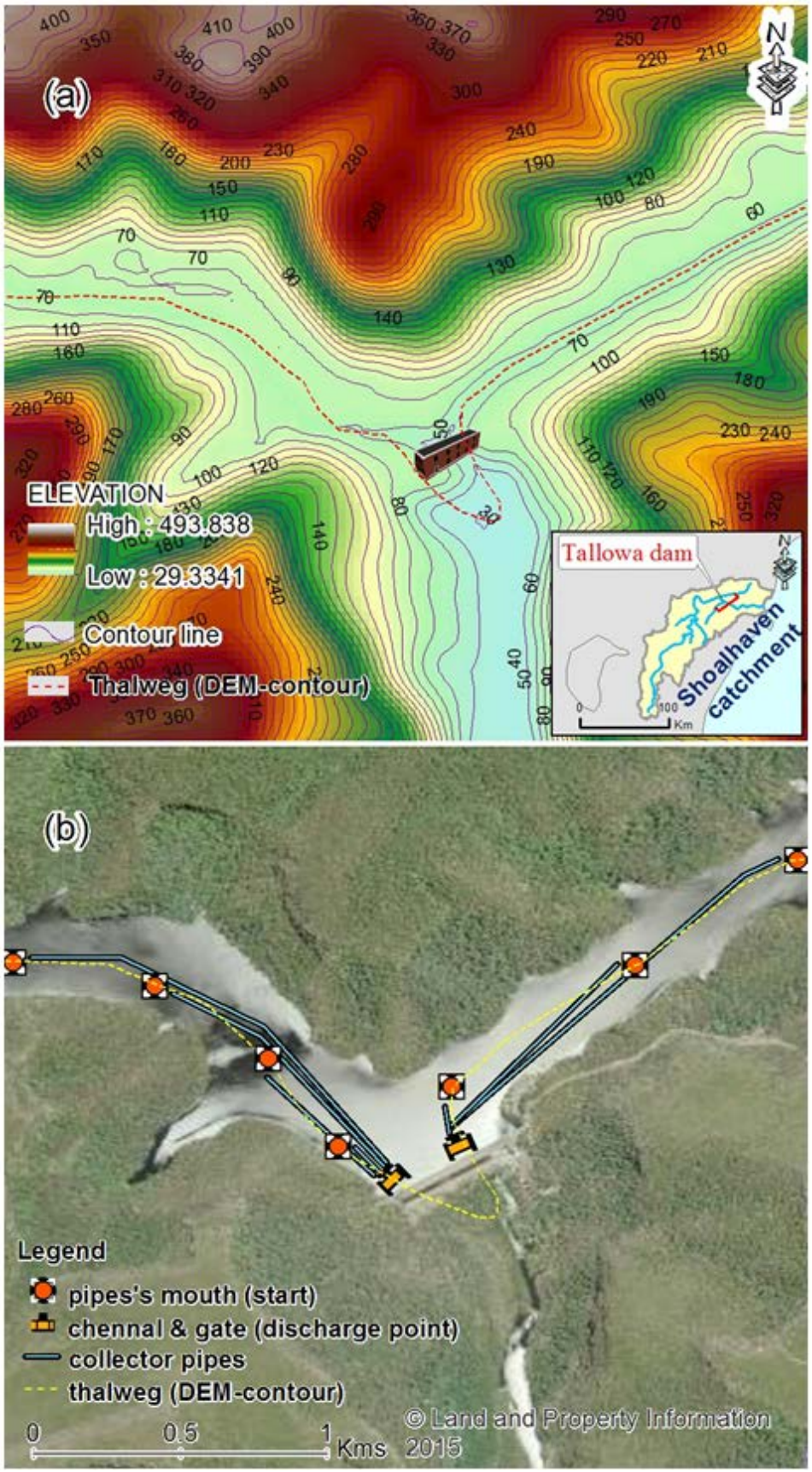

Figure 3-6. (a) The high slope shown on (a) the study site' contour lines and DEM, the thalweg line of the lake, overlying on the DEM and showing the elevation ranges (29-494 m) and the lowest line in the area, generated using data from Geoscience Australia © Commonwealth of Australia (2011), (b) suggested collection points to extract sediment and water through the pipes.

to get the exact subaqueous reservoir surface topography, and to find more accurate results for the locations of the sediment reservoirs. So far, it gives an average slope for the basal surface of the reservoir of 3.8°, which was derived from the DEM and contour surface analysis (Fig. 3.6).

A balance needs to be attained between stored water levels for urban consumption, and applying this proposed sediment bypass solution to sustain the water quality itself and the ecosystem below the dam (coastal section). Thus, these collector pipes need to have specially designed discharge channels and gates.

3.4.5 Designing the pipes and the controlling gates

The pipes need to have a specific slope designed so that they could be merged into a single channel at the dam wall. Then an auto-mechanical gate would control the water and outstanding payload released, as follows.

3.4.5.1 Water storage control gates

The water storage will be controlled by auto-mechanical gates. The auto-mechanical gate operation is illustrated in Fig. 3.7. The operation of these gates depends on the head pressure of the water level without the need for human-intervention. The head pressure affects the float that, if raised above the 31 m ideal storage level, will cause the gate to open until the water level is reduced back to 31 m. The gate is susceptible to the force of the water that depends on the density of the water (ρ), gravity (g) and the height of the water level as represented in equation 1 (Çengel *et al.*, 2010). A retiring spring could be used to assist the gate to return to the closed position.

$$F = \rho . g . A . h \qquad (1)$$

Where;

F= water force on the gate (Newton);

ρ = water density (1000 kg/m^3); A= gate area; and

h= relative height of water levels.

In addition, sustainable natural fibre reinforced composite materials could be used for the pipes and gates. These materials consist of two or more components, such as natural fibres and polymer matrix, in order to fabricate a new material with different characteristics from standard pipes. The characteristics and potential of these materials, such as high strength-weight ratio, renewable, recyclable and resistant to chemical effects (corrosion), make them more environmental friendly and an attractive ecological alternate to other materials (Fuqua *et al.*, 2012; Uddin, 2013).

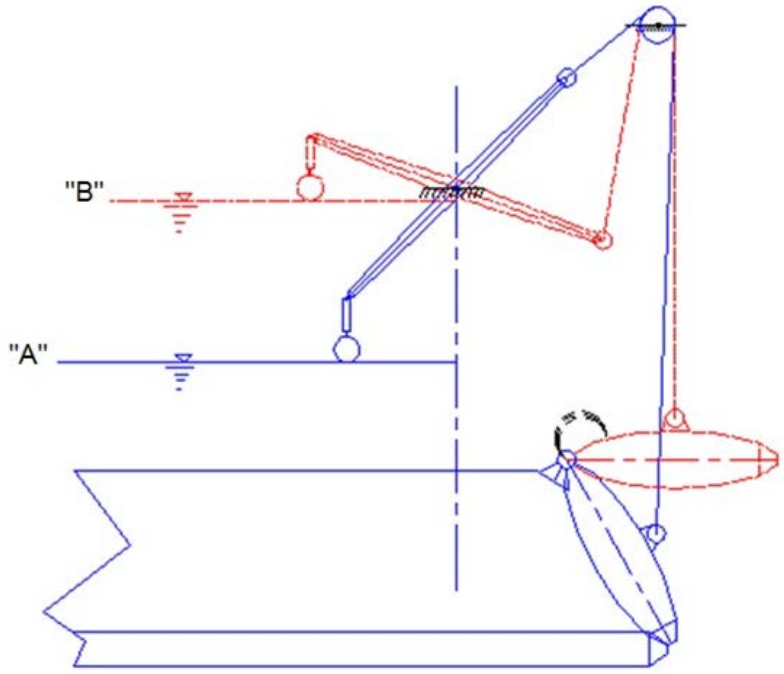

Figure 3-7. The designed auto mechanical gate operation method is shown with the bypass channel located through the base of the dam. The auto-mechanical gate controls water flow; at low water level "A" the gate is closed to save the water in the lake, whereas at high water level "B" the gate opens to allow the over-storage water to flow from the grid pipes through the gate to sustain ecosystems below the dam.

3.4.5.2 Effective slope for fluid transport

It is very important to find an effective and suitable slope and aspect ratio for the pipes and channels to allow sediment transportation. It is well known that the natural river catchment has variable slopes that influence rates of erosion and deposition. Accordingly, the rate of sediment transportation and the effective weight of the transported sediment and attached pollutants is one of the problems that could block this suggested system. The quantity and grain size of transported sediment is also affected by development in the catchment landscape. All this river-borne sediment enters the reservoir where the bedload is deposited as deltas and the suspended load can be transported in suspension throughout the reservoir. In order to control subsequent sediment transportation within and from the reservoir, and hence the effective size and weight of the sediment grains that can be moved, the slope of the transportation pipes and channels through the dam and the dimensions (aspect ratio of the pipes) should be specified.

There is a clear relationship between fluid flows and the entrainment and transport of sediment (Julien, 1998; Parker, 2007; Frey, 2014). In the past decades, bedload sediment movement in open channel flow has been investigated many times but most practical and theoretical work has been done under conditions of gentle or even horizontal channel slopes (Chien & Wan 1999; Cheng & Chen, 2014). Only limited studies on the calculation of sediment transport rates have been achieved (*et al.et al.et al.*Cheng & Chen, 2014). Fernandez Luque &

Van Beek (1976) have investigated the slope effect on the velocity of the sediment particles and transport rates.

The formula that is used widely for sediment transportation in channels based on experiments using sand and gravel was developed by Meyer-Peter & Müller in 1948, as below:

$$q_b = a(\frac{\tau_b^1}{(\rho s - \rho)gd} - \theta_{cr})^{3/2} \quad (2)$$

Then etymologically "α" is:

$$a = 8\sqrt{\left(\frac{p_s}{p-1}\right) gd^3} \quad (3)$$

Where q_b is the volumetric transport per unit bed width; d is the grain size of the sediment; r'_b is the bed shear stress; and θ_{cr} = 0.047 represents the dimensionless critical shear stress which also represents the Shields parameter.

Smart (1984) included bed shear stress and sediment sorting elements to derive the slope correction that is represented below:

$$M = \frac{c}{2\sqrt{g}} (\frac{d_{90}}{d_{30}})^{0.2} \left[S^{0,6}\sqrt{\frac{\theta}{\theta - \theta_{c\beta}}}\right]^2 \quad (4)$$

Where, C is the Chezy coefficient, d_{90} and d_{30} are the diameters of grains for which 90% and 30% of the sediment sample are finer, *S* is the channel slope, and $\vartheta_{c\beta}$ represents the critical Shields factor for primary motion of sediment within the horizontal-bed scenario (Cheng & Chen, 2014). However, Smart's equation is valid for downslope flow only.

Cheng & Chen (2014) reported that, to predict the sediment transport rate, Damgaard *et al.* (1997) developed the Meyer-Peter & Müller (1984) method by involving the following slope correction:

$$\text{For } \beta \geq 0 M = 1 \quad (5)$$

$$For \quad < 0 M = 1 + 0.8(\frac{\theta_{c0}}{\theta_{c\beta}})^{0.2}(\frac{1-\theta_{c0}}{\theta_{c\beta}})^{1.5+x} \quad (6)$$

Where;

$\vartheta_{c\beta}$ represents the reduced ϑ_{c0} and x = $\vartheta_{c\beta}/\vartheta_{c\beta}$.

All the previously used factors of slope correction are empirical, and they include different variables (Cheng & Chen, 2014).

$$\theta_{c\beta} = k\,\theta_{c0} \quad (7)$$

$$K = \frac{sin(\alpha-\beta)}{sin\,\alpha} \quad (8)$$

Cheng & Chen (2014) suggested a different procedure for slope correction to find out the slope influence on sediment transport using a uniform open channel. Sediment is considered to be entrained under both drag forces and lift forces, however, it is believed that the drag force is dominant while the lift force can be ignored. After using simple equilibrium equations, as shown in Fig. 3.8, the correction factor was:

$$\eta = cos\beta \, tan \, \alpha - sin \, \alpha \qquad (9)$$

where η is a slope correction factor, Δg is the reduced gravity of the submerged particle (i.e. effective particle weight/unit mass), $tan \, \alpha$ = coefficient of friction and β is the slope of the channel-bed. The force parallel to the surface of the bed F_D was written as:

$$F_D = \eta \, \Delta g \, \rho \, V_s \qquad (10)$$

$$\Delta = \frac{(\rho_s - \rho)}{\rho} \qquad (11)$$

where V_s is the volume of the particle; ρ_s = density of the particle; ρ = fluid density; and Δ is the relative density-difference.

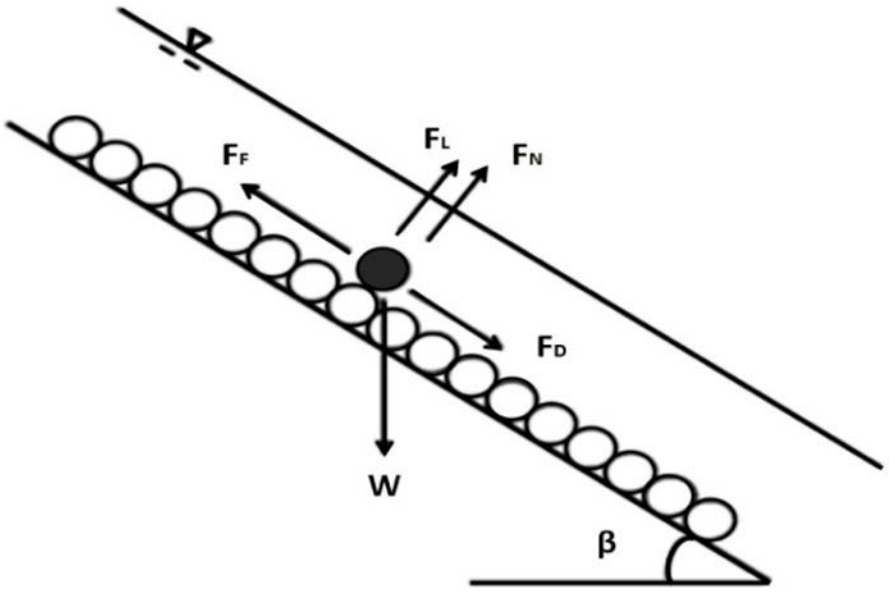

Figure 3-8. An open channel flow showing the forces acting on a moving particle: in the derivation, the lift-force has been ignored; (after Cheng & Chen, 2014).

For the proposed slope correction to be validated, experimental data were collected from the research of Fernandez Luque & Van Beek (1976), Damgaard *et al.* (1997) and Recking *et al.* (2008) for both closed and open channels. The experiments are detailed in Cheng & Chen (2014) as shown in Fig. 3.8 and could be applicable for the Tallowa Dam as a case study, by modifying this design from an open channel to a closed pipe.

Finally, this project has made a comparison between Cheng & Chen's (2014) study with other correction factors. In the study done by Cheng & Chen (2014) the proposed corrected slope factor was compared with Meyer-Peter & Müller (1948) because Fernandez Luque & Van Beek (1976), Damgaard *et al.* (1997) and Recking *et al.* (2008) all used the formula of Meyer-Peter & Muller (1948) to develop the slope correction formula. Therefore, only this earlier formula was employed for comparison purposes. However, the indication based on the formula of Meyer-Peter & Muller is practicable merely for shear stress more than the critical shear stress (Cheng & Chen, 2014). The proposed correction factor showed better agreement with experimental results compared to the previous studies.

Thus, Cheng & Chen's (2014) method (equation 9) provides the most suitable and applicable slope at the suggested take off points in this case study when it is extended for application to closed pipes. The water head pressure applies another drag force acting on the moving particles. The drag force from water head pressure is assumed to be equal to F_D. To determine the acting force on the particles from the water head pressure, Bernoulli's equation is adopted.

According to Bernoulli's equation, the force that results from the water head pressure that acts on the particles is:

$$Fw = ½\,\rho\, g\, L\, sin\beta\, v \qquad (12)$$

By combining equations 10, 11 and 12, the optimum slope of pipes that reduces particle accumulation is:

$$½\,\rho\, g\, L\, sin\beta\, v + \rho\, g\, v\, sin\beta = cos\beta\, tan\alpha\, 0.5\,\rho\, g\, v$$

Where tanα = 0.14 since the coefficient of friction is 14% for the proposed use of composite material (El-Sayed *et al.*, 1995) and L = pipe length 50 m (applicable to use a different length).

$$Then, \beta = tan^{-1}[0.07/\,(0.5 \times L + 1)]$$

$$\beta = 0.15 \text{ degrees.}$$

This means that the parameters (especially using the composite material at a 15 m water head pressure) have suggested a slope recommendation of 0.15° to use for the pipe grid. However, the reservoir slope is 3.8° allowing a higher pipe slope that could deal with mixed suspended and bedload sediment during floods and rain storms. Also, not all the reservoir is at the same depth, as the 15 m is an average depth, thus a comprehensive field investigation and equation replication is needed to establish the most suitable slope from each of the take-off points. The number of take-off points depends on the river twists and turns, thus this project suggests

take-off points should be in the middle of the reservoir approximately every 400 m in the twisted reaches, and 600 m in the less twisted reaches (Fig. 3.6). The collector pipes should have straight design, or arced if necessary, to minimise frictional resistance to the flow and prevent any sediment accumulation. Fig. 3.9 shows a diagrammatic view of these results.

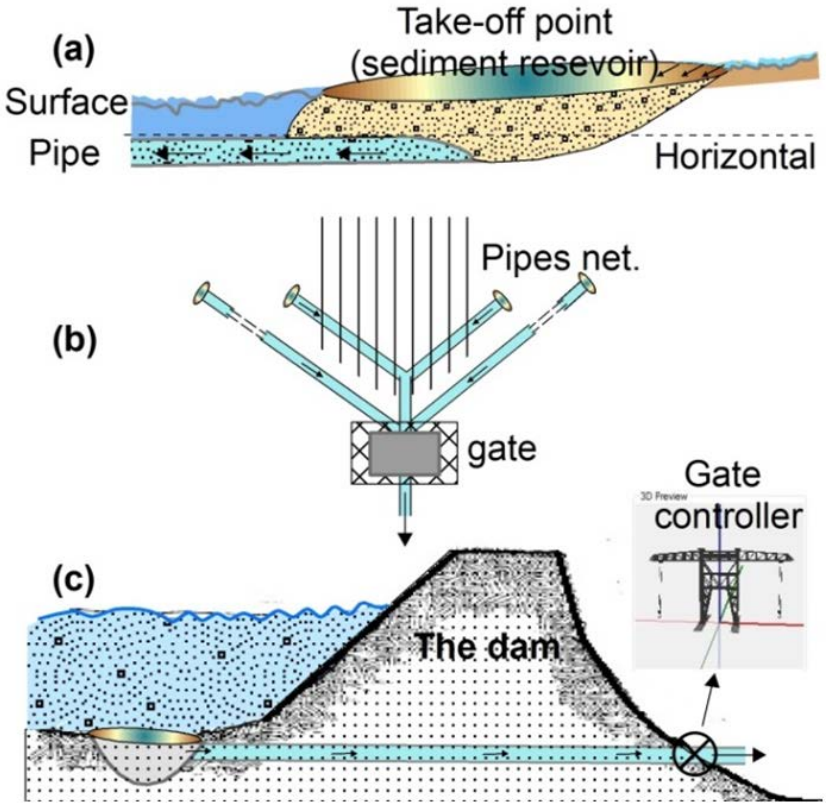

Figure 3-9. Showing; (a) sediment reservoir and the take-off points that link from the centre bottom of the reservoir, (b) the pipe network that could be combined together using same gate. (c) The gate collection and discharge points that are controlled by the gate controller.

This scheme should be instigated during the construction phase of a dam. It could possibly be retro-fitted to the Tallowa Dam, as well as other current dams worldwide. A retro-fit would cause more difficulties and cost more than instigating it during the construction phase of a dam.

3.5 Conclusions

In order to find a better sustainable solution for geomorphic ecosystems and water quality of dammed rivers, a case study has been chosen from the Shoalhaven River at Tallowa Dam, southeastern NSW, Australia.

The water discharge and suspended sediment, which have been blocked by the dam, have led to high sediment accumulation rates in the reservoir. Meanwhile, supplementary sediment problems have caused several eco-geomorphic threats in the downstream section of the river,

such as higher erosion rates and salinity intrusion. Analysing the existing situation of the dam's reservoir has proven that the water quality has been influenced by the increasing sediment accumulation, particularly with the deposition of mud particles that are more abundant than sand components (58.5% and 41.5%, respectively). That has increased the amount of chemical pollution, such as heavy metals and nutrients that has accumulated in the mud sequences, which may eventually affect the water users.

Civil-infrastructure design of a grid of collector pipes on the reservoir bottom could play an important role to minimise sediment quantity and enhance water quality providing a longer storage time in the Tallowa basin. The proposed grid of collector pipes from the reservoir should be considered in terms of eco-geomorphic sustainability. Spatial data analysis has been used to determine the best location of the pipes in the lowest zones of the reservoir. The equations of Cheng & Chen (2014) can be adapted and used to determine the slope and aspect ratio of the transportation channels for comparison with the subaqueous topography of the reservoir. Using sustainable natural fibre reinforced composite materials would be environmental friendly and an attractive ecological alternate material that could be applied when considering an integrated sustainable approach.

Chapter IV: A Spatio-Temporal Assessment of Landcover and Coastal Changes at Wandandian deltaic System

4.1 Abstract

Large numbers of people live along and depend upon the world's coastal resources. Human modifications of the coastal zone, in combination with climate induced environmental changes, have had a major effect on the natural ecological systems. GIS analysis of remote sensed data, combined with fieldwork and laboratory tests, can be used to determine the resultant eco-geomorphic changes that need to be managed sustainably on a worldwide scale. Modelling the eco-geomorphic dynamics between 1949 and 2016 on the Wandandian Creek delta (southeastern NSW, Australia) provides a case study of management options for such coastal resources. Results from the Wandandian Creek delta show that sand/silt sediment derived from the partially (22%) modified terrestrial catchment has prograded into the wave-dominated St Georges Basin where it is impacted by nearshore processes. Clear spatio-temporal growth of the areal extent and elevation of the deltaic levees and sandspits, with their associated mangroves and saltmarshes, has occurred over the past 65 years. Although the growth rate has fluctuated during the study period, due to flood events in 1974, 1990s and 2010, the overall subaerial and subaqueous delta area has had an average growth of 4168 m^2 annually with the shoreline extending 1.451 m/year on average. This geomorphic growth has stabilised the estuarine deltaic habitats with high proportions of nutrients and organic matter, particularly within saltmarsh, mangrove, *Casuarina*/*Juncus* and other mixed native plant areas. This research shows the importance of analysing morphological changes observed on the delta that can be related to both anthropogenic modifications and natural processes to the catchment and thus should be used in the development of catchment and coastal management plans.

Keywords: *anthropogenic modifications; eco-geomorphology; remote sensing; GIS-modelling; sediment progradation.*

4.2 Introduction

Many coastal ecosystem management strategies have become more focused on the conservation and sustainability of coastal wetlands (Aarts & Nienhuis, 1999; Day *et al.*, 2008)

locally (Al-Nasrawi *et al.*, 2015b, 2016b, 2017b), regionally (Akumu *et al.*, 2010) and globally (Kirkpatrick, 2012) according to their unique ecosystem function roles (Costanza *et al.*, 2008). However, they are located in sensitive zones where anthropogenic and climate change stressors are concentrated, such as estuaries and deltaic platforms (Ehrenfeld, 2000; Morris *et al.*, 2002; Lee *et al.*, 2006). For effective management of such areas it is imperative that comprehensive knowledge of their environmental responses to current anthropogenic and climatic stressors is known, along with the factors that have driven such responses within the last few decades, to enable prediction of their future behaviour.

One of the most cost effective methods of studying changes in coastal ecosystems is through geographic information system (GIS) analysis of aerial photograph and satellite images (Kirkpatrick, 2012; Costanza *et al.*, 2008; Ozesmi & Bauer, 2002; Cho *et al.*, 2004). Ozesmi & Bauer (2002) provided an overview of the most appropriate satellite data and classification methods to use for studying wetlands. They also discussed how complimentary information could be obtained from aerial photographs, thus providing the opportunity to extend equivalent analyses back before satellite data became available to study longer term changes to wetland composition and shoreline positions. Some studies have relied entirely on satellite data, such as the study by Cho *et al.* (2004) who successfully mapped wetland and shoreline changes on a broad scale in southeastern India. The same techniques have been applied when mapping vegetation and shoreline changes in inland wetland situations, such as study of Haack (1996) of the distribution and dynamic nature of small isolated wetlands in the plains and highlands of Kenya and Tanzania, and Roshier & Rumbachs' (2004) mapping of temporary wetlands in the arid areas of the Darling River basin in eastern Australia. The success of these studies led us to instigate a case study modelling the current and historic coastal ecosystem dynamics on the Wandandian delta (St Georges Basin, southeastern Australia) as a method for providing data to assist in developing local catchment and coastal management plans.

The aim of this study is to use the Wandandian delta as a case study to monitor and measure sensitive shoreline, land cover and vegetation changes in a deltaic system and its associated coastal wetland in order to assess potential options for conserving and managing the wetlands. This study (i) employs spatial technologies to determine the ecological and geomorphological (eco-geomorphic) growth of the estuarine system within the last few decades, (ii) considers the direct and indirect influences of anthropogenic and environmental trends on the catchment runoff and sedimentation factors, (iii) assesses the historical eco-geomorphic trends to determine the main factors likely to affect the future ecosystem health, and then (iv) indicates how these findings could be extended to other estuarine deltaic regimes and important coastal wetlands worldwide. This work is relevant to management because it

indicates how susceptible the estuary is to shoreline expansion or contraction, which causes changes in ecosystem accommodation space as a function of sediment transport and deposition from the catchment.

4.2.1 Background

The Wandandian deltaic eco-geomorphic system is located on the southeastern coast of New South Wales (35°06'23.4" S 150°33'20.5" E), about 194 km south of Sydney (Fig. 4.1). The coastal eco-geomorphic system of the Wandandian delta is located at the end of Wandandian Creek where the channel is actively prograding into St Georges Basin (Fig. 4.1) that is separated from the South Pacific Ocean by a sandy barrier (Murray *et al.*, 2005). The shallow St Georges Basin has rock outcrops that control where the Wandandian fluvial sediment can accumulate and build the deltaic system over time (Hopley, 2004; Hopley & Jones, 2006).

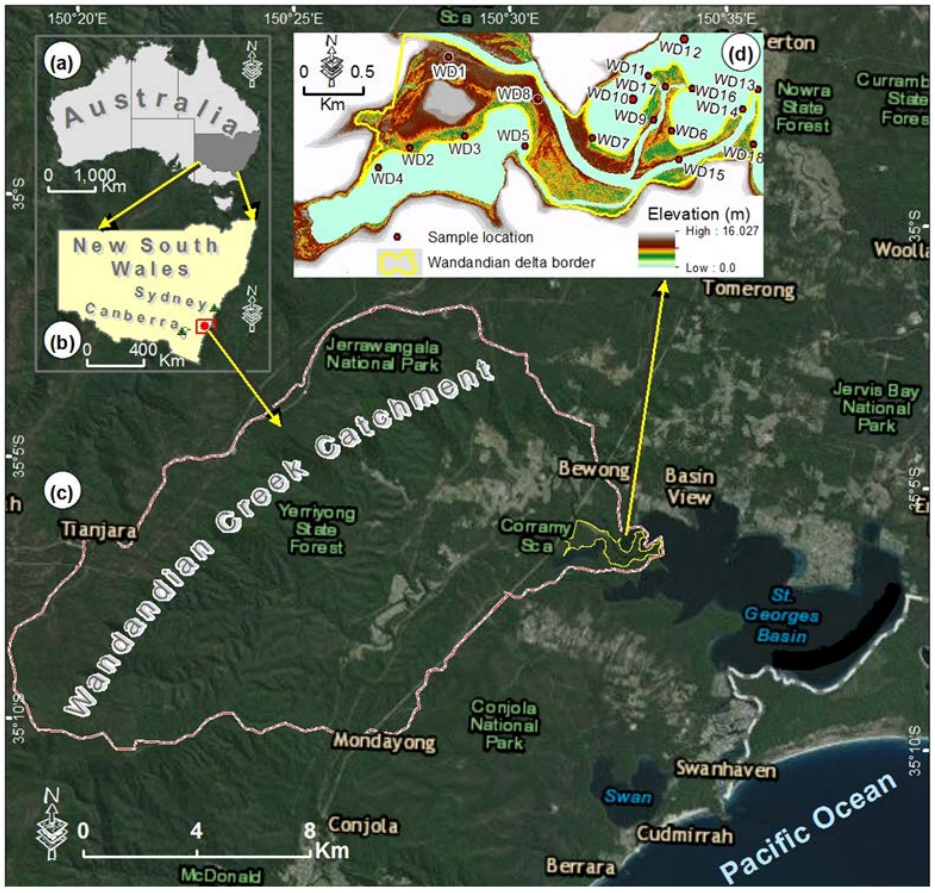

Figure 4-1. The study site, of the coastal deltaic section of Wandandian Creek, southeast NSW, Australia, illustrating; (a) location of New South Wales (NSW) in eastern Australia, (b) the study site located on the mid-southern NSW coast, (c) the regional setting showing the St Georges Basin and the catchment area of Wandandian Creek, and (d) illustrates the deltaic border, elevation and the sampling locations (WD1 to WD18).

The Wandandian eco-geomorphic system has been considered as a sensitive area that includes (i) fluvial platforms, and (ii) intensive vegetation cover, such as mangroves and *Casuarina*

(Shoalhaven City Council, 1998; ALUM, 2010).

Wandandian Creek is 25 km long starting from the eastern cliffs of the Tianjara Range (part of east Australian Great Dividing Range) to indirectly discharge to the southern Pacific Ocean via St George Basin, a typical wave dominated estuarine platform (Roy *et al.*, 2001; Hopley, 2004). The 1.6 m deep Wandandian Creek drains about 46% of St Georges Basin catchment (Windley, 1986). The deltaic system built by the Wandandian Creek sedimentary processes contains small areas of coastal wetlands (including mangrove, saltmarsh and back swamp) and intertidal flats on a fluvial bayhead delta (Hopley & Jones, 2006).

4.2.2 Catchment and land use classes

Wandandian Creek has a small catchment draining about 202.3 km^2 ranging from high to irregularly sloped terrain with elevations from 0 to 709 m along the ~25 km long Wandandian Creek. This represents an average 3.5% slope along the main creek channel, but the slope is much higher in the upper parts of the valleys (Fig. 4.2a; Murray *et al.*, 2005). The Wandandian Creek catchment contains the Wandandian, Bewong, Tullarwalla and Jerrawangala villages that are neighboured by quite intensive rural activities (Hopley, 2004). This region has a population of about 15,000 (Murray *et al.*, 2005; Australian Bureau of Statistics, 2017) but this will increase as urban development expands (Murray *et al.*, 2005). St Georges Basin is a popular holiday destination known for its recreational activities such as sightseeing, bushwalking, fishing, water skiing and sailing.

Human settlement in the catchment began in 1830 and by 1900 had established grazing, urban areas and other modifications over 22% of the catchment (see Fig. 4.2b). These transitions in land use were associated with clearing native vegetation, resulting in changes to the drainage network hydrology and eco-geomorphologic characteristics of the catchment and its runoff and sedimentary processes (Al-Nasrawi *et al.*, 2016a; Al-Nasrawi *et al.*, 2016b). Large areas of the catchment are still covered with native vegetation (74.2%) including a state forest and a national park along the eastern cliffs of the Tianjara Range (Fig. 4.2). Early land clearing affected the eco-geomorphic systems in the lower catchment and its dependent downstream areas but during the study period has only included minor additional urban development (Fig. 4.2). Sand mining operations for construction materials in the late 1960s through to the early 1970s in the lower deltaic reach of Wandandian Creek increased water depths and affect sedimentation rates for over a decade. The dredging also opened the creek to recreational users and wake waves enhanced bank erosion.

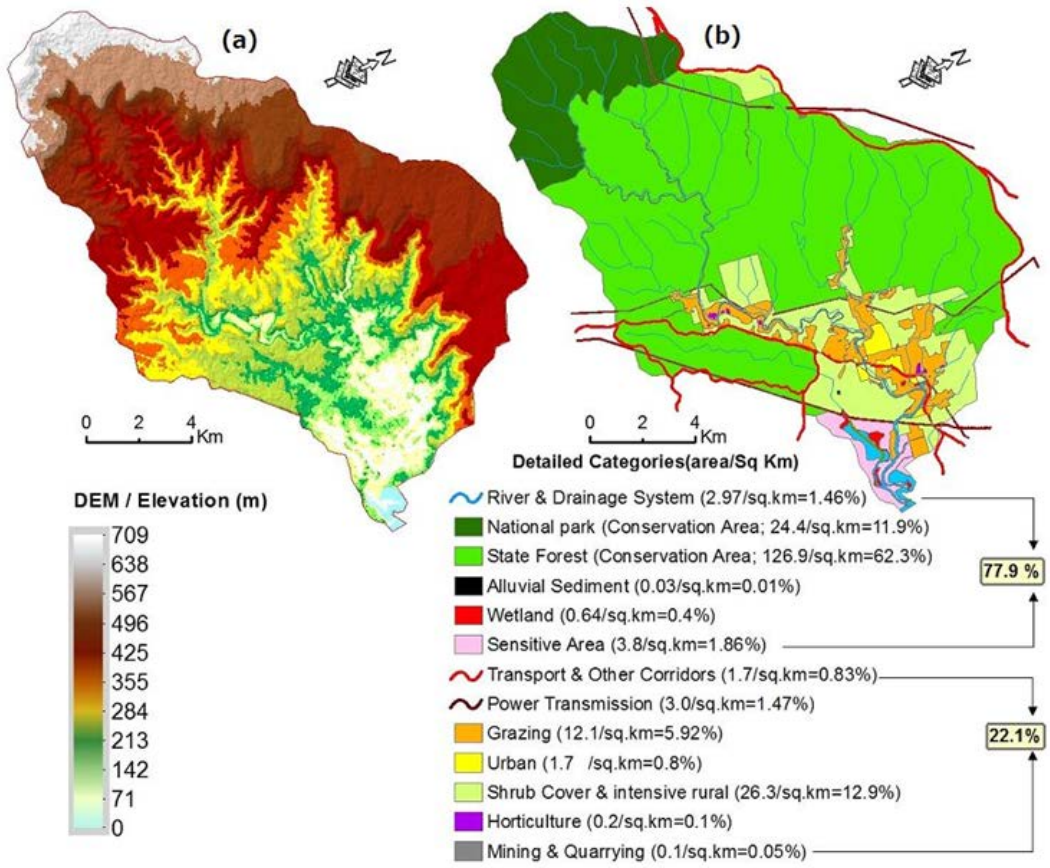

Figure 4-2. Landcover elevation and patterns within Wandandian Creek catchment area, showing; (a) the elevation of the catchment illustrating the terrain and high sloped watershed (using Australian height vertical datum at 1.024 m MSL), the 1-metre digital elevation model (DEM) is derived from C3 LiDAR (Light Detection and Ranging) obtained by LPI on 19 September 2016 (LP-DAAC, 2017). (b) Land use classes and areas (km^2). Source; (after; Hopley, 2004; Shoalhaven City Council, 1998; ALUM, 2010; LP-DAAC, 2017).

4.2.3 Local climate conditions

The main climate factors that could have major effects on the eco-geomorphic processes are precipitation (and the resultant river discharge in the Wandandian watershed area), temperature and mean sea level at/around the deltaic system (Figs 4.3 and 4.4).

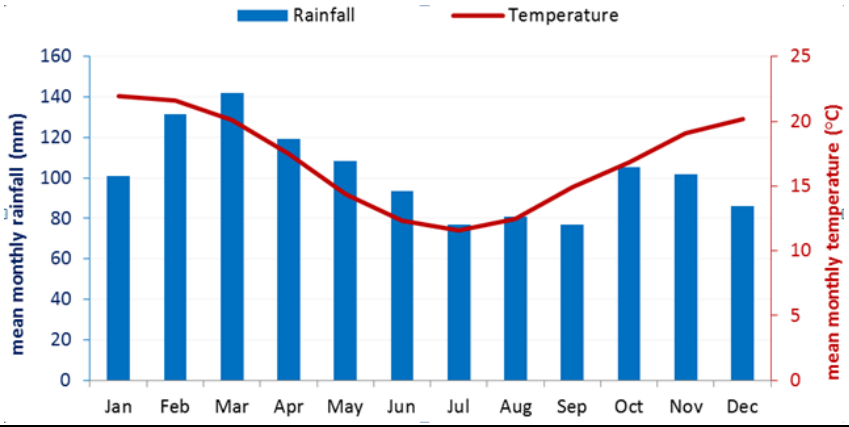

Figure 4-3. Monthly data for temperature and precipitation for Wandandian area during this study period show that the highest seasonal temperature occurs during the south hemisphere summer, particularly in January and February. At the same time, February and March are the wettest months in the records (BOM, 2017b; KNMI, 2017).

Wandandian catchment has a temperate oceanic climate (Cfb) with no dry season (Bureau of Meteorology, 2017b), which promotes weathering and sediment production (Mkpenie *et al.*, 2007). The average temperatures range from 11.5 °C in winter (July and August) to 21 °C during summer (January and February; data from Sussex Inlet Bowling Club gauging station; Fig. 4.3; (Hopley, 2004). Rainfall in the Wandandian catchment is highest in late summer and autumn, whereas the lowest rainfall occurs in late winter and spring (Bradshaw, 1987; Hopley, 2004).

Average rainfall in the Wandandian catchment is 1300 mm/year leading to an estimated annual runoff of 400 mm (Hopley & Jones, 2006). Five major flood events between 1985 and 2015 have been identified within the Wandandian catchment (Fig. 4.4a,b). They occurred in March 1959, October 1959, February 1971, June 1991 and August 2015. Nine additional minor flood events occurred in May 1953, February 1958, March 1961, March 1975, March 1976, October 1976, February 1992, September 1993, April 1994, March 2011, March 2012 and June 2013 (Fig. 4.4a,b); (BOM, 2017; Webb McKeown & Associates, 2001; BOM-NSW Weather, 2017).

In terms of climate change at the study site, temperature and sea level are slowly rising (Fig. 4.4c,d), which reflects the global warming trend (Day *et al.et al.*, 2008; Hughes, 2003). Air temperature shows a clear overall increase during the last five decades, with numerous fluctuations. The increasing temperature would affect sedimentological processes and plant productivity, which logically would have an effect on the eco-geomorphic system.

The reported local mean sea level rise (MSLR; Fig. 4.4d) is caused by global warming and climate change (Hughes, 2003; Day *et al.*, 2008). It is based on mean water level relative to the nearest local tide gauging station at Port Kembla, which is located ~45 km away but has an observation record extending from 1957 to recent (BOM-NSW, 2017).

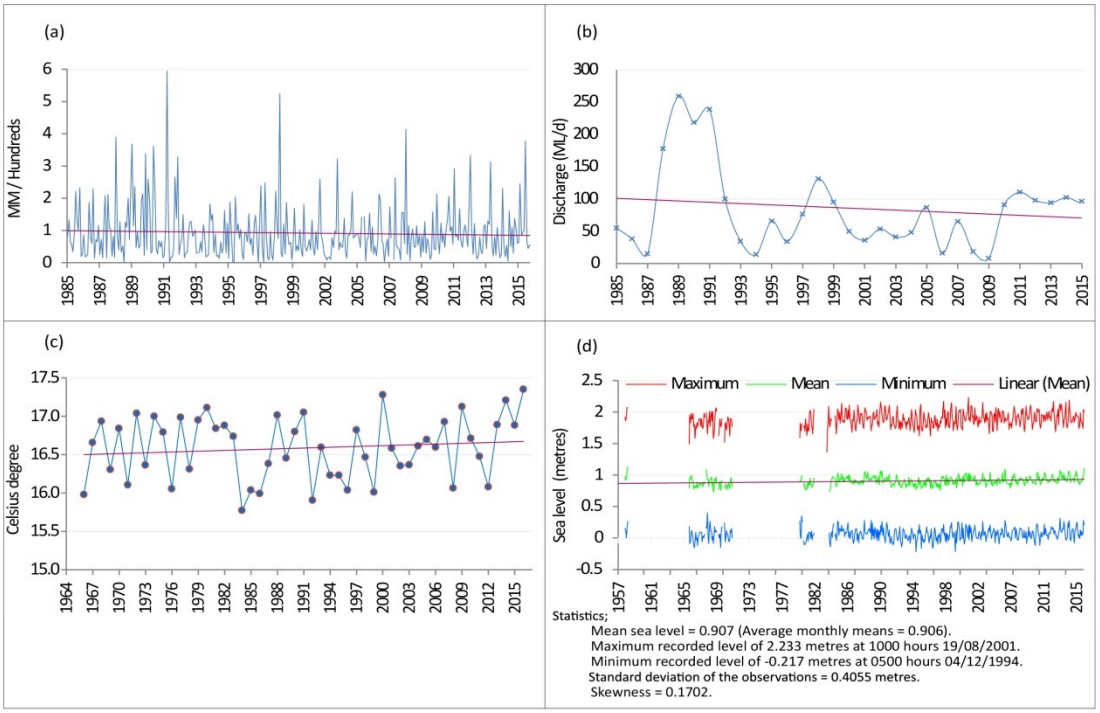

Figure 4-4. Climate trends for Wandandian Creek estuary; (a) the total monthly precipitation, (b) annual flow discharge in Wandandian Creek, (c) mean annual air temperature, and (d) monthly mean sea level at Port Kembla (1957 to 2016; red is the maximum, green is the mean, and blue is the minimum). Sources BOM (2017) and KINMI climate explore.

Analysis of monthly data from this gauging station is based on 60 years' time-series of sea-level measurements from 1957 to 2016. Fig. 4.4d clearly shows that sea level at Port Kembla has fluctuated and risen. The monthly average mean sea level at Port Kembla is 0.907 m, and the maximum recorded was 2.233 m on 19 August 2001, whereas, the minimum recorded was on 4 December 1994 at −0.217 m. The overall average trend of SLR at Port Kembla is 0.035 m from 0.895 to 0.930 m during last six decades.

The channel linking St Georges Basin to the open ocean is restricted and the basin has a much reduced tidal range and an elevated water level of about 1.23 m AHD (data from Island Point Station 216415 in northern St Georges Basin). This means water level fluctuations within St Georges Basin have less influence than in other coastal examples since there is very little tidal influence coming into this large basin with restricted connection to the Pacific Ocean. Thus, water flows from Wandandian Creek will always be attenuated as they enter the basin giving rise to more sediment deposition opportunities on the delta that can develop habitat accommodation and ecosystem diversity. Sea level rise is still likely to influence the basin and can be used to assess the eco-geomorphic changes, such as shoreline dynamics and coastal wetland responses.

4.3 Material and Methods

This chapter is based on a GIS mapping, monitoring and modelling has been used to investigate the landcover classes dynamics, shoreline movement, sedimentation rates and the general deltaic progradation based on local literature, aerial photography, and satellite imagery. The GIS analysis was supported by previous investigations of vegetation, sediment sampling, particle size, X-ray diffraction (XRD), loss on ignition (LOI) and water quality analyses (Hopley & Jones, 2006). This study divided the methodology into three parts, as seen in Fig. 4.5.

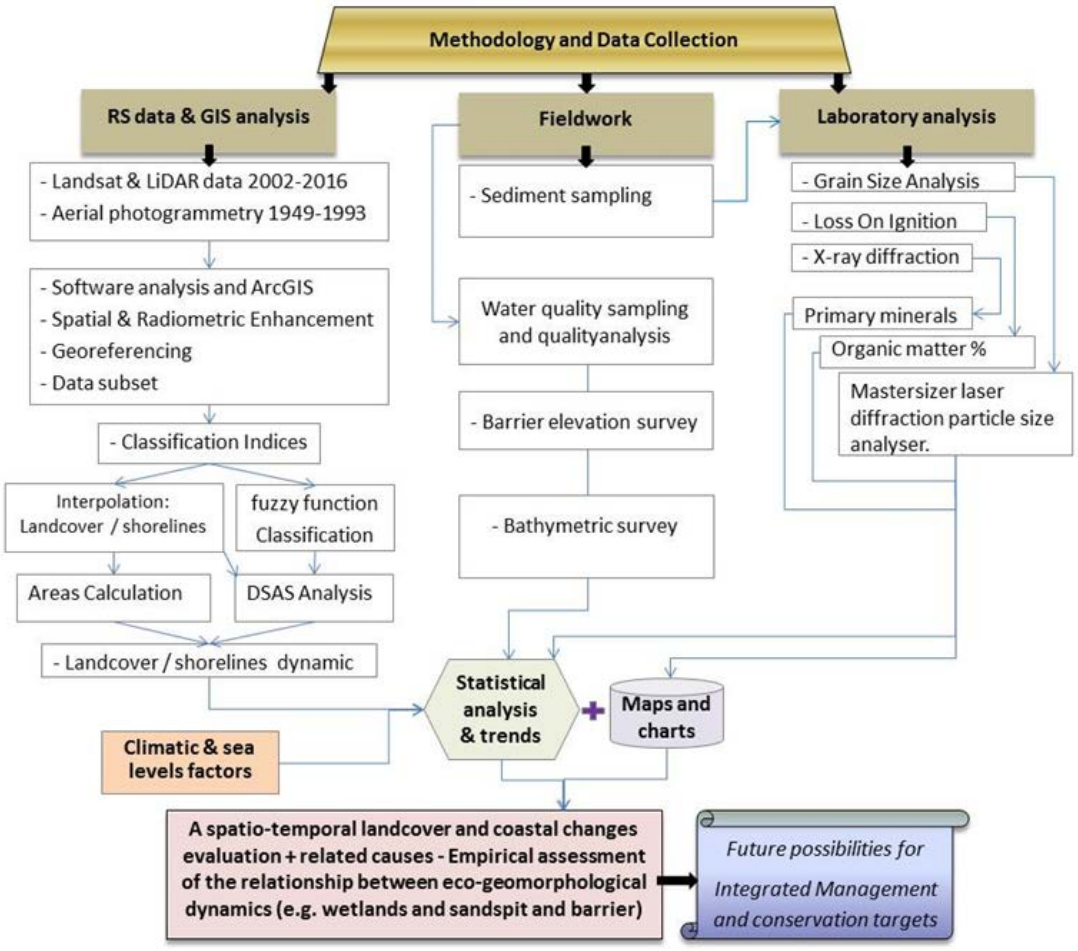

Figure 4-5. Methodology; data collection and analysis sequences.

4.3.1 Data Collection and processing

Various data have been collected to achieve the study aims. RS and GIS datasets were used to analysis land covers. Light Detection and Ranging (LiDAR; 2004 and 2010) and SRTM (2011) data have been used in ArcGIS to create DEMs. These survey data for the Wandandian area were provided by the Department of Land and Property Information (LPI) in NSW. These data record the surface elevation as heights (Z values) relative to a local zero level datum. The data also incorporated the actual local mean sea level at the time of the survey based on the

tidal/time dynamics from the local ground base-stations at the Sussex Inlet Bowling Club and the Island Point Station in St Georges Basin. The DEM was generated using a TIN and the contour spatial analyst tools in ArcGIS. Meanwhile, aerial photography was obtained from the LPI and the landsat satellite imagery from the USGS (https://earthexplorer.usgs.gov/).

Sediment and soil samples were collected as vibracores from the Wandandian delta (Fig. 4.1) to represent all the recognized sedimentary facies (Hopley & Jones, 2006). Surface material was subsampled and analysed for grain size, mineralogy (using X-ray diffraction; XRD, Panalytical, Almelo, Holland) and organic matter (by loss on ignition; LOI, Ceramic Engineering, Sydney, Australia) to categorise each facies. The pH, conductivity, dissolved oxygen, salinity and turbidity were measured in the field using a Yeo-Kal 615 multi-parameter water quality analyser. These data were combined with previous detailed stratigraphic data from the vibracores (Hopley & Jones, 2006).

A collection of remote sensing datasets and GIS analytic tools were utilised in assessing the landcover dynamics at the landscape scale from 1949 to 2016. The multitemporal imagery classification of Landsat data has enough detail to capture the eco-geomorphic distribution and dynamics of deltas and estuaries at the landscape level (Giri *et al.* 2011). However, small patches (< 900–2700 m2) of classes along a small coastal estuary cannot be identified from these data (FAO 2003). Thus, Landsat datasets have been combined with high-resolution (50 cm) satellite remote sensing datasets from LPI and aerial photographs, to assess and monitor the Wandandian site. A Digital Elevation Model (DEM) was created by analysing LiDAR (2010) point cloud dataset in ArcGis10.2. Kriging, clipping and masking were also used in ArcGis10.2 to incorporate the resultant fieldwork/laboratory analyses. Meanwhile, regarding the photogrammetry to shoreline digitising, higher resolution historical aerial photogrammetry of the Wandandian deltaic eco-geomorphic system was used to model the spatial and temporal dynamism. ERDAS IMAGEN v2014 software was used to orthorectify the digitised aerial photographs, with at least six to ten points as ground-control distributed around the estuarine area on each image to define the estuarine eco-geomorphic systems. If carried out carefully, the image-to-image techniques give accurate correlation of spatial features over time (Hughes *et al.* 2006; Hopley & Jones, 2006; Al-Nasrawi *et al.* 2017b, 2018a). Finally, catchment land cover classes were obtained from the Australian Land Use and Management authority (ALUM).

4.3.2 Data Analysis

All images were rectified by using 20 training points within an average of 15 to 25 pixels as a finger print; this has been done for each class in every single satellite tail. We used the pixel to

pixel validation method using an existing vector based classification of this study site provided by LPI in 2014. The vector layer was then converted to a raster and the ERDAS IMAGINE validation tool was run to test our results, which showed high accuracy.

Assessment and measurement are based on the land cover derived from aerial photographs (1949, 1961, 1972, and 1993) and satellite images (2002 and 2016) over time using the standard self-adaptive/minimum distance-adjustment combined with the fuzzy membership function. The fuzzy classification method distinguishes the spatial features on the imagery according to fuzzy rules about the pixels membership functions to give more reliable and realistic outputs. Simultaneously, it will not allow pixels to be incomplete-members of multiple classes, which could lead to ambiguous/uncertain assignation of the resultant classes (BOM-NSW/Tide Gauge Metadata; Hofmann, 2016; Foody & Cox, 1994). Analysis of the shoreline has determined the progradation of Wandandian deltaic system. Changes to the levees and shorelines and their associated wetlands, including mangrove and saltmarsh areas (as a land cover function), illustrate the shoreline position and elevation stability in the area. This project entails assessing potential threats, such as shoreline erosion and sediment delivery problems. In addition, the effects of artificial modification in the catchment are the principle element addressed.

The project targets are achieved at several levels, starting with GIS and RS-based analysis to identify and classify the land cover and shoreline changes at specific study sites depending on recent and historical records of aerial photography, satellite and LiDAR data. This was combined with sampling the water, soil and sediment.

Pre-processing of the employed imagery and aerial photographs was done to produce radiometrically and geometrically rectified framework parameters, including the local coordinate system and datum (GDA-MGA-1994/zone 56), atmospheric issues, and pixel size. To analyse datasets with various resolutions and to make the multi-temporal data comparable for valid use in research, this research has scaled the pixel sizes to a uniform spacing and converted the imagery pixels to the same scale as the resolution of the aerial photographs to assure common pixel extents, which resulted in errors of ±0.0125 to ±0.0375 m. As part of the standard procedure, statistical weighting was used to cope with rescaling to a common pixel spacing and to accommodate images across multiple dates. During this rescaling some neighbourhood weighting is needed to make sure that the output values are radiometrically equivalent, rather than visually smooth.

To analyse shoreline changes, the Digital Shoreline Analysis System (DSAS) was used on the dynamic shoreline positions of the delta (after dividing them into sections a–f; see Fig. 4.10) derived from the employed datasets between 1949 and 2016. The DSAS also quantified the

rate of deltaic progradation over a 66-year period (Fig. 4.10). The DSAS analysis used many transects sampled along shorelines at 50 m intervals from an offshore baseline around the deltaic facies and levees (Fig. 4.10a–f). To calculate the rates of shoreline changes over the study period, two statistical methods were used: the net shoreline movement (NSM)/envelope to track the changes, and the linear regression rate (LRR) to evaluate the results (Thieler *et al.*, 2009; Tran Thi *et al.*, 2014).

4.4 Results

A spatiotemporal deltaic dynamic evaluation has been established, using a stratigraphic description derived from remote sensing datasets, GIS analyses and fieldwork sampling, to highlight the deltaic changes including shoreline erosion/accretion rates and landcover change (e.g., vegetation canopy). Eco-geomorphic changes to the Wandandian delta were detected using ArcGIS, digital shoreline analyses system (DSAS) and geomorphic change detection (GCD) based on aerial photography and satellite imagery. These changes were related to most effective controlling factors through sedimentology analyses and catchment assessment. Thus, a three level simulation approach for evaluation of the Wandandian deltaic system was based on geochronological data at the landscape scale.

The coastal eco-geomorphic changes, caused by deltaic progradation and land use development have resulted in expansion of the Wandandian deltaic eco-geomorphic systems, including growth and establishment of saltmarsh, mangrove and mudflat shorelines (Figs 4.6 and 4.7).

4.4.1 Multitemporal imagery classification

The multitemporal analysis of remote sensing and GIS data (Fig. 4.6) indicates that the river channel has actively prograded moving sediment brought down from the catchment to the mouth of the delta. This has built an interesting deltaic system at the Wandandian Creek mouth, which has grown geomorphologically since at least 1949 to offer suitable ecosystem habitats for wetland colonisation. In addition, there is clear evidence of landcover development on the main deltaic platform since the 1940s (Fig. 4.6).

The Wandandian delta is under constant eco-geomorphic growth due to both natural (e.g., weathering/erosion, deposition) and indirect anthropogenic forces (including human activities, climate change and sea level rise). During the Holocene, the Wandandian delta started to infill and prograde into the western part of St Georges Basin (Hopley, 2004; Hopley & Jones, 2006) with more accommodation space being generated during the current sea level rise (Fig. 4.6

shown in red and pink).

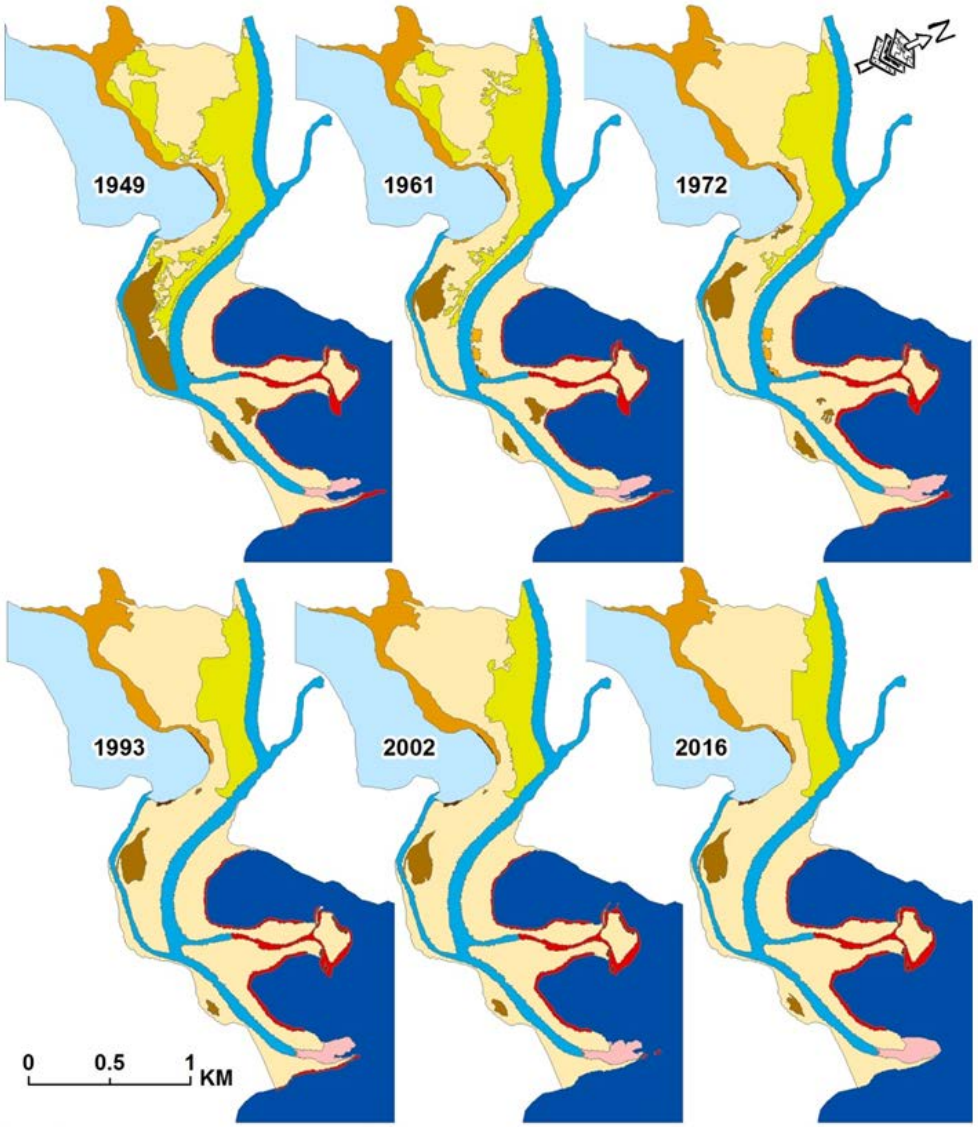

Figure 4-6. Multi-temporal high resolution aerial photograph classifications for 1949, 1961, 1972, 1993, 2002 and 2016 show progressive changes of Wandandian deltaic landform classes and shorelines. The clearest changes have occurred on the levee and backswamp facies where increasing native and mixed vegetation canopy indicates progressive eco-geomorphic stability. Prograded sand and silt bars have grown since 1949 and added more geomorphic accommodation habitat, thus allowing ecological development to continue.

Geomorphic development has led to ecosystem expansion onto sensitive deltaic areas as shown by the landuse classes (Fig. 4.6). Growth of the Wandandian deltaic eco-geomorphic system of vegetation canopy and deltaic facies is due to the protected ecosystem allowing sediment accumulation. This has resulted in the active channel levees prograding into St Georges Basin (Fig. 4.7) with elevations up to 1.5 m above water level (Hopley, 2004). Vegetation canopy growth has played an important role in stabilising and expediting the shoreline/levee expansion and vertical accretion (Fig. 4.7).

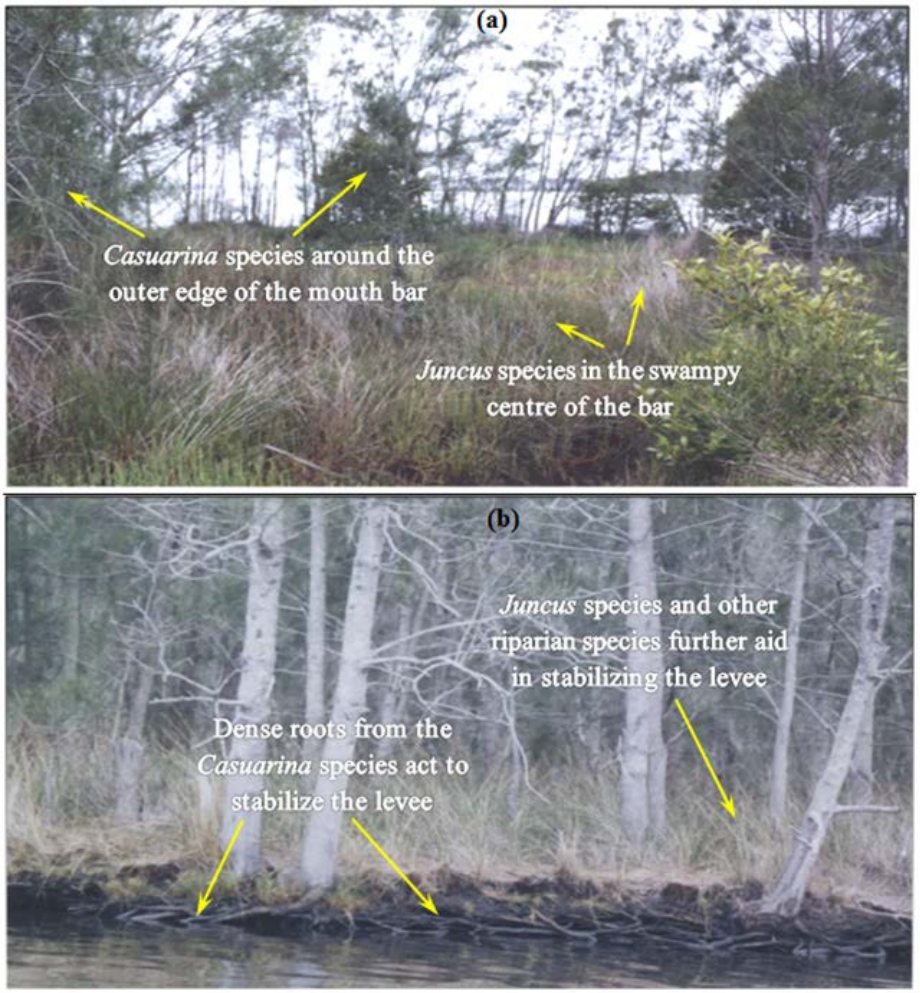

Figure 4-7. Vegetation canopy acting positively to assist the geomorphic growth and to develop the deltaic ecosystem; (a) *Casuarina* has vegetated the outer edge of the subaerial portion of the mouth bar whereas the depressed swampy portion in the centre of the bar is dominated by *Juncus*. (b) *Casuarina* and *Juncus* stabilising and expediting vertical accretion of the subaerial portions of the Wandandian Creek delta (levees and mouth bars; after, Hopley, 2004).

Charcoal in the basal fraction of the palaeoswamp facies suggests that at the time of deposition relatively frequent fire events occurred in the area (Hopley, 2004; Hopley & Jones., 2006). Growth of levees and delta front facies have become suitable habitats for new ecosystems, including; mangrove and saltmarsh, as well as the native plants such as *Casuarina*, eucalypts and *Juncus*, which have continued to stabilise the estuarine deltaic ecosystem (Fig. 4.7a,b). The biotic detritus has accumulated as organic matter within the sedimentary sequences.

The high-resolution aerial photography analysis (Fig. 4.6) shows Wandandian deltaic facies progradation and growth into St Georges Basin in red and graded red. Clear spatial patterns of accelerated accumulation of sediment in the Wandandian system are shown in Figs 4.6 and 4.7. Measurements of deltaic progradation including rates, total and net growth are summarised in Table 1 and Fig. 4.8.

4.4.1.1 Wandandian deltaic growth (1949-2016)

Figures 4.6 and 4.8 have derived growth evidence from the Wandandian deltaic eco-geomorphic system, particularly on the delta front facies and the adjacent shorelines. The area of the delta has been calculated for: (i) the subaerial, (ii) subaqueous delta borders and (iii) the total area (Table 1) thus providing annual rates of sedimentation during the study period (1949–2016), as illustrated in Fig. 4.9.

Table 1 shows that the delta grew by 14% (242,860 m^2) over the study period (1949–2016) at an average rate of 4168 m^2/year, with highest rates being 5283 and 8554 m^2 for 1949–1961 and 1961–1972, respectively. The reduced delta growth between 1972 and 1993 probably reflects sediment trapping in the sand mining area on Wandandian Creek. The subaerial area has grown by 29,130 m^2, allowing suitable ecological accommodation to be inhabited. The intertidal and subaqueous area grew by 213,730 m^2 into a protected part of St Georges Basin preparing a great opportunity for the subaerial area to expand more positively in the future (Fig. 4.8).

Table 4-1*: Area analyses of Wandandian delta for the overall delta growth, subaqueous area, total sensitive area, and average deltaic progradation.

Aerial Photograph	Subaerial area (km^2)	Subaqueous area (km^2)	Total sensitive area (km^2)	Total growth (km^2)	Growth/year (km^2/year)
1949	1.7112	0.1679	1.8791	-	-
1961	1.7125	0.23	1.9425	0.063400	0.005283
1972	1.7134	0.3232	2.0366	0.094100	0.008554
1993	1.7298	0.3319	2.0617	0.025100	0.001195
2002	1.7356	0.364	2.0996	0.037900	0.004211
2016	1.74033	0.38163	2.12196	0.022360	0.001597
Changes (m^2)	29130	213730	242860	*0.242860*	*0.004168*

** Sources: Figures 4.6 and the calculate geometry tool of the data management package in ArcGIS, (after Hopley, 2004; LPI, 2017).*

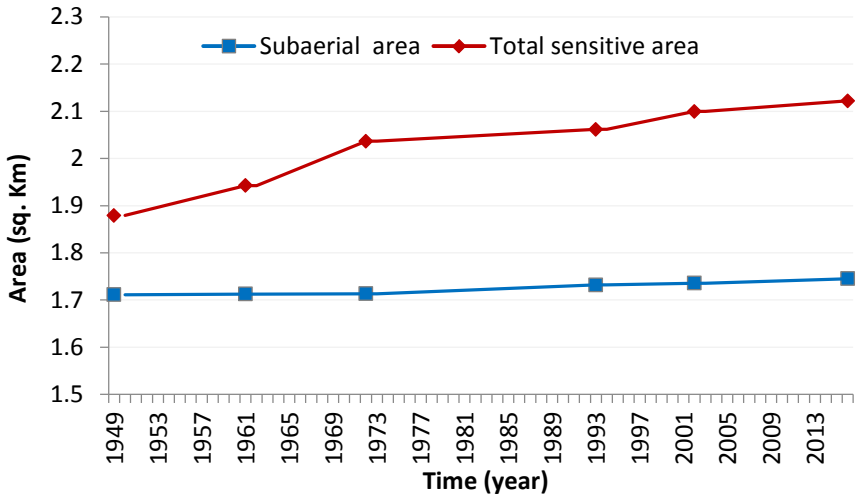

Figure 4-8. Wandandian deltaic growth, illustrating the overall growth of the delta itself and its levees/shorelines (blue), as well as the total growth of sensitive subaqueous areas (red). (Sources; Table 4.1, Fig. 4.6).

4.4.1.2 Tracing the shoreline temporal movement

Evidence of shoreline movements in Figs 4.6–4.8, and the more detailed example in Fig. 4.9, is a call for more shoreline dynamic analysis. The frictional interaction between the outflowing river water and the sediment surface (Carter & Woodroffe, 1997) within the western shallow channel resulted in an accumulation of a large triangular midchannel bar, which has resulted in the channel becoming bifurcated forming a typical fluvial-dominated birdsfoot delta morphology (Hopley, 2004; Hopley &Jones, 2006). The subaqueous portion of the delta coarsens upwards whereas the subaerial portion of the interdistributary bar fines upwards from relatively clean mouthbar sand to muddy finer sand interbedded with dark carbonaceous silt lenses (Hopley, 2004; Hopley & Jones, 2006).

Most of the fluvial sediments passed into delta mouth via the active tidal channel are eroded and redeposited on the margins of St Georges Basin (Fig. 4.9). A more detailed dynamic analysis of the deltaic shoreline is shown in Fig. 4.10.

Figure 4-9. Subaqueous and subaerially exposed levees associated with the western distributary channel of the Wandandian Creek delta. Source: LPI, 50 cm Jervis Bay and Ulladulla surveys of January 2014.

Shoreline movements of Wandandian Creek delta have been captured using the digital shoreline analysis system (DSAS). Figure 4.10 shows clear growth (green) in the active delta areas. On the other hand, some erosion occurred along the landward side of the upper active channel (Fig. 4.10a,b,f) part of its southern bank, as well as small portion of the delta-front island (Fig. 4.10e).

The overall average shoreline extension was 1.451 m/year (Fig. 4.10) but some zones show shoreline erosion rates of up to 0.348 m/year. These changes occurred along some parts of the deltaic landform facies and are more concentrated on the southern part of the delta at the creek mouth. Accretion was concentrated on the left side of the delta (on and around the large island, Fig. 4.10d and levees of sections b and c), with a net shoreline movement of 2.87 m over the past 65 years. Most of the sediment movement occurs during flood conditions but movement around the delta margins is also affected by minor tidal flows and wind-wave action.

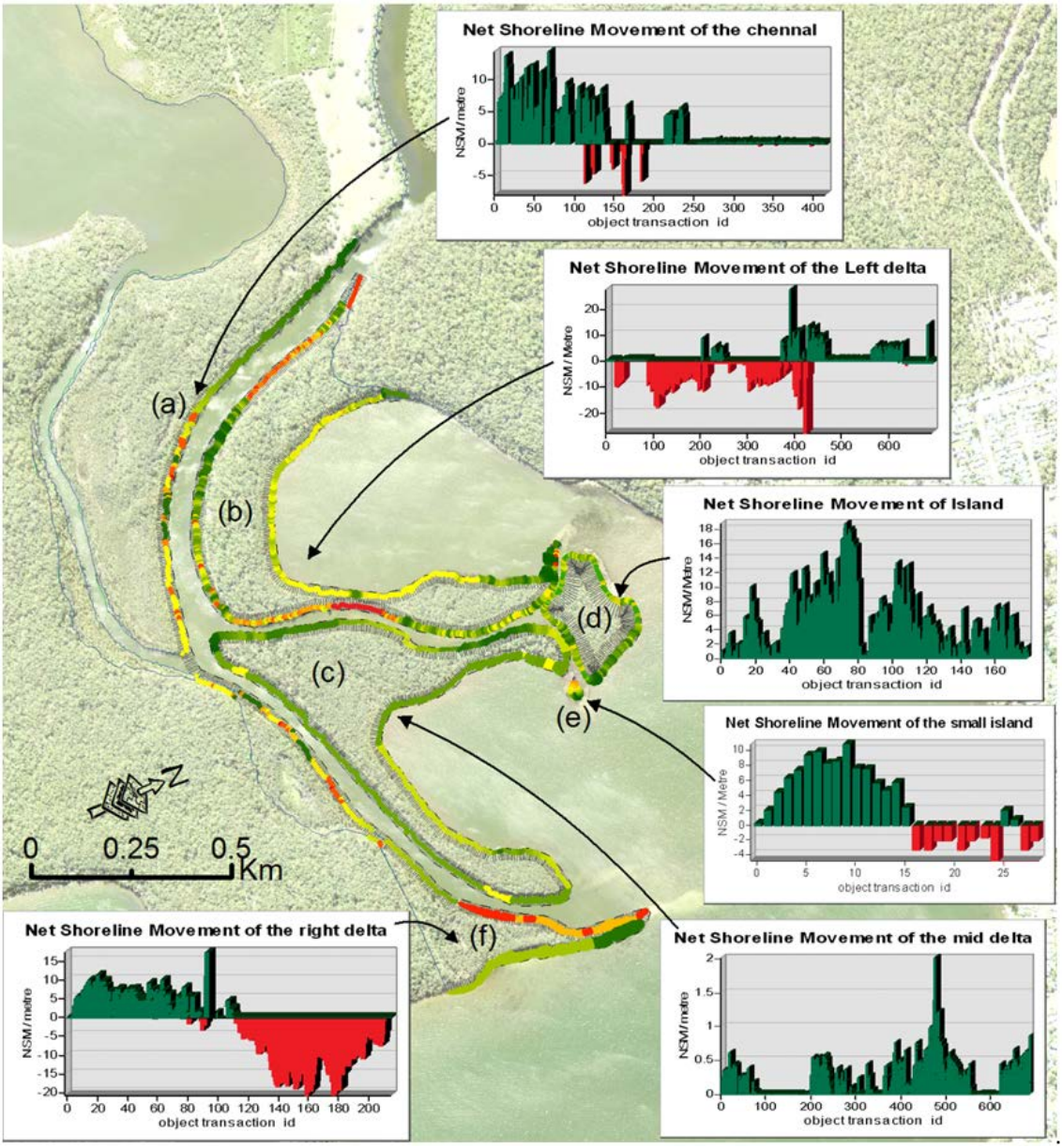

Figure 4-10. Digital shoreline analysis system (DSAS) applied to the sensitive Wandandian delta shows shoreline erosion in red, accretion in green while yellow represents the stable zones. Attached charts show the net shoreline movement envelope between 1949 and 2016: (a) the upper channel; (b) western portion of the delta; (c) the mid delta; (d) large interdistributary island; (e) small mouthbar island; and (f) eastern portion of the delta.

4.4.2 Fieldwork, sampling and modelling

4.4.2.1 Soil and sediment samples

4.4.2.1.1 Particle Size Analysis

The soil and sediment sample locations (Figs 4.1 and 4.12) and analyses have linked the detected shoreline changes to a better understanding of the Holocene facies distribution and sedimentation patterns. A detailed description of the stratigraphy of the Wandandian delta and its substrate has been presented in (Hopley, 2004; Hopley & Jones, 2006). Initial deposition of fluvial sands and overbank deposits progressively filled the Pleistocene low stand palaeochannel before reaching St Georges Basin. Progradation of the Wandandian delta into the broader embayment on the western margin of St Georges Basin began approximately 3.5–4 ka (Hopley & Jones, 2006) with the prodelta/lagoonal mud facies being overlain successively by the delta-front sandy silt facies and the prograded sand facies (Fig. 4.11b). However, in the inner part of this embayment the latter two facies are mainly separated by 1–2 m thick organic-rich accumulations representing a palaeoswamp environment (Fig. 4.11a). The prograded sand facies includes mouth bar, subaqueous channel and levee, and wave-reworked delta-front deposits. In the innermost protected part of the embayment the prodelta sand facies is overlain by a younger prodelta/lagoonal mud facies recorded in WD7.

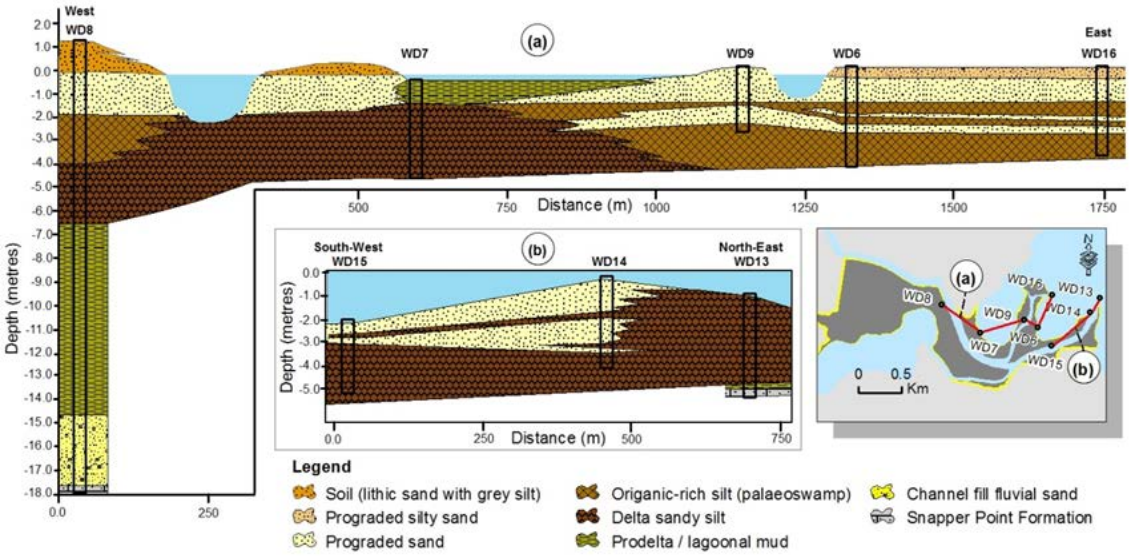

Figure 4-11. Cross-sections showing the distribution of prograded sand and organic-rich silty sequences in the Wandandian deltaic facies, which provide suitable bases for eco-geomorphic growth. (a) Progradation of the western distributary into the embayment in St Georges Basin along vibracores: WD8 (west), WD7, WD9, WD6 and WD16 (east). (b) Eastern distributary through drill-holes WD15 (southwest), WD14 and WD13 (northeast). Its eastern extent is controlled by an outcropping to shallow subsurface basement high (after Hopley, 2004; Hopley, & Jones, 2006).

The sandy facies are prograded into St Georges Basin and covering the delta front sandy/silt (Fig. 4.11b). The sediment is characterised by prograded sand facies and more varied than the front sandy/silt facies of the delta (Table 4.2). Characterising the basal prograded sand facies from the sandy/silt facies of the delta front was complex, yet analysis of sedimentation particle size visibly distinguish the two facies. Comparing to the front-delta, the prograded sand facies within the basal sediments are silty-sands. The prograded sand facies are having quartz contents that marginally greater comparing to the delta-front sandy silt facies (88.1 ± 2.1 % comparing with 82.4 ± 1.8%), which is shown that the mineralogical composition also aids in differentiating these facies. These growing sandy facies are including a range of wave-reworked delta-front deposits, subaqueous channel and levee, mouth bars (Hopley & Jones, 2006).

Table 4-2. Sediment and mineral analysis of samples taken from the Wandandian Creek*

Facies	Mean grainsize	Sorting	Mineralogy (%) (SIROQUANT XRD)	Colour
Levee/floodplain	Medium sand to fine sand	Poorly sorted	No analysis	Buff yellow to brownish black.
Palaeoswamp	Silt	Very poorly sorted	Quartz (54.6+1.0), kaolin (20.5+0.4), illite – smectite (18.6+0.8), illite (14.9+1.0), muscovite (11.2+0.8), pyrite (5.9+20.5), albite (0.6+0.5)	Black
Prograded sands	Very fine to very coarse sand	Moderately to poorly sorted	Quartz (88.0+2.1), kaolin (1.1+0.6), illite – smectite (4.1+1.0), illite (3.2+1.4), muscovite (0.8+1.1), albite (2.1+0.7)	Pale yellowish white to very dark greyish brown.
Delta sandy silt	Silt	Very poorly to poorly sorted	Quartz (82.35+1.8), kaolin (1.65+0.5), illite – smectite (6.75+1.0), illite (3.9+1.3), muscovite (4.35+1.9), pyrite (0.1+0.2), albite (0.5+0.6)	Dark olive to greyish black.
Prodelta/lagoonal mud	Silt	Very poorly to poorly sorted	Quartz (54.53+1.06), kaolin (3.9+0.4), illite – smectite (3.5+0.9), illite (6.1+0.2), muscovite (33.9+0.9), pyrite (0.1+0.2)	Dark olive brown to black.
Pleistocene sediment	Fine sand	Very poorly sorted	Quartz (81.2+1.76), kaolin (2.9+0.6), illite – smectite (1.9+0.8), illite (4.8+0.9), muscovite (6.5+1.1), albite (0.8+0.7)	Light grey with common orange, red mottles and rare olive mottles.
Pleistocene channel-fill sands	Medium sand	Very poorly sorted	Quartz (86.1+2.9), kaolin (2.9+0.8), illite – smectite (6.5+0.6), illite (3.4+1.9), muscovite (0.1+1.5), albite (1.1+0.9)	Greyish yellow sand with rare white quartz pebbles.
Pleistocene palaeosol	Very fine silty Sand	Very poorly sorted	Not analysed	Light yellowish brown, light brownish grey, pale grey and olive brown.

**Source; after, (Hopley, 2004; Hopley & Jones, 2006).*

The rate of progradation of sandy facies in the Wandandian Creek delta is difficult to establish in the dynamic fluvial and delta mouth areas. Very few macrofossils live within these facies and most of the recorded shells are reworked or broken making them unsuitable for accurate dating since they are not in situ (Hopley, 2004; Hopley & Jones, 2006; LPI, 2017). Thus, gaining

knowledge about accumulation rates through remote sensing datasets and the GIS analytic system would create a better framework for assessing deltaic systems here and worldwide.

4.4.2.1.2 X-ray diffraction

The mineralogy and grain size of the deltaic facies shows a clear relationship to the depositional energy reflected in the relative proportions of quartz in the sand facies and clay in the fine facies (Table 2).

Table 4-3. X-ray diffraction analyses of sediment samples from the Wandandian delta showing mineral proportions*.

Facies	Quartz %	Albite %	Illite-Muscovite %	Mixed Layer Illite-Smectite %	Kaolinite %	Calcite %	Pyrite %
Prograded Sand	85.7	4.3	8.8	0.3	0.8	0.1	0
	86.6	2.5	0.5	7.9	2.4	0	0.1
	92.1	0.2	3.2	4.2	0.3	0	0
Palaeoswamp	51.1	0.2	27.0	14.4	1.6	0	5.7
	59.1	1.4	26.5	4.2	2.7	0	6.1
Delta sandy Silt	86.1	0.7	9.7	2.8	0.6	0	0.1
	78.5	0.4	7.3	10.8	2.9	0	0.1
Prodelta/ Lagoonal Mud	51.5	0.1	31.6	6.2	3.9	0.2	6.5
	56.3	0.1	28.8	3.8	5.2	0.1	5.7
	58.3	1.3	23.3	7.8	3.1	0	6.2
Channel Fill Fluvial Sand	87.2	0	0.6	9.3	2.9	0	0
	84.7	2.4	6.4	3.6	2.9	0	0

**after; Hopley (2004).*

Clay content in the samples is highest in the low energy environments in sheltered reaches, but also occurs in the fluvial lithic sands through the diagenetic alteration of feldspar and rock fragments (Fig. 4.12). Pyrite indicates reducing conditions in the organic-rich palaeoswamp and prodelta/lagoonal mud facies.

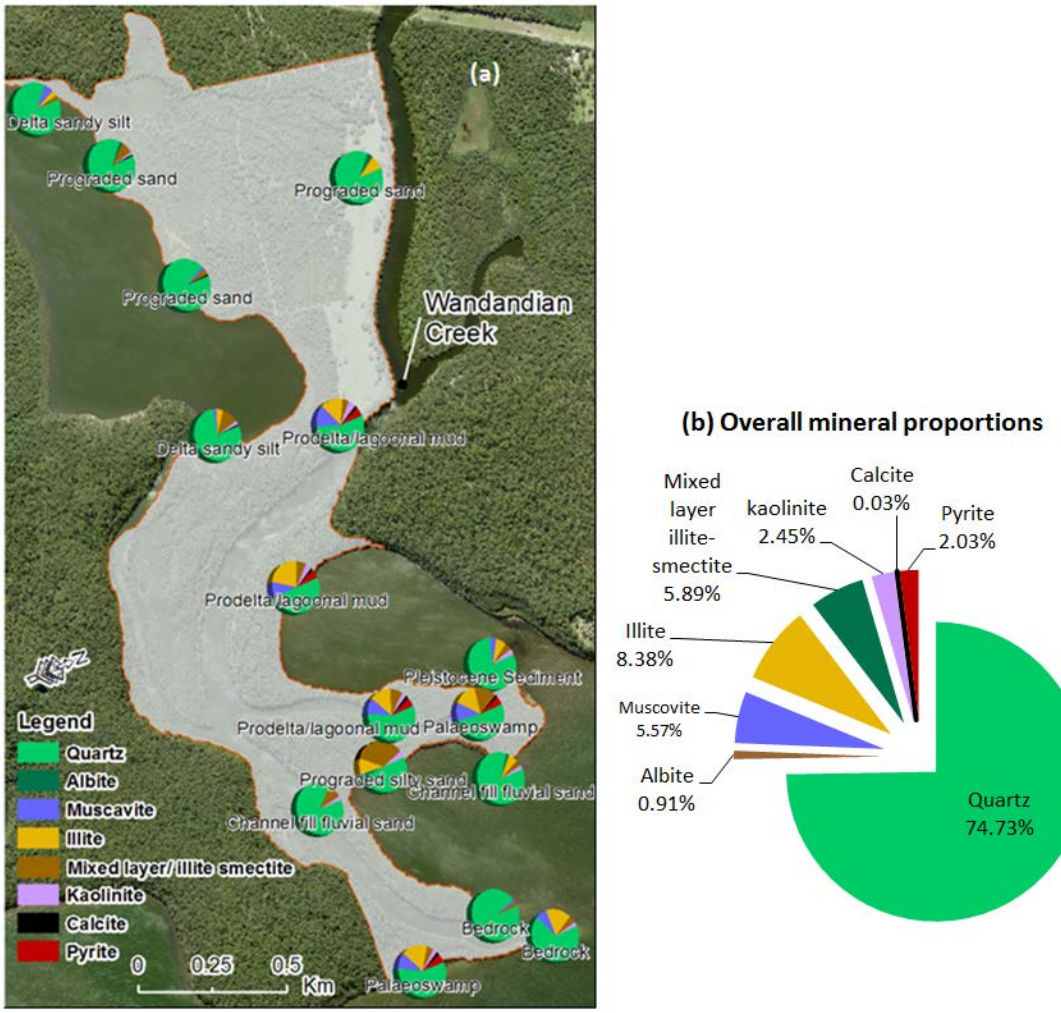

Figure 4-12. Soil and sediment samples from the Wandandian deltaic landform, illustrating: (a) mineral contents in each sediment sample and represented facies, with a clear dominance of quartz, (b) the overall mineral proportions in the sediment samples. (The background is from a Jervis Bay 50 cm Orthorectified Image obtained from LPI for January 2014; Chakravarty *et al.et al.*, 2017).

4.4.2.1.3 Organic matter

Organic matter plays an important role in the ecosystem development and growth on intertidal sedimentary deltaic landforms. The amount of organic matter in the sediment is controlled by the rate of organic decomposition in the sediment (Murray *et al.et al.*, 2005). In general, high rates of total carbon dioxide (TCO_2), ammonium (NH_4^+), and silicate (SiO_4^{4-}) production, and oxygen (O_2) consumption indicate high respiration rates and correspond to high organic contents in the sediment (Murray *et al.et al.*, 2005). As the organic matter degrades nutrients are released into the water column and become available for plant growth and ecosystem development. Organic matter components (%OM) are concentrated (Fig. 4.13) in the downstream part of the delta, where the wetlands are distributed.

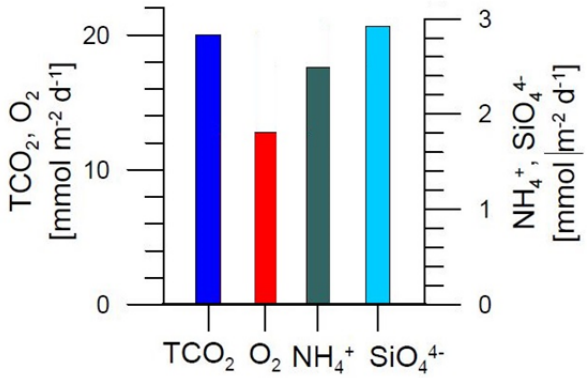

Figure 4-13. Average (n=3) organic matter (benthic nutrient), TCO_2, O_2, NH_4^+, and SiO_4^{4-} in Wandandian delta. Note that NH_4^+, SiO_4^{4-}, and TCO_2 were fluxing out of the sediment, whereas O_2 was fluxing into the sediment. TCO_2 was determined by alkalinity and conductivity titrations for this study site (after; Murray *et al.*, 2005).

While the Wandandian delta had low TCO_2, O_2, NH_4^+, and SiO_4^{4-} fluxes, the SiO_4^{4-} and TCO_2 "fluxes exceeded the NH_4^+ flux indicating that denitrification, carbonate dissolution or decoupled decomposition of organic matter were more important than respiration" (Murray *et al.et al.*, 2005). Aerobic respiration in coastal and estuarine sediments generally shows a flux ratio of $1TCO_2$: $1.3O_2$ but the TCO_2 flux in the Wandandian delta exceeded this ratio indicating the importance of anaerobic degradation in these deposits. This was confirmed by the large amount of gas, including H_2S, released during vibracoring (Hopley, 2004; Murray *et al.*, 2005; Hopley & Jones, 2006).

4.4.2.2 Water quality analysis

Water quality was assessed under average flow conditions to indicate downstream changes in the main water quality parameters. Figure 4.14 shows increases in conductivity, dissolved oxygen and salinity towards the mouth of the delta while the temperature and pH show a very slight increase, due to shallower water that was easier to heat (Table 3). In contrast, turbidity has shown a decline in the downstream direction because suspended sediment has flocculated and accumulated along the delta channels as salinity increases. At the same time, the active channel flows more slowly towards the coastal end of the delta especially during rising basin water levels (due to floods, tides or seiches), which makes the river less able to transport both bedload and suspended sediments. These results clearly indicate that abundant sediment is transported to the delta leading to high rates of deposition and bank accretion in these downstream areas. Thus, the sediment is basically spread across the entire estuary and the suspended sediment becomes less and finer during its movement along the Wandandian delta due to flocculation.

Table 4-4. Table 3. Profile depth and analysis of water temperature, salinity, dissolved oxygen (DO), conductivity and turbidity.

Sample No.	Depth (m)	Temperature (°C)	Salinity (±0.05 ‰)	DO (%)	Conductivity (±0.05 mS/cm)	Turbidity (NTUs)
WD8	−0.6	19.8	28.8	89.4	14.5	20.54
WD9	−1.1	21.2	29.1	82.6	16.8	19.1
WD17	−1.5	21.1	30.3	80.9	17.12	19.1
WD16	−2.4	21.3	29.6	79.8	18.9	19.1
WD11	−1.96	21.4	30.7	79.55	20.4	21.9
Average	1.5	21.0	29.7	82.5	17.5	19.9

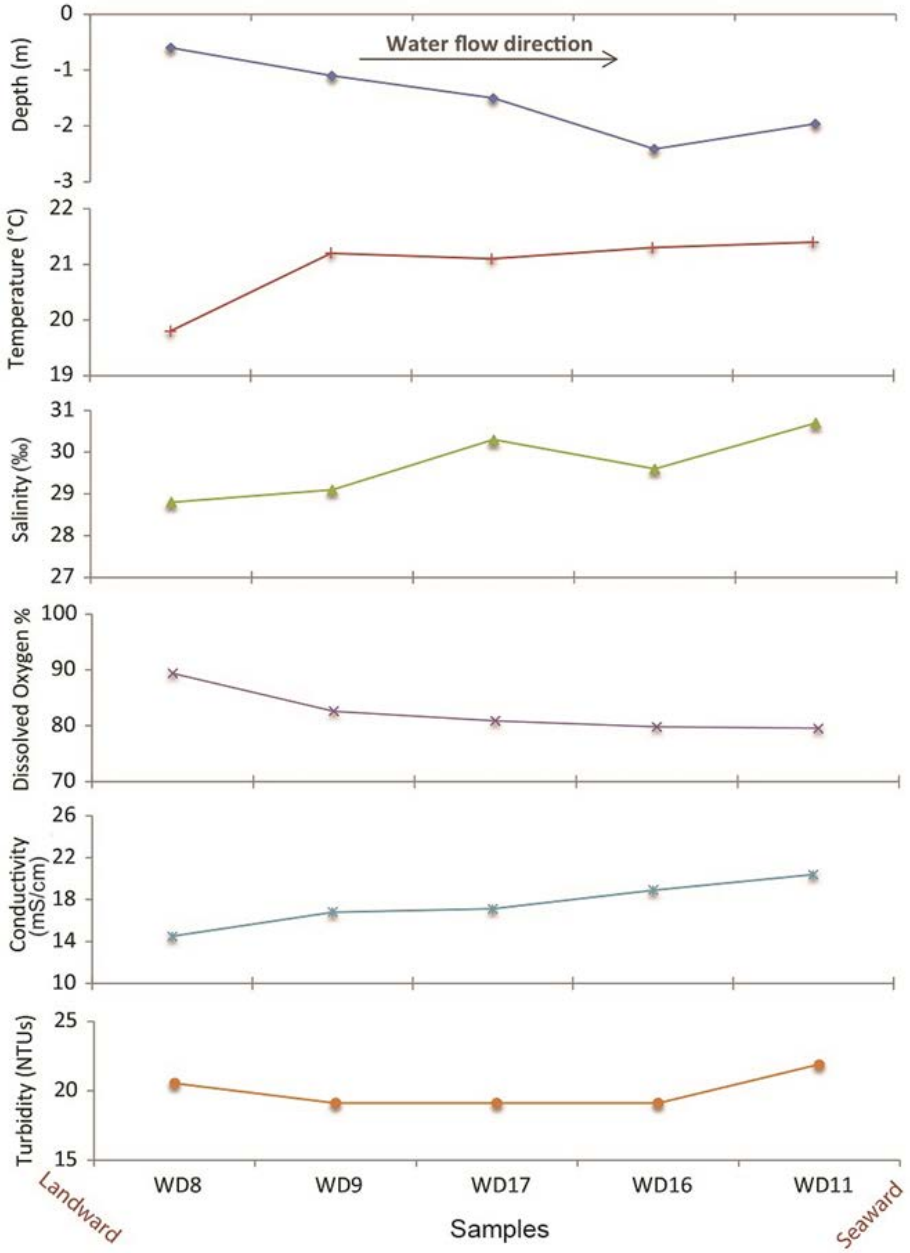

Figure 4-14. Water sample analyses show spatial changes in; conductivity, salinity, dissolved oxygen and turbidity, (sample locations have presented on Fig. 4.1).

4.5 Discussion

The knowledge gained by assessing accumulation rates through remote sensing datasets and the GIS analytic system creates a better framework for assessing deltaic systems here and worldwide. The multi-temporal changes analysis approach was able to quantify the eco-geomorphic changes on the Wandandian delta case study, and shows a qualitative picture of changes in the pattern of land cover, banks and broad changes in the delta area since the start of suitable historical photographic data in 1949 (Figs 4.7–4.9 and Table 4.1). The main features shown by the multitemporal deltaic changes between 1949, 1961 and 1972 are in the delta front facies, which involved growth of the levees, deltaic shoreline facies, a reduction in the width of the active channel, and changes to the areas of mangrove, saltmarsh and some native plant canopy (Figs 4.6–4.8). The subaqueous zone and the active delta channel, as well as some of the internal shorelines, experienced net accretion in all five analysed time intervals between 1949 and 2016 but especially from the 1940s to 1970s. Consequently, most of the extended areas have increased land covers by expansion of mangroves and saltmarshes.

The active channel of Wandandian Creek has bifurcated with the eastern distributary prograding onto the shallow rocky bed on the western side of the St Georges Basin producing an elongate delta. In contrast, the western distributary extends into the middle of the bay forming a small birdsfoot delta. These delta extensions have resulted in expanded geomorphic units including levees, floodplain, sandspits and their associated land covers (Figs 4.6 and 4.10; (Hopley, 2004). Both distributaries are characterised by well-defined subaqueous and subaerial levees up to 1.5 m above water level. These levees consist of coarse fluvial sand that fine upwards to silty sands with interbedded dark organic-rich silt lenses. The subaerial levees are rapidly stabilized mainly by *Casuarina* and *Juncus* (Fig. 4.7b). Additionally, most of the native plants and the new saltmarsh areas (seen in 1949) were growing on the stable sensitive areas and started mixing with mangroves in the tidal zones as an effect of sea level and the consequent table water rise (Figs 4.4d and 4.6). The mangrove cover has gained ground as a result of the shoreline expansion (Figs 4.6 and 4.8).

The minimal wind-wave reworking in the western embayment of St Georges Basin means that it represents an ideal environment for silt and organic matter accumulation as Wandandian Creek discharges load through the delta. A reduced sediment carrying capacity through the delta may reflect a lower river discharge (lower rainfall) or more probably represents gradual filling and abandonment of previously active channels (Coleman & Wright, 1975). The large woody detritus and abundant organic material present in the palaeoswamp and prodelta/lagoonal mud facies were mainly transported as rafted plant debris into these quiet

water environments. Two distinct sand sheets in the upper part of the palaeoswamp facies (Fig. 4.11a) probably represent large flood events. The palaeoswamp deposits typically have a distinctive hydrogen sulphide smell caused by anaerobic decomposition of organic matter in the presence of sulphate ions.

Suspended sediment fluxes from the catchment and the progradation of geomorphic units are the major influences controlling this delta growth in an inner estuary, like St Georges Basin (Hopley, 2004; Hopley & Jones, 2006). The results of this study reveal some important aspects of human and natural effects influencing the sedimentary facies, shoreline growth and water quality of Wandandian Creek and its deltaic zone (Figs 4.6–4.10).

Water quality analysis (Table 3 and Fig. 4.14) has shown that sedimentation increases towards the delta head providing continued accumulation processes. The salinity shows a gradual increase downstream towards the marine influenced St Georges Basin. The water temperature also increases due to the stagnated water and limited ocean water exchange in the inner parts of St Georges Basin (Hopley, 2004; Murray *et al.*, 2005). Meanwhile, the conductivity and turbidity have fluctuated but show a slight increase towards the delta mouth reflecting the influence of salinity and suspended sediment transport and accumulation along the creek. In contrast, dissolved oxygen shows a declining trend seaward, indicating that O_2 consumption in the water column exceeded any replenishment from photosynthesis or the atmosphere.

The deltaic progradation evidence comes from the geomorphic growth of 242,860 m^2 over the study period (4168 m^2 annually, Table 1). Growth has resulted from the sediment delivered to the coastal zone through the Wandandian Creek drainage system from intermediate moderately modified catchment. This growth has provided good ecosystem accommodation for plant colonisation, with common organic matter accumulating within the sediment along the shorelines and in the interdistributary bays.

This study has illustrated how careful analysis of remote sensing data using a GIS platform can lead to a detailed understanding of the growth and evolution of deltaic and estuarine systems and is similar to the results presented for other Australian coastal systems (Kench, 1999; Hopley& Jones, 2007; Sloss *et al.et al.*, 2007; Akumu *et al.et al.*, 2010; ALUM, 2010; Al-Nasrawi *et al.et al.*, 2016b). This implies that the methodology can be broadly applied to study morphological changes over relatively short timeframes in other coastal lagoon systems both in eastern Australia and more generally to any similar systems around the world.

4.6 Conclusions

This investigation has effectively used remote sensing and GIS analysis to quantify historical and existing eco-geomorphic situations in deltas and use these to predict their future responses to related environmental stressors. Proven deltaic progradation has shown how estuaries can keep up with sea level rise through continuous sand/silt sediment accumulation derived from a partially modified catchment.

The morphology of the Wandandian Creek delta has been influenced by both the shape of the shallow bedrock and Pleistocene outcrops and by recent anthropogenic modifications within the catchment. Delta growth into the western arm of St Georges Basin began at 3.5–4 ka with the delta-front sandy silt facies overlying a very thin prodelta mud facies. Seaward extension of the overlying prograded sand facies formed a coarsening-upward sequence that was probably facilitated by the lowering of regional sea-level by about 1.5 m after 4 ka (Sloss *et al.*, 2007). The fall in sea-level reduced the available accommodation space farther up Wandandian Creek releasing more sediment for delta growth. As the delta prograded into a broader and deeper part of St Georges Basin its form became less restricted, and the western distributary has formed a typical classic birds-foot delta [37–39, 42, 44]. The large amount of organic matter in the fine-grained delta facies indicates subaqueous deposition in a low energy environment at water depths similar to or slightly higher than at present (Hopley & Jones, 2006). The upper delta floodplains, levees and backswamps partly overlie the lower delta plain subaqueous units described above but elsewhere they directly overlie fluvial sands. These fluvial-dominated areas show a typical fining-upwards sequence, and hosted an extensive vegetation canopy, such as mangrove vegetated shorelines and backswamps with saltmarsh habitats.

European modification of the Wandandian Creek catchment (22.1%) has had a limited impact on sedimentation and progradation rates of the delta [15, 16]. However, dredging in the Wandandian river channel in the 1970s reduced the amount of bedload transport into St Georges Basin restricting delta progradation. The effects of modifications such as this means that short term intensive investigations based on remote sensing and GIS analysis are highly recommended in all such areas worldwide.

The eco-geomorphic interpretation from this study could assist the Shoalhaven City Council and local landowners on the lower Wandandian Creek floodplains to make informed decisions about the future environmental management of the delta. The findings from this study can be extended locally and globally when considering the Holocene development of coastal lagoons. For example, the widespread occurrence of pyrite- and organic-rich delta-front deposits at relatively shallow depths could lead to the formation of acid sulphate soils if they were drained

and oxidized. This would have a large impact on the surrounding environment.

This thesis has established that remote sensing datasets and GIS analysis, in combination with sedimentological and morphological data, can clearly document the evolution of the Wandandian deltaic eco-geomorphic system as it progrades into St Georges Basin, southeastern NSW, Australia. The understanding of how the deltaic landforms have evolved in the past can then be used to help establish their probable vulnerability/adaptability into the future. Equivalent analytical methods can be extended to and replicated in similar lagoonal estuaries worldwide.

Chapter V: An assessment of anthropogenic and climate stressors on estuaries using a spatio-temporal GIS-modelling approach for sustainability: Towamba estuary

5.1 ABSTRACT

Monitoring estuarine eco-geomorphic dynamics has become a very important aspect of coastal studies in relation to current climate change and worldwide infrastructure development in coastal zones. Together these factors have altered the natural eco-geomorphic processes, and caused changes in estuarine regimes, especially coastal wetlands. To ensure the sustainable use of coastal resources, comprehensive modelling can help managers make appropriate decisions. This study uses Towamba estuary (southeastern NSW, Australia) as a case study to demonstrate the importance of modelling estuarine dynamism to investigate the rates of eco-geomorphic change and the consequences of these changes. This research employs several data-based modelling approaches over time to explore and assess how climate change and human activities have altered this estuarine eco-geomorphic setting.

Multi-temporal trend/change analysis of land cover, shorelines and sediment delivery, estimated from remote sensing data, GIS analysis and fieldwork, show significant spatio-temporal changes to the areal extent and elevation of estuarine facies (for instance; mangroves, saltmarshes and sandspits) in the Towamba estuary over the past 65 years. Overall land and wetland area has grown by 169608 m^2 (2609 m^2 annually), but some erosion has occurred in the tidal channel and on the landward side of the coastal barrier. Geomorphic growth has resulted in stability of the estuarine habitats, particularly within saltmarsh, mangrove and mixed native plant areas. Geomorphic changes have occurred due to a combination of sediment runoff from the mostly unmodified terrestrial catchment, nearshore processes (ocean dynamics) and human activities. The construction of GIS models, in conjunction with water and sediment samples to characterise physical processes within the ecosystem (for instance; sediment transport and erosion/deposition) quantifies changes within the ecosystem. Such robust models will allow resource managers to make more informed decisions and evaluate potential consequences of changes to the existing ecosystems.

ADDITIONAL INDEX WORDS: *Anthropogenic modifications, eco-geomorphology, ecosystem management, GIS-modelling, sediment transport.*

5.2 Introduction and Background

The ecosystems on Earth, particularly in the coastal zones, have become a balanced and stabilised since the mid Holocene (Troedson *et al.*, 2004; Murray-Wallace & Woodroffe, 2014). Early Sumerians (Mesopotamia 4500 BC – southern Iraq nowadays) and most ancient civilisations inhabited coastal and estuarine environments, which have provided people with many ecologically valuable services, including food, transport and access within a specific ecosystem (Postgate, 1992). Since then, habitation attractions have increased for economic and environmental reasons, impacted directly on the estuarine areas and/or indirectly through their relevant catchments (Cherfas, 1990; Pendleton, 2010; Neumann *et al.*, 2015). Coastal ecosystems are threatened as a result of the rapid population growth that concentrates anthropogenic stressors on coastlines around the world (Neumann *et al.*, 2015). Anthropogenic pressure include deforesting, farming, urbanisation and related industrial and recreational activities, which influence the current ecological and geomorphological (eco-geomorphic) processes and potentially add adverse pressures on the environment (Baban, 1997; Lee *et al.*, 2006; DSE, 2007; Hardisty, 2008; Al-Nasrawi *et al.*, 2016b). More recently, environmental stressors have risen, including increasing severe storms/flood events, climate change, rising sea level and habitat alteration, which threaten the eco-geomorphic functions that have supported coastal habitats historically (Michener *et al.*, 1997; Nicholls, 2004). Human and natural processes/hazards that influence coastal eco-geomorphology should therefore be monitored, whether for the direct threats of loss to the estuary eco-geomorphic system itself or indirect adverse impacts from land use practices within the catchment. Kingsford (1990) revealed that direct and indirect human impacts can change estuarine habitats, which can then affect the conservation management plans and policies. Indirect negative effects include modifying land covers in the catchment and its water usage (Saintilan & Imgraben, 2012; Al-Nasrawi *et al.*, 2016a, 2016b, 2018a). That has reflected several eco-geomorphic losses, including estuarine saltmarshes decline in southeastern NSW (Saintilan & Williams, 2010). The Towamba River estuary (southeastern NSW, Australia) represents an example of an infilled and prograding river-dominated estuary within a near-pristine catchment area where natural processes have controlled downstream runoff and sediment supply to the estuary zone to establish the modern geomorphological landforms and the associated habitat as a coastal ecosystem.

Morphological changes to estuaries and associated changes to their accompanying wetland may produce complex results for the biota that are not intuitive because of biological interactions (Day *et al.*, 2008). Unfortunately, numerous coastal ecosystems, including

wetlands, have been degraded and a lot of artificial-wetlands have been unsuccessful to reproduce the varied ecosystems within such wetlands, such as some of the Louisiana coastal wetlands (Penland *et al.*, 2005).

Comprehending the causes that have influenced the current geomorphology and process regime of the estuary is vital in terms of erosion, transport and deposition process of terrigenous clastic sediments, that are basically controlled by river, human activities on Earth and climate factors (Blott *et al.*, 2006). Clastic sediments are delivered to the estuarine environments by rivers from the catchments recording the effects of tectonic, climatic and sea-level changes and anthropogenic land-use that act as major factors controlling temporal and spatial changes in coastal estuarine ecosystems (Zhu *et al.*, 2010).

There are vitally needed to monitor, evaluate and quantify changes in an estuary's geomorphology, sedimentary characteristics, water quality and impacts of human settlement on estuarine ecosystems at all development stages. This study quantifies threats to a coastal estuarine regime, such as shoreline erosion and sediment delivery problems, through continuous monitoring methods at a landscape scale. Methods include; remote sensing, GIS analysis and fieldwork investigations at a chosen estuarine site as a case study, to model potential modifications that can be used for rehabilitation of the associated coastal wetlands. Additionally, the effects of artificial modifications (for example, the grazing and farming growth as a dynamic land cover function) in the catchment are another principle element addressed.

In order to monitor and evaluate the estuary's current eco-geomorphic status and the possible future changes that will occur, modelling and understanding the existing situation is an essential role for eco-geomorphic system managers (Al-Nasrawi *et al.*, 2015a, 2016b, 2018c). Modelling estuarine eco-geomorphology, however, is restricted by a relative shortage of measuring data, computational expense and uncertainty. Many recent researches have established the groundwork for developing strong calibration and simulation methods for estuarine geomorphic change (Thom *et al.*, 1975; Ball, 1994; Carter, 1999; Roy *et al.*, 2001; Blott *et al.*, 2006; Bianchi & Allison, 2009; Batzer & Sharitz, 2014; Venter *et al.*, 2016).

Approximately 15-16×10^9 tons of sediments are estimated to be delivered every year to the oceans under current climatic conditions (Zhu *et al.*, 2010). Riverine estuary studies have focused on many eco-geomorphic aspects including: (i) fluvial geomorphology and sedimentology (Jones *et al.*, 1993); (ii) hydrology (Zhu *et al.*, 2010); (iii) sediment transport - including erosion and weathering (Wei *et al.*, 2007; Zhu *et al.*, 2010); (iv) the characteristics/dynamics of the riverine sediment transport regarding their particle size (Yang

et al., 2009); (v) the mineralogical properties of the sediment (Sondi *et al.*, 2008; Zhu *et al.*, 2010); (vi) the geochemistry aspect (Jones *et al.*, 2003a); (vii) the characteristic assessment/evolution of a delta (Jones *et al.*, 2003b; Zhu *et al.*, 2010); (viii) general environmental research (Hu *et al.*, 2009); (ix) climate change studies of the late Quaternary (Hudson, 1991; Zhou *et al.*, 2005) (Zhu *et al.*, 2010); and (x) sea level change (Sloss *et al.*, 2007; Al-Nasrawi *et al.*, 2015a, 2018c).

The object of this research is to (1) determining the estuarine system spatial eco-geomorphic growth within the last few decades, (2) investigating the direct and indirect interactions between the anthropogenic and environmental trends on the catchment's sedimentation and runoff factors, and then (3) determine the implications of the eco-geomorphic assessment trends for the future health of estuarine deltaic ecosystems that would be applicable to coastal wetlands worldwide. The importance of this work to management is that it gives an idea of the sensitivity of the estuary to sand flat and shoreline extension, which allows more ecosystem expansion as the sediment accumulates.

Previous spatio-temporal evaluations have used RS datasets, GIS analyses, and fieldwork sampling to highlight the estuarine changes, including shoreline change rates and associated landcover change.

GIS simulation and RS data analysis combined with field work sampling provides a quantifiable approach to developing accurate models of spatial and temporal changes in estuarine systems. GIS analysis of aerial photographs, satellite images, LiDAR data and fieldwork (water analysis, sediment sampling, bathymetry and GPS surveys) overcome difficulties in extracting geomorphic changes, such as shoreline position and detection of shoreline changes, as well as identifying sediment sources and determining sedimentation rates.

5.2.1 Study site specifications

The formation of an estuary depends on the position of sea-level compared to the level of fresh water flow from the river (Wright, 1970; Woodroffe *et al.*, 2000). Estuarine systems within southern NSW coast provide examples of disturbed geomorphological regimes. NSW estuaries infilled late Quaternary low-stand incised valley systems (Roy *et al.*, 2001; Sloss *et al.*, 2006b, 2010). The landward sediment movement from the continental shelf after the Last Glacial Maximum (LGM) low-stand accumulated in the river mouths and formed Holocene coastal estuarine sand barriers (Sloss *et al.*, 2006b, 2010, Roy & Crawford 2011). Over the Holocene highstand of sea levels, estuarine systems started to simultaneously infill with

marine sediment and with sediment derived from the river catchment. NSW estuaries vary greatly in their rate of infilling depending on their sediment supply and the geomorphic ability to keep the sediment within the estuary, depending on the balance between the river and nearshore ocean energies. Towamba River drains into Twofold Bay which is affected by two opposing oceanic water masses: a cold current from the Southern Ocean and the warmer East Australian Current (Yassini & Jones 1995) that both have a major effect on the microfossil ecology of the bay (Dean & De Deckker 2013).. Twofold Bay is the largest commercial fishing port in New South Wales and has been an important place for many anthropogenic activities, ranging from large boat traffic, Australian Navy activities, timber export, recreational fishing and whaling to mussel farming (Dean & De Deckker, 2013).

Successive erosion and deposition cycles in NSW estuaries have resulted in ecological and morphological changes over time (Roy *et al.*, 2001). Furthermore, there has been a clear increase in the possible effects of changes in natural environmental aspects, such as dynamics of the sand bodies. This have resulted from, i) climate change, including rising mean sea-level and the frequency of high energy storms; and ii) anthropogenic influences including farming, industrial development and urbanisation within the catchment, dredging of the channel, embankment modification within estuarine ecosystems (Roy *et al.*, 2001). These geomorphic changes have also led to ecological responses, particularly within estuarine/coastal wetlands, because of their sensitivity and relatively rapid responses (Al-Nasrawi *et al.*, 2016b, 2017a). Responses include developing vegetation canopy (mainly mangrove, *Casuarina* and some *Juncus* sp.) particularly within shoreline zone, as well as saltmarsh areas, that offer suitable accommodation and habitat for other ecological and biological communities to develop.

The Towamba estuary is located on the southeast coast of New South Wales near Eden (Fig. 5.1). The main coastal ecosystem of the Towamba estuary is located at the end of the Towamba River delta where it enters Twofold Bay. The active tidal channel has an average depth of 1.15 m. and is constrained by rock outcrops, resulting in restricted estuarine shape (Fig. 5.1). Towamba is mostly a fluvial sandy estuary, with sediment derived from volcanic, volcaniclastic and mudstone rocks in the source area; muddy components only accumulated in low energy areas resulting in a Quaternary alluvium with little structural strength.

According to Roy *et al.*'s (2001) classification, Towamba is a mature wave-dominated barrier estuary that has infilled and is now dominated by fluvial processes and sediment bypass to the estuary mouth. It has an open estuary mouth into Twofold Bay, with the water and sediment mainly derived from Nullica State Forest and the other mostly untouched forests in the

catchment area (Blay 1944). The source of the perennial Towamba River is at Mount Marshall in the South Coast Range that forms part of Great Dividing Range (SOC 2010).

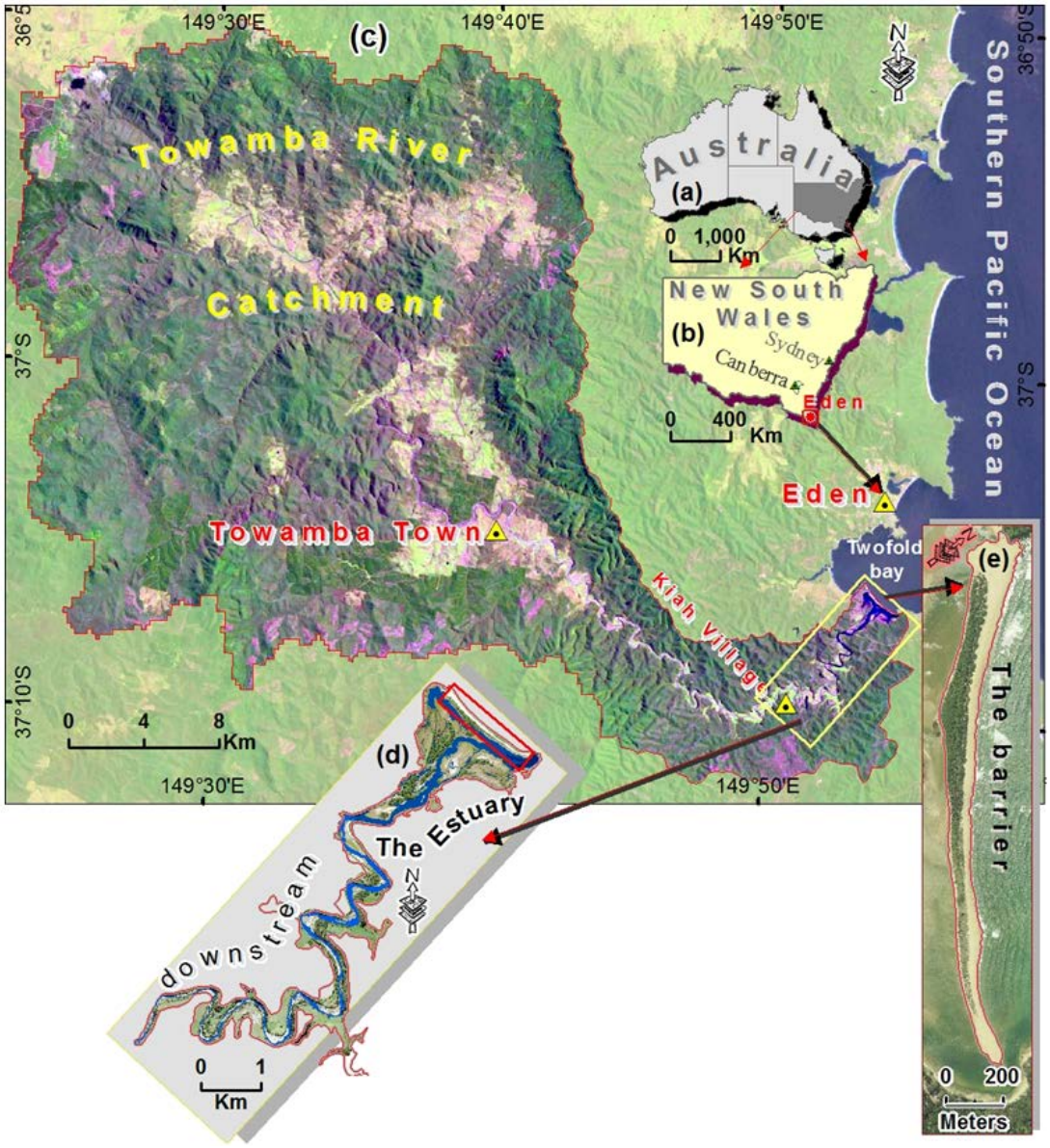

Figure 5-1. The study site in the coastal estuary section of Towamba River, southeast NSW, Australia (a and b), showing; (c) the study site region and the river catchment, (d) the downstream river and estuary, and (e) the wave-dominated estuarine barrier that secures the estuarine eco-geomorphic system.

The river flows generally southeast and then northeast, joined by 12 tributaries, before flowing into Twofold Bay southeast of Eden near East Boyd (Hudson 1991). The river descends 533 m over its 86-km course (Roy *et al.* 2001; DPI/OW 2017) passing through part of the South East Forest National Park in its upper reaches. Farther downstream the river forms the northern boundary of Mount Imlay National Park. Towamba River is also known as Kiah River since the Princes Highway crosses the river at Kiah (Fig. 5.1) which is about 6 km up from the estuary (SOC 2010).

The estuary area is 2.7 km^2 and includes interesting coastal wetlands, native plants, a dynamic barrier island, sandspits, tidal banks, tidal/active channel and other sandflats with palaeo-delta facies underlying them. The estuarine barrier hinders direct sediment discharge, leading to more deposition within the estuary, supporting the rapid growth of eco-geomorphic features over time. It protects a large area of seagrasses, saltmarshes and mangroves that are important for biodiversity and ecosystem service roles. Towamba River transports weathered sediments downstream from a mostly untouched catchment area of 1034 km^2. The river was deeply incised during the last low stand of sea level while the post-glacial sea level rise submerged the section of the river adjacent to the coast, forming an estuarine inlet. The estuary is partly enclosed by a sand flat/spit formed at the river mouth by coastal processes. Deposition has occurred gradually over thousands of years, filling the estuary with sediments from the river, and it is now dominated by sediment bypass in a mature estuarine system prograding into Twofold Bay (Roy *et al.*, 2001; Jones & Byrne 2014, p.203; DPI/OW 2017). The Towamba River has a series of interconnected channels forming a braided network. The slope of the river was critical in the formation of the estuary. Deposition can occur either at the bayhead delta, in the estuary or in Twofold Bay in front of the river mouth (Roy *et al.*, 2001; Young, 2011; DPI/OW, 2017).

Historically a few sections of the river near Kiah village (Fig. 5.1) became unstable and resulted in high erosion rates on both sides of the river where the bank consisted of alluvial sediment. This erosion was enhanced by undercutting, bank slumps, tree falls and the uncontrolled access to the banks by livestock. The erosion was localized along the river and only occurred where alluvial fill rather than bedrock occurred in the banks (Ian, 2013). This increased the volume of sediment moving downstream into the estuary and resulted in rapid expansion of the bayhead delta into the southwestern Twofold Bay. That may explaining why very little mudflat occurs along the margins of the estuary, which are mostly covered by saltmarsh and mangrove wetlands, including Grey Mangrove (*Avicennia marina*; fieldwork observation; DPI/OW, 2017). Fieldwork observations indicate dynamic changes to the wetlands caused by interactions between the sedimentary characteristics and rising sea level.

5.2.2 Related Local climatic conditions

Climate factors (precipitation and the resultant river discharge, temperature and mean sea level) have significant effects on the eco-geomorphic processes and runoff amount around Towamba estuary. Although the Towamba site is also affected by coastal weather systems, a clear decline in precipitation has occurred over last forty years (Fig. 5.2a). The Towamba River

catchment has experienced a fluctuating decline (2.4 mm/a) in annual rainfall from 974 to 879 mm during study period (Fig. 5.2a). However, it is still providing adequate flow rates (average of 387.4 ML/day since 1970s) in the main Towamba River channel (Fig. 5.2b) that transports the weathered sediments and associated nutrient elements into the estuarine eco-geomorphic system where they have accumulated. However, there has been a clear decline in average of Towamba River discharges over the last forty years (see Fig. 5.2b; BOM, 2017b; DPI/OW, 2017).

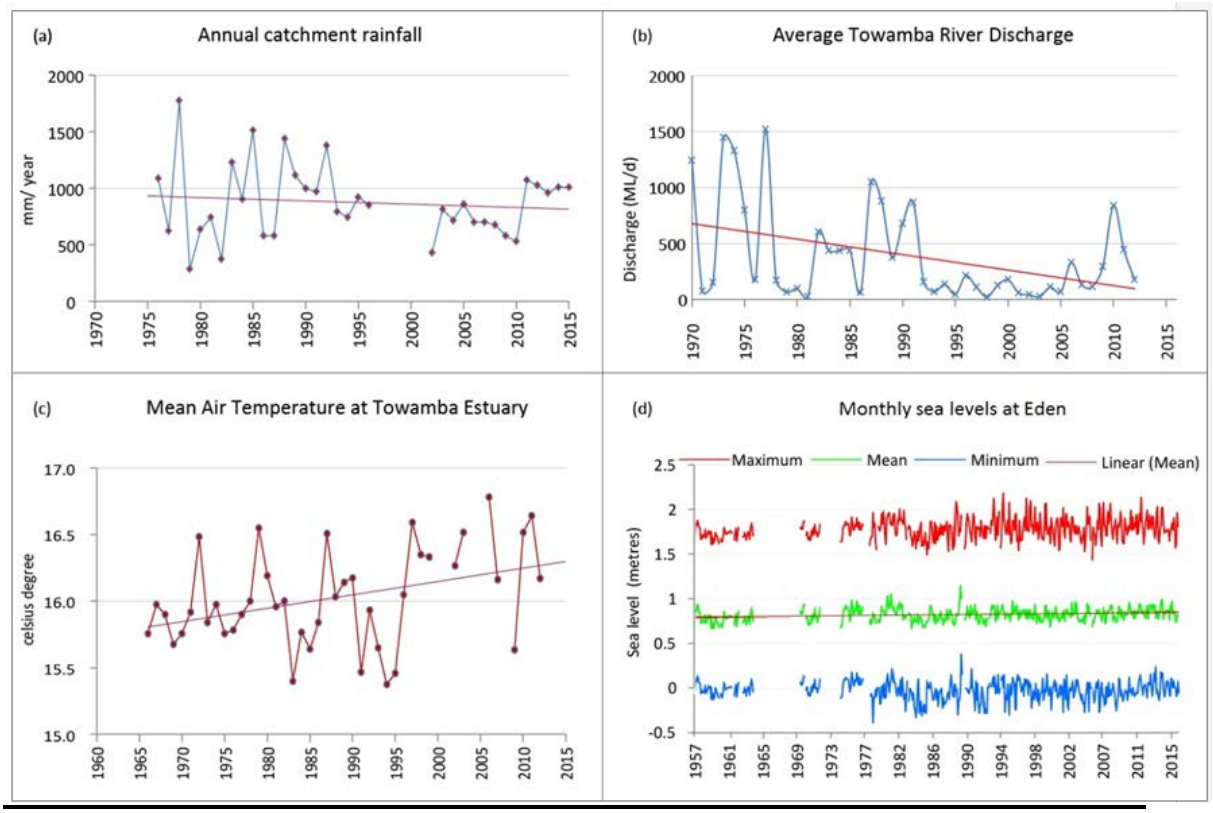

Figure 5-2. Climate trends affecting the Towamba River estuary; (a) the annual precipitation, (b) flow discharge, (c) mean air temperature, and (d) monthly mean sea level (at Australian height datum). (BOM, 2017b, and KINMI climate explore).

Air temperature has increased over the past 55 years since 1960, with some fluctuations (Fig. 5.2c). This reflects the global warming trend. Towamba estuary has a temperate oceanic climate (Cfb) with an average temperature of 15.38°C - 16.78°C (BOM, 2017b).

Global warming and climate change are also responsible for the recorded local mean sea level rise (Fig. 5.2d) from the tide gauging station at Eden. Monthly analysed data from 1970 to 2015 from the Eden gauging station yielded a positive trend with sea level rising by 0.036 m over the last 45 years. The average monthly mean sea level is now at 0.836 m; the maximum recorded sea level was 2.187 m on 14th June 1999, whereas the minimum record was -0.380 m on 2nd December 1986 (BOM, 2017b).

5.3 Methods

Changes in the areas of the eco-geomorphic estuarine units, like wetlands and sandspits, have been assessed by measuring the landcover on RS datasets over time using a GIS analysis approach supported by fieldwork investigations and related laboratory analysis. Analyses of the shoreline have determined the changes in erosion/accretion rates at the study site whereas changes of mangrove and saltmarsh areas (as a landcover function) illustrate the shoreline and vegetation canopy stability in the Towamba estuary.

This project was implemented using a multifaceted methodology. It started with GIS and RS based analysis to identify and classify the landcover, shoreline and vegetation changes at this specific study site depending on recent and historical records of aerial photography, satellite imagery and LiDAR data. This was combined with fieldwork – sampling the water, soil/sediment, a GPS barrier survey, and the bathymetry of the active channel. Laboratory analysis of the samples was involved as well.

This research quantifies and divides the methodology into three main parts (Fig. 5.3).

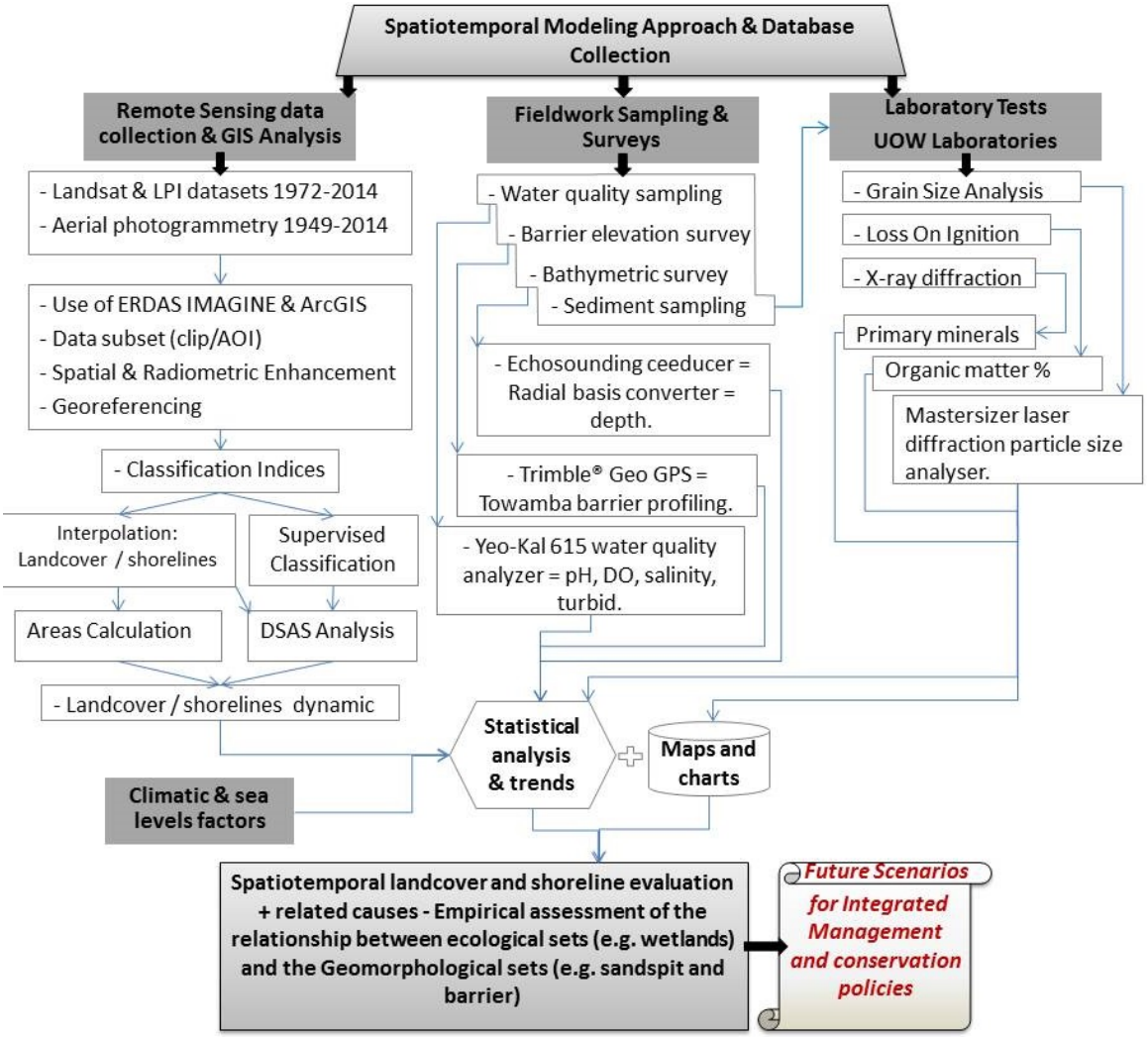

Figure 5-3. The spatiotemporal eco-geomorphic changes modelling approach, database collection and analysis sequences.

5.3.1 Remote sensing data collection and GIS analysis

Remote sensing and GIS datasets, which have optimum relevance according to the current literature (Calzadilla *et al.*, 2002; Hughes *et al.*, 2006; Giri *et al.*, 2011; Al-Nasrawi *et al.*, 2017a, 2017b), were used to classify landcover classes from 1949 to 2015 using fuzzy membership function. LiDAR (2004 and 2010) and SRTM (2011) data have been analysed in ArcGIS10.2 to create the DEMs. LiDAR and SRTM data sets have been used to extract various DEMs using TIN and surface analytic GIS tools for elevation analysis and validations. Kriging, clipping, and masking have also been used in ArcGIS10.2 to incorporate the resultant fieldwork analyses.

5.3.1.1 Photogrammetry; shoreline digitizing

Historical aerial photogrammetry of the Towamba estuary was used to model the spatiotemporal estuary dynamics. The whole estuary has been captured at; May 1949, June 1972, June 1998, and April 2014. ScanMaker 9800XL Plus (A3 Colour Scanner) having a resolution of 600 dpi was used to digitalize the selected photographs. The sources for these images include Land and Property Information (LPI, 2014), Land and Property Management Authority (LPMA, 1998), Department of Lands (1972) and Army Survey Core (1949). ERDAS IMAGEN v2014 software was used to orthorectify the digitised aerial photographs, with at least six points as ground-control distributed around the estuarine area on each image to defining the estuarine eco-geomorphic systems.. For increased accuracy of the orthorectified images, the chosen points were digitised with a maximum root mean square error of 0.05. In addition to the ground-control points, a digital elevation model was used for orthorectification. The most accurate digital elevation model (derived from LiDAR data; Land and Property Information, NSW (LPI)) available for the Towamba estuary area, was accurate to 1 m in the horizontal plane. If carried out carefully, the image-to-image techniques give accurate correlation of spatial features over time (Hughes *et al,.* 2006; Hopley & Jones, 2006; Al-Nasrawi *et al.,* 2017b).

5.3.1.2 Multitemporal imagery classification

Landsat-resolution data has enough detail to capture the eco-geomorphic distribution and dynamics of estuaries (Giri *et al.* 2011). However, small patches (< 900–2700 m^2) of classes along a small coastal estuary cannot be identified from these data (FAO 2003). Thus, Landsat datasets have been combined with high-resolution (50 cm) satellite RS data from LPI (Fig. 5.4a), and aerial photographs, to assess and monitor the study site, as shown in Fig. 5.4b.

Imagery classification helps monitor the estuary and is the first step in checking the historical records for eco-geomorphic changes. Landsat images of MSS, TM, ETM+ and LPI supervised

classification were used to identify, group and label features in an image according to their spectral fingerprint. In supervised classification, pixels are clustered together based on spectral homogeneity and spectral distance using an identified fingerprint from each class. ERDAS IMAGEN software has been used to provide supervised classification, using eight classes and ignoring the zero values. Figure 5.5 shows the results and traces the general multitemporal dynamics over the last 43 years (1972, 1984, 1993, 2004, 2010 and 2015).

5.3.1.3 Future estuarine scenario

Another modelling exercise/implementation has generated the future scenario of the estuary, by using the resulted shapefiles of the Towamba estuary and its growing rates. Simulating future growth scenario technically is as in the following steps to estimate and detecting the areas that will be gaining ground in 21st Century; using Animation manager tool of the ArcScene 10.4, by converting the resulted shapefile above to a raster grid format, which would generate a gradient pixel values for each specific class type that considering the neighbouring class relationships. Now, these pixel values will be considered as a Z values in the simulation processes. Then, creating a polygon (to be blued second layer representing water bodies) covering the area to and to be zero levelled. After that, from the Display menu of the raster properties, Cubic convolution (for continuous data) need to be used to choose the; Base Heights, floating on a custom surface, and change the custom default elevation (to 300 or whatever will make a logical 3D shape), after that Calculate from extent tool, from the ScenLayers properties, will generate the 3D shape. Finally, create Animation Key frame (for the polygon) from the Animation manager tool, add number of these keys and change their “Z” value to the historical rates of landcover and shorelines of the existing situation to generate the future scenario, however, the growth rates need to be revised oppositely (for example positive values to negative values) to allow the eco-geomorphic sets to inundate the water bodies (the zero levelled polygon), and then simply run and save the scenarios using animation controls panel.

5.3.1.4 Shoreline change tracing using DSAS analysis

"The Digital Shoreline Analysis System (DSAS) is a freely available software application that works within the Environmental Systems Research Institute (ESRI) Geographic Information System (ArcGIS) software. DSAS computes rate-of-change statistics for a time series of shoreline vector data. The last version is 4.0, which was released in May 2009 and is compatible with most of ArcGISs. It is supported on both Windows XP and Vista operating systems" (Thieler *et al.*, 2009).

DSAS has been utilised to track the shoreline position on the most dynamic part of the estuary (the estuarine barrier) utilising RS data from 1949, 1972, 1998 and 2015 and the DSAS was used to quantify the rate of barrier changes over a 65 year period (Fig. 5.12). The DSAS analysis has used 274 transects sampled along the front and back (137 each) at 50 m intervals along the barrier shorelines using a centred baseline (offshore) on the middle of the barrier (Fig. 5.12a). To calculate the rate of shoreline changes over the study period, two statistical methods have been used: the net shoreline movement/envelope and the linear regression rate (Thieler *et al.*, 2009; Tran Thi *et al.*, 2014).

5.3.2 Fieldwork sampling, laboratory and modelling methods

GIS and RS changes monitoring the evolution of the Towamba estuary eco-geomorphic changes during the past 65 years were combined with fieldwork in November 2015 consisting of 35 sediment samples, 16 water quality sample analyses, and 11.13 km of bathymetric and barrier elevation surveys. The downstream river portion located just upstream from the estuary was included in the fieldwork investigations to allow more understanding of the existing situation.

5.3.2.1 Soil and sediment samples

35 sediment and soil samples from the estuary were analysed for grain size and loss on ignition, and the mineralogy was assessed using X-ray diffraction. Samples of sediment were obtained in November-2015, ranging from a 500 m/point grid at the estuary mouth to 1 km spacing at the lower-river section (see Fig. 5.8 for sample distribution).

(a) Particle Size Analysis

Grainsize, sorting, skewness and kurtosis were determined to evaluate the transport distances, source and depositional conditions of each sample. Coarse fractions of the samples were washed with fresh water, sub-sampled to ~100 g aliquots and dried at 60°C. The Blott (2010) GRADSTAT TM v8.0 method was used for grain-size analysis. Using Krumbein and Pettijohn's (1938) approach, the phi scale was used to calculate the logarithmic particle parameters. A Mastersizer 2000 laser diffraction particle size analyser was used to measure fractions finer than 2 mm.

A kriging interpolation tool was employed in ArcGIS, to produce a gridded map with 10 m spatial resolution over the Towamba estuary based on the 35 sampled locations. The sediment grain characteristics, including percentage of sand, gravel, silt/clay (mud), skewness and sorting was then visualised for spatial pattern assessment.

(b) Loss on ignition (LOI)

The 35 soil and sediment samples were analysed for organic matter components (% OM) using LOI to evaluate its involvement in changes in elevation with respect to the water table, as well as, it helps to develop the ecosystem abilities such as soil stage/ability. The sediment samples were dried at 60°C, crushed and five grams was placed in the ignition oven at 450°C/24 hours, as it is the best temperature can be applied to fluvial bed sediments according to Sutherland's (1998) approach. Samples were weighed again after organic matter had been burned to evaluate the LOI.

(c) X-ray diffraction (XRD)

XRD analysis was conducted on 35 representative samples to determined primary mineral composition within the various facies (Table 5.4). The samples were dried at 60°C and then crushed. The XRD utilised a PW1130 copper tube, a Spellman DF3 generator and SIE 112 software. The samples were analysed from 4° to 70° 2θ and the diffraction traces were assessed using Traces, UPDSM and SIROQUANT software to identify the minerals present.

5.3.2.2 Water quality analysis

Water quality of 16 samples was determined in the field using a Yeo-Kal 615 water quality analyser to assess the health of the eco-geomorphic system. This system is influenced river by water quality and flow, including the quantity of suspended sediment and salinity levels. The water quality analyser provided real-time readings of turbidity, salinity, conductivity, pH, and dissolved oxygen between Kiah (Fig. 5.1) to the seaward end of the estuary as shown in Fig. 5.10.

5.3.2.3 Bathymetric survey

Bathymetric data was collected using a UOW-boat-mounted Ceeducer echo-sounder. Sounder accuracy was checked and confirmed using a hand held high resolution-GPS (10 cm) and a 3 m measuring stick. The initial bathymetric survey was conducted over a two day period in November 2015. A bathymetric survey was conducted along the active channel of the estuary and adjacent river using an echosounding Ceeducer in combination with an RTK-antenna-GPS linked to the nearest ground-control stations and 4G mobile phone. This achieved an accurate bathymetric survey with true time and location accuracy according to the local height datum (zero level) to avoid any tidal-dynamic effects.

Collected data, in the form of an X, Y, Z point cloud, recorded every one second from the estuary entrance to 11.13 km upstream. A total of 10726 bathymetric points were collected. The data were downloaded from the echo sounder, using 'Ceeducer download utility'

software, prior to being filtered using 'echo sounder data reader' software, which analyses the data and removes any obvious errors in it. In addition to the software filtering, manual data filtering was used to identify and remove inaccurate bathymetric depth data points. The filtered data was imported into ArcGIS where the data were further assessed and remaining inaccurate data points deleted. The remaining corrected data points were then interpolated and projected in 'ArcGIS 3D analyst' to produce a draft bathymetric model. The bathymetric data were converted to a suitable format that can be acceptable in ArcGIS processing environments using Microsoft Excel. After that, they were imported in ArcGIS 10.2 as a table data-base by choosing the 'Display x, y, z data tool' that identified the easting, northing and the Z value (choosing the suitable coordinate system is part of this step), and then interpolating the surface by using 'Radial Basis Functions' (Geostatistical analyst tool) and using the Completely Regularized Spline to get the gridded surface. Finally, some of the masking and extracting tools were used to produce a suitable shape for the layout results (Fig. 5.11).

Visual assessment of the draft model indicated that some areas lacked sufficient data coverage. To rectify this, additional bathymetric survey data points were collected using the same methodology as outlined above. Webb, McKeown & Associates (1993) noted that the tidal range within the central portion of the basin is only 0.037 m. Due to the limited tidal range it was deemed unnecessary to account for it as it would have a negligible effect on the data collected.

5.3.2.4 Coastal barrier elevation survey and profile analysis

A high resolution-GPS surface survey of the Towamba estuary and coastal barrier was carried out using the high accuracy Trimble® Geo GPS (10 cm) during fieldwork (Fig. 5.12a) for: (i) the site investigations and for (ii) the remote sensing data geo-referencing (orthorectification). This equipment was connected to a mobile phone's 4G (internet access) for position correction to achieve the true time and position. The system is connected to the nearest ground-GPS-control station (Eden station) to get the elevation relative to the local height datum (zero level) to avoid the tidal-dynamic effects. The analysis generated a gridded DEM for the barrier island (Fig. 5.12b), and a raster elevated according to this DEM (Fig. 5.12c). The barrier profile was checked for accuracy along three sections as shown in Fig. 5.12c, d.

5.4 Results

The results show significant coastal eco-geomorphological change, caused by estuary geomorphic growth and land use development. This has resulted in expanding the coastal

estuary ecosystems, such as growing and establishing saltmarsh, mangrove and mudflat zones.

5.4.1 Catchment and land use classes

Both the existing situation and historical records have been utilized. Most of this study of the Towamba River catchment was conducted through imagery. Land use classification has determined the proportion of human modification within the Towamba basin and assessed the extent that these human activities have impacted on sediment availability, transport and deposition (Fig. 5.4; Table 5.1).

Figure 5.4a is a DEM of the catchment surface that shows a high-sloped terrain and complex surface with elevations from 0 to 1368 m along the Towamba River for ~58.6 km representing an average 2.3% slope. In fact the slope is much higher in the upper parts of the valleys, while limited human clearing (12%) occurs in the middle catchment (Fig. 5.4b). The more detailed supervised classification map (Fig. 5.4c) proves that this area actually has about 14% modification, and 86% remains as untouched area.

Figure 5.4d is based on high spatial resolution datasets from Australian Land Use and Management (ALUM, 2010), that shows a mostly unmodified catchment (86%) in dark and light green.

Human settlement has established grazing, urban areas and other modifications (see Fig. 5.4). These transitions in land use are associated with clearing native vegetation, resulting in changes to the drainage network hydrology and eco-geomorphologic characteristics of catchments and their runoff. These landuses around the catchment are changing the amount of the sediment availability in the long term, as well as affecting water quality by contaminants, such as organic matter, entering the waterways. Together these modifications can alter the eco-geomorphic characteristics and in some cases cause serious degradation. This results in a series of sedimentation problems in the estuary that could increase the shoreline erosion rates and cause ecosystem losses, such as wetland communities.

The Towamba River catchment contains small towns: Kiah, Towamba, Pericoe, Burragate, New Buildings, Coolangubra, Wyndham and Rocky Hall. Very low populations live in these towns, for example, the highest population is in Towamba town with just over 360 people (ABOS, 2007). Thus most of the catchment is uninhabited (86%) with natural processes controlling the eco-geomorphological systems in the catchment. Figure 5.4 and Table 5.1 show large areas of the catchment (63%) covered with native vegetation, such as the national parks at Mount Imlay, Towamba State Forest and Nullica State Forest, plus 21.9% of tree and sub-canopy cover along the river/drainage system and the downstream wetlands. Only 14% of the land cover has

been modified or controlled by human settlement for rural and urban land uses (Fig. 5.4; Table 5.1).

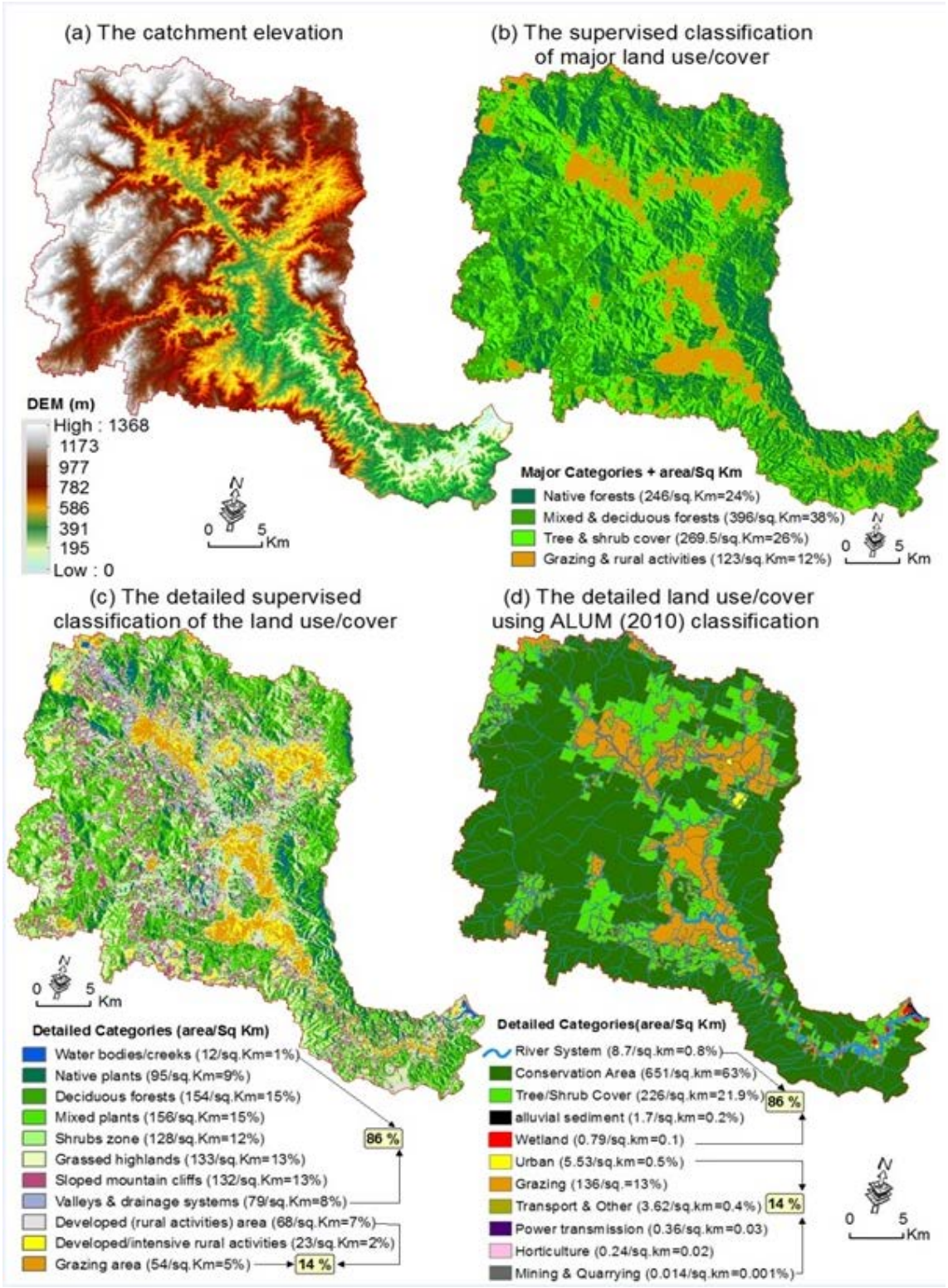

Figure 5-4. (a) Elevation of the catchment showing the terrain and high-sloped watershed. (b-d) Towamba River catchment showing; land use classes and area (km^2) from (b) major categories supervised classification, (c) detailed supervised classification, and (d) detailed categories using ALUM (2010). Sources; (ALUM, 2010;USGS-LANDSAT, 2016; LP-DAAC, 2017).

All of the catchment analysis methods have proven that the catchment has a small proportion

of human activities and modification (rare worldwide) representing a mostly untouched catchment, whereas the DEM has shown a high-sloped basin area which allows natural geomorphic processes and high runoff velocity to dominate.

Table 5-1. Landuse classes in Towamba River catchment showing area, percentage of each category and type of major category process

Landuse Classes	Area (km^2)	Each category (%)	Major Category (%)
River and drainage system	8.77	0.8	Natural processes controlled area
Conservation area	651	63	
Tree and shrub cover	226	21.9	
Special category	1.68	0.2	
Wetland	0.79	0.1	**86%**
Urban	5.53	0.5	Human modified area
Grazing	136	13	
Transport and other corridors	3.62	0.4	
Power transmission	0.36	0.03	**14%**
Horticulture	0.24	0.02	
Mining and quarrying	0.014	0.001	
Total	**1034**	**100**	**100**

Source: Attributes and metadata are from land classes generated using ArcGIS 10.2 in Fig. 4d. Classes have been derived from ALUM (2010)

5.4.2 Multitemporal imagery classification of the estuary

Supervised classification (Fig. 5.5) obtained using ERDAS IMAGINE employing the 'Maximum Likelihood Classification tool' with the 'Training Sample Manager' (8-10 chosen training-area of each class as a finger print to identify each landform distribution, to achieve the maximum accuracy). Maximum likelihood (ML) has been used as it can give the best results, as Woodward et al, (1984) have stated: "those ML techniques are normally superior to other methods for imagery component distributions" (Woodward *et al.*, 1984). The classification process has resulted in four major classes represented in raster gridded distribution (Fig. 5.5). Later the 'Zonal Geometry As Table' (a spatial analyst tool in ArcGIS) was used to calculate the landcover area changes (excluding the statistic attributed areas of these rasters) for each year (Table 5.2 and Fig. 5.6).

Figure 5.5 shows the multi-temporal analysis of RS data using GIS tools, which indicates that the Towamba estuary and its eco-geomorphic systems have achieved a significant growth of deltaic facies (approximately 0.8 km^2) due to sediment accumulation. This has resulted in the tidal channel being restricted and a seaward movement of the barrier. Additionally, it indicates that most of the vegetation canopies (like *Casuarina* and *Juncus*) and the new saltmarsh areas (seen in 1949) were growing on the stable sandspit areas and started mixing with mangroves in the tidal zones as a result of sea-level rise. The mangrove cover (grey mangrove - *Avicennia*

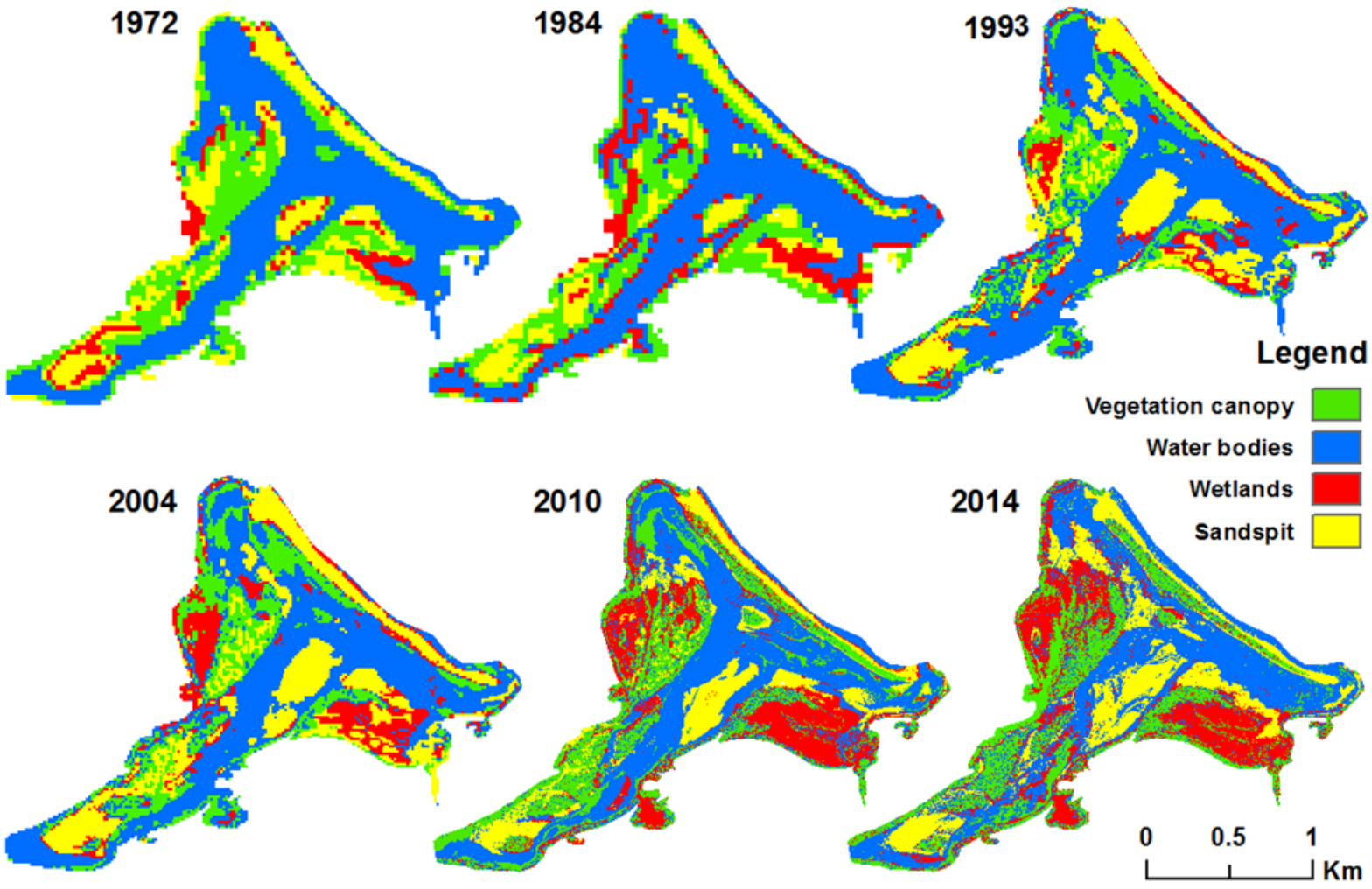

Figure 5-5. Supervised classification (raster gridded) of the Landsat imagery (MSS-1972, TM-1984, TM-1993, ETM+2004, ETM+2010 and ETM+2016) shows a clear increase in all coastal landform covers (classes) associated with a decline in water bodies. Sources: (LPI, 2010 & 2014; USGS-Landsat, 2016).

marina) has gained ground because of the prograding shoreline. New geomorphic areas have become suitable habitats for ecosystem growth, such as mangrove and saltmarsh, as well as the native plants such as *Casuarina* and *Eucalyptus*, which have continued to stabilise the estuarine delta.

Table 5-2. The total and rates of growth of the Towamba estuarine eco-geomorphic landform system*.

Platform class	1972	1984	Rate of change (%)	1993	Rate of change (%)	2004	Rate of change (%)	2010	Rate of change (%)	2016	Rate of change (%)
Vegetation canopy	225232	268434	1.59	367475	3.65	393926	0.98	409206	0.56	532897	4.56
Water bodies	2318485	2244074	-2.74	2002143	-8.92	1926616	-2.78	1786311	-5.17	1443878	-12.63
Wetlands	111010	135656	0.91	216142	2.97	241906	0.95	432957	7.04	519023	3.17
Sandspit	57328	63891	0.24	126294	2.30	149607	0.86	83581	-2.43	216257	4.89

*Note; for more accuracy, all the imagery has been georeferenced and converted to the local Australian Datum GDA-MGA-1994/zone 55, and the root mean square error (RMSE) was ±5.32 metres.

Qualitative changes in the pattern of land cover, river banks, channels and broad changes in the inter-tidal area since 1949 have been determined (Figs 5.5, 5.6a, b, 5.7a-c and Table 5.2). The main features shown by the multitemporal estuary changes between 1949, 1972, 1998 and 2014 involve growth of the barrier, the land cover of native plants, mangroves and saltmarsh, and a reduction of the tidal channel. Spatial patterns of accelerated accumulation of sediment in the Towamba estuary are shown in Fig. 5.5b. Net accretion and erosion in different areas/classes are summarized in Fig. 5.5c. The sub-tidal zone and the estuary tidal channel experienced net accretion (and size reduction) in all four time intervals, as well as the barrier, but especially from the 1990s to recent time. At the same time, the tidal channel and the rocky edges around the estuary have been restricted and lost area by sediment accumulation during the whole period of this study with only a slight reversal between 1998 and 2014. The narrowed and shallowed channel forced the Towamba River entrance to discharge farther eastward mainly due to the barrier/island growth, as shown in Fig. 5.7.

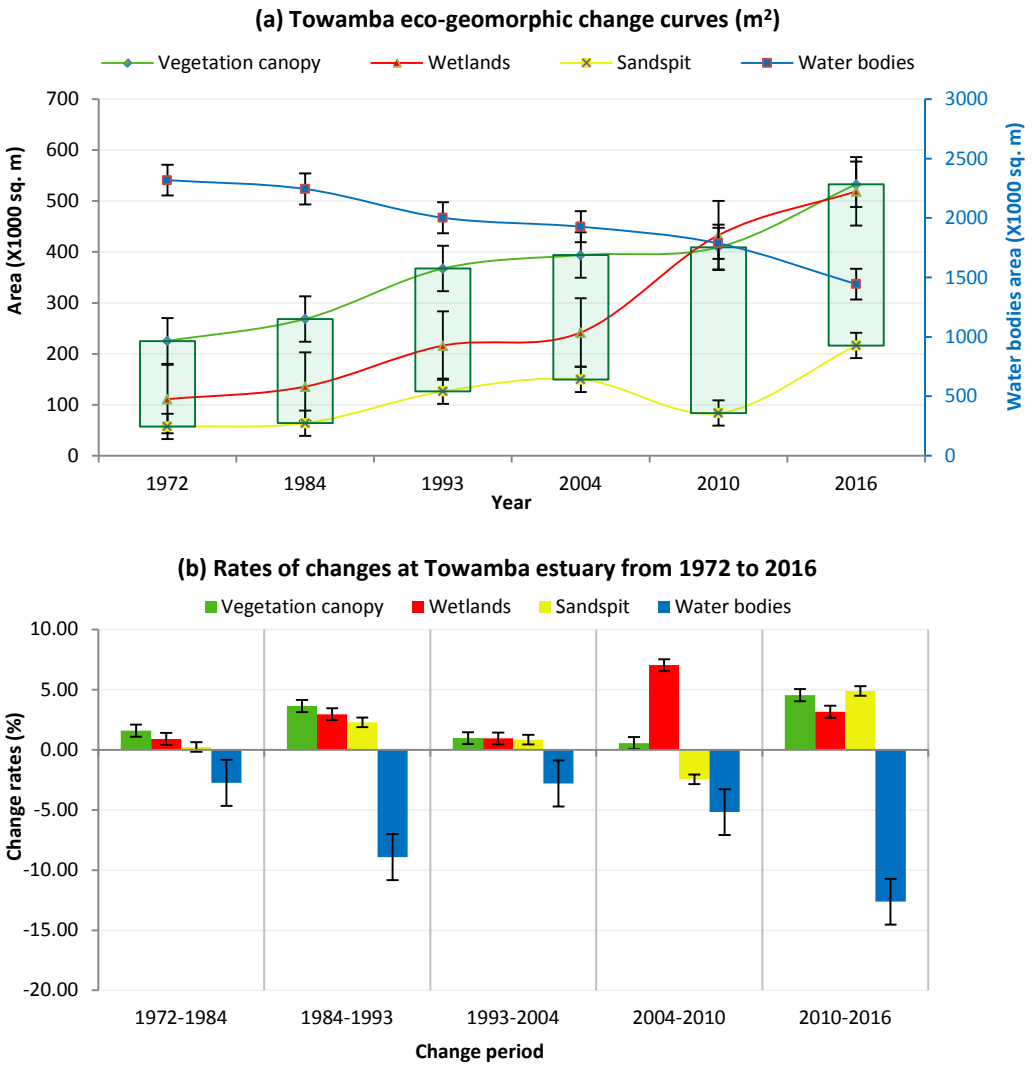

Figure 5-6. (a) Growth of Towamba estuarine eco-geomorphic landform areas (green, red and yellow) and a decline in water bodies (blue). (b) Rate of change percentages between 1972 and 2016. (Uncertainty bars based on standard deviation error of average 5%).

The shallow/active channel of the Towamba River has divided the estuary into two sides with floodplain, sandspits and the associated land covers, and continues building on both sides. It was also a prominent feature which had evidently extended the land classes between 1949 and 2014 (Fig. 5.7a,c) by the following amounts: sandy banks (82377 m^2), barrier (57989 m^2), native plants (97372 m^2), mangrove (17891 m^2) and saltmarsh (163774 m^2). Simultaneously, there was a clear decrease of tidal channel (-149584 m^2) and rocky bed (-100211 m^2) area during same study period.

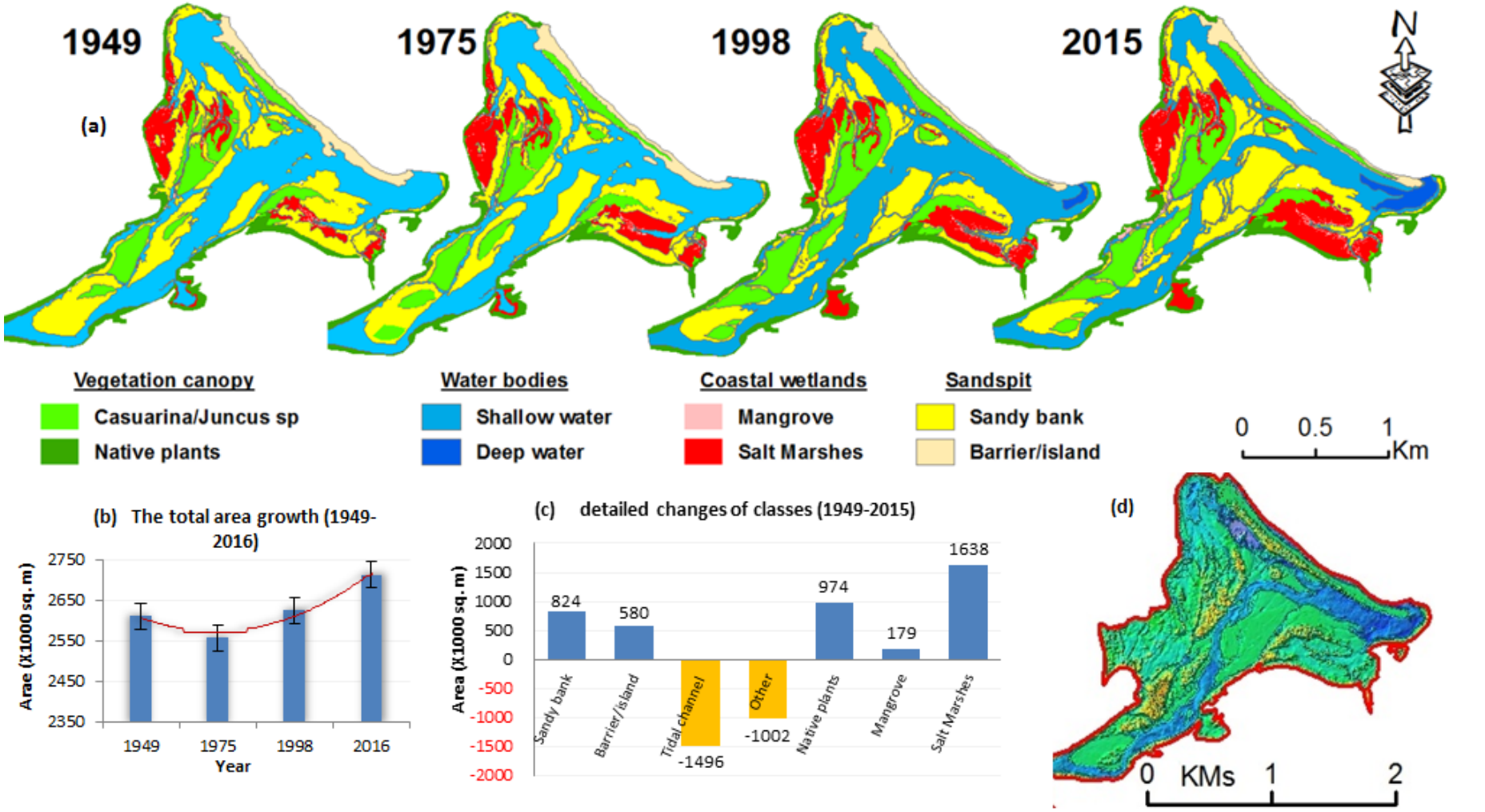

Figure 5-7. (a) Multitemporal (vector characterised) high-resolution imagery classification (aerial photographs; 1949, 1972, 1998 and 2016) showing a clear distribution changes of Towamba estuary classes and shorelines. (b) Total estuarine changes since 1949. (c) Total changes that occurred in each class. (d) The future scenario of the Towamba estuary resulting from continued vectored classes growth (resulted from sediment accumulation) estimated by GIS simulation tools using the historical change rates (1949-2014).

Finally, Fig. 5.7b shows a clear positive total growth, except for the 1975 decline. The total of growth was 169608 m^2 over the study period at an average of 2609 m^2/yr. Figure 5.5b shows a series of scenarios for sediment accumulation over time during the study period and, by applying GIS simulation tools, it has resulted in a predicted future situation that is presented in Fig. 5.7d. According to the rates of accretion and extension of the estuarine plains and habitats over the study period (1949-2014), the whole estuary will be filled by 2100 and the remaining tidal discharge channel will be very narrow with an infilled swamp on the western bank due to easier discharge flow out on the eastern side of the estuary (Fig. 5.7d).

5.4.3 Tracing the temporal-barrier changes

Towamba barrier is attenuating the waves to secure the ecosystem habitats behind it. The barrier and its vegetation cover have been clearly affected by erosion on its landward side (Fig. 5.8a, b). This has resulted in a loss of the seagrass beds and *Juncus* and *Casuarina* on the elevated island. In contrast accretion has occurred on the seaward side (Fig. 5.8c). In the meantime, the far south tail of the barrier is still active and too unstable to be vegetated (Fig. 5.8d).

Figure 5-8. The geomorphic changes on the Towamba estuarine barrier, showing; (a) location of the photos on the barrier, (b and c) erosion effects on the inside of the barrier (landward, middle and south respectively), (d) high accretion rates at the front of the barrier (seaward), (e) geomorphic-instability of the southern tail of the barrier.

Some of the eroded fluvial and barrier sediments pass into Twofold Bay via the active tidal

channel and are redeposited on the seaward side (Fig. 5.8c,d). A more detailed shoreline dynamic analysis of the barrier is shown in Fig. 5.9.

Figure 5.9a-c shows erosion along the landward side of the Towamba barrier, which has a shoreline maximum movement of about -84 m during last 65 years at a mean erosion rate of -1.294 m/yr. These changes occurred all along the landward side, except far north and south parts, with erosion more concentrated on the southern part. Significant accretion occurred on the seaward side of the barrier, with a maximum shoreline movement of 119 m within last 65 years at an averages accretion rate of 1.831 m/yr.

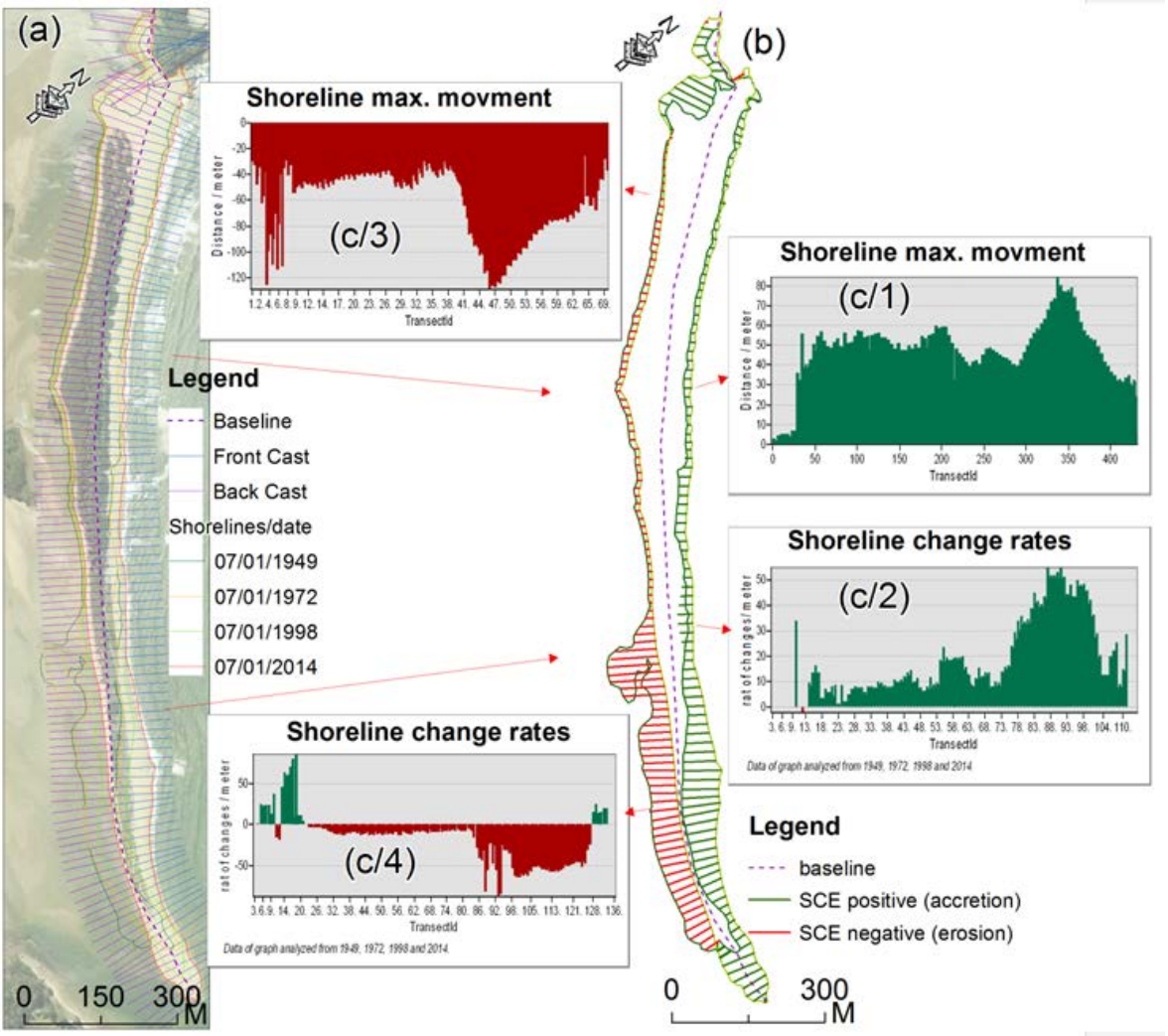

Figure 5-9. Digital shoreline analysis system (DSAS) has used to investigate the changes on the front and back sides of the barrier, showing; (a) the coastal barrier shorelines overtime and the DSAS transect/base lines, (b) the net shoreline movement (NSM) between the 1949 and 2014 shorelines: (c) c/1, 2, 3 and 4 show net shoreline maximum movements and the linear regression rate for the front and back sides of the barrier, respectively (red is erosion and green is accretion).

5.4.4 Samples analysis and modelling

5.4.4.1 Soil and sediment samples

(a) Particle Size Analysis

The soil and sediment sample analysis has generated the results shown in Figs 5.10 and 5.11. Most of the estuary is made of sand (up to 98% sand), especially along both sides of the barrier and in the active tidal channel, where wave and tidal energy has a significant effect on the construction of these parts of the estuary (Fig. 5.11a). Figure 5.11a also shows high sand proportions in the upper part of the estuary and lower part of the river. Clay and silt constitute more than 20% of the samples along the middle part of the Towamba estuary (Fig. 5.11b), especially on the left and right banks where sediment was derived from the river catchment and deposited by flocculation in the higher salinity wave attenuation zone.

The mean particle size of the samples ranged from 166-1013 µm (Fig. 5.11c). The coarser samples are limited to the upper river samples, whereas medium to coarse sand with minor gravel component (0.3 to 5%; Table 5.3 - Towamba 7 and 30) are concentrated in the lower estuarine parts, especially along the barrier (Fig. 5.11a). Contrariwise, the mud component (0.0 to 53.3%; Table 5.3 - Towamba 2 and 3) is mainly distributed along the middle of the Towamba estuary (Fig. 5.11b).

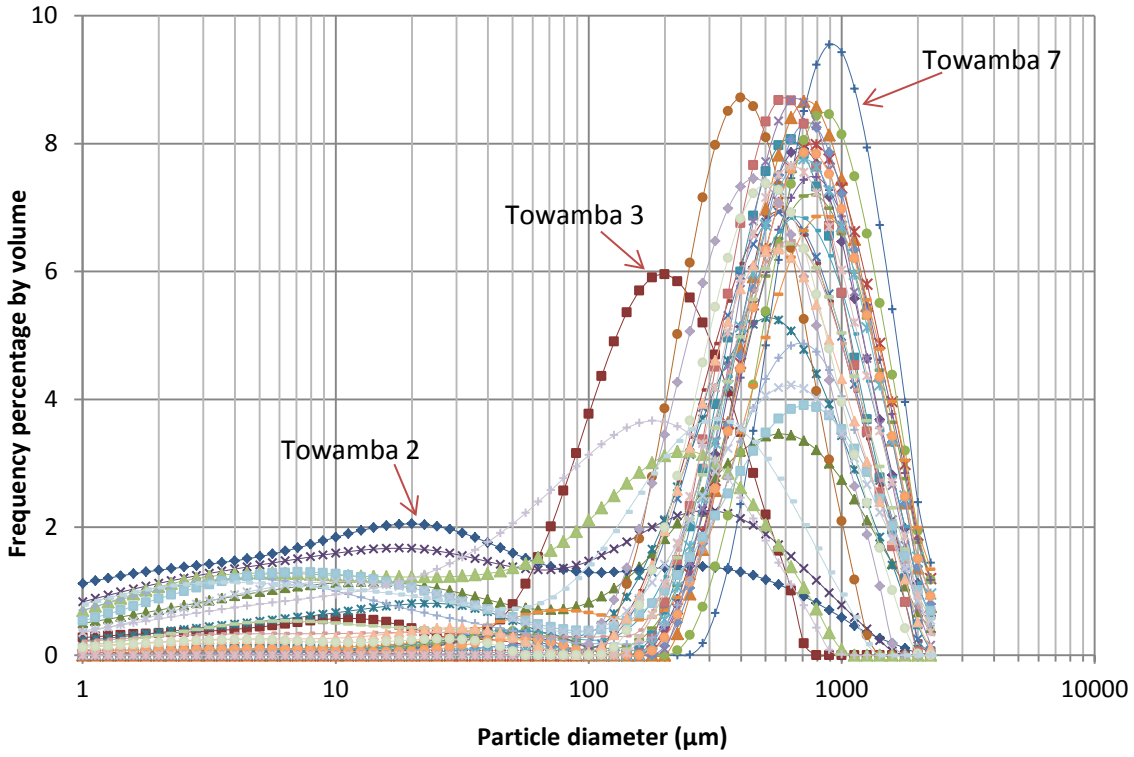

Figure 5-10. Particle size analyses of the 35 sediment samples (multi-coloured) have shown that the accumulated sediment in Towamba estuary mostly contains a large proportion of sand. The sediment samples have been taken from the estuary and the lower Towamba River, from the river mouth to Kiah village.

Many of the 35 sediment samples have a range of particle sizes from clay to silt and sand, with samples such as Towamba 2 being dominated by mud (Fig. 5.10 and Table 5.3). Other samples have high fine sand components (e.g. Towamba 3) while samples from the sandspit consist entirely of sand (e.g. Towamba 7; Fig. 5.10 and Table 5.2).

Table 5-3. Representative particle size analyses of the sediment samples from Towamba estuary, showing the proportion of sand and mud (silt plus clay).

Sample No.	Sand %	Silt %	Clay %	Mean grain size (µm)	Mode 1 (µm)	Mode 2 (µm)	Sorting (phi)	Skewness
Towamba 2	46.0	48.3	5.7	166	54	372	2.48	-0.01
Towamba 3	86.0	12.8	1.2	281	306	35	1.38	0.43
Towamba 7	100.0	0	0	1013	976	0	0.49	0.02
Towamba 30	93.6	6.2	0.2	632	626	68	1.11	0.33
all sample averages	**88. 4**	**10.7**	**0.9**	**649**	**701**	**73**	**1.26**	**0.24**

The sediment in the middle of the estuary (the central mud basin) contains silty clay and clayey silt, representing the suspended load that flocculated in the higher salinity zone. These deposits are represented in the saltmarsh, mangrove and associated habitats as a developed ecosystem.

Particle analysis shows that the sediment samples are typically poorly-sorted along the estuary, with well- to moderately-sorted sands concentrated on the sandspit (Fig. 5.11d).
Figure 5.11e shows the sandy samples in the northwestern part of the estuary have a normal (symmetrical) grain size distribution whereas most of the estuarine and river samples are fine to strongly fine skewed (0.1 to 0.67) indicating a higher proportion of fines compared to a normal grain size distribution. This corresponds to the higher mud contents through most of the estuary.

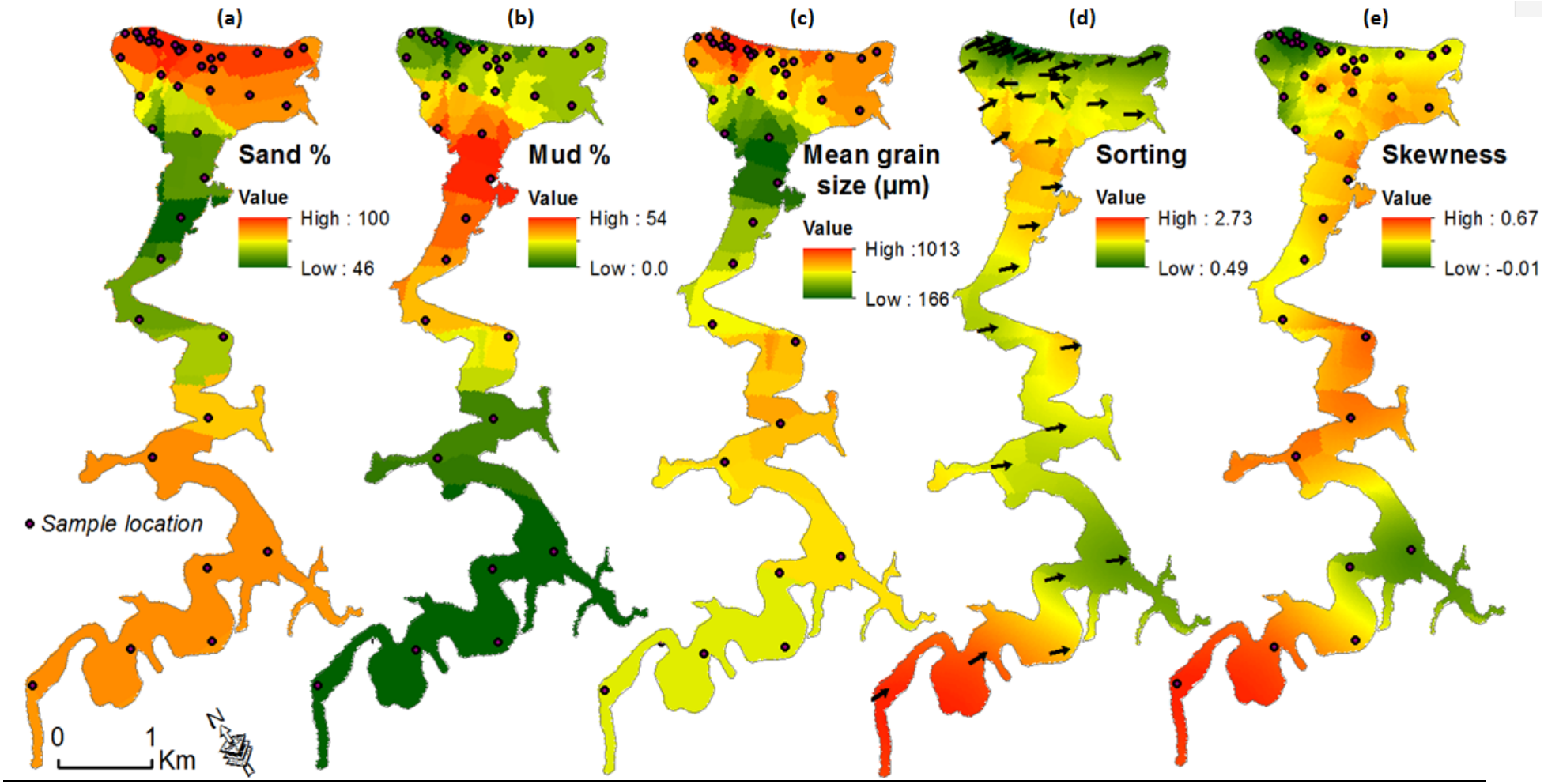

Figure 5-11. Soil, sediment samples and grain size analysis from Towamba River estuary; (a) sand proportion (including very small amount of gravel in some samples), (b) mud proportion (clay and silt), (c) sediment mean grain size, (d) sediment sorting (including the approximate sediment transport direction represented by the black arrows), and (e) Towamba estuary skewness. Note: the legend scales of (a) to (e) show different percentages across the colours.

(b) X-ray diffraction (XRD)

XRD results show a clear relationship between the estuary and the catchment sedimentary sources (Fig. 5.12a). All 35 sediment samples are dominated by quartz (average ~59%), while some parts of the estuary have more than 70% quartz (for example; sample Towamba 3, Table 5.4), especially those along the estuary channel and barrier/island where wave action has eliminated most of the softer minerals and clays (Fig. 5.12a). In the middle of Towamba estuary, both left and right banks and the active channel areas extending 6 km upstream, K-feldspar, albite and lithic sand grains form prominent components representing fluvial sands derived from volcanic, volcaniclastic and mudstone rocks in the catchment source area (for instance; Table 5.4 samples 3, 19 and 30). Clay content in the samples is highest in the low energy environments in sheltered reaches, but also occurs in the fluvial lithic sands through the diagenetic alteration of feldspars.

Table 5.4. Representative XRD analyses of the sediment samples from Towamba estuary showing the mineral proportions.

	Quartz	Albite		Illite	Illite-smectite		
Sample		**K-feldspar**	**Labradorite**		**Chlorite**		**Kaolinite**
Towamba 3	78.1	6.6	3.4	2.2	3.2	5.8	0.4	0.3
Towamba 19	61.3	17.7	13.2	4.9	0.9	1.6	0.2	0.2
Towamba 30	52.5	25.8	17.8	1.2	0.8	1.4	0.3	0.2
all samples average	**59.1**	**17.0**	**12.8**	**4.3**	**4.1**	**1.1**	**1.0**	**0.6**

(c) Loss on Ignition (LOI)

LOI data show three main areas have the highest proportion of organic matter (OM; Fig. 5.12b and Table 5.5). One area on the barrier has up to a maximum of 11% OM (for instance; sample Towamba 34), which represents the native plants that have grown on the barrier. The second area is near the eastern bank (Fig. 5.12b) in the muddy middle portion of the estuary that has up to 24% OM (for example; sample Towamba 4) represented by saltmarsh and mangrove areas. The third section occurs near the western bank (Fig. 5.12b) in the very muddy area with the highest density of native plants mixed with saltmarsh and mangrove cover that contains up to 46% OM (for example; sample Towamba 2) in the northwestern part of the estuary. In contrast, some sandspit samples have the lowest OM% (e.g. 0.2, 0.4 and 0.6 in samples 24, 7 and 19, respectively). This reflects how much the OM is involved in the surface accretion and estuarine wetland elevation dynamics.

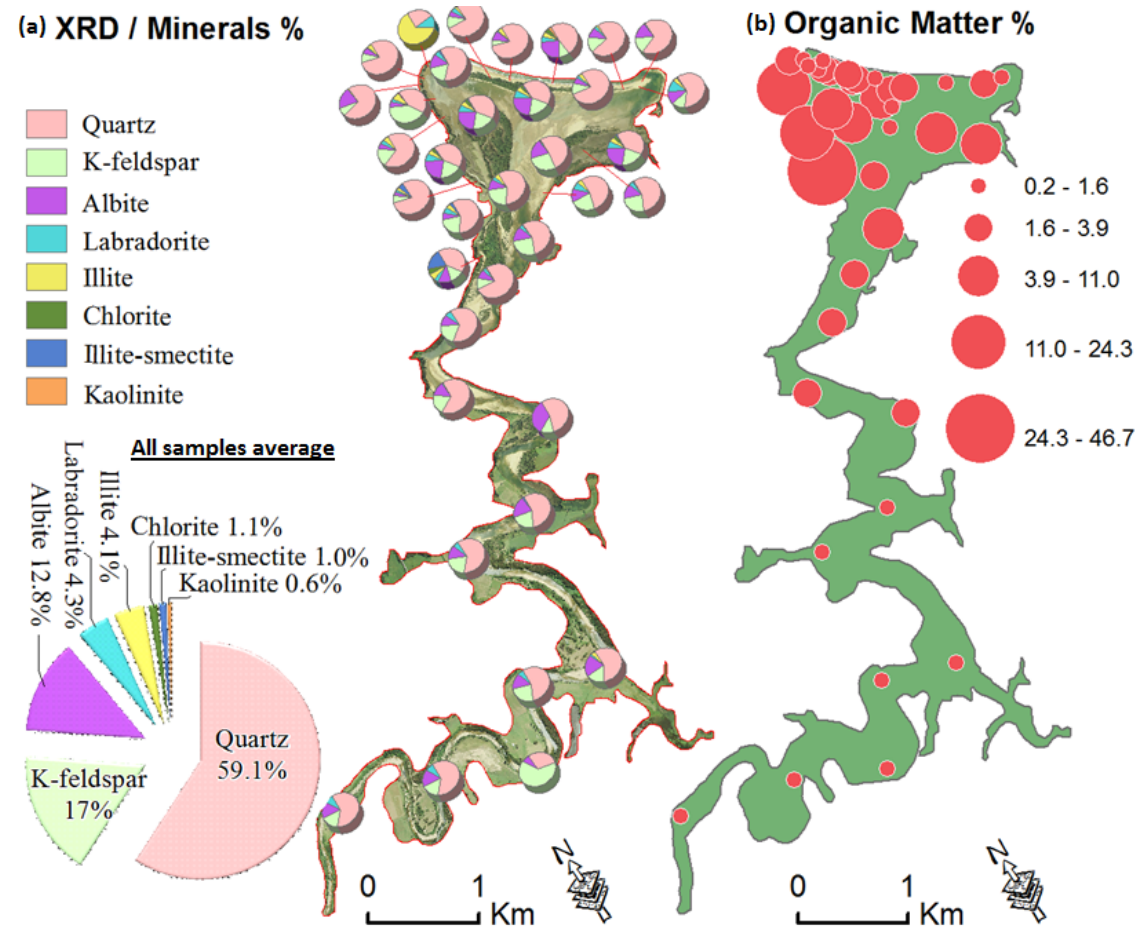

Figure 5-12. Soil and sediment samples from Towamba River estuary; (a) XRD results showing the mineral contents in the sediment samples at Towamba estuary, with a clear dominance of the quartz component, (b) organic matter components (%OM) based on loss on ignition, that clearly shows organic matter concentrated in the downstream part of the estuary, particularly on the wetlands sites.

Table 5.5. Representative loss on ignition (LOI %) analyses of the sediment samples from Towamba estuary showing the proportion of the organic matter.

Sample no.	***LOI (OM%)***	***Sample no.***	***LOI (OM%)***	***Sample no.***	***LOI (OM%)***
Towamba 2	46.71	Towamba 7	0.36	Towamba 30	1.21
Towamba 3	15.6	Towamba 19	0.58	Towamba 34	11.03
Towamba 4	24.27	Towamba 24	0.21	***All samples average***	***4.36***

5.4.4.2 Water quality analysis

Figure 5.13 shows a significant increase in conductivity, dissolved oxygen and salinity towards the mouth of the estuary while the temperature and pH show a very slight increase, due to shallower water that was easier to heat. In contrast, turbidity has shown a clear decline in the downstream direction, representing less suspended sediment that has flocculated and accumulated along the estuary as salinity increases. At the same time, the active channel flows more slowly towards the coastal end of the estuary especially during rising tides, which makes the river less able to transport both bedload and suspended sediments. These results clearly prove that abundant sediment is transported to the estuary leading to high rates of deposition

and bank accretion in these downstream areas. Thus the sediment is basically spread across the entire estuary and the suspended sediment becomes less and finer during its movement along the Towamba estuary due to flocculation.

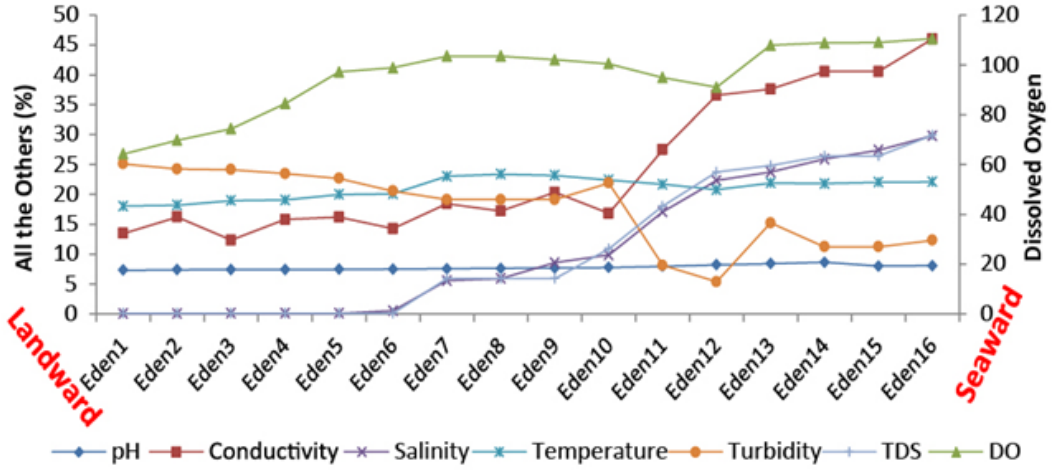

Figure 5-13. Water sample analyses show significant spatial changes in; conductivity, salinity, dissolved oxygen and turbidity.

5.4.4.3 *Bathymetric survey*

A bathymetric survey was conducted along the active and adjacent channels of the estuary showing that 1.15 m is the averaged depth and 2.99 m is the maximum (Fig. 5.14.

Figure 5.14 shows variations in water depth along the Towamba estuary and the adjacent river. It is clear that the deepest zones are at the ocean end of the estuary, where the narrow channel is discharging the runoff with its suspended sedimentary material. However, most of the river and estuary bottom has shallow water represented in the light green colour (Fig. 5.14) except for scour hollows on tight meander bends.

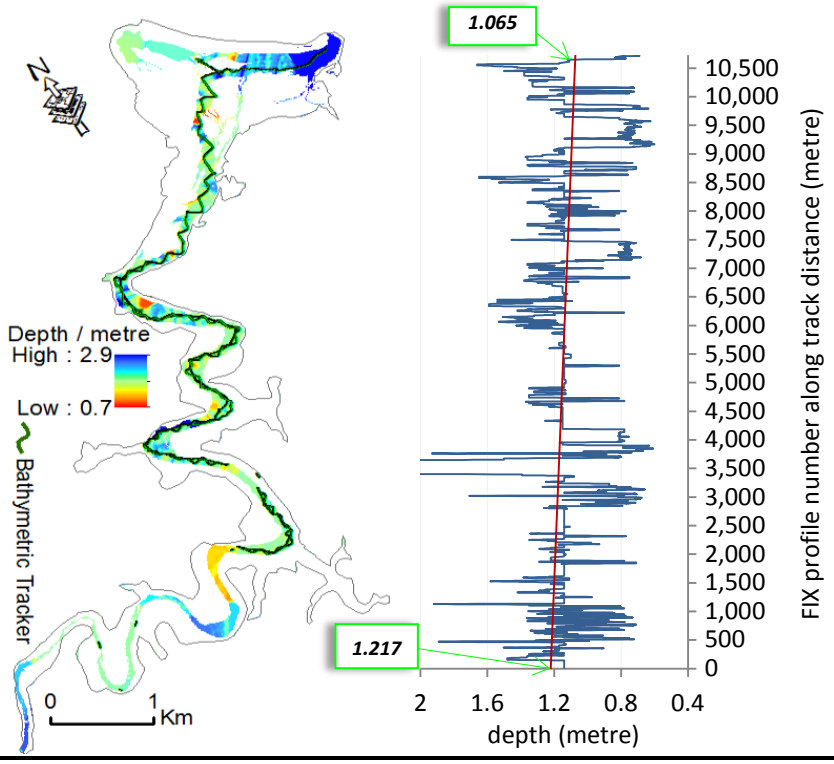

Figure 5-14. Bathymetric survey data and ArcGIS analysis are showing water depths along the Towamba estuary and adjacent river.

5.4.4.4 Barrier elevation survey and profile analysis

The collected datasets of the GPS survey were utilised to generate the island's Digital Elevation Model (DEM), and a raster elevation model according to this DEM (Fig. 5.15). The island profile was checked for accuracy along three surveyed sections as shown in Figure 5.15d. The barrier is 135 m wide in the north, 134 m in the middle and 51 m in the south (representing the youngest geomorphic stage) with an island length of 1913 m.

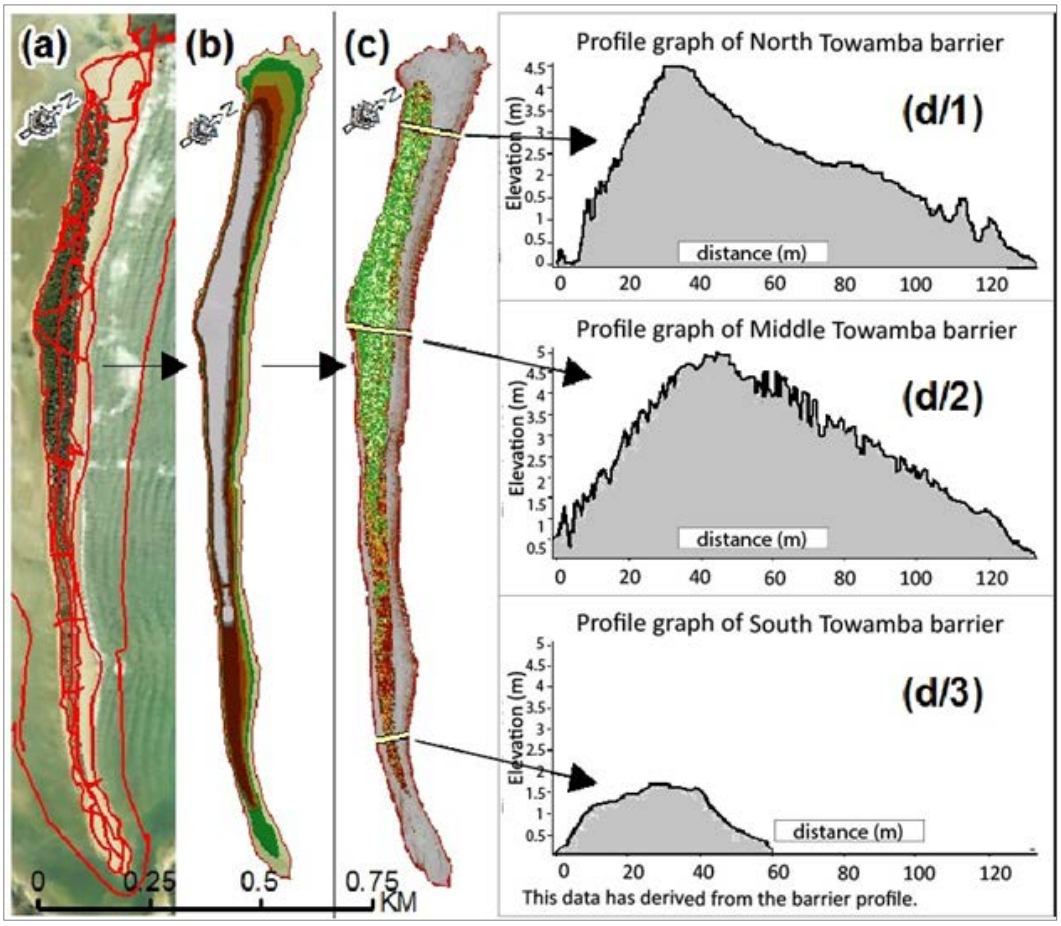

Figure 5-15. GPS elevation survey and barrier profile analysis of the Towamba barrier that has accrued at the end of the estuary. (a) GPS survey path tracker, (b) DEM generated, (c) 3D raster elevation, d/1, d/2 and d/3 are cross-sections through the north, middle and south of the island respectively.

Towamba barrier has the structure of a standard coastal sand barrier where, open water, beach, dune, mud flat, saltmarsh and mangrove sections are present in the standard order with appropriate vegetation cover (Fig. 5.16).

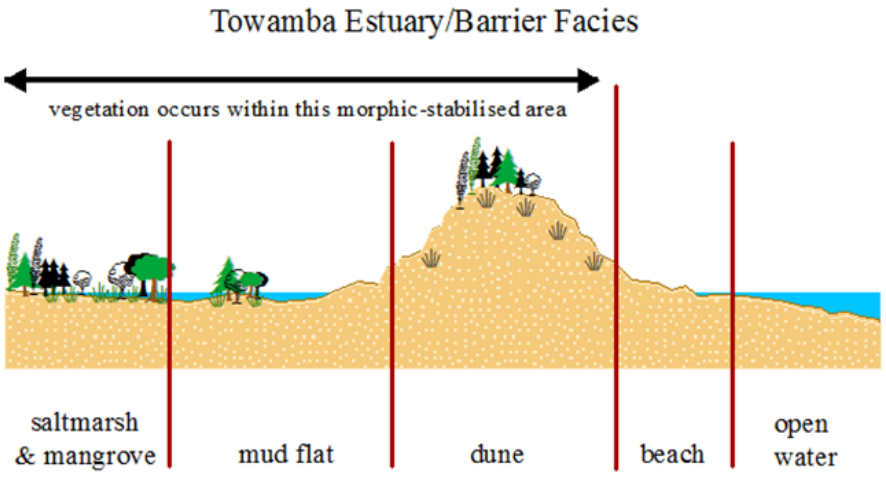

Figure 5-16. Towamba River estuary and coastal barrier is structured in a standard estuarine and barrier format. It has the five standard profile sections of open water, beach, dune (associated with mixed native plants, such as *Casuarina*), mud flat (associated with some plants such as *Juncus* species and saltmarsh/mangrove (associated with sea grasses).

5.5 Discussion

During the last century increased population and rural, urban and industries activities have been concentrated on coastal areas and have stressed and even overloaded these coastal ecosystems, threating the ecosystem's balance and even its loss globally (Parmesan & Yohe, 2003; Neumann *et al.*, 2015; Al-Nasrawi *et al.*, 2016a, 2016b, 2017b, 2108a, 2018b, 2018c). On the other hand, temperature increases during the 21st Century are causing climate change and mean sea-level rise (IPCC, 2014), significantly threatening many ecosystems, particularly within low-lying estuarine landforms/wetlands (Michener *et al.*, 1997; IPCC, 2014). Regionally and globally, estuarine ecosystems have high estimated economic values (in US$/year) per hectare as follows: lakes/rivers 8,498, tidal marsh/mangrove 9,990 coastal sea grass/algae beds 19,004, swamps/floodplains 19,580 and estuaries 22,832 (Batzer & Sharitz, 2014). Hence protecting wetland systems is very important both ecologically and economically.

5.5.1 Eco-geomorphic dynamics

The multitemporal analysis of RS and GIS data indicates that the Towamba tidal channel has clearly filled up as sediment was transported downstream from the catchment to the mouth of the estuary. This has added to the barrier at the end of the estuary, which has grown since 1972 (the oldest satellite data observations) to secure the eco-geomorphological system behind it and allow it to expand and develop its habitats. There is clear evidence of sediment deposition in front of the barrier on the embayment side since the 1990's (Figs 5.5-5.7). Towamba estuary is under constant eco-geomorphic growth due to both natural (weathering/erosion and deposition) and indirect anthropogenic forces (e.g. climate change and sea level rise). In the last few decades, Towamba estuary has mostly filled but the current sea level rise has produced additional accommodation space (Fig. 5.5a). The used data have consisted uncertainties errors, the reported changes are actually gained from different spatial resolution of satellite imagery and aerial photography, this limitation have been considered as a standard error within average of 0.5.

The multi-temporal change analysis approach (Fig. 5.3) has shown a steady eco-geomorphic growth and development at Towamba estuary in both sand flats and vegetation canopies (Figs 5.5, 5.6a/b and 5.7a-c). Results indicate that the Towamba estuary and its eco-geomorphic systems have achieved a growth of deltaic facies by approximately 0.8 km^2 due to sediment accumulation. However, erosion in some parts of the estuary (Figs 5.5-5.7) due to some big flood event, including in 1974 (Fig. 5.2b), restricted the net total growth to 169608 m^2 over the

study period at an average of 2609 m^2/yr. Results from this study predicted that the whole estuary will become filled by 2100 and the remaining tidal discharge channel will be very narrow with an infilled swamp on the western bank due to easier discharge flow out on the eastern side of the estuary (Fig. 5.7). The mud flats have a mixed zonation of sea grass, saltmarsh and mangroves while the barrier vegetation mainly consists of mixed native plants covering the northern and mid parts of the barrier and the southern area is grass covered except for the very south end that is too unstable for vegetation.

Figure 5.4a shows the characteristically high-sloped catchment surface and its river network with an average slope of 2.3% that has reduced the human impact to 14% (Fig. 5.3c, d; and Table 5.1) and has allowed natural-geomorphic processes to control 86% of the catchment area. Together these features provide a large runoff after rainfall events with sufficient discharge and velocity (Fig. 5.2a, b) to move sediment, through a shallow channel (averaged 1.15 m; Fig. 5.14), into the coastal estuarine area. Lower velocities caused by embayment attenuation, especially during rising and high tides and the slowly rising sea level (Fig. 5.2d), forces the accumulation of bedload and suspended sediment in the mouth of the estuarine zone. The mixing with saline water causes flocculation of the finer components (silt and clay) that are mainly accommodated in lower velocity areas away from the main channel. This has resulted in high deposition rates near the mouth of the estuary and into the embayment and fast ecosystem development, particularly in the muddy middle part of the estuary where more eco-geomorphic sequences such as saltmarshes and mangroves are forming. Coarser sediment is being added to both the inside and outside of the coastal barrier. In some cases the sedimentation styles and sequences can be related to events such as the flood history records and rising sea level.

The river basin consists of an elevated and sloped watershed surrounded by mountains and unmodified uplands that result in a highly variable discharge patterns. This determines the rate of transport and erosion. Within the downstream part the bank of the river is mostly composed of sandy unconsolidated Quaternary alluvium with little structural strength. Therefore, they are vulnerable to erosion through frequent slumping especially in areas with steep banks. Lastly, while riparian vegetation binds the banks preventing erosion, some areas have been cleared with no vegetation along the river bank which triggers slumping and the sediment is readily entrained by the flow and carried towards the river mouth.

5.5.2 Sediment characteristic impacts

LOI, XRD and grain size analyses of the sediment samples yielded the proportions of organic

matter, minerals and grain size (Fig. 5.11a-d). LOI (mainly due to organic matter) was use to evaluate its involvement in changes in elevation with respect to the water table. Also, XRD and grain size analyses of samples were used to assess their particle size, sources, depositional conditions and whether they represent ocean or river sediments. The rates of sedimentation and types of sedimentary sequences would then be related to events such as the flood history records and sea level rise. The modelled transport directions (black arrows; Fig. 5.11d) specify that the sediments were generally moving seaward through the estuary with local movement towards the main channel. The sediment has accumulated along the estuary sandspit with the excess discharged to Twofold Bay to be redistributed along the seaward side of the barrier by wave energy (Fig. 5.11d).

The sediment accumulations that form the eco-geomorphic habitats in the Towamba estuary are mostly characterized by sand (Fig. 5.11a, b) except in mid-parts of the estuary that have higher mud and organic matter components (Figs 5.11b and 5.12b). This muddy sediment was derived from the catchment (Fig. 5.12a) and the estuary development represents an eco-geomorphic system that is dependent on its catchment sedimentary sources.

Although the rate of geomorphic growth is high, the wetlands are expanding more slowly because the sediment reaching the estuary is mostly quartz (~59%; Fig. 5.12a and Table 5.4) and lithic sand (averaged of 88.5%; Figs 5.10, 5.11a and Table 5.3). A limited component of mud (max. 54% within a very limited area but averaging ~12%; Fig. 5.11b and Table 5.3) is present aiding the development of wetlands and their associated habitats. More habitable areas will help with soil accumulation and surface accretion due to their biotic and abiotic roles (Aarts & Nienhuis, 1999; Cronk & Fennessy, 2001). The poorly sorted organic-rich sediment in the wetlands (Fig. 5.11d) accumulates more slowly than the higher geomorphic growth rates of sand facies. This situation is reflecting the estuary catchment that has characterized by a high-sloped terrain with mostly unmodified natural geomorphic processes (Fig. 5.3) driving a large amount of such poorly sorted sediment downstream to accumulate in the estuary.

Instability of some of the sandy geomorphic units in the estuary has resulted in unsuitable platforms for wetlands to develop on, particularly on the inside of the sandspit. The elevated estuarine barrier (Fig. 5.15) presents an example of the unstable pattern in the Towamba estuary; it has an average seaward movement of 1.831 m/yr (Fig. 5.9) and has a narrowing vegetation development, especially on the unstable southern end of the barrier, even though the temperature average allows a long warm growth season (Fig. 5.2c).

Bathometric analyses (Fig. 5.14) shown that Towamba narrow channel is mostly shallowed and

has flatted bottom surface, allowing smooth runoff and suspended sediment material to be discharged. That would allow more sediment to be transferred downstream to continue to build the estuarine eco-geomorphic system and keep it moving seaward.

5.5.3 Water quality roles

Measuring the water clarity through turbidity will show that increasing the suspended sediment including silt, clay, plankton and detritus, would resulted in declining water clarity to be more muddy appearance. That have indicated how much suspended sediment entering the estuary to be accumulated (Herben *et al.*, 2012). Salinity (and resultant conductivity) is another important factor in the development of ecosystem habitats such as wetlands, since it controls the borders between the mangroves, saltmarshes and *Casuarina* zones. The acidity of the water reflects the amount of organic matter and nutrients entering the water body from the catchment, and is related to natural and anthropogenic processes. pH and dissolved oxygen play important roles in the development of benthic biotic and abiotic components in the middle estuary, and act as ecological development accelerators.

Figure 5.13 shows a slight increase in pH and temperature that is linked with the higher salinity downstream through the estuary. The equivalent increase in dissolved oxygen reflects mixing with more oxygenated marine water and better developed ecosystem communities, such as sea grasses. In contrast, turbidity decreases within the estuary reflecting flocculation and accumulation of the suspended sediment along its way to the ocean discharge point in the tide-dynamic controlled area (Fig. 5.13). However, the remaining bedload sediment that reaches the ocean reforms as part of the dynamic coastal sandy barrier (Fig. 5.9).

5.5.4 Climatic factors and sea level effects

Although Towamba River has quite a small catchment (1034 km^2), it receives an average rainfall of 926.5 mm annually (Fig. 5.2a) giving a high average discharge flow of 379.3 (ML/d), with some flood event recorded during the 1970s, 1990s and 2010 (Fig. 5.2b). The high surface slopes in the catchment and its drainages result in high runoff volumes and velocities, particularly upstream that transport sediment downstream to build and develop the estuarine eco-geomorphic systems.

The increasing temperature affects plant productivity and the growing season length, which logically would have an effect on the estuarine ecosystem directly, while in the elevated parts of the catchment, the increasing temperature and declining precipitation would influence sediment production and transportation rates (Al-Nasrawi *et al.*, 2016a, 2016b, 2018a). This

increasing temperature would also affect the soil salinity and its nutrients (Mkpenie *et al.*, 2007).

Climate changes including rising sea-level have clearly affected the local Towamba weather. Local sea level rise affects the estuarine eco-geomorphic units directly providing impetus for slow vertical accretion. The temperature and rainfall affect plant growth in the estuarine section directly, as well as indirectly through discharge from the catchment that is controlled by both natural and anthropogenic factors.

Locally and regionally, this research is contributing to part of the New South Wales Government natural resources evaluation and reporting program to monitor estuarine habitat availability and condition/health indicators for mangrove, saltmarsh and seagrass together with water clarity (OEH, 2013). For the future sustainability and conservation management, eco-geomorphology and climate change influences have to be considered. Thus to successfully secure and manage such areas, a comprehensive understanding and clear evaluation of the existing situation has to be provided to allow prediction of the future vulnerability of estuarine systems. Increasing this understanding of such sensitive ecosystems, will assist land managers to better forecast the implications of management decisions and the potential impacts of climate change and human influences.

5.6 Conclusions

This research has established that imagery processing of remotely sensed data and GIS analysis, in combination with sedimentological and morphological data, can document the evolution of the Towamba estuary landcover dynamics as it progrades into Twofold Bay, southeastern NSW, Australia. An understanding of how the estuary has evolved in the past can then be used to help establish the probable vulnerability/adaptability of the estuary into the future, and can be used to assess similar estuaries worldwide.

The GIS-based morphodynamic modelling and assessment of the estuarine eco-geomorphic system and shoreline changes at Towamba River between 1949 and 2016 have shown a significant erosion/accretion around this estuary. The main Towamba estuary's changes were at the geomorphic features (such as sandspit extension and barrier growth) and its associated habitats (such as saltmarshes, mangroves and the mixed native plants, for instance; *Casuarina* and *Juncus*). The total area of growth was 169608 m^2 over the study period at an average rate of 2609 m^2/yr. The barrier island also provides proof of these changes, with an average landward erosion rate of -1.29 m/yr, and a seaward accretion rate of 1.83 m/yr indicating that

more accretion is occurring than erosion. The scenario for the future has estimated that, even with the predicted sea level rise, the whole estuary will be filled by 2100 and the remaining active tidal discharge channel will be very narrow with some remaining infilled swamps and lagoons.

The unmodified (mostly) and high-sloped catchment has a large sediment load available for discharge downstream to fill the estuarine area. This has three main influences: (i) positively, it would result in high sediment accumulation rates in the estuarine zone, allowing faster geomorphic growth; (ii) negatively, the high deposition rates have built poorly sorted and coarse-grained geomorphic features in the estuary (for example the sandspit) with very limited muddy areas; and (iii) this has limited the growth of ecological patterns of coastal wetlands and its associated saltmarsh and mangrove habitats.

The results of this research will assist scientists in forecasting areas that are at risk of erosion and/or accretion in the future. The method applied in this study can be directly applied to the many similar estuaries and lagoons along the east coast of Australia, South Africa and elsewhere in the world. Results obtained from this study, and future equivalent studies elsewhere, will aid scientists to predict areas with the highest risk of erosion or accretion over the next hundred years. It will also help decision makers and managers to propose appropriate measures for incorporating coastal/wetland management plans into both local and national conservation strategies. The results will contribute towards forming effective, catchment-wide coastal zonation management plans to respond to climate change and sea level rise, and also current and possible future human modification, preservation and restoration plans.

Quantifying historic estuarine eco-geomorphic change can be used to predict future responses to related environmental stressors. Results show that a spatiotemporal and statistically accurate approach to the development of GIS-based models can be used to upscale local field-datasets to provide a quantifiable spatiotemporal analysis. The incorporation of unmodified estuarine intertidal sedimentary landforms in eco-geomorphic models would be relevant to similar modelling activities, both regionally and globally.

The broad-scale methodology in this study is applicable worldwide for evaluating eco-geomorphic changes to estuaries and helps provide more understanding of the factors responsible for the changes. These factors can then be considered when estimating responses to future climate change in such coastal ecosystems and be used as sustainable and effective management tools. Valuable information on current and future climate changes scenarios of rainfall and river discharge can be predicted and these trends will change the amount of

sediment driven from the catchment. Also future human modification might increase significantly in the catchment area, which would impact the runoff and all the relatively natural processes. These will all have different levels of negative influences depending on the change proportions. Thus, future research should consider these factors in the preparation of applicable preservation and restoration plans.

Chapter VI: Geoinformatic analysis of Vegetation and climate change on intertidal sedimentary landforms in: use of NDVI from 1975–2015

6.1 Abstract:

Vegetation canopies can be used to represent the main ecosystems on intertidal landforms and they clearly reflect any responses to changes in the coastal environment such as global warming. Climate change, such as temperature, precipitation, and rise in sea level, are affecting the health and distribution of coastal vegetation, as well as the runoff and sedimentation rates that can impact on coastal areas. This study has used the normalized difference vegetation index (NDVI) to investigate vegetation canopy dynamics on three different coastal sites (south-eastern Australia) over the past 47 years (1975-2015). Satellite imagery derived from Landsat 1-8 has been analysed in ERDAS IMAGINE, building the NDVIs temporal-datasets, and then regressed to the climatic and geomorphic variables in RStudio software, with a focus on the NDVI-greenness scale. The results have shown clear increases in NDVI on Towamba and Wandandian sites but a declined at Comerong Island. Sedimentation rate has the most significant positive impact on the NDVI since it has a potential to provide additional space for vegetation. Temperature and sea level rise have positive effects, except on Comerong Island, but rainfall has no significant effect on the NDVI at any site. Different NDVI reflection trends have been recorded at these three coastal sites reflecting different correlations between the vegetation, climatic and geomorphic (as independent) variables. The geomorphological characteristics of the highly dynamic intertidal estuarine landforms, that are subject to active erosion and deposition processes, have the largest/highest impact on vegetation cover, and hence on NDVI. Assessing the vegetation canopy using NDVI as an evaluation tool has provided temporal-dynamic datasets that can be correlated to the main individual environmental controls. Such knowledge will allow resource managers to make more informed decisions for sustainable conservation plans following evaluation the potential consequences of any environmental changes.

Keywords: *ecosystems; climate changes; vegetation response; NDVI; GIS-Analyses; remote sensing.*

6.2 Introduction

There is much concern about climate change impacts as demonstration in various scenarios, such as on the ecosystems of the Earth (Costanza, 1999; Pittock, 2003; Zinnert *et al.*, 2011; IPCC, 2014). The clearest and widest ecosystem responses to climate change are represented in the vegetation canopy dynamics of such ecosystems (Goward & Prince, 1995; Donohue *et al.*, 2009). At global, regional to local landscape levels, the responses of the vegetation canopy are influenced by whichever climatic elements characterise the principal plant growth's control factors (Donohue *et al.*, 2009). Within coastal-dynamic setting, vegetation condition dynamics could be categorised as these affected by the main atmospheric energies of temperature and precipitation that impact growth and productivity, as well as those that affect the landform stabilities, including sea level and sedimentation dynamics (Woodroffe, 1990; Meyssignac & Cazenave, 2012).

Coastal ecosystems and specifically wetland habitats are highly productive natural ecosystems (Matthews, 1993; Mitsch & Gosselink, 1993; North Central C.M.A., 1998; Ehrenfeld, 2000; Perillo *et al.*, 2009). Coastal wetlands are also the most sensitive and responsive coastal ecosystems to environmental pressures than others, such as climate change, the rising sea level and the current stage of human settlements that control most of the coastal processes (Al-Nasrawi *et al.*, 2015b, 2016a). Coastal ecosystems may be affected by a local surge in surface temperature, precipitation decline and sea level rise (SLR) under current climate scenarios. On top of that, human activities have been shown to have a substantial effect on coastal systems, including as clear a biodiversity reduction and habitat destruction (Al-Nasrawi *et al.*, 2016b), which implies that there is a great need to find out and forecast changes in ecosystem functioning.

Coastal environmental studies have become more focused on the applications of climate change scenarios within the coastal zones to assess the vulnerability of its ecosystems and/or landforms (Goward & Prince, 1995; Costanza, 1999; Watson, 1999; Nicholls, 2004; Semeniuk & Semeniuk, 2013; Al-Nasrawi *et al.*, 2015b, 2016b, 2018a). So far, these studies have indicated an important climate – eco-geomorphic correlation. However, limited discussion has focused on examining the vegetation trends associated with climate related factors at specific geomorphic-estuarine sites in coastal wetlands. This case study from the southeastern Australian coast shows the relationships between different environmental conditions, geomorphic and human pressures, and demonstrate success in this case that recommends the use of these methods in other ecosystems worldwide.

The aims of this exploratory study are to:

i) quantify the temporal change-trends of coastal vegetation canopies,

ii) quantify the spatial change-distribution within sensitive wetted landforms.

These aims were achieved by analysing the vegetation trends over time and establishing correlations between change stressors and the vegetation response, which can be used to predict future response scenarios of such landscapes along the southeastern Australian coast. The research objectives have been based on a literature review augmented by imagery modelling, including the pre-processing, clipping-sub-setting, re-scaling-classifying and all the followed geospatial analysis (using RS and GIS) and subsequent correlation statistical analysis that can offer a qualitative outcome, which could be based on for informal conservation solutions with potential worldwide applications.

6.2.1 Use of satellite remote sensing for monitoring changes in coastal wetlands vegetation

Earth observations through multiple satellite imagery sources have provided important monitoring and classification approaches, which have led to a significant method for landform-dynamic observations to check the historical records of any eco-geomorphic change (Borre *et al.*, 2011; Franke *et al.*, 2012). Thus, imagery classification has been widely adopted in several fields, including ecology, geomorphology, and climate change assessment (Kerr & Ostrovsky, 2003; Jeong *et al.*, 2016). Classification of satellite images is a sorting pixels process (with values scaled from 0-255) to a narrower individual classes/categories according to their pixel-values. For instance, pixels will be assigned to a particular class/category that corresponds to their criteria If the each pixel has satisfied the certain criteria of that class (Nguy-Robertson & Gitelson, 2015; Peng *et al.*, 2017). Many classification approaches have been used as methods of diagnosticating, and specifying features within the satellite image as per their spectral values (Fernández *et al.*, 1997; Kerr & Ostrovsky, 2003). For example, within Normalised Difference Vegetation Index (NDVI) classifications, pixels are converted and clustered together (from -1 to +1) based on spectral homogeneity and spectral distance (Turner *et al.*, 2003).

The most commonly publicly available imagery, Landsat, has a spatial resolution ranging from 15 m (panchromatic bands on Landsat 7 and 8) through the dominant 30 m (spectral bands on Landsat 4-7) to 80 m of Landsat 1-3. Any of these pixel sizes are adequate to give multiple pixels within a patch of the classes of interest in this study, namely intertidal sedimentary landforms of estuaries, and their ecological and geomorphological (eco-geomorphic) distribution and dynamics, which could be linked to provide better eco-geomorphic

understanding and monitoring tools at the landscape scale (Giri *et al.*, 2011; Hamylton *et al.*, 2016, 2017). At the same time, temporal resolution of various earth observation satellite datasets can be used to track dynamic vegetation trends (see Table 6.1). The many different spatiotemporal satellite datasets can generate varied NDVIs over land-patch/time (Pettorelli *et al.*, 2005). The limitations of data derived from different satellite sensors mean that a high temporal resolution (rapid repeat time) requires a wide swath and coarser pixels, whereas finer spatial detail limits the time interval between equivalent images (Pettorelli *et al.*, 2005). Thus, the spatial detail needed to define the landforms must be balanced against the time interval needed to document changes. For example, the very-high-accurate radiometer and advanced-Level three (time series dataset) is derived from the National Ocean and Atmospheric Administration (NOAA-AVHRR/PAL, GVI, and GIMMS; see Table 6.1) provides pixels either 8 or 16 km on a side resolution, and records are available from 1981 to present. Meanwhile, Level two NDVIs-datasets, with a resolution of 250-1000 m, can be obtained from the Moderate accuracy of the Spectroradiometer imagery (TERRA satellite (EOS AMI) with MODIS instrument; see Table 6.1) datasets, which offers a medium-scale but shorter term data-series going back to 2000 only (Pettorelli *et al.*, 2005). Meanwhile, a freely-available high resolution (Level one) datasets can be obtained from Landsat 1-8 missions (sensors: MSS, TM, ETM+ and OLI with 30 to 79 m resolution and extending from July 1972 to present;

Table 6-1. Main satellite imagery sources of earth observations*

Data set	Satellite	Instrument	Archive extent	Temporal resolution	Spatial resolution	Sources
PAL	NOAA	AVHRR	July 1981-SEP.2001	1 day , 10 days, monthly, seasonal	8 km	http://daac.gsfc.nasa.gov/guides/GSFC/guide/avhrr_dataset.gd.html
GVI	NOAA	AVHRR	May 1982 - present	Weekly, monthly, seasonal	16 km	http://www2.ncdc.noaa.gov/docs/gviug/index.htm
GIMMS	NOAA	AVHRR	July 1981-present	15 days	8 km	http://ltpwww.gsfc.nasa.gov/gimms/htdocs/
MOD13	TERRA (EOS AMI)	MODIS	Feb.2000-present	16 days	250 m - 1 km	http://modis.gsfc.nasa.gov/
	MSS	Landsat 1-5	July 1972-Dec. 1993	18-16 days	79 m	http://Landsat.usgs.gov/
	TM	Landsat 4-5	July 1982 – June 2013	16 days	30 m	http://Landsat.usgs.gov/
	ETM+, OLI	Landsat 7 - 8	April 1999 - present	16 days	15 m – 30 m	http://Landsat.usgs.gov/

*Sources: (Pettorelli *et al.*, 2005; Parcher, 2012; Nguy-Robertson & Gitelson, 2015; USGS-Landsat, 2017; USGS, 2017b).

see Table 6.1) represent scale data with the best satellite imagery-series that could be utilised for NDVI indexing (Horn & Woodham, 1979; Baban, 1997; Nguy-Robertson & Gitelson, 2015; Peng *et al.*, 2017; USGS, 2017a). Thus, related to the current study sites' specifications that average 3-4 km^2 in area, the Landsat datasets would provide the best data that could be used

to achieve this study's targets in terms of sensor resolution (MSS = 60-79 m, TM, ETM+ and OLI=30 m; see Table 6.1) and longer archive recorded that goes back to 1972.

6.2.2 Vegetation indicators

Vegetation changes can be monitored over time using the Normalised Difference Vegetation Index (NDVI) from satellite imagery (Fuller, 1998; Donohue *et al.*, 2009). It is possible to empirically correlate changes in NDVI with direct and indirect environmental changes, which has been an important consideration in recent ecological studies and analysis methods (Fuller, 1998; Weier & Herring, 2000; Pettorelli *et al.*, 2005). Over last decade numerous environmental studies have obtained new knowledge regarding the immediate and consequential impacts of ecological change through using the NDVI (Fuller, 1998; Weier & Herring, 2000; Pettorelli *et al.*, 2005; Nguy-Robertson & Gitelson, 2015).

The red with near-infrared reflected lights have defined the NDVI ratio (Huete *et al.*, 2002)

$$\mathrm{NDVI} = \frac{\lambda\,\mathrm{NIR} - \lambda\,\mathrm{RED}}{\lambda\,\mathrm{NIR} + \lambda\,\mathrm{RED}} \qquad (1)$$

Where: RED/NIR are exhibiting the red-light and near infrared quantities, and are sensed, using the satellite's sensor, the vegetation light reflections (Weier & Herring, 2000). Since mesophyll leaf structure will reflect NIR yielding a high NIR-band pixel value whereas RED would be absorbed by chlorophyll yielding a low RED pixel value for the same pixel, the NDVI is normalized to produce a continuous variable with a potential a range of -1 to +1, where negative values represent the non-existence of vegetation (Weier & Herring, 2000; Pettorelli *et al.*, 2005).

Initially in their history NDVI images were used visually to allow experts to manually interpret the patterns on the landscape. Only later were quantitative methods applied to defining the patterns thus perceived (Tucker *et al.*, 1985; Pettorelli *et al.*, 2005; Nguy-Robertson & Gitelson, 2015).

Vegetation biomass and dynamics have been linked to NDVI, and could easily be regressed with the related controlling and resultant variables, such as climatic factors, across many ecosystems worldwide; Table 6.2 has included most of the commonly used applications of NDVI.

Table 6-2. Some of the NDVI applications, examples and references that have successfully applied in relating to vegetation canopy aspects locally, regionally and worldwide.

NDVI applications	Implied example and/or case studies	References
Correlation between the vegetation and its productivity	Capturing absorbed photosynthetically active radiation	Asrar *et al.*, 1984; Sellers *et al.*, 1992; Fuller, 1998; Weier and Herring, 2000; Pettorelli *et al.*, 2005
Vegetation and influential environmental parameters	Climate and ecosystem habitat distributions and performances at coarse spatiotemporal scale, including coastal ecosystems	Reed *et al.*, 1994; Vourlitis *et al.*, 2003
NDVI with climatic variables and atmospheric patterns of change	Effect of climate influences on vegetation biomass by defining vegetation classes through their phenological patterns.	Fuller, 1998; Donohue *et al.*, 2009; Pettorelli *et al.*, 2005; Donohue *et al.*, 2009
Local ecosystem monitoring	Local ecosystem monitoring that could be affected by the influence of recreational impacts, to assess the anthropogenic interactions of parkland covers - whether they are forested or grassed.	Justice *et al.*, 1985; Goward and Prince, 1995; Weier and Herring, 2000; Pettorelli *et al.*, 2005
	In variegated ecosystem conditions, so, it has applied not only in dry to semi-arid regions in Australia but also in a thick shade, e.g. Congo Forest.	Huete *et al.*, 2002; Pettorelli *et al.*, 2005
Risk and hazard assessments relating the vegetation canopies (RHAVC) and drought	Dynamic fire risk in Mediterranean areas, and forest fires in Spain	Maselli *et al.*, 2003; Fernández *et al.*, 1997
	Assess vegetation changes related to dry seasons, fires, and surges of drought land covers depends on the index to vegetation aridity, a noteworthy component for fire incidence	Maselli *et al.*, 2003; Tait and Zheng, 2003; Wang *et al.*, 2003
Biophysical studies (BS)	Biophysical performance for vegetation indices	Myneni *et al.*, 1995; Huete *et al.*, 2002
Analysing vegetation dynamic (AVD)	Vegetation trend analysis	Tian *et al.*, 2015
The net ecosystem exchange (NEE) of carbon flux	CO2 fluxes within a steppe & sagebrush's ecosystem	Wylie *et al.*, 2003
Agriculture investigations	Cotton yield and crop production in Senegal	Fuller, 1998; Dalezios *et al.*, 2001
Ecological applications	Vegetation biomass and elements in different environmental communities	Fuller, 1998; Weier and Herring, 2000; Pettorelli *et al.*, 2005
	Assess ecological responses to environmental change	Sellers *et al.*, 1992; Kerr and Ostrovsky, 2003; Pettorelli *et al.*, 2005
Ecosystems predictions	Correlation between the NDVI and climatic variables enable it to be used for monitoring and predictions of the ecosystems. Atmosphere, vegetation, and ecosystem habitats are forming dynamics over coarse spatio-temporal scale	Asrar *et al.*, 1984; Sellers *et al.*, 1992; Pettorelli *et al.*, 2005; Donohue *et al.*, 2009

The Enhanced-Vegetation-Index (EVI) is another popular index, which has used the MODIS datasets for vegetation analysis after 2000 (Peng *et al.*, 2017). Along these lines, in bare lands, SAVI (soil-adjusted-vegetation-index) has been suggested rather than NVDIs (Huete, 1988; Despland *et al.*, 2004).

The correlation between the NDVI index and vegetation is more accurate than indices such as EVI and SAVI for coastal ecosystem assessment, and it can be correlated to other factors (e.g. climatic factors) comprehensively (Goward & Prince, 1995; Costanza, 1999; Zheng *et al.*, 2012; Raynolds *et al.*, 2015).

The NVDI is affected sometimes by the soil radiation reflectance within scantily vegetated regions that have a leaf area index (LAI) of <3. However, within LAI >4 (such as a territories with thickly vegetation canopy) the correlation between the NIR & NVDI becomes saturated (Asrar *et al.*, 1984; Huete, 1988; Nguy-Robertson & Gitelson, 2015; Peng *et al.*, 2017).

The ecosystem related measures that can be acquired from an NDVI dataset can be confounded/confused or reliable according to the ecosystem consideration issues. Using data on a yearly scale; within areas where a variable rainy season is present, the analysis should concentrate on the more stable and less vegetation dynamic season (summer) to determine the NDVI as part of the practical sensed data (Weier & Herring, 2000; Pettorelli *et al.*, 2005; Kumar, 2011; Peng *et al.*, 2017). However, for easier explanation to be understood (from this point and on), the summer dates that were processed of a year, will be recalled of that chosen year, for example, the summer-data of 1985 will be called 1985-NDVIs.

6.2.3 Climate indicators

The Earth has encountered some rapid climatic changes in the past a few decades (Pachauri *et al.*, 2014). It has been recorded that after 1980 the climate has experienced the warmest mean temperatures in modern records ever (within past century), and considerable change has been recorded in terms of intense storm events, and declining precipitation (Michener *et al.*, 1997). There have been major changes along the Australian coast areas in cloudiness and monsoon dynamics (Steffen *et al.*, 2009). Knowledge of these progressions is imperative since they are directly linked with the climatic system, specifically in terms of the energy, water and biogeochemical cycles on the Earth's surface due to respiration, photosynthesis, transpiration and surface albedo (Scavia *et al.*, 2002; Bianchi & Allison, 2009; Wookey *et al.*, 2009; Zinnert *et al.*, 2011; Semeniuk & Semeniuk, 2013).

Ecosystem processes are related to many controller variables including: temperature, season of growth, precipitation, flooding, storminess, erosion, accretion, tidal levels, salinity and hydrodynamics are factors to be adapted within a time frame. Therefore, all these factors need to be understood in terms of recent climate change (Al-Nasrawi *et al.*, 2015a, 2016b, 2018c). Then there is a need to quantify whether these factors are going to impact these ecosystem future and by how much (Costanza, 1999; Nicholls *et al.*, 1999; Gedan *et al.*, 2011). The major factors that may affect coastal wetlands, as shown in other cited studies, will likely be temperature, precipitation, sea level rise, sedimentation (erosion and accretion) and human settlement within coastal ecosystems (Fuller, 1998; Weier & Herring, 2000; Kumar, 2011). In reality, they also represent factors that we can now gather reliable data to test, largely satellite-image derived (Tian *et al.*, 2015). Intensities of long-term changes (in average) of these factors will drive vegetation and habitat distribution in the future (Newton *et al.*, 1998; Christiansen *et al.*, 2000; Zedler & Kercher, 2005).

Sea level rise (SLR) has become the main issue of many scientific studies, which threatens coastal ecosystems including wetlands. However, human modifications on: catchment and upper stream (including sediment characteristics/runoff)also affect coastal ecosystems by changing the sediment budget that can keeps coastal wetlands and estuaries in a kept-pace synchronous with SLR (Al-Fadhli, 2013; Al-Nasrawi *et al.*, 2015a, 2018c). Also, natural processes in coastal wetlands can be altered by high-energy events such as riverine floods, storms and tsunamis (Nicholls, 2004). On the other hand, early civilizations inhabited estuarine and coastal areas (e.g. Mesopotamia; Postgate, 1992) and nowadays 70% of the human population and 86% of Australians live along the coasts for ecological and economic reasons (Cherfas, 1990; Pendleton, 2010). Thus, SLR plus human-induced stressors that resulted in challenges of degradation have increased since the last century and caused losses of estuarine and coastal ecosystems, particularly within coastal wetlands (DSE, 2007; Al-Nasrawi *et al.*, 2016b). The productivity of wetlands as natural ecosystems is essential for sustaining the conversation within such areas.

The pattern, in general, and the span of the seasons in the southern hemisphere have become longer due to the environmental changes interlinked with the recorded warming trends, which should have amplified the vegetation productivity, structure and arrangement. Since the 1960s, this should have resulted in an increase in the amount of the persistent O_2 cycle (Vourlitis *et al.*, 2003), though in dry regions like Australia, radiative forces (climate forces) have led to soil dryness and a decrease in vegetation (Boto & Wellington, 1984; Tongway & Ludwig, 1990; Qi *et al.*, 1994; Hughes, 2003; Notaro *et al.*, 2007). These vegetation variations

might have changed the sediment, nutrient and hydrological cycles, trophic associations as well as the entire coastal environment (Costanza, 1999; Zinnert *et al.*, 2011; Davies & Stewart, 2013). Another significant climatic variable apart from air temperatures is precipitation, which has more impact in semiarid and arid areas, like Australia, and has distinctly decreased in the past few decades (Watson, 1999; Nemani *et al.*, 2003; Fensholt *et al.*, 2013). Along with climate, other elements that influence vegetation growth should also be characterized, like morphodynamics (e.g. shoreline movement and sedimentation rates), varieties of vegetation (e.g. mangrove and saltmarsh), nutrient availability (e.g. the organic matter in the sediment) and anthropogenic modification levels in estuarine and coastal ecosystem areas and there relevant catchment (Davies, 1974; Tongway & Ludwig, 1990; Chapin *et al.*, 2005; Goetz *et al.*, 2005).

Various studies have recorded that natural inter-decadal (e.g. El Niño) irregularity and anthropogenic forcing, particularly at the local (continental/basin) scale, leads to inter-decadal environmental change (Hughes, 2003; Davenport & Davenport, 2006; Lee *et al.*, 2006; Kumar, 2011; Liu, 2012; Pachauri *et al.*, 2014). Eastern Australian coastal environments are under the climate dominant influence of the Pacific Ocean. The inter-decadal irregularities in atmosphere over various areas of the Pacific Ocean, including Australia, are significantly affected by the El Niño/Southern Oscillation (ENSO) (Henley *et al.*, 2015) that has been shown to cause more drought and warmer weather, as shown for example by the 1997 and 2010 El Niño events (Michener *et al.*, 1997; Hughes, 2003; BOM, 2017b).

The wave-dominated Australian east coast has been subject to hotter and more intense atmospheric events than in the past, particularly showing effects in the eastern coastal ecosystems (Michener *et al.*, 1997; Hughes, 2003; Day *et al.*, 2008; USAID, 2016). Therefore vegetation in this region may also be particularly vulnerable to climate change (Preston & Schmidt, 2006; Notaro *et al.*, 2007).

The above correlations can be applied to have a comprehensive practical view. Thus, this research has focused on three estuaries, as ideal case studies, along the Australian southeastern coast. Australian southeastern coastal ecosystems in the temperate zone have experienced considerable vegetation dynamicity during the last few decades of climate change, particularly after the 1980s. A comparative investigation of the relationships between vegetation dynamics and climate change is urgently required, with empirical case studies to prove the theoretical statement of this framework research to be useful and applicable worldwide. Satellite imagery series allow us to perform this for the past four decades, since the maximum imagery availability, using GIS. Then, we utilized RStudio liner regression, correlation

analysis to deal with the correlations between these three vegetation dynamic study sites and the atmosphere related indicators: temperature, precipitation and sea level rise, as well as with the human impact (mainly) on erosion dynamic represented by the sedimentation rates. Anthropogenic impacts have a geomorphic interaction that has included the dynamics of the loaded sediment from the catchments that have been impacted by human activities, as well as the direct anthropogenic modification within the coastal environment.

This study has focused on the NDVI data from 1975 to 2015. This exploratory study investigates the response of ecosystem dynamics, represented by its vegetation, to the climate change trends along the southeastern Australian coast. The study has been based on Landsat empirical imagery, GIS-modelling and subsequent statistical analysis (for both the NDVI, climatic and geomorphic indicators) that can provide a numerical outcome, which would be able to offer a future informal and adaptable ecosystem' solution. This methodology tests this research's hypothesis that the ecosystem dynamics respond directly to environmental changes at these study sites. Such findings reflect local ecosystem responses to such global changes and thus serve as an applicable worldwide approach for use by environmental scientists, government agencies, bio-ecologists, geomorphologists, meteorologists, GIS/remote sensing users, ecosystem managers and conservation policy makers.

Examining the existing situation of vegetation trends to provide a comprehensive view at the current stage of climate change is an important approach; locally (community benefit, e.g. local lifestyle convenience and property prices), regionally (government and state benefits, e.g. management plans), and globally (gathering the international legislation efforts, e.g. UN-UNEP, 2016-DELC/environmental laws).

6.2.4 Study sites general setting

This study has selected three sensitive coastal ecosystems on the Australian southeastern coast (Fig. 6.1) that are not safe against the effects of changes in climate and they can represent the worldwide ecological responses (Blay, 1944; Wright, 1970; Yassini & Jones, 1995; Kench, 1999; Sloss *et al.*, 2006b; Hopley, 2013; OEH, 2013).

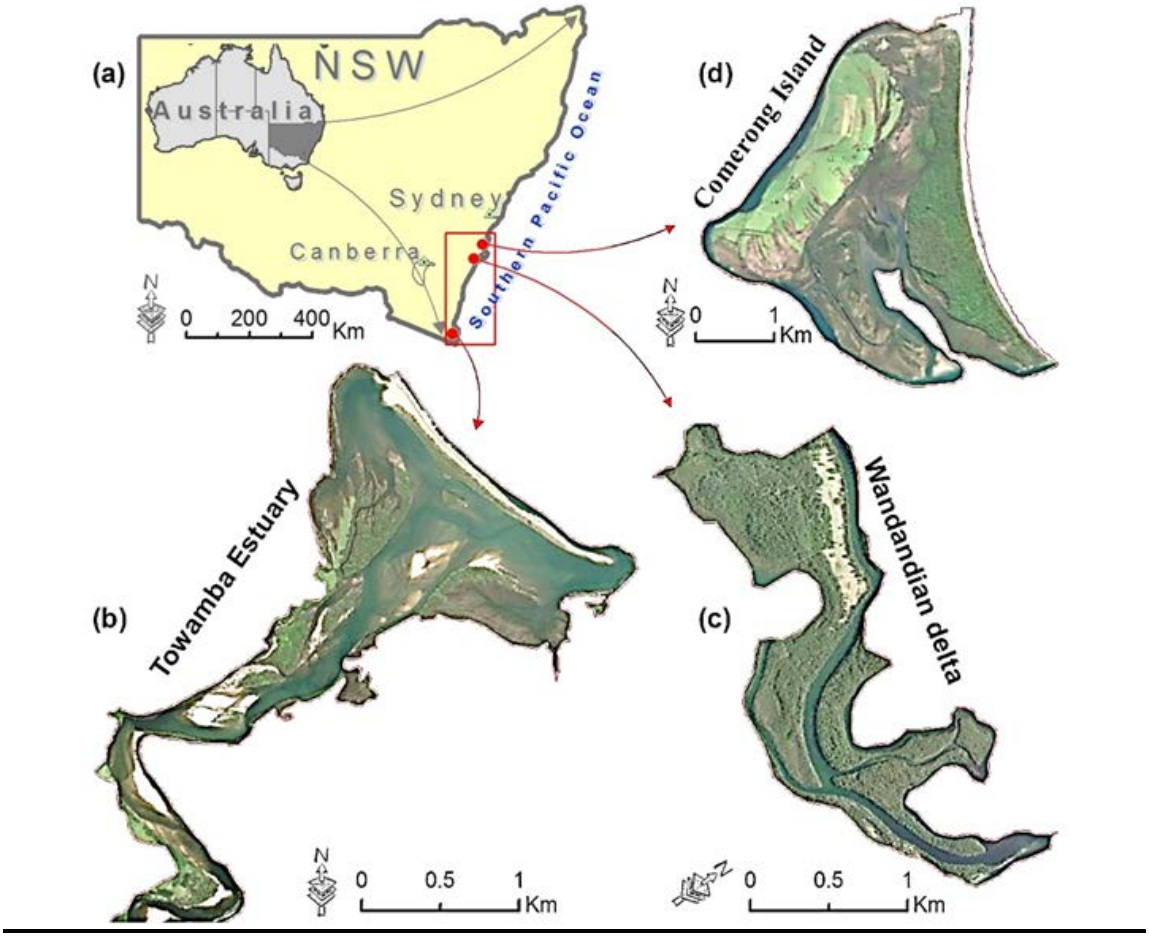

Figure 6-1. (a) Study site locations along the NSW coast in southeastern Australia. From south to north they include the (b) Towamba estuarine ecosystem, (c) Wandandian estuarine delta and (d) estuarine portions of Comerong Island.

The southeastern Australian coastline includes protected lagoonal and wave-dominated beach natural assets that make an enormous contribution to the economy (Roy *et al.*, 2001; Pendleton, 2010; Kirkpatrick, 2012). Estuarine ecosystems at Towamba, Wandandian delta and Comerong Island provide representative applicable case studies of ecosystem responses (Fig. 6.1).

6.2.4.1 Towamba estuary

The estuary is located on the south NSW coast, 486 km southern of Sydney, on the border with Victoria (NSW; 37°06'38.0"S 149°54'10.7"E, Fig. 6.1a,b) with a temperate oceanic climate (Cfb), the Towamba catchment has a no distinct dry season with temperature that ranging between 11°C and 20°C in winter and summer respectively, and an average precipitation of 882 mm annually (BOM, 2017a). Towamba River has built its specific estuarine eco-geomorphic system at the meeting point between the high-elevation and steep mountains/catchment area and the Pacific Ocean (Hudson, 1991; Dean & De Deckker, 2013; Al-Nasrawi *et al.*, 2018a; DPI/OW, 2017). Although this estuary ecosystem is only 2 km^2 it receives a huge amount of sediment

annually from the steep terrain and mostly untouched catchment of 1034 km^2 (Roy *et al.*, 2001; DPI/OW, 2017). The estuary is mostly surrounded by rocky outcrops that have limited estuary growth. This has resulted in forcing the sediment accumulation and growth to occur in the middle and open water sides of the estuary, leading to a narrow main active channel and forcing the barrier island to grow seawards (Hudson, 1991; Dean & De Deckker, 2013; Al-Nasrawi *et al.*, 2018a; DPI/OW, 2017).

According to the Roy *et al.* (2001) classification, it is a wave-dominated barrier estuary in the mature stage of ecosystem development. It has an open estuary mouth into Twofold Bay in the Tasman Sea discharging water and sediment mainly derived from the Nullica State Forest (national park) and other untouched forests in the catchment area. The source of the perennial Towamba River is at Mount Marshall within the Great Dividing Range - South Coast Range (Roy *et al.*, 2001; DPI/OW, 2017). The river normally runs/discharging southeast to be turned northeast just north Kiah Village. twelve reaches are joining the main Towamba River including Wog-Wog river & Mataganah Creek to be discharged into Twofold Bay just southeast of Eden near East Boyd. The river descends 533 m over its 86 km course (Roy *et al.*, 2001; DPI/OW, 2017).

6.2.4.2 The Wandandian estuarine delta

Located about 200 km south of Sydney, on the St Georges Basin (west-corner)(35°06'23.9"S 150°33'21.8"E, Fig. 6.1a,c). It has a temperate oceanic climate (Cfb) with no dry season and average temperatures ranging from 11.5°C in winter (July and August) to 21°C during summer (January and February, data from 'Sussex Inlet Bowling Club' gauging station; BOM, 2017a), average precipitation is 1264 mm annually, with 400 mm estimated runoff (Hopley & Jones, 2006; BOM, 2017a). The delta area is about 3.1 km^2 while its catchment is approximately 152 km^2 (DPI/OW, 2017). The Wandandian delta has built out during the Holocene and consists of fluvial sediments (gravel, sand, silt and clay) and it is still growing nowadays (Hopley & Jones, 2006). Wandandian Creek is the main water and sediment supplier to the delta, being 125 km long extending from the Tianjara Range (part of the Australian Great Dividing Range) before discharging into the St Georges Basin (Windley, 1986; Hopley & Jones, 2006; Al-Nasrawi et al., 2017b, 2018b).

6.2.4.3 Comerong Island

Located about 30 km north of the Wandandian site on the mid-NSW coast (34°53'08.2"S 150°44'14.3"E, Fig. 6.1a,d), Comerong Island has a warm oceanic to and humid subtropical climate (Cfa), with no dry season and a hot-warm summer (BOM, 2017a). The average

temperature ranges from 16°C in winter (July and August) to 25°C during summer (January and February, data from 'Greenwell Point Bowling Club' gauging station; (BOM, 2017a) and the average precipitation is 1127 mm annually, with 350 mm estimated runoff (Nott *et al.*, 2002; ASCPSS, 2009; BOM, 2017a). Comerong Island is about 4.5 km^2 in area, and is located at the end of the Shoalhaven River-Crookhaven Heads forming a barrier-deltaic island on the NSW coast. Comerong Island has been internationally recognized as habitat for a range of waders and shorebirds, and it has an amazing wetland distribution consisting of mangroves and saltmarshes (Kingsford, 1990; Al-Nasrawi *et al.*, 2016a, 2016b). At the same time, it represents a clear example of an ecosystem affected by human influences (associated with a developed catchment) accompanied by sea-level rise resulting in changing shorelines and vegetation extent (Wright, 1970; Kingsford, 1990; Nott & Price, 1991; Daly, 1996; Christiansen *et al.*, 2000; Christian & Hill, 2002). Geomorphically the island has been built as a small estuarine barrier at the Shoalhaven River mouth by fluvial sedimentation behind the marine sand barrier during mid of Holocene (Umitsu *et al.*, 2001). The delta migrated northwards and the entrance was frequently blocked so in 1822 Alexander Berry constructed a canal that linked the Shoalhaven and Crookhaven Rivers (~4 km south of the old river entrance) to alleviate the high river water levels that threated the estuary and all associated human settlements (Thompson, 2012). This resulted in the final shape of Comerong Island, but the lower water levels threated some island ecosystems, such as saltmarsh areas (Al-Nasrawi *et al.*, 2016b, 2018c).

6.2.4.4 Climatic conditions along the south east Australian coast

The Australian east coast is subject to varying climate conditions over a substantial land scale, variable geology, air/sea currents and different coastal environmental systems, making speculations troublesome in light of the Köppen climatic framework (Hughes, 2003; Dee, 2006; Ward & Butler, 2006; BOM, 2017b). Thus, the Australian Bureau of Meteorology (BOM) has modified the Köppen classification system to meet the local specifications (BOM, 2017a).

The eastern coast of Australia has north-south stretched climate zones, affected by the coastal wave-dominated air/ocean currents, especially the warm East Australian Current. Thus the tropical and subtropical weather conditions are stretched farther south than normal. This could also be enhanced by global warming that causes similar shifts in different parts of the globe. This has caused a range of unstable weather event, such as cyclones, floods, droughts and other sporadic natural disasters at the study sites or in their catchments, that have caused damage costing millions of dollars annually(Hughes, 2003; Fensham *et al.*, 2005; Semeniuk & Semeniuk, 2013; BOM, 2017a).

Interestingly, while the eastern Australian coast is prone to such climate changes, their recurrence intervals are liable to become more frequent and intense. Present and future vegetative changes and present rate of ocean level rise and the accompanied immersion of eastern Australian low-lying waterfront habitats (e.g. estuaries and coastal wetlands) are affected differently at present, and are anticipated to change due to global warming (Semeniuk & Semeniuk, 2013; BOM, 2017a).

6.2.4.5 Precipitation variation along the east Australian coast

Precipitation records have a tendency to fluctuate along the east Australian coast, especially on the southern NSW coast, where all three study sites are located (Fensham *et al.*, 2005; BOM, 2017a). However, the Australian general climate indicators, including those on the southeastern coast, show a clear trend of declining precipitation over the last few decades, which is part of the global climate trend (Fig. 6.2; BOM, 2017b).

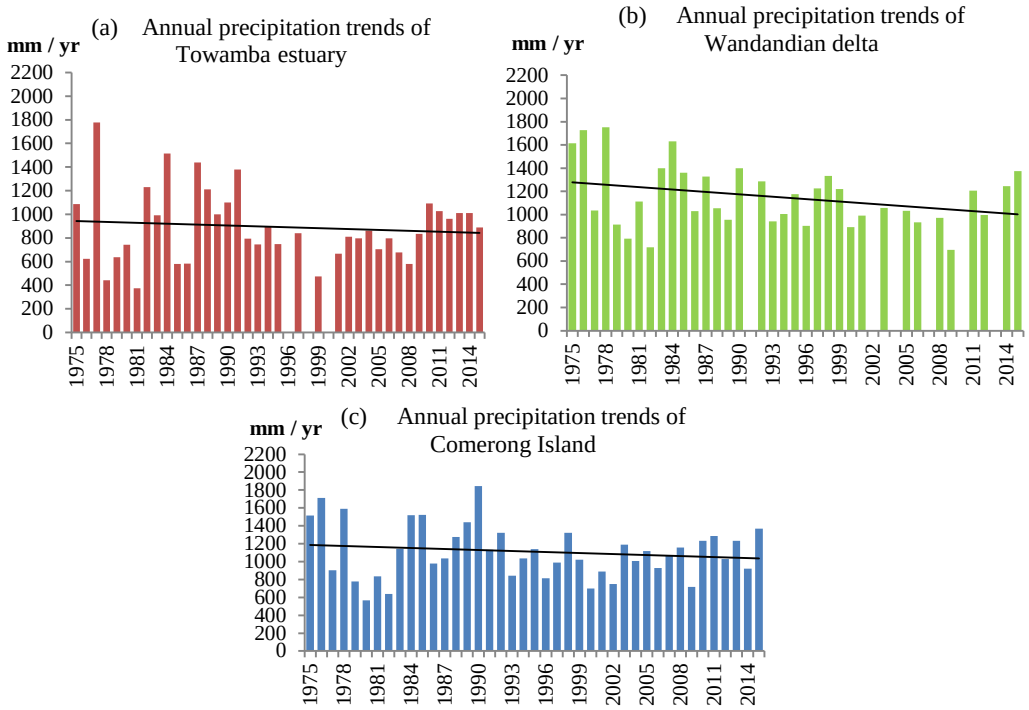

Figure 6-2. Annual precipitation records (1975-2015) at the study sites: (a) Towamba precipitation, (b) Wandandian precipitation and (c) Comerong precipitation. The overall trends show a decline in precipitation over the study sites during the past forty years, (BOM, 2017b; KNMI, 2017). *Note, the overall trend is presenting by the grey line on a-c.

The Towamba estuarine ecosystem receives an average precipitation of 882 mm annually (Fig. 6.2a; BOM, 2017a; data from the 'Marine Rescue Eden' gauging station, located 1.4 km away from the estuary). The overall average Towamba precipitation trend shows a slight decline during the last forty years (Fig. 6.2a), from 974 to 879 mm (2.38 mm/a). In contrast, the Wandandian deltaic ecosystem receives annual average precipitations of 1264 mm (Fig. 6.2b;

BOM, 2017a; data from 'Sussex Inlet Bowling Club' gauging station, located 11.2 km away from the delta). The overall average Wandandian precipitation trend shows a significant declined over the last forty years (Fig. 6.2b) from 1350 to 952 mm (9.95 mm/a). Whereas, Comerong Island estuary receives an average precipitation of 1127 mm annually (Fig. 6.2c; BOM, 2017b; data from 'Greenwell Point Bowling Club' gauging station, located 0.4 km away from the island). The overall average Comerong precipitation trend has also declined during the last forty years (Fig. 6.2c) from 1203 to 1026 mm (4.43 mm/a).There is also a clear decrease in precipitation along the coast from north to south that could be related to the regional and global precipitation distributions, which usually decrease towards higher latitudes. However, the case study sites, which are located at different latitudes and receive different amounts of precipitation, all show a similar decline in the overall records from 1975 to 2015 (Fig. 6.2).

6.2.4.6 Temperature

Increasing the overall temperature will affect the season's length and average temperature, which would affect plant productivity and the growing season length, and these effects should be clearly indicated in the NDVI records. The mean annual temperature data for the last five decades (1966-2016) at the case study sites have been analysed (Fig. 6.3). At these sites air temperature has clearly increased (Fig. 6.3), representing the combined effects of local and regional global warming trends, and would have a positive impact on vegetation growth especially in coastal ecosystems with enough water resources, like wetlands (Raynolds *et al.*, 2015). Figure 6.3 shows that the average air surface temperature has fluctuated but shows a rising trend within last a few decades over all three case studies. The Towamba estuarine ecosystem (with Cfb weather conditions) is the highest latitude site that records higher global warming impacts, and as Figure 6.3a shows the mean temperature is 16°C, but the overall trend has significant increased by 0.4°C, from 15.8 to 16.2°C. Whereas, Wandandian estuarine delta (with Cfb weather conditions) has a temperature average of 16.5°C with a slightly increase of 0.2 from 16.4 to 16.6°C (Fig. 6.3b), and Comerong Island estuary (with Cfa weather conditions) has a slightly increased temperature trend by 0.2°C as well, ranging between 16.5-16.7°C with an of average of 16.6°C (Fig. 6.3c).

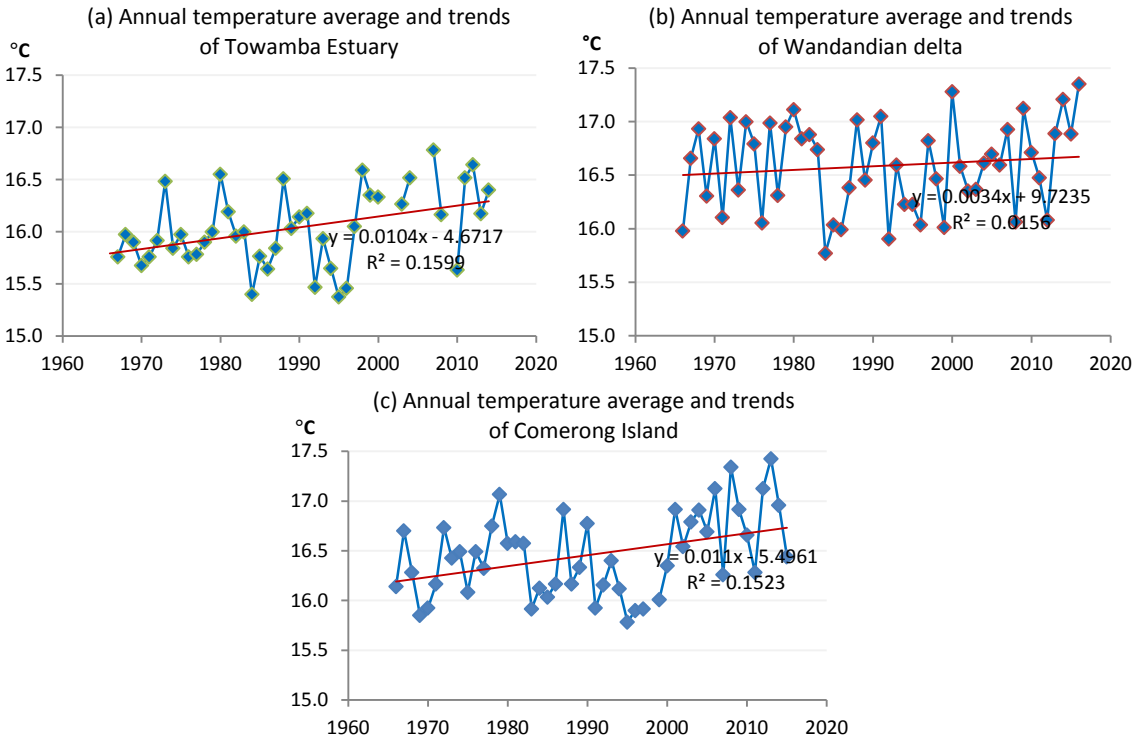

Figure 6-3. Mean annual air Celsius temperature (1968-2015) at the study sites: (a) Towamba, (b) Wandandian and (c) Comerong. The temperature trends at the three study sites have increased during the past 49 recorded years (BOM, 2017b; KNMI, 2017).

The results of monthly (mean) temperature and precipitation data for all three study sites have been analysed and are shown in Fig. 6.4. They indicate that January and February (south hemisphere summer) are the warmest months while February and March are the wettest months in the records (Fig. 6.4). The monthly precipitation records show that these sites have no dry season but precipitation declines slightly during winter, especially from July to September (Fig. 6.4).

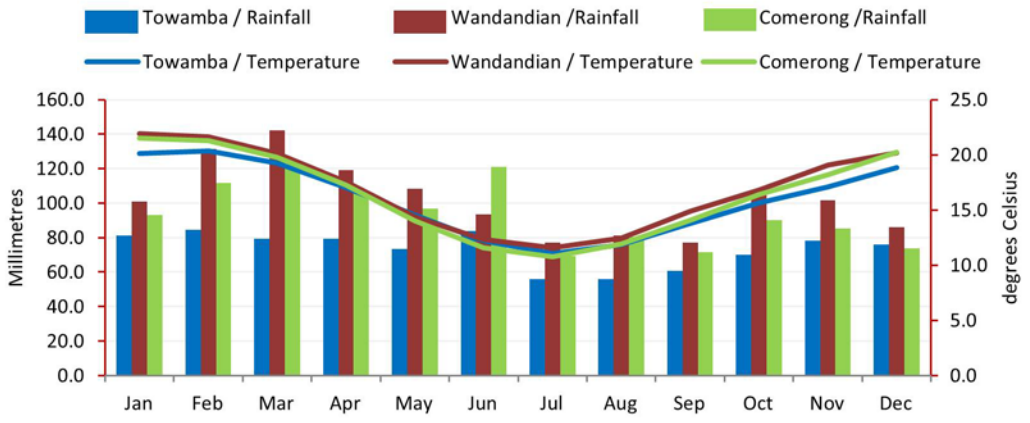

Figure 6-4. The temperature and precipitation (monthly data) for all study sites (together) during 1966-2015, which have shown the highest seasonal temperature occurs during the south hemisphere summer, particularly in January and February. At the same time, February and March are the wettest months in the records (BOM, 2017b; KNMI, 2017).

The best vegetation growing months are January and February at such coastal ecosystems, which is combined with a stability of tidal stage at this time of the year. These two months would have the highest NDVI values recorded during the long warm growing season. This summer period is associated with enough water resources: (i) brackish water in the intertidal habitats (e.g. mangrove and saltmarsh); and (ii) precipitation for the elevated vegetation on the estuarine barrier (Towamba and Comerong, about 4 and 6 m above AHD), as well as the high deltaic zone (Wandandian, about 1.5-3 m above AHD) where some mixed native plants like eucalypts are present and are rainfall dependent (Jones *et al.*, 1999; Weier & Herring, 2000; Al-Nasrawi *et al.*, 2016b, 2018b).

6.2.4.7 Mean sea level

Coastal ecosystems, particularly coastal wetlands (e.g. mangrove, salt marsh and associated habitats) would be strongly influenced by sea level rise (SLR) in terms of their zonation, position, and elevation characteristics (Barnett, 1983; Woodroffe, 1990; Gedan *et al.*, 2011; Church *et al.*, 2013). These habitats can be subjected to losses of area, extent and distribution, as well as the wellbeing of productivity (Costanza *et al.*, 2008). Coastal ecosystems are the most sensitive, responsive and vulnerable ecosystems on Earth to SLR (Nicholls *et al.*, 1999). Coastal wetland ecosystems are well developed and conserved along the extensive Australian coasts and shorelines, including southeastern NSW (Roy *et al.*, 2001; Zedler & Kercher, 2005; DSE, 2007; Department of Environment, 2010). However, changes are not exclusively restricted to SLR since, nowadays, direct and indirect climate change and human development have had significant impacts on such ecosystems worldwide (Michener *et al.*, 1997).

Stratigraphic and sedimentological literature of the sediments underlying coastal wetlands and their unique associated habitats (e.g. mangrove and salt marsh) indicate that there have been considerable changes in the extent of these wetlands as a direct result of historical sea level fluctuations (Thom, 1967; Woodroffe, 1990; Michener *et al.*, 1997; Deconto & Pollard, 2016). In addition, the indirect human settlement effects of modifying the catchments have led to a series of sedimentary problems, which would leave the coastal wetlands less able to keep up with SLR (Davenport & Davenport, 2006; Lee *et al.*, 2006; Al-Nasrawi *et al.*, 2016b, 2017b, 2018a, 2018c).

In general, as observed from prior studies, stressors would, in either a direct or indirect way (or both), lead to losses of coastal wetland vegetation extent, surface canopies and land classes. Hence, the response of coastal ecosystems, especially coastal wetland ecosystems, to SLR would depend on the existing coastal topography, rates and sources of sedimentation, and the SLR rate itself (Michener *et al.*, 1997; Costanza, 1999; Nicholls, 2004).

The reported mean sea-level rise (MSLR) locally, which is relevant to the study sites, forms part of the global rise of mean sea-level that has resulted from the global climate changes (Church *et al.*, 2013; Pachauri *et al.*, 2014). It is based on mean sea level relative to the local or nearest tide gauging stations to the case study sites as follows. Towamba site has used the Eden tidal gauge station (1.4 km away) and the observation period has been extended from 1986 to present time (it has some unavailable observations in 1957-1958, 1960-1972, 1983-1984). Sea level data for both the Wandandian and Comerong sites was derived from the Port Kembla tidal gauge, located ~45 km away but it has a longer observation record extending from 1957 to recent time (BOM-NSW, 2017), as shown in Figure 6.5.

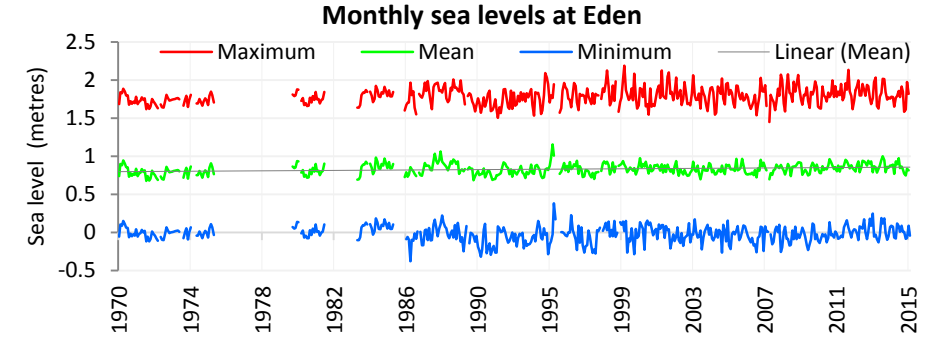

Statistics;

Mean sea level = 0.838 (Average monthly means = 0.836)
Maximum recorded level of 2.187 metres at 1100 hours 14/06/1999.
Minimum recorded level of -0.380 metres at 0500 hours 02/12/1986.
Standard deviation of the observations = 0.4009 metres.
Skewness = 0.1321.

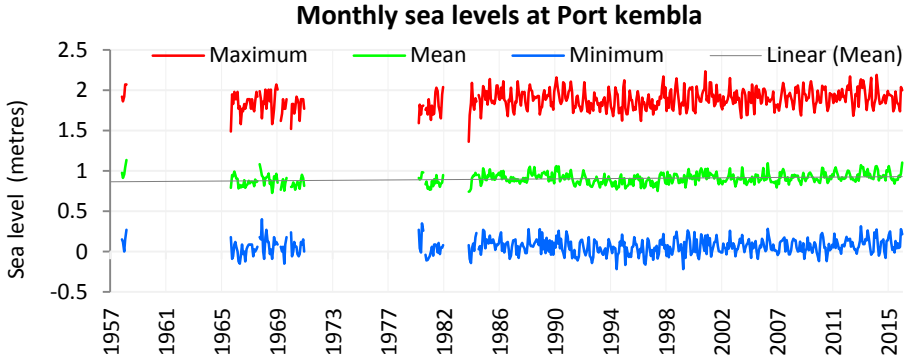

Statistics;

Mean sea level = 0.907 (Average monthly means = 0.906).
Maximum recorded level of 2.233 metres at 1000 hours 19/08/2001.
Minimum recorded level of -0.217 metres at 0500 hours 04/12/1994.
Standard deviation of the observations = 0.4055 metres.
Skewness = 0.1702.

Figure 6-5. Monthly sea levels records (the tidal range in m) for; Towamba estuarine ecosystem (Eden - 1986 to 2015), Wandandian estuarine delta and Comerong Island estuary (Port Kembla - 1957 to 2016). Red is the maximum, green is the mean, and blue is the minimum (BOM-NSW, 2017).

Primary analysis of these monthly data from the above gauging stations, based on the 59 year time-series of sea-level measurements from 1957 to 2016 (in general), conceded a statistically notable SLR trend during the past few decades. The standard deviation of data observations is

equal to 0.4 at both gauging stations (BOM, 2017a). Figure 6.5 clearly shows that sea level at both gauging stations has fluctuated and risen as follows.

Towamba site; the average mean sea level is 0.84 m, and the maximum recorded sea level was 2.19 m on 14th June 1999, whereas the minimum recorded was on 2nd December 1986 at -0.380 m. The overall average trend of SLR at Towamba is a rise of 4.5 cm from 0.815 to 0.860 m during the last three decades.

Wandandian and Comerong sites: monthly average mean sea level is 0.907 m, and the maximum recorded was 2.233 m on 19th August 2001, whereas, the minimum recorded was on 4th December 1994 at -0.217 m. The overall average trend of SLR at Wandandian and Comerong is 3.5 cm from 0.895 to 0.930 m during the past six decades. Thus, the average of five years used as trend of a chosen year for the sea level in the regression model to assess their correlation with the NDVI trend reflections.

6.3 Methodology and datasets collection

The main methods used in this study are GIS modelling and statistical analyses, which have been applied to the three case studies for the period from 1975-2015 at 5 year intervals, as follows (see Fig. 6.6):

- The GIS analysis was based on imagery analyses for NDVI, including imagery spatial/radiometric enhancements, classification indices; clipping/expression, temporal trend analysis and raster attribute analysis (collecting the pixel values for the statistical analysis).
- The statistical analysis using RStudio included analysing the climatic indicator trends for precipitation, temperature and mean sea level, as well as regression analysis to determine the liner correlation between these climatic factor trends and the NDVI trends (pixel values) spatiotemporally.

6.3.1 Landsat Imagery Data (1975-2015)

Landsat 1-8 imagery at five-year intervals from 1975 to 2015 (Table 6.3) was utilised to create the NDVIs to determine vegetation trends for each case study site. The analysis was based on a Landsat MSS, TM sensor summer dataset with a resolution of 79 m or 30 m from a single satellite image covering each-site/each-year. The imagery was chosen from southern hemisphere summer images since they have the best weather conditions that may affect the surface/canopy radiation wave reflections recorded by the satellite, particularly within such coastal ecosystems at the case study sites.

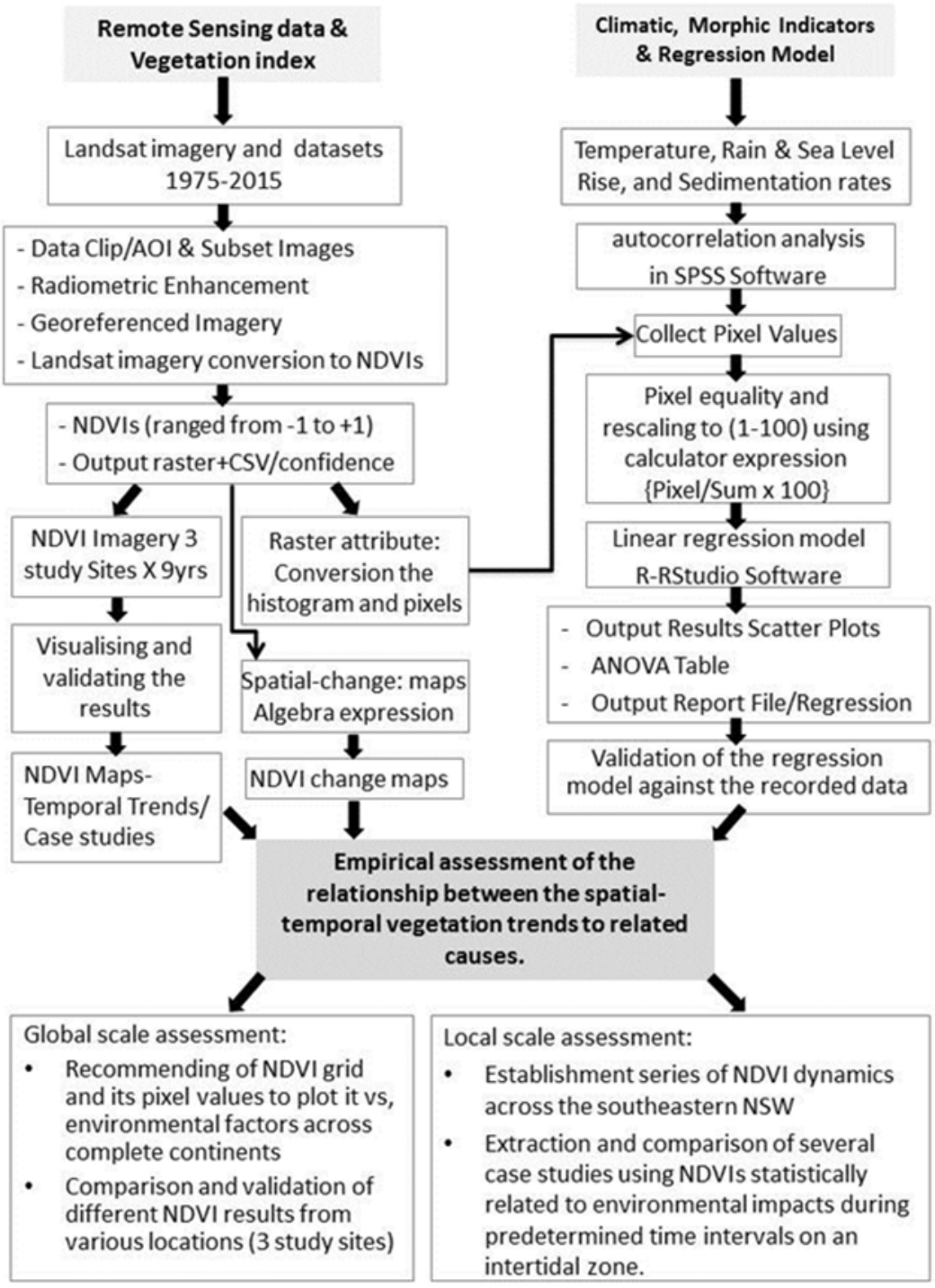

Figure 6-6. Methodology of the modelling approach steps used in the study. It has been applied to the Landsat satellite imagery and climatology datasets, using ERDAS IMAGINE 2014, ArcGIS 10.2 and R-RStudio (RStudio).

The Landsat images have been radiometrically and geometrically rectified to meet the framework parameters including coordinate systems, atmospheric issues, and pixel size, as well as clipping the Landsat datasets for all three case study sites every five years from 1975 to 2015 according to each site boundary separately to be presented, but the whole data of pre-chosen year (data in intermediate years) will be included in the processes to get the average

NDVIs for that chosen year (Fuller, 1998; Pettorelli *et al.*, 2005; Nguy-Robertson & Gitelson, 2015; Tian *et al.*, 2015; Peng *et al.*, 2017).

Table 6-3. Landsat satellite sensors utilized for the case studies*.

Sensor	Satellite	Overpass/orbit Frequency	Data Record (years)	Spatial Resolution
MSS	Landsat 1-3	18 days	Jan, Feb 1975, & 1980	79 m
TM	Landsat 4-5	16 days	Jan, Feb 1985, 1990, & 1995	30 m
ETM+, OLI	Landsat 7-8	16 days	Jan, Feb 2000, 2005 , 2010, & 2015	30 m

*(USGS-Landsat, 2017; USGS, 2017b)

Meanwhile, to make the multi-date data are comparable for valid use in research, This thesis is using the assuring geometric accuracy, including scaling of pixel sizes to a uniform spacing and converting the imagery pixels (30 and 79 m) to be equally scaled from 0 to 100, especially needed when using both MSS and TM and OLI, with different native bit depths, assuring common pixels extent. Some of the standard procedure, statistical weighting, is used to cope with rescaling to a common pixel spacing to accomplishes with the multiple date images. Using the standard procedure for coming to a uniform spatial scale would be to use some kind of neighbourhood weighting, where the respacing comes before the analysis, which usually used to make sure that the output values are radiometrically equivalent, rather than visually smooth. That determines the weighting used. That resulting of analysing the various resolutions of the Landsat datasets (Table 6.3), guided this study to develop a specific equation to give an equal opportunity for the NDVI pixel values to be presented, and the 79 m resolution is equity-compared with the 30 m resolution datasets statistically, as shown in equation (2)

$$\mathbf{DE} = \frac{\boldsymbol{\lambda DN}}{\sum \boldsymbol{DNs}} \times (\mathbf{100}) \qquad (2)$$

Where; DE is the dataset equality, λ DN is the digital number of the pixel value (NDVI value) of each pixel in the single satellite image, and the ∑DNs is the pixels total value (sum of NDVI of that image) in the same satellite image.

Negative values of NDVI (values nearer to -1) relate to not vegetated surface including barren rocky territories, snowy or sandy surfaces. Values from zero to one (0 to 0.1), for the most part relate to vegetation canopies. It will depend on the relative NIR and RED reflectance of the particular rock and sand in particular image, rests on testing the cutoff values for the chosen images and areas (Weier & Herring, 2000; Pettorelli *et al.*, 2005). Apparently at the local coastal ecosystem, low positive values relate to bush and meadows of saltmarsh (roughly 0.02 to 0.04), whereas higher values determine mild/tropical mangroves and blended plants, for

example, *Casuarina* (values drawing closer 1). The typical reach is between about -0.1 (for a not exceptionally green territory) to 0.6 (for an extremely green zone; Goward & Prince, 1995). Values under zero commonly do not have any ecological significance, thus, this research is considering the whole range -1.0 to 1.0, but it gives more attention to 0.0 to +1.0 ranges. Higher values result from a clear difference from the Near-Infrared to RED radiation received by the satellite sensor that can be equated with the very photosynthetically-dynamic green canopy. Meanwhile, a small distinction between the NIR and RED signals will reflect low NDVIs. This occurs when there is minimum photosynthetic activity and no reflectance of NIR light such as reflections from water bodies (Goward & Prince, 1995; Pettorelli *et al.*, 2005; Donohue *et al.*, 2009).

6.3.1.1 Creating a NDVI using ERDAS IMAGINE

The major focus of this chapter is to find out and assess the ecosystem dynamics by classifying the satellite images with NDVI over time focusing on vegetation radiometric reflection trends in each satellite image from the study site/time. NDVI modelling tool from ERDAS IMAGINE 2014 has been used and multispectral Landsat datasets, because they have RED and NIR, as well as other bands (USGS-Landsat, 2017). After that, the NDVI series converted to colour-ramped (visualised-able) maps and their pixels attribute converted to a CSV format to be analysed and plotted to their influences factors.

6.3.1.2 Pixels distribution and length management

The image surface (Fig. 6.7a) is actually a digital background representing a digital surface (Fig. 6.7b,c); this surface has been divided into rows and columns producing pixels. Each pixel has its own value that represents a specific phenomenon of the captured area, within the resolution allowance, and its position on the digital surface is represented by its unique latitude and longitude. However, many continuance phenomena would have the same pixel values, which could be reorganised, as in Fig. 6.7c, and be statically analysed by regression. Consequently, the pixel values have been plotted (as a scale) according to their time of appearance (as frequency).

Figure 6.7c illustrates this idea; the chosen (example) value of 0.241 (in yellow) has appeared five times on the digital surface (Fig. 6.7b); it is then simply reorganised to appear as one value (Fig. 6.7c) plotted based on its frequency which is 5 (note the actual repetition of the pixel value of 0.241 for this whole Landsat tail was 1986). This process has been repeated for all other Landsat tails, and the resultant NDVI pixel values have been plotted according to their supposed influence by independent variables using the database in Fig. 7d and equation 7e. This resulted in the linear correlations shown in Fig. 6.7f.

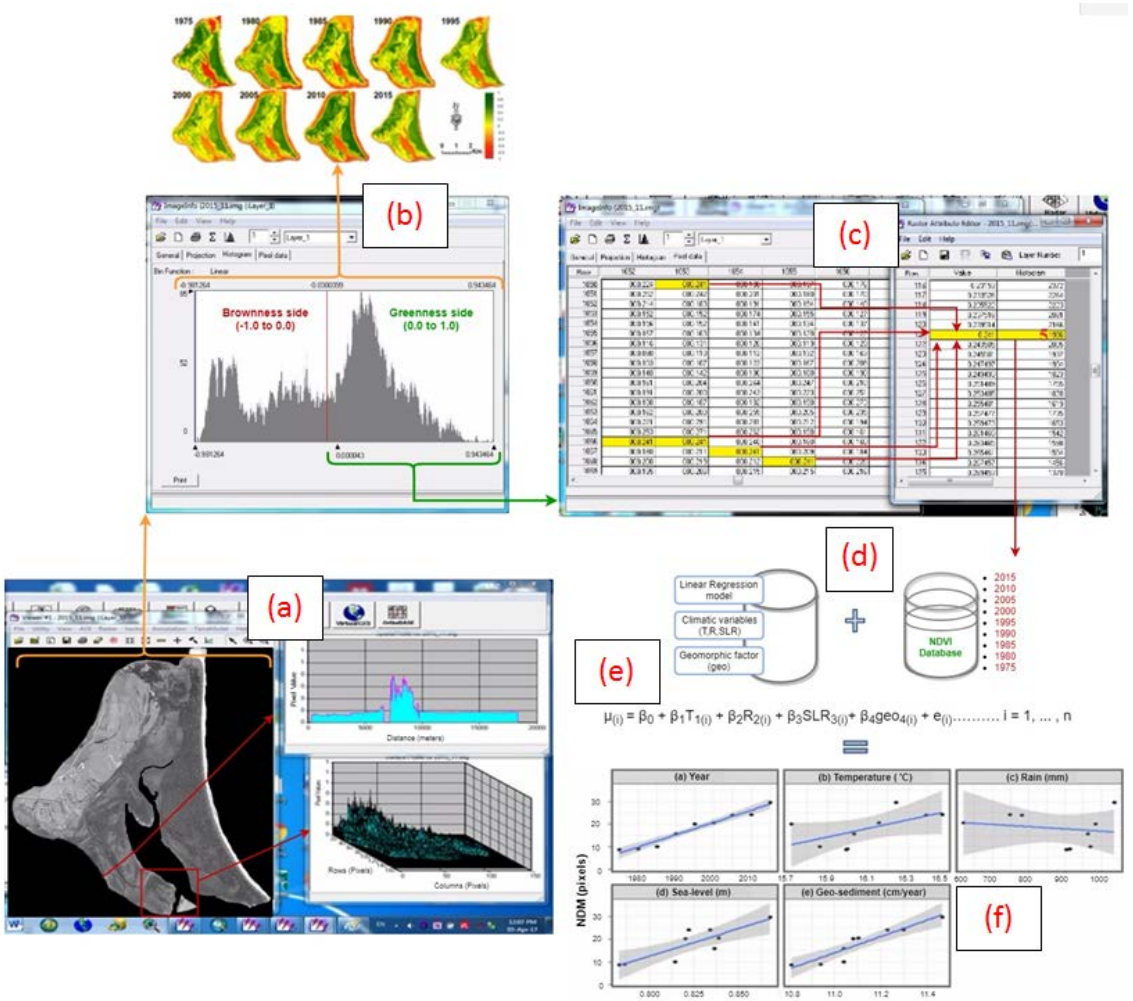

Figure 6-7. An example of preparing/interpolating the Landsat datasets and pixels distribution management in ERDAS IMAGINE and RStudio.

This method allows the data values to be dealt with statistically and ignores their specific locations (as in Fig. 6.7c,d); thus the pixel values pretend to act as a data scale and the frequency is shown as a data histogram. Figure 6.7a also shows a profile section and surface of the southern part of Comerong Island, as illustrated on the right hand side. It shows a clear vegetation concentration in the middle of the channel shoreline indicating that the shoreline dynamics will essentially impact the vegetation canopies and the resultant NDVIs. Figure 6.7b shows the NDVI histogram scaled from -1 to +1 and representing both brownness and greenness sides on the visualised NDVI figure. The statistical analysis has considered the -1.0 to 1.0 range, but later analysis is more focused on the greenness side, as Figs 6.7b and c show.

Using images with different resolutions would affect the total number of rows and columns and hence the resultant pixels on the digital surface. The equivalent attribute table for the image would be either shorter or longer depending on the resolution, which will also affect the statistical analysis. Thus, an equation needs to be developed to give equal weight comparison to the all the used data.

A separate trend analysis of vegetation change in the NDVI datasets, based on an algorithm developed by Fuller (1998), has produced regression coefficients in an imagery format. The approach developed by Los (1993) has been adopted to minimize sensor-related trends, and radiometric errors, which are corrected for sensor degradation effects and different pre-launch calibration coefficients. Then, the NDVI trends are calculated from the mean annual NDVIs over 40 years, and each was examined for statistical significance. Landsat imagery-tails were also inspected for their association with land-cover as matched by Hopley & Jones (2006), ALUM (2010), Thompson (2012) and Al-Nasrawi *et al.* (2016b, 2017b, 2018a).

6.3.2 Climate related indicators

Climate datasets of the monthly temperature, precipitation and mean sea level were obtained from the historical records of the local gauging stations at the study sites. With a specific end goal to evaluate the this study has additionally utilised other air temperature, precipitation and sea level datasets from KNMI-Climate-Explorer, and has examined the missing information from nearby stations too (KNMI, 2017; BOM, 2017a). This study has utilized the local gauging station to demonstrate whether the local impacts (weather conditions) at the study sites belong to regional and global systems that are affecting all the sites, such as El Nino and La Nina (BOM, 2017b).

6.3.3 Regression Model

Statistical regression was used to explore the relationship between NDVIs as an indicator of wetland vegetation and a range of potential climate drivers for corresponding years. The liner regression-models (multiple linear) were employed by exporting the remote sensing datasets into RStudio (at each study site) were combined, with consideration to their time scale order, in the dataset to maximize variability across the variables explored.

For each data case (the three case studies) there was an RS measure of NDVI vegetation (dependent variable) and regressed against the values of three climatic indicators; temperature, precipitation and sea level rise as well as sediment rates (independent variables). The sedimentation data for the Towamba, Wandandian, and Comerong sites were obtained from previous research (chapters 2,4,5) that concentrated on the geomorphic dynamism of these sites (Al-Nasrawi *et al.*, 2015b; Al-Nasrawi *et al.*, 2016b; Al-Nasrawi *et al.*, 2017b; Al-Nasrawi *et al.*, 2018a). Data preprocessing has been applied to the whole datasets. Because this research is focused on the permanent vegetation statue that resulted from the environmental conditions over years, we used the five-year-average technique of calculating

the NDVIs, climatic and sedimentation rate and then run the regression model. For example, the NDVI values of 1980 are gained by averaging pixels over a spatial area of pre-1980 five years (1976 to 1980), which has been applied to all NDVI series (except 1975 that is based on the previous 3 years only). That has been done, also, for all other variable datasets to gain the averages of climate and sedimentation conditions. Then the regression model plotted the average (mean) pixel values for each year of the NDVIs, climatic and sediment rate factors at each location to determine the coefficients of variation β_0 to β_4, and the variation proportions accounted for by each regression model. For the regression procedure, this was achieved by inputting data cases into the following equation (3).

$$\mu_{(i)} = \beta_0 + \beta_1 T_{1(i)} + \beta_2 R_{2(i)} + \beta_3 SLR_{3(i)+} \beta_4 geo_{4(i)} + e_{(i)} \quad i = 1, \dots, n \qquad (3)$$

where:

- μ = NDVI pixel value average for the year (dependent variable),
- T_1 (temperature), R_2 (rain), SLR_3 (sea level rising), and geo_4 (sedimentation rates as geomorphic factor) are the independent variables,
- $e_{(i)}$ is the independent, normally distributed error term,
- **n** is the number of pixels each year at each study site, and
- $\beta_0, \dots, \beta_4$ are coefficients estimated.

Separate regressions were run for each of the case study sites on the southern NSW coast.

6.3.4 Pixel value subtraction of NDVI change maps

The spatial distribution of NDVI change maps was calculated from the raster calculator expressions, which allows the power of basic algebraic expression to be achieved on raster maps (Cordeiro *et al.*, 2005; ESRI, 2017). An expression was written in which the NDVI rasters of, for example, earlier (1975) were subtracted from the later (2015) NDVI sets to generate a raster representing spatial-NDVI changes over the study period, and so on for all the input images, to detect and demonstrate any trends. Which is simply subtracting the pixels from each other within the same latitude and longitude to create new pixels at the same locations, but with remaining values of NDVIs, whether positive or negative values, they will indicate spatial vegetation growth or decline respectively.

To limit the errors that are often introduced by choice of start and finish time, we have chosen different start and finish times in the datasets. Also, for more accuracy and validation, there is a considerable literature in the remote sensing change detection and analysis field that looks

at many ways to deal easier with multiple date datasets. Thus, we used a change vector (a visual method), which shows for a pixel or collection of pixels the trajectory of change throughout your period.

6.4 Results

6.4.1 Ecosystem dynamics; (Vegetation/NDVI trends and statistical regression model)

Visualizing and analysing the vegetation dynamics of the three study sites has been accomplished using NDVI derived from Landsat data over the last 40 years (1975-2015; Figs 6.8-6.14). NDVI has rearranged the pixel values from the Landsat data from a multispectral scale of 0-255 to the NDVI form -1 to +1. Visually, the NDVIs have resulted in Figs 6.8a, 6.10a, and 6.12a that show a clear trend of dynamic 'brownness and greenness (-1 to +1)' land-cover changes at the study sites over time. This can determine the whole land ecological and geomorphological cover dynamics. Statistically, however, this study has more focused on the ecological side, as presented by vegetation dynamics (greenness), so only the positive values have been interpolated statistically (0 to +1), which represent greenness canopies (Figs 6.8b, 6.10b, and 6.12b).

In general, the NDVI analyses have shown noticeable overall NDVI value increases at the Towamba estuary and Wandandian delta (Figs 6.8 and 6.10), whereas at Comerong Island a decline in the overall NDVI values occurred over the study period (Fig. 6.12).

6.4.1.1 Towamba estuarine ecosystem

The Towamba ecosystem has been analysed for its vegetation canopy dynamics using the NDVI and Landsat data from 1975 to 2015 (Fig. 6.8).

In general, Figure 6.8 shows significant estuarine ecosystem growth and changes within the last forty years in all eco-geomorphic land-covers, including vegetation canopy in graded green, sandspit patterns in yellow, and water bodies in red (see Fig. 6.8a). More accurately, a concentrated statistical vegetation analysis (see Fig. 6.8b) has shown a clear growth of the greenness of the land-covers.

Figure 6.8a,b shows the spatial distribution of the NDVI values at Towamba estuary, which has gradually increased overall during the last four decades, with some fluctuations (e.g. 1990-2000). Relating these changes over time to the relevant climatic trends can be examined by regressing them with the NDVI trends. Linear regression model analysis has been done using RStudio software, and Fig. 6.9 and Table 6.4 details the relationship of averaged climatic and geomorphic factors (temperature, precipitation, sea level and sedimentation rates) as independent variables that could affect the averaged NDVI trends (as the dependent variable) at the Towamba site.

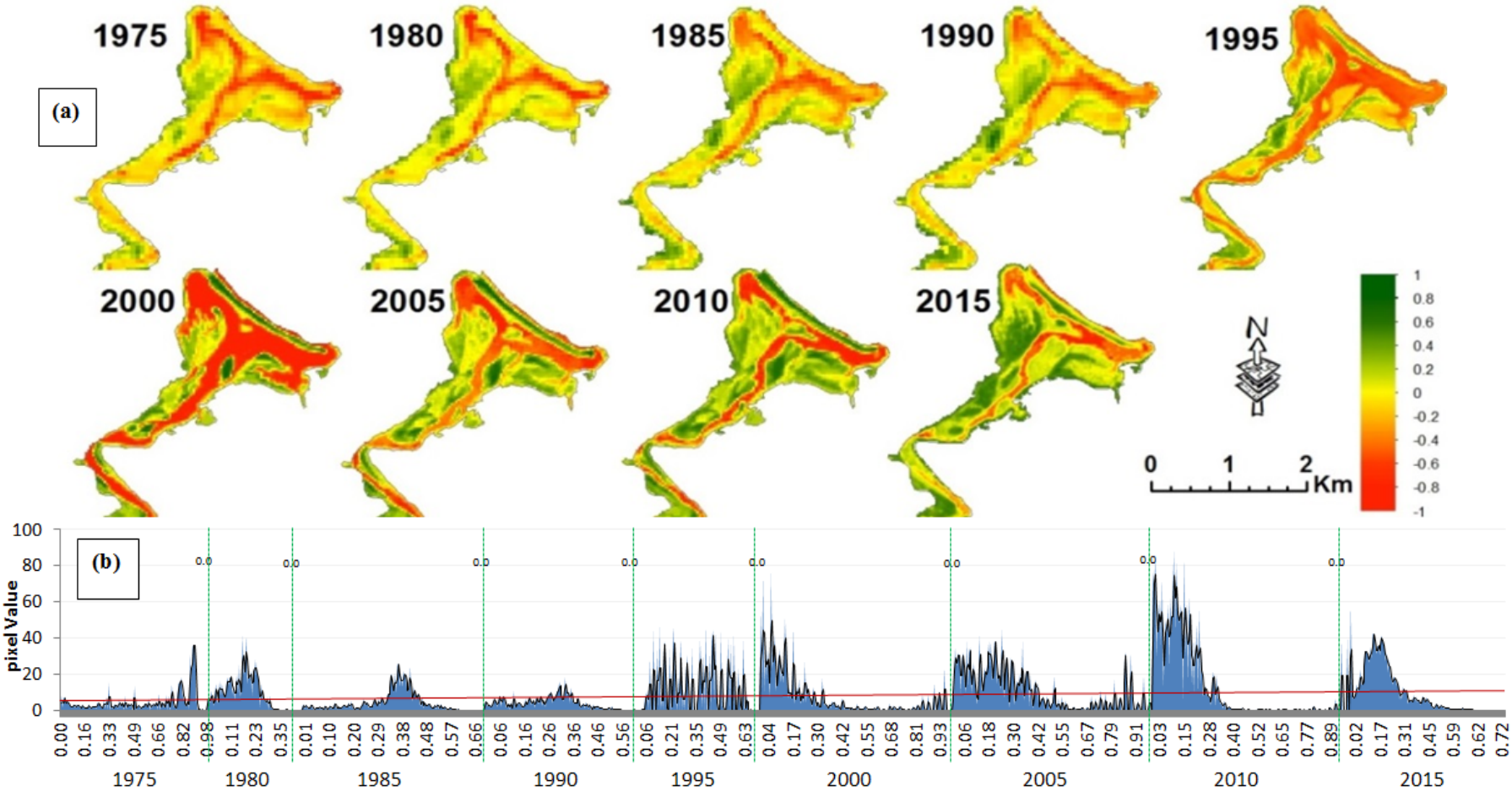

Figure 6-8. Ecosystem dynamics at a landscape level for the Towamba estuary investigations from 1975 to 2015 represented by the NDVI values. (a) Maps are showing a clear vegetation growth trend in all estuary classes (-1 to +1 of the NDVI values), and (b) histograms of the statistical analysis of the greenness side only (0 to +1 values of the NDVI scale) that show a significant trend of vegetation growth over the study period.

[Note: on the y axis, all NDVI positive values have rescaled from (0 – 1) to (0 – 100) using equation (2) to make whole numbers. On the x axis, the original range of the NDVI (pixel scales 0 to +1) is displayed, which has recorded at each year and separated by the green vertical line.]*

From the scatter plot (Fig. 6.9a) and Table 6.4 we can see a significant positive linear relationship between the dependent variable (NDVI) and the explanatory variable (time in years). NDVI has a weak positive linear relationship with temperature that is not significant at the 95% level (Fig. 6.9b). Rainfall is also not significant at the 95% level and it shows a very weak negative linear relationship with NDVI (Fig. 6.9c). However there is a moderate positive linear relationship between the sea level and the NDVI (Fig. 6.9d) that is statistically significant. Finally, plotting NDVI vs sedimentation rates (Fig. 6.9e) illustrates a significant strongly positive linear relationship between the variables.

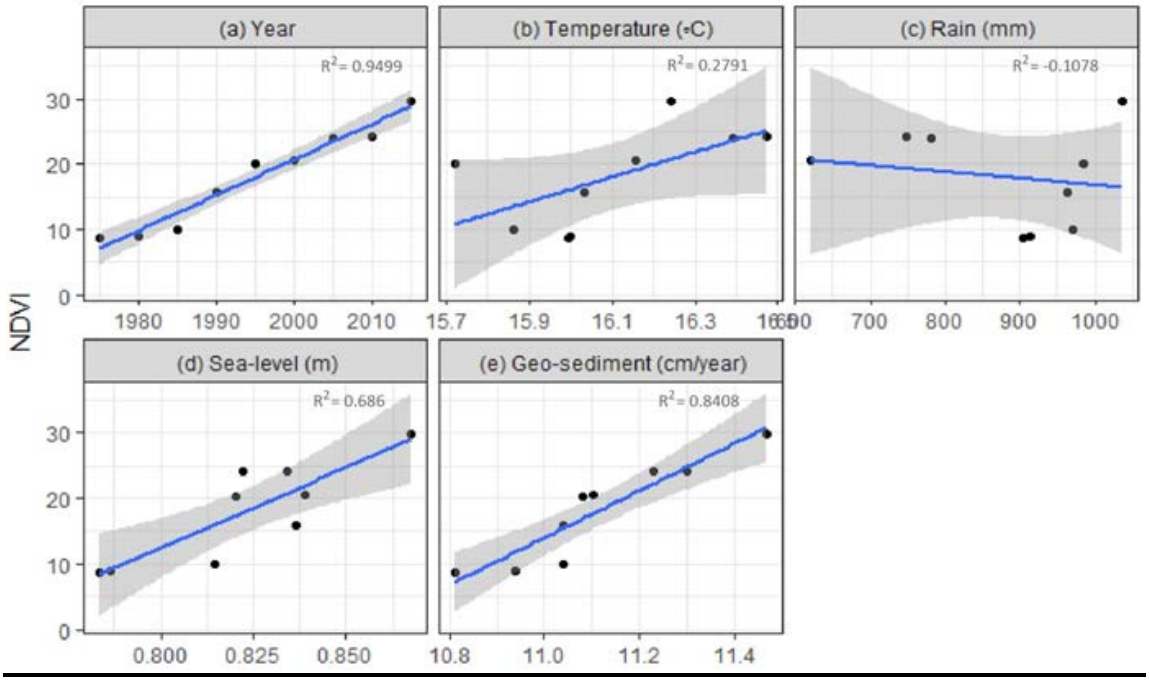

Figure 6-9. Results of Towamba site of the linear regression model are showing a positive relationships between NDVI and (a) time, (b) temperature, (d) rising sea level and (e) the sedimentation rates, but a negative relationship with (c) rainfall records. The grey area is the standard deviation of the data.

Table 6-4. Correlation summery of the regressed variables for the Towamba site, shows the R-squared, p-value and the impact level.

Variables	R-squared	p-value	Effects
Year	0.9499	$5.206e^{-06}$	P
Temperature	0.2791	0.08261	P*
Rain	-0.1078	0.652	N*
Sea levels	0.686	0.003571	P
Sediment rates	0.8408	0.0003113	P

* Means not significant, P is positive and N is negative.

6.4.1.2 Wandandian estuarine delta

Analysis of the Wandandian ecosystem dynamics at a landscape level is represented by its vegetation canopy changes, which have been monitored using the NDVI calculated from the past four decades of Landsat data (Fig. 6.10).

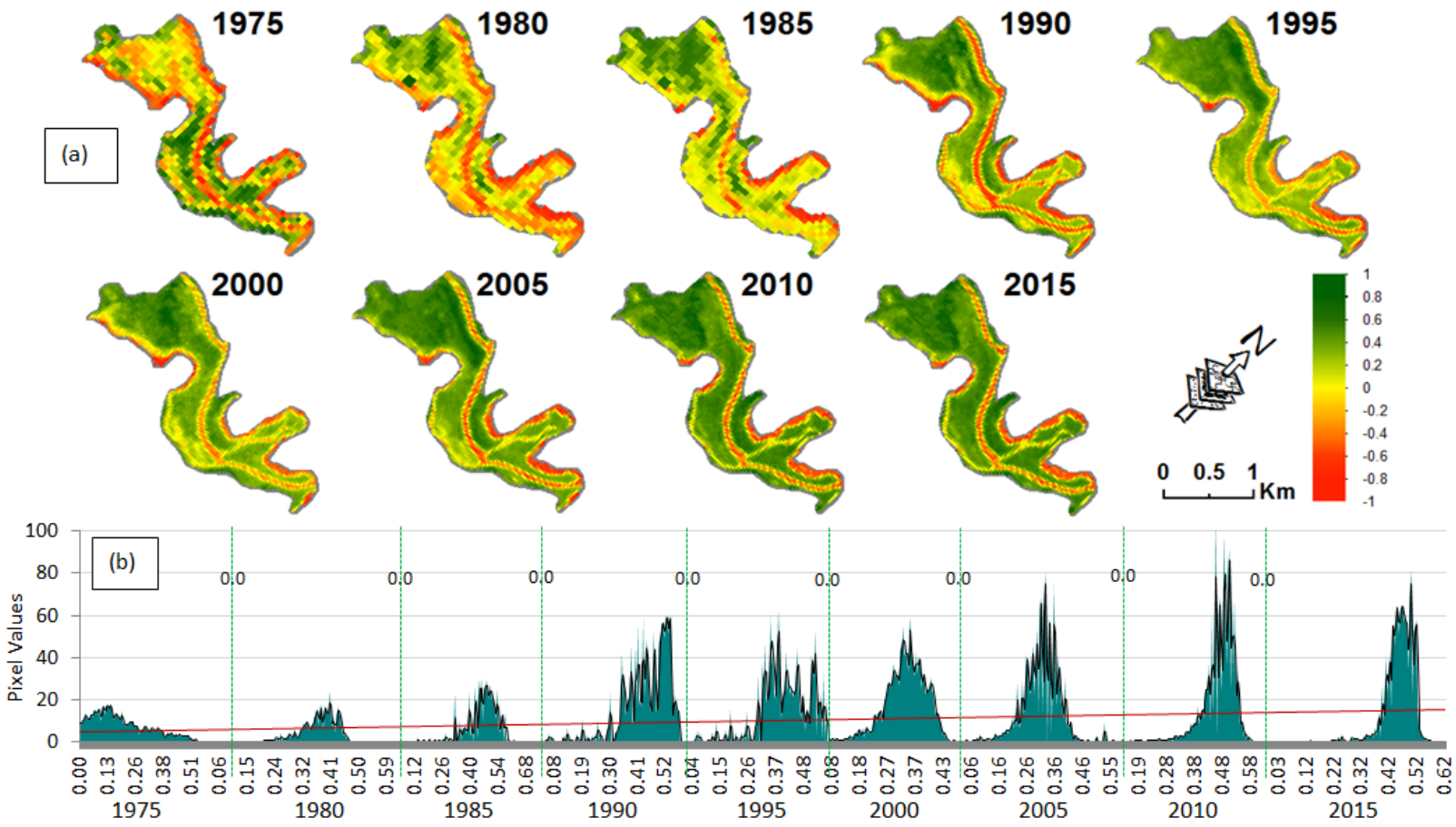

Figure 6-10. Ecosystem dynamics at a landscape level for the Towamba estuary investigations from 1975 to 2015 represented by the NDVI values. (a) Maps are showing a clear vegetation growth trend in all estuary classes (-1 to +1 of the NDVI values), and (b) histograms of the statistical analysis of the greenness side only (0 to +1 values of the NDVI scale) that show a significant trend of vegetation growth over the study period.
[Note: on the y axis, all NDVI positive values have rescaled from (0 – 1) to (0 – 100) using equation (2) to make whole numbers. On the x axis, the original range of the NDVI (pixel scales 0 to +1) is displayed, which has recorded at each year and separated by the green vertical line.]*

Figure 6.10a,b shows significant estuarine deltaic ecosystem growth during the study period (1975-2015) in all eco-geomorphic land-cover classes, including vegetation canopies shown in graded green, sandspit patterns in yellow, along with a decrease in water bodies in red (Fig. 6.10a). Objectively, a concentrated statistical vegetation analysis has shown a significant growth of the greenness of the canopies (Fig. 6.10b)

Figure 6.10 is supporting the literature finding of deltaic growth (Hopley & Jones, 2006) in shorter-term variability though, and shows a clear vegetation growth over time both visually and statistically for the whole eco-geomorphic platform (Fig. 6.10). The NDVI spatial and statistical distribution trend shows a significant overall increased brownness and greenness during the last four decades (Fig. 6.10). This has documented the overall ecosystem growth, with a clear smoothing of the spatial distribution. A slight fluctuation occurred during 1990 to 2000 (Fig. 6.10a).

Results from the linear regression analysis model provide details of the climate-related factors plus the sedimentary processes that could affect the NDVI trends at the Wandandian site (Fig. 6.11 and Table 6.5).

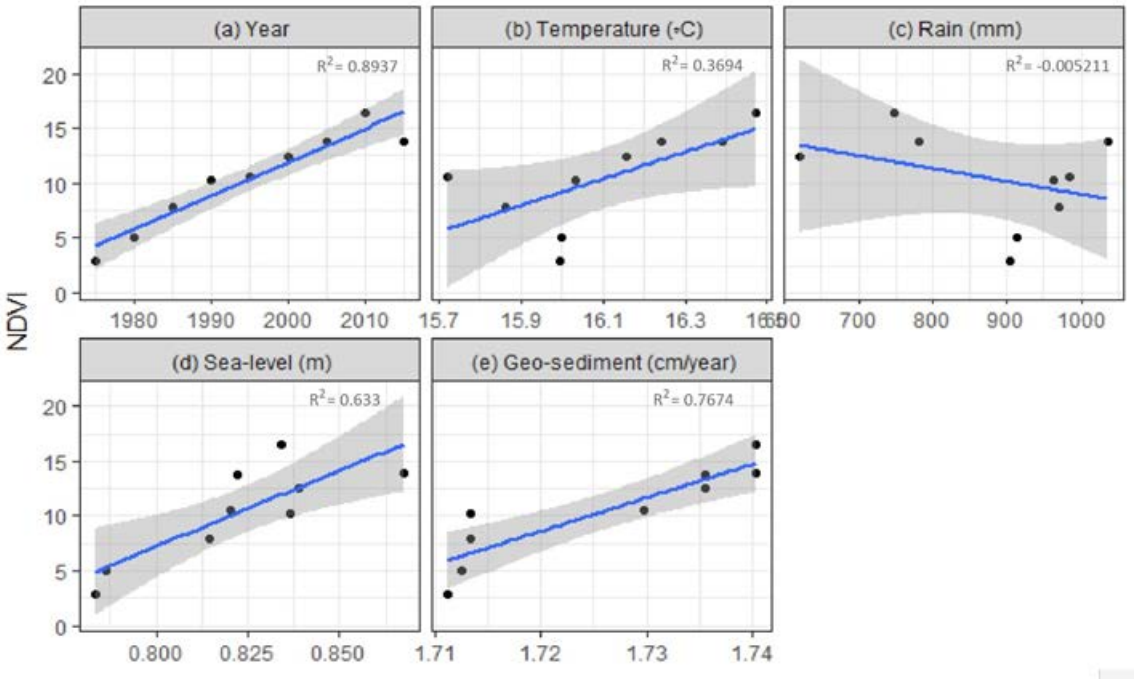

Figure 6-11. Wandandian site' results of the linear regression model with different significant p-values, showing a positive relationship between NDVI and (a) time, (b) temperature, (d) rising sea level and (e) sedimentation rates, but a negative relationship with (c) rainfall records. The grey area is the standard deviation of the data.

A strong positive linear relationship illustrated between the dependent variable (NDVI) and the explanatory variable (time in years; Fig. 6.11a, Table 6.5). Secondly, the relationship between the NDVI and temperature (Fig. 6.11b) is significant at the 95% level (p-value = 0.0486) indicating that temperature has a moderate positive linear relationship with NDVI. Rainfall does not have a significant effect on NDVI (Fig. 6.11c). In contrast, strong and positive linear correlation accruing between NDVI / SLR (Fig. 6.11d) and between NDVI and sedimentation rate.

Table 6-5. Correlation summery of Wandandian site, shows the R-squared, p-value and the effects value

Variables	R-squared	p-value	Effects
Year	0.8937	$7.407e^{-05}$	P
Temperature	0.3694	0.04856	P
Rain	-0.005211	0.3414	N*
Sea levels	0.633	0.006316	P
Sediment rates	0.7674	0.001207	P

* Means not significant, P is positive and N is negative.

6.4.1.3 Comerong Island Estuary

Figure 6.12 shows the ecosystem dynamics, at a landscape scale, of Comerong Island as represented by the vegetation canopy based on the NDVI reclassification of the Landsat data from 1975 to 2015.

Eco-geomorphic land-cover classes on Comerong Island show a slight decline in all ecosystem land-covers over the last forty years (Fig. 6.12a). Statistically, Figure 6.12b shows a clear decrease in the land-cover greenness by concentrating statistical analysis on the vegetation side only (0 to +1).

Figure 6.12 confirms the literature finding on Comerong Island of high southern shoreline erosion rates (Thompson, 2012) and northern slight sandspit growth (Carvalho and Woodroffe, 2013). The greenness trend shows a slight decline on Comerong Island during the past 40 years, with a clear spatial heterogeneity of fluctuations over the island and its shorelines. The NDVI spatial distribution on the island (Fig. 6.12) has gradually decreased during the last four decades, with some fluctuations with higher greenness being recorded (e.g. 1975 and 2010), and declining after that in 2015.

Hence, a statistical regression model can be used to examine and estimate which climate factors or sedimentary features have the most effect on the NDVI trends (Fig. 6.13 and Table 6.6).

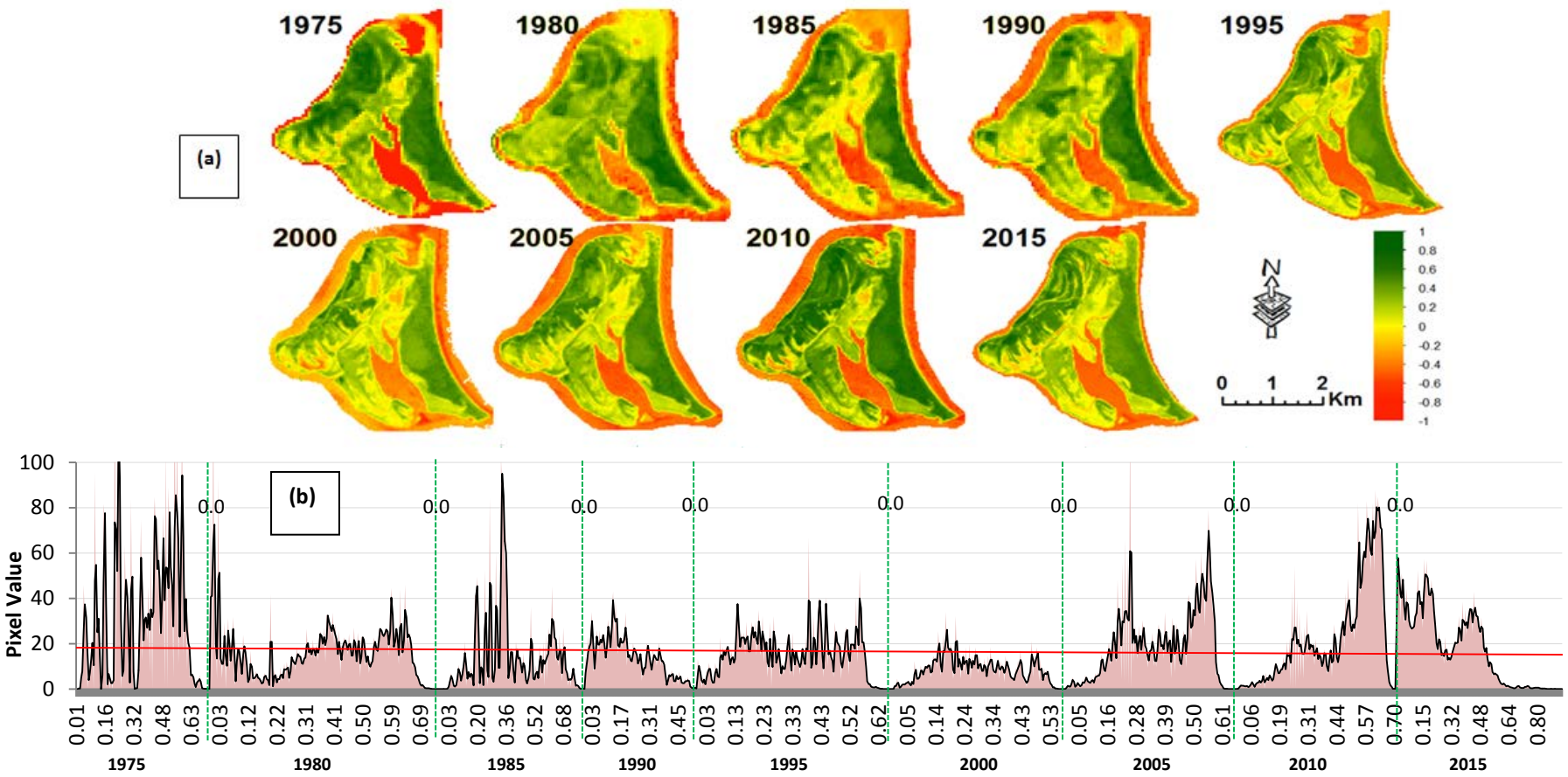

Figure 6-12. Ecosystem dynamics of the Comerong site investigation from 1975 to 2015 presented as NDVI values. (a) Shows a fluctuated visual declining trend of the island classes overtime (-1 to +1 of the NDVI values), and (b) histogram of the statistical analysis of the greenness side only (0 to +1 of the NDVI values), that shows a slight statistical decline in the overall trend of vegetation dynamics over the study period.

[Note: on the y axis, all NDVI positive values have rescaled from (0 – 1) to (0 – 100) using equation (2) to make whole numbers. On the x axis, the original range of the NDVI (pixel scales 0 to +1) is displayed, which has recorded at each year and separated by the green line.]*

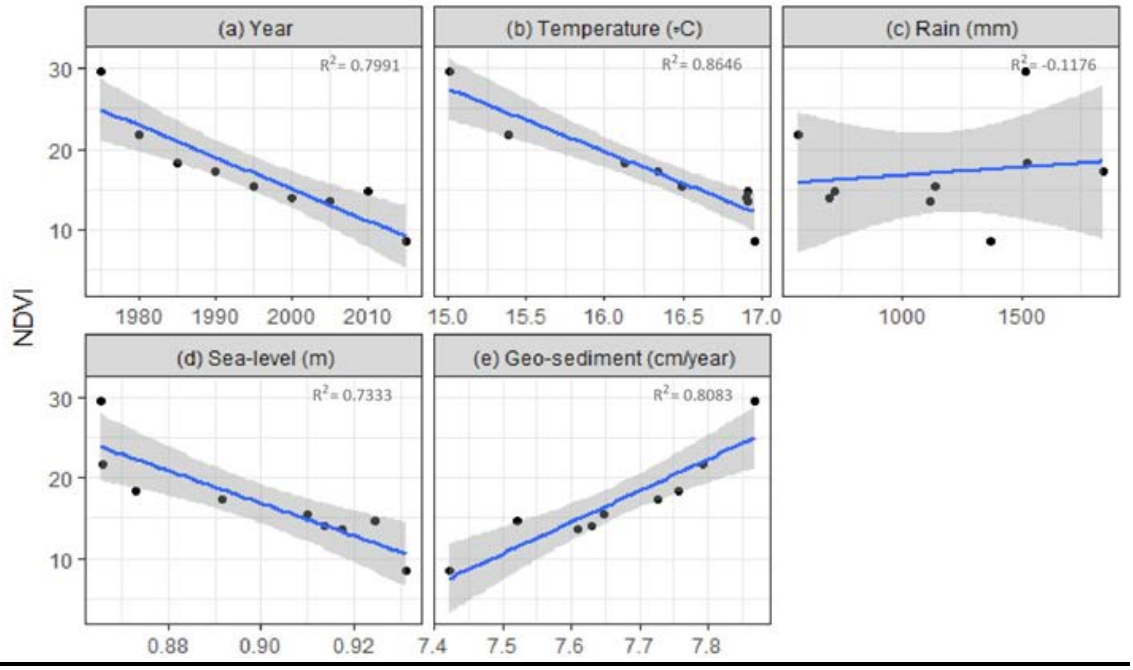

Figure 6-13. Results of the Comerong' linear regression model, is showing a negative relationship between NDVI and (a) time, (b) temperature, and (d) rising sea level, but positive with (c) rainfall records and (e) the sediment rates. The grey area is the standard deviation of the data.

The scatter plot (Fig. 6.13a) of the NDVI over time demonstrates a strong negative linear relationship that is statistically significant at the 95% level (Table 6.6). There are also significant strong negative linear relationships between temperature and NDVI (Fig. 6.13b) and between NDVI and sea level (Fig. 6.13d). In contrast a very weak positive linear relationship can be seen between NDVI and rainfall (Fig. 6.13c). It can be concluded that NDVI may not be impacted by rainfall at the Comerong site. The scatter plot between sedimentation rate and NDVI (Fig. 6.13e) suggesting a significant strong and positive linear correlation between those factors.

Table 6-6. Comerong site' summery of the linear model correlation, shown R-squared, p-value and the effect relationship levels.

Variables	R-squared	p-value	Effects
Year	0.7991	0.000714	N
Temperature	0.8646	0.0001749	N
Rain	-0.1176	0.7028	P*
Sea levels	0.7333	0.001977	N
Sediment rates	0.8083	0.0006031	P

** Means not significant, P is positive and N is negative.*

6.4.2 Spatial distribution of NDVI change maps (using Raster Calculator)

High values of the NDVI index equate to the presence of more vegetation, thus simple comparisons has been drawn between values of the index on different dates to assess vegetation reflection. For example, to subtract an index calculated for one (earlier) date from an index calculated for another (later) date have yield positive values for vegetation gain (in green) and negative values for vegetation loss (in red). In this way, a map of the spatial

distribution of vegetation change has been established for these coastal wetland cases in southeastern Australia, the NDVI canopy changes, including some geomorphic bases/sets, overtime identified using the map-algebra expression (using more than one start and end point), as well as the change vectors method (Fig. 6.14).

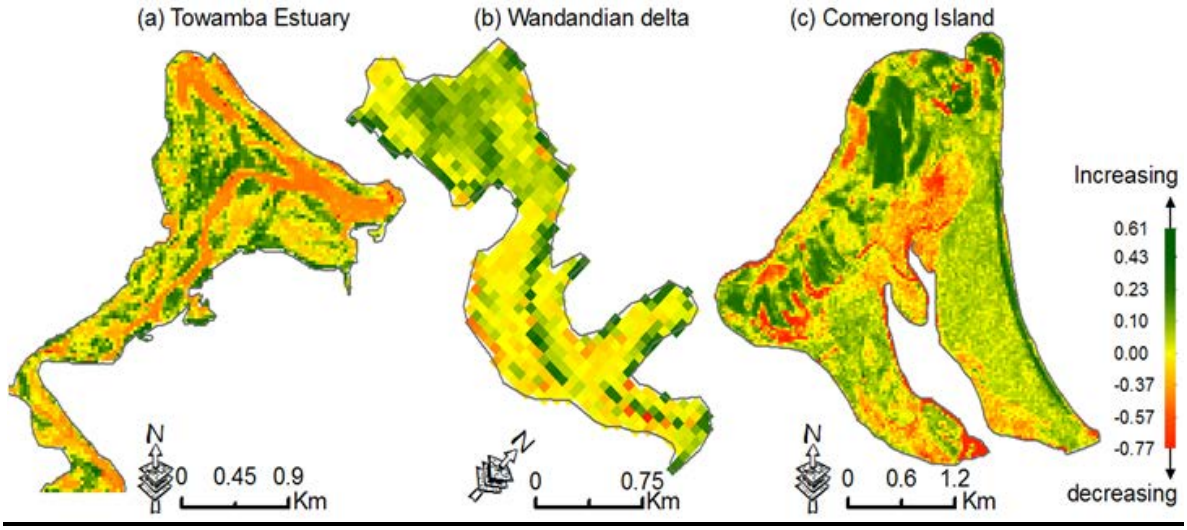

Figure 6-14. Raster calculator analyses (NDVI differences) are showing; the spatial distribution of NDVIs changes at the study sites over time, using the map-algebra expression. The maps are based on the differences between the NDVI pixel values between 2015 and 1975.

Figure 6.14a,b shows clear increases in the NDVI values within the Towamba (ignoring the discharge channel in orange) and Wandandian sites, which reflect high vegetation growth rates at both sites. However, decreases in emergent estuarine wetland vegetation canopy were detected on Comerong Island (Fig. 6.14c) showing the decline has scaled from orange to red on the island landform itself.

6.5 Discussion

6.5.1 Towamba vegetation dynamics

6.5.1.1 Towamba NDVI trend

The Towamba ecosystem, (at a landscape scale) and its habitat growth evidence, shows a clear spatial heterogeneity. The spatial distribution of the NDVI values in the Towamba estuary (Fig. 6.8) has gradually increased overall during the last four decades, with some fluctuations (e.g. 1995-2000) that may relate to a flood event that occurred in late 1990 and eroded the active channel and low-lying sandspits. However, Figure 6.8 shows that erosion has affected the active channel bed more than the greenness cover over the estuary, and then the eco-geomorphic system started growing again. The overall growth represented by the mean NDVI

(-1.0 to +1.0) over the study period increased by 9.5%, from 29.1% to 38.6% of the total wave reflections of Towamba area (i.e. Fig. 6.8b), whereas the greenness portion (0.0 to +1.0) average increased as well by 5.9% from 5.1% to 11%. This indicates that the Towamba estuary is growing both ecologically and geomorphologically. Interestingly, the bare geomorphic units (brownness; -1.0 to 0.0) have increased from 24% to 28.6% at the Towamba site and are significantly larger than the greenness cover. Over 4 decades this might be due to the sedimentary characteristics of the estuary, whereby sediment infills the estuary providing ground on which vegetation can later become established.

6.5.1.2 Towamba regression model

The reason the linear regression test (Fig. 6.9 and Table 6.4) shows an important interrelationship between NDVI and all climate and sediment factors may be because the positive correlation with increasing sea level and sediment rate as well as temperature allows a longer growing season and higher photosynthetic productivity in addition to gaining ground geomorphologically in this coastal system where water resources are available. Consequently, rainfall has not impacted the vegetation growth temporally since water dependent plants mostly consist of mixed native plants on the elevated barrier island, which represents a very small area (~0.14 km^2, or 7% of the estuary). Sea level rise provides a significant positive affect in this correlation, at the current rising rates, which may allow more accommodation for accumulating sediment and increasing ground-wetted areas, which would help develop ecosystem stability of habitable wetlands as well as the other communities at Towamba estuary. It might also reflect severe erosion during the 1974 floods on the east coast causing extensive scouring before this analysis started.

The Towamba site is really interesting since the increasing annual temperature trend shows an insignificant positive correlation (at 95% level) with increases in the NDVI values, while it has a significant positive correlation at the other two study sites. These differences may relate to the Towamba higher latitude being located about 500 km south of Sydney. That has even resulted in different weather conditions, whereby the temperate oceanic climate (Cfb) has a slightly shorter growing season than other sites that have a warm oceanic to humid subtropical climate (Cfa). Thus, it seems that an increasing temperature trend during climate change would lead to a longer growing season in this estuarine system since suitable water and sediment resources are available to support a growth in vegetation canopy.

6.5.2 Wandandian vegetation dynamics

6.5.2.1 Wandandian NDVI trend

Extension of the delta during the Holocene by continuous accumulation of sediments via Wandandian Creek from its partially developed catchment, has led to large areas in St Georges Basin bring infilled providing a good habitable estuarine area for a range of coastal ecosystems, such as wetland vegetation and associated communities. The NDVI spatial and statistical distribution trend shows a significant overall increase (brownness to greenness) during the last four decades (Fig. 6.10). This has documented the overall ecosystem growth, with a clear smoothing of the spatial distribution. A slight fluctuation during 1990 to 2000 (Fig. 6.10) may be related to the drought and low rainfall recorded from 1993-1995, as well as the flood events that hit the area from 1998 to 2000 (Fig. 6.4) and may have caused some shoreline erosion, and the El Niño influences after 2010 (BOM, 2017a).

The overall ecosystem growth represented by the mean total NDVI over the study period increased by 10.7% from 8.4% to 19.1%, whereas, the greenness portion (0.0 to +1.0) has increased by 7.3% from 6.9% to 14.2%. This indicates that the Wandandian site eco-geomorphic system is also growing ecologically and geomorphologically, but the ecological rate of growth is higher (7.3%) compared to the geomorphic growth of only 3.4% (from 1.5% to 4.9%). This could be because the low lying wetlands have been well preserved and growing over the last few decades. However, it could also be related to the availability of sediment from the partially developed catchment, and because the Wandandian delta is slowly accumulating under low wave energy conditions in the inner St Georges Basin (Hopley, 2004) providing ideal habitat conditions for vegetation.

6.5.2.2 Wandandian regression model

Regression model analyses have shown clear vegetation growth over time for the whole ecosystem and statistically represent a preponderance of control by the three regressed climatic plus geomorphic factors on the NDVI values. The NDVI growth trend evidenced on Wandandian delta can be interpreted from the linear regression test (Fig. 6.11 and Table 6.5) that shows an insignificant negative relationship with rainfall, but a positive relationship with temperature, sea level rise and sedimentation rates. This indicates that increases in sea level have a significant positive correlation with the NDVI trend due to the long shorelines with low slope, as well as the large area of low lying wetlands that include large mangrove and saltmarsh areas. The latter have a direct connection with St Georges Basin whereby rising sea level would influence the estuarine inundated areas in conjunction with the increasing

sedimentation rates. Meanwhile, rainfall has a slight negative influence (-0.080 only) on vegetation radiation, especially on the elevated parts (~3-4 m) of the delta that are controlled by a shortage of water resources. Temperature has a significant positive affect on vegetation health as it provides a longer growing season.

6.5.3 Comerong Island vegetation dynamics

6.5.3.1 Comerong NDVI trend

Comerong Island has been generated by the Shoalhaven River as part of a wave-dominated delta, which also built the estuary and the associated ecosystems and habitats (e.g. unique wetlands) on the landward margin of the delta. Nowadays, however, although the Shoalhaven River has a huge catchment area of about 7200 km^2, which is the sixth largest catchment in NSW, the construction of Tallowa dam restricted the amount of sediment delivered downstream to balance the erosion/deposition rates along the island's shorelines. This has caused higher erosion rates along the western and southern sides of the island and resulted in loss of area at some eco-geomorphic sites (e.g. shorelines and associated intidal habitats like mangrove; (Thompson, 2012; Al-Nasrawi *et al.*, 2016a, 2016b). This loss of vegetated area would effectively influence the vegetation radiation and hence the NDVI values. In contrast, a small part of the northern end of the island has been growing (Carvalho & Woodroffe, 2013) at the same time because the original river mouth has been closed allowing sedimentation to occur in this inactive region.

Comerong Island has been analysed for its ecosystem vegetation canopy dynamics using the NDVI and the Landsat datasets from 1975 to 2015. The greenness trend shows a slight decline on Comerong Island during the past 40 years, with a clear spatial heterogeneity of fluctuations over the island and its shorelines. This could be related to specific climate events, such the El Niño that hit eastern Australia between 2010 and 2012, which resulted in higher temperatures and flood events at this site (BOM, 2017a). Specifically, the middle and southern parts of Comerong Island have been more influenced than the other sides (Fig. 6.12a).

The overall decrease represented by the mean total NDVI over the study period fell by 1.4% from 24.6% to 23.2% (Fig. 6.12a,b), whereas the greenness average decreased by 3.2% from 18.3% to 15.2% Fig. 6.12b). This indicates that Comerong Island is deteriorating ecologically and geomorphologically. But the rate of ecologic decline is higher, which may be due to: (i) geomorphic decline (caused by less sedimentation supplements plus sea-level rising); (ii) leading to a decline within the vegetation growth trend, plus (iii) the rising temperature and falling precipitation that influences the more rain dependent elevated

habitats and mixed plant communities on the elevated 4-6 m sandy barrier. Altogether, sedimentological and climatic factors have negatively affected Comerong Island with lost shoreline area leading to vegetation/habitat losses as well.

6.5.3.2 Comerong regression

The linear model for Comerong Island (Fig. 6.13 and Table 6.6) shows: (i) a significant negative correlation between the NDVI trend over time with temperature, rainfall and sea level factors, which means a warmer climate with higher sea levels would result in a declining trend of vegetation greenness (NDVI values); and (ii) higher temperature would increase drought conditions particularly on the elevated barrier side, whereas, rainfall could play another role (insignificantly though) by affecting the river discharge and sediment transport/erosion that directly/indirectly effects the shorelines. However, (iii) a significant positive sedimentation rate influence has been shown by the NDVIs on Comerong Island's low-lying platforms. This positive relationship occurred because they have a similar declining trend in sediments and NDVIs.

6.5.4 Spatial distribution of NDVI change maps (using Raster Calculator)

Changes in vegetation distribution on these estuarine intertidal ecosystems have been explored over the study period (Fig. 6.14) as follows. (i) The Towamba estuary ecosystem shows a slight increase in the NDVI green distribution, with some steady areas and losses on/around the main channel shorelines in yellow and orange, respectively. (ii) Wandandian delta shows a clear NDVI increase in the northwestern parts with a mainly steady trend on the other parts of the delta (Hopley, 2004). These features are related to the availability of multiple water resources at these two study sites and the high sediment accumulation rates that result in geomorphic growth at both Towamba estuary and Wandandian delta, which has provided a more suitable habitat for ecological developments (Hopley, 2004). (iii) Comerong Island, in contrast, has a clear NDVI increase on the northern portion with a slight increase on the middle and barrier sides, which are both extending geomorphically (Carvalho & Woodroffe, 2013). Some areas show steady records in yellow. However, there has been a significant decline in NDVI values in the middle, west and southern parts of the island as shown in orange to red. These arose because of increased salinity introduced by the decline in Shoalhaven River discharge since dam constructed in 1976 (Al-Nasrawi *et al.*, 2016a), and shoreline erosion (Thompson, 2012; Al-Nasrawi *et al.*, 2016b), as well as, storm surge and regional drought conditions following cyclones in the 1990s and El Niño conditions since 2010 (BOM, 2017a).

6.6 Conclusions

Although the climatic and sea level factors have slightly different values at each study site, all sites have tended to show a SLR and temperature increases with clear rainfall declined. This reflects the homogeneous coastal conditions that simulate the global trends with the small differences being related to the latitude at each site. However, a clear variation of vegetation reaction has occurred at these three coastal sites, resulting in different NDVI trends and different correlations with the climatic and sea level factors. Consequently, the NDVI may have been affected by another independent variable, which has been identified as the sedimentation rates since it impacts on the area of vegetation reflection. Hence the geomorphological characteristics underlying the vegetation cover have a significant impact in such highly dynamic intertidal estuarine landforms subject to active erosion and deposition processes.

Another finding of this research is that by using the maximum available RS datasets, which exhibit a variety of spatial resolutions through the study period, fixable and fairly comparable though. A specific dataset equality equation has been designed for NDVI-imagery and allows the 79 m and 30 m resolution data to be compared statistically over time.

The NDVI was used to assess the sensitivity of coastal wetland vegetation at the study sites to the main climatic variables. Values of this index were calculated from Landsat 1-8 imagery across a range of wetland vegetation types growing on various geomorphic landforms.

6.6.1 NDVI surface analyses and trend

The Towamba estuary is growing ecologically and geomorphologically, with the rate of geomorphic growth being faster and wider than the plant communities. Over the last 4 decades this reflects the sedimentary characteristics of the estuary, whereby sediment infills the estuary providing ground on which vegetation can become established.

The Wandandian site eco-geomorphic system is also growing ecologically and geomorphologically, but the ecological rate of growth is higher (7.3%) than the geomorphic growth of only 3.4%.

In contrast, the NDVI spatial distribution on Comerong Island (Fig. 6.12) has gradually decreased during the last four decades, with some fluctuations showing higher greenness (e.g. 1975 and 2010). This indicates that Comerong Island is deteriorating ecologically and geomorphologically but the rate of ecological decline is higher. These changes can be attributes to sediment erosion and rising sea level.

6.6.2 Regression model

The reactions of the dependent variable (NDVI) to the regressed independent factors (time, temperature, rainfall, sea level and sedimentation rates) are provided in Table 6.8.

Table 6.7. Effect of five variables in three areas on NDVI at 95% significance level

	Time	Temperature	Rainfall	Rising Sea level	Sedimentation rates
Towamba	P	P*†	N*	P	P
Wandandian	P	P	N*	P	P
Comerong	N	N	P*	N	P

** Means not significant, P is positive and N is negative.*

(† at Towamba site, temperature is significant at the 90% confident level).

The variables time (year), rising sea level and sedimentation rate have significant effects on NDVI trends whereas temperature and rainfall have insignificant effects on increasing the NDVIs on the Towamba intertidal estuarine eco-geomorphic landforms. At Wandandian delta all the variables have significant positive effects on the Wandandian NDVI index, except rainfall. In contrast, at the Comerong site time, temperature and sea level rise have significant negative impacts on the NDVI, whereas rainfall has an insignificant effect on NDVI and sedimentation rate has a positive influence.

From all three study sites, at 95% confident level (which is the target of this research), it can be concluded that:

- Rainfall does not have a major impact on NDVI at any of these areas.
- The sedimentation rate effect is positive and significant on the NDVIs at all of the study sites.
- Temperature effect is significant in the Wandandian and Comerong sites, whereas it is insignificant at the Towamba site.
- At Comerong Island, year, temperature and SLR have a significant negative effect on NDVI but, they have a positive effect in the other regions.

Generally, the correlation between NDVI and the climatic and geomorphic factors is very significant at Towamba, Wandandian and Comerong indicating that these factors (except the remaining R square of other non-regressed factors) are the main controllers that will disturb the NDVI at such intertidal landforms during the 21st Century.

6.6.3 NDVI change maps

The spatial distribution of NDVI change maps were important to show, easily and clearly, the change in vegetation distribution at each study site, which may be informative about the causes and/or drivers of change at the local scale. NDVI change maps have effectively

employed the map-algebra expression (raster calculator tool) to Landsat datasets, to show a clear pattern of changes at particular areas over time (Cordeiro *et al.*, 2005; WRC, 2012).

The zoned changes, that have been detected, have smoothly interpolated and mapped the dynamic changes of NDVI distributions over the study sites/period. This has allowed these zoned changes to be related to the responsible factors, such as water shortage on some elevated parts of Wandandian delta and erosion of shorelines around Comerong Island.

Modelling the relationship between NDVI and the environmental conditions across 40 years, for each site on the southeastern Australian coast, has been based on: (i) NDVI trend surface analysis, (ii) a correlation regression model, and (iii) NDVI change map distributions. This study has used the NDVI index to assess spatial and temporal changes of vegetation radiation at chosen coastal sites. Then it regressed these vegetation multispectral wave reflections with the related climatic and geomorphic trend factors (temperature, rainfall, sea level rise and sedimentation rates). Visually, the resultant NDVI maps have shown clear vegetation changes over time, as well as other land cover attributes (water bodies, sandspit). Furthermore, more accurate results can be gained by understanding and statistically comparing these greenness (vegetation) changes with climate related factors, especially when using the positive NDVI values (0.0 to 1.0) that represent the vegetation canopy, and ignoring the negative values (-1.0 to 0.0) that represent the bare-lands and water. The regression model has shown the significant impact that the environmental changes have on the NDVIs (Towamba Fig. 6.9, Wandandian Fig. 6.11 and Comerong Fig. 6.13), and indicates that some non-regressed factors (accounting for the remaining R square) are affecting the vegetation of these areas. Moreover, mapped NDVI distribution dynamics over the study sites/period has clearly indicated the change zones, which need more investigation to determine the responsible causes within these sections.

The unique wetlands habitats of coastal ecosystems are among the most productive and sensitive natural ecosystems on the Earth. They are highly responsive to environmental pressures both ecologically and geomorphologically. Climate change (particularly; temperature, rainfall and sea level rise) and coastal geomorphic processes (sedimentology) have clearly impacted most ecosystems worldwide. The vegetation canopy indicator has notably represented the coastal ecosystem dynamics at a landscape scale. This exploratory study has investigated the response of coastal vegetation to climate changes and sediment rates along the three sensitive coastal ecosystems on the southeastern Australian coast. Published literature has argued “that the ‘Normalised Difference Vegetation Index (NDVI)’ is the” best vegetation dynamic representative. Landsat imagery modelling and subsequent

statistical analyses have provided a qualitatively significant outcome that can be used to offer possible sustainable management solutions with worldwide applications.

Chapter VII: Geoinformatic vulnerability predictions of coastal ecosystems to sea level rise

7.1 Abstract

Geomorphic changes, such as increased shoreline erosion rates, are clearly affecting coastal eco-geomorphic systems worldwide, which have resulted from global warming, particularly rising sea levels (SLR). The existing situation for coastal ecosystems in southeastern NSW, Australia, has been affected by both global SLR and anthropogenic modifications. These impacts have mainly resulted in the loss of coastal wetland ecosystems. Coastal environments and ecosystems are sea level dependant and they are controlled by tidal stressors in estuaries and deltas where there is a complex interaction between eco-geomorphic and hydrologic processes.

This project applied future IPCC-SLR scenarios to assess its impact on the eco-geomorphic aspects of coastal ecosystems in terms of risk assessment and sustainability. Comerong Island is used as a case study and is compared with other ocean influenced (Towamba) and lagoonal deltas (Lake Illawarra and Wandandian) to evaluate the regional influences of SLR. Applying IPCC (2013, 2014) hydro-scenarios to the chosen geomorphological coastal datasets resulted in a hydro-geomorphic model that shows the Comerong Island study site was already under pressure in 2015, about 18% of the island will be covered by sea water by 2050, and using the maximum sea level rise scenario approximately 43% of the island will lost by 2100. Similar losses of wetlands are also expected to occur at the other study sites and can be extended to the remaining estuaries in southeastern Australia. Applying this broad scale application of simulation and classification using LiDAR data, topographic layers, remote sensing data and local sea level records in ArcGIS together with the various IPCC (2013, 2014) sea level rise scenarios will be necessary to assess future ecosystem sustainability management plans for coastal zones worldwide.

Keywords: *Ecosystems Vulnerability, climate changes, remote sensing, GIS modelling, conservation.*

7.2 Introduction

The Earth as a planet has had balanced and sustainable Holocene ecosystems (eco-sustainability) for thousands of years (Siddall *et al.*, 2003; Carlson *et al.*, 2008). Although it has faced fluctuating Quaternary weather conditions (Fairbanks, 1989), like glaciations followed by warm periods (Siddall *et al.*, 2003), its coastal ecosystems have become balanced and stabilised during the mid of Holocene, especially within last 4000 years in Australia (Carlson *et al.*, 2008; Steffen *et al.*, 2009). However, during the last century the increased population and rural, urban and industrial pollution has stressed these coastal ecosystems, and even overloaded them, threating the ecosystem's balance and even its loss (Parmesan & Yohe, 2003; Neumann *et al.*, 2015; Al-Nasrawi *et al.*, 2016a, 2016b). For example temperature increases during the 21st Century as a result of CO_2 emissions are causing climate change and mean sea level rise (IPCC, 2014), significantly threatening many ecosystems, especially coastal environments such as wetlands (Watson *et al.*, 1998; Michener *et al.*, 1997; IPCC, 2014).

Mean sea level started to rise globally in the 19th Century, but significant rises have occurred since the 1950s and it has been estimated that sea level will continuously rise throughout this 21st Century (Watson *et al.*, 1998; IPCC, 2013, 2014; Nicholls *et al.*, 1999; Hughes, 2003; Meyssignac & Cazenave, 2012; Deconto & Pollard, 2016). Sea levels are expected to keep rising, according to range of scenarios of CO_2 emission, by 26-55 cm by 2100 AD under low emission estimates, whereas high estimates suggest a rise of 52-82 cm according to IPCC (2013). Moreover, under the most popular projections, rate of SLR is probable to increase and will exceed the records from 1971-2010 based on the current global warming rates and gas emissions that will lead to increased ice sheet melting. In fact, the post-1990 SLR rate is already faster than in the preceding 20 years (IPCC, 2013, 2014; Cazenave *et al.*, 2017).

During the last few decades, the United Nations Intergovernmental Panel on Climate Change (IPCC) and many scientists have outlined a range of future emissions scenarios to explain the existing and forecast future geomorphological strategies to cope with SLR. Many of these methods depend on digitizing and analysing remote sensing data. Several methods have been developed to simulate geomorphological surfaces to create digital elevation models (DEMs; Arun, 2013). Examples of models include elevation changes within coastal ecosystems that have led to the invention of several methods and devices, such as Sediment Erosion Tables (SETs) designed by Boumans & Day (1993), and its subsequent modification to Surface Elevation Tables (SETs) allowing very accurate surface dynamic measurements (Whelan *et al.*, 2005). However, SETs are generally costly, have a limited areal coverage, and take a long time to obtain accurate trend results. SETs may need up to 20 years on average to get accurate

results (McIvor *et al.*, 2013; Cahoon, 2015). Thus, since higher resolution and more accurate remote sensing data has become available to represent geomorphological surface patterns (Patel *et al.*, 2016), like Light Detection and Ranging (LiDAR) clouded datasets (Gillin *et al.*, 2015), environmental scientists have been using the DEMs as a surface dynamic analyser. It is accurate enough, cheaper and faster than using SETs and can be based on several modelling methods (White & Wang, 2003; Gillin *et al.*, 2015). DEM analyses may be utilised as ecosystems management, modelling and decision support tools (National Parks and Wildlife Service, 1998; Haq *et al.*, 2012; Arun, 2013).

DEM analyses are used to measure characteristic geomorphological aspects of the surface (Wood, 1996). Several software tools can be used to create DEMs (Omran, 2016; Al-Nasrawi *et al.*, 2017a). However, a geographic information system (GIS) provides the most advanced and accurate results that can be achieved at present (White & Wang, 2003). A number of datasets, like SRTM and LiDAR datasets, can be used to suit the purpose of making the DEMs (White & Wang, 2003). A GIS format can be developed to characterize three specific objectives, namely to identify spatial patterns, to identify scale dependency in form and to allow visualization of results (Wood, 1996).

Approximately one third to half of the major coastal environments on Earth have been degraded, including eastern Australian coastal wetlands, during the past decades (Watson *et al.*, 1998; Valiela & Fox, 2008; Saintilan & Williams, 2010; Al-Nasrawi *et al.*, 2016a, 2017b, 2018a). An additional 6-22 % of sensitive coastal ecosystems (such as coastal wetlands) are expected to be lost by 2080, with little anthropogenic contribution, by applying different natural climate change scenarios (Nicholls *et al.*, 1999). However, anthropogenic modifications are expected to have more impact than the magnitude of SLR within wetlands during the 21st Century (IPCC, 2013, 2014). Losses of 36-70 % by 2080 are expected when considering combined natural and human change scenarios (Michener *et al.*, 1997; Wall, 1998; Nicholls *et al.*, 1999; Morris *et al.*, 2002; Nicholls, 2004).

7.2.1 Case study and setting

Comerong Island, 120 km south of Sydney in southeastern NSW, Australia (Fig. 7.1a), is used as a main case study to show the influence of mean sea level changes on changing the island's elevation and ecosystems. Comerong Island is located at the end of the Shoalhaven and Crookhaven Rivers, and represents an example of large scale biodiversity habitats like saltmarsh and mangrove (and their associated oysters, fish, animals and birds) where the shorelines and vegetation extent are being influenced by climate change (Kingsford, 1990;

Thompson, 2012; Al-Nasrawi *et al.*, 2016b). Comparative study sites with different geographic settings include Wandandian Creek delta (Fig.1b), Towamba estuary near Eden (Fig. 7.1c) and the Macquarie Rivulet and Mullet/Hooka Creek deltas in Lake Illawarra (Fig. 7.1d).

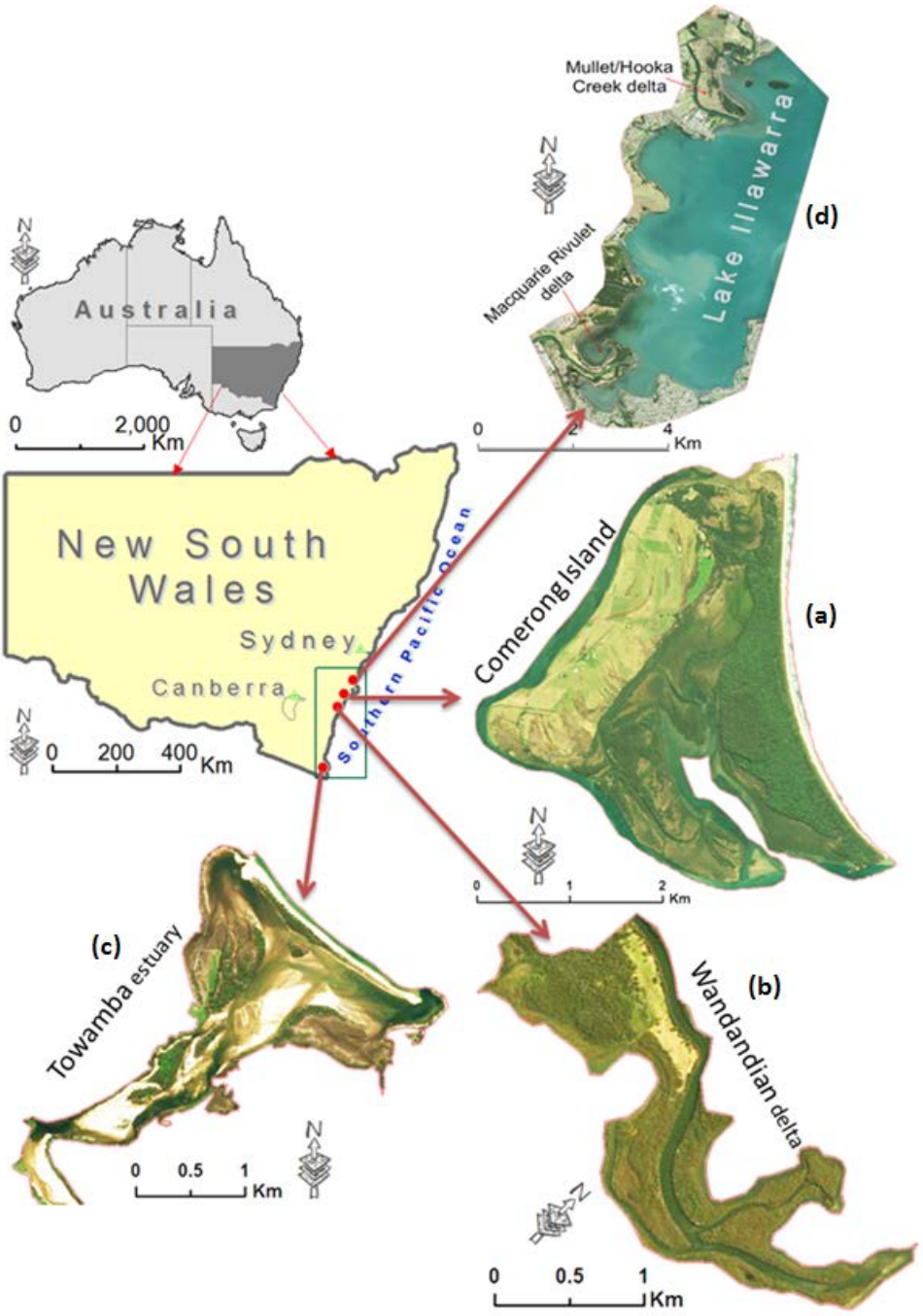

Figure 7-1. New South Wales location in Australia showing: (a) the study site, Comerong Island, in southeastern NSW, with a complicated mostly intertidal eco-geomorphic wetlands system created by tidal and river interactions, and the comparative examples on the southern NSW coast as follows; (b) Wandandian delta, (c) Towamba estuary, and (d) Macquarie Rivulet and Mullet/Hooka Creek deltas in Lake Illawarra.

Comerong Island is mostly made of sand, and it has important coastal wetlands that were escaped any degradations for many centuries. Situated on the eastern coast to the Southern Highlands, the riverine and coastal area is now degraded in its ability to adjust ecologically and

geomorphologically as a result of human settlement, landscape modification and sea level rise (Al-Nasrawi *et al*., 2016a, 2018b, 2018c). This has culminated in a series of changes in the coastal wetlands and the distribution of habitats like saltmarshes and mangroves (Thompson, 2012; Al-Nasrawi *et al.*, 2016b).

The major natural processes affecting coastal wetlands into the future are likely to be Global Mean Sea Level Rise (GMSLR), erosion, sedimentation and altered rainfall patterns. These processes will initiate changes to the long-term average wetlands distribution and drive habitat changes in the future. Other factors such as salinity, rainfall and flooding are also expected to have effects on the coastal environment's characteristics. The processes currently affecting Comerong Island, and the level of influence that each process has on the coastal wetland growth/persistence, need to be understood. Previous studies on Comerong Island have shown clear shoreline erosion and wetland losses on the western side, adjacent to Berry Canal (southwestern), and the southern and middle portions of the island (Fig. 7.2; Thompson, 2012; Al-Nasrawi *et al.*, 2016b).

This research has focused on southeastern NSW to investigate the possible future responses to environmental changes caused by GMSLR. Several parameters of the coastal ecosystems need to be addressed in order to estimate and apply a suitable modelling approach. Such parameters include historical shoreline responses, grain size distributions and their vulnerability to the tidal dynamic stressors. Meanwhile, it should be understood that tidal planes (levels) up an estuary will change depending on the estuarine type and shape. The study site is recognised as having a significant ecological value and the island is mostly classified as a conservation area under NSW biodiversity legislation (State SEPP-14), which aims to ensure preservation and protection of the wetlands both environmentally and economically. For these reasons, future sustainability of the coastal ecosystems needs to build on the previous investigation by Al-Nasrawi *et al.* (2016b) that assessed the existing situation on Comerong Island and its past temporal and spatial changes.

The historical and current situation on the island have been checked and mapped by Al-Nasrawi *et al.* (2016b) using remotely sensed data including aerial photographs for 1949, 1961, 1970, 1981, 1993, 2002 and 2014 (fig. 4 in Al-Nasrawi *et al.* 2016b). These analyses have shown significant shoreline changes around Comerong Island; the northern part of the island has expanded by 0.41 km^2, whereas, the western, southwestern and southern parts have been eroded by 0.73 km^2 (Fig. 7.2; Thompson, 2012; Al-Nasrawi *et al.*, 2016b). This situation has resulted from interrupting the natural sediment delivery and erosion/deposition cycles (Al-Nasrawi *et al.*, 2016a, b). The eco-geomorphic processes around Comerong Island have been significantly influenced by human infrastructure upstream, such as the Tallowa Dam, and the

increased fine sediment runoff from agricultural land. These changes, combined with the rising ocean tidal prism, have caused a reduction in sediment delivery that cannot balance the erosion/deposition around the island caused by natural processes (Thompson, 2012; Al-Nasrawi *et al.*, 2016a, 2016b).

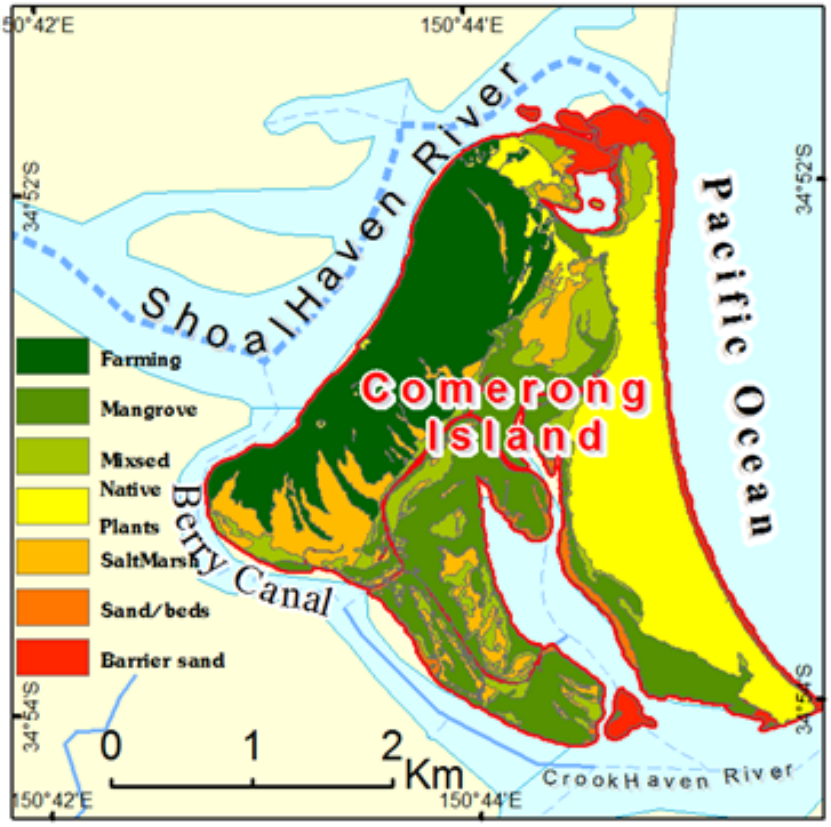

Figure 7-2. Study site at Comerong Island in southeastern NSW, Australia, showing the complicated mostly intertidal eco-geomorphic wetlands system created by tidal and river interactions (after Al-Nasrawi *et al.*, 2016b).

Grain size analysis of 113 sediment samples (Fig. 7.3) has shown the vulnerability of Comerong Island, which mostly consists of sand (96.4%; Al-Nasrawi *et al.*, 2016b). This sandy non-cohesive sediment means that tidal currents associated with GMSLR will have a greater effect on Comerong Island and its ecosystems than if there was a rocky foreshore. Although, most coastal wetlands in NSW have ecosystems developed on unconsolidated sediments, Comerong Island has an additional sediment delivery problem caused by the construction Tallowa Dam on the main Shoalhaven River, which has limited the amount of sediment derived from the sixth largest catchment in NSW (7177 km^2). Altogether, these factors are likely to increase erosion rates and decrease the amount of deposition at the same time.

Four other study sites have been investigated to examine the proposed methods, geomorphic settings and to prove the study findings. They are Wandandian delta, Towamba estuary, Macquarie Rivulet delta and Mullet/Hooka Creek delta (see Fig 7.1).

The delta of Wandandian Creek is actively prograding into St Georges Basin (western side), and it is located about 155 km south of Sydney (Fig. 7.1b). The length of the delta is about 25 km with average of 1.5-3 m elevation.(Hopley & Jones, 2006).

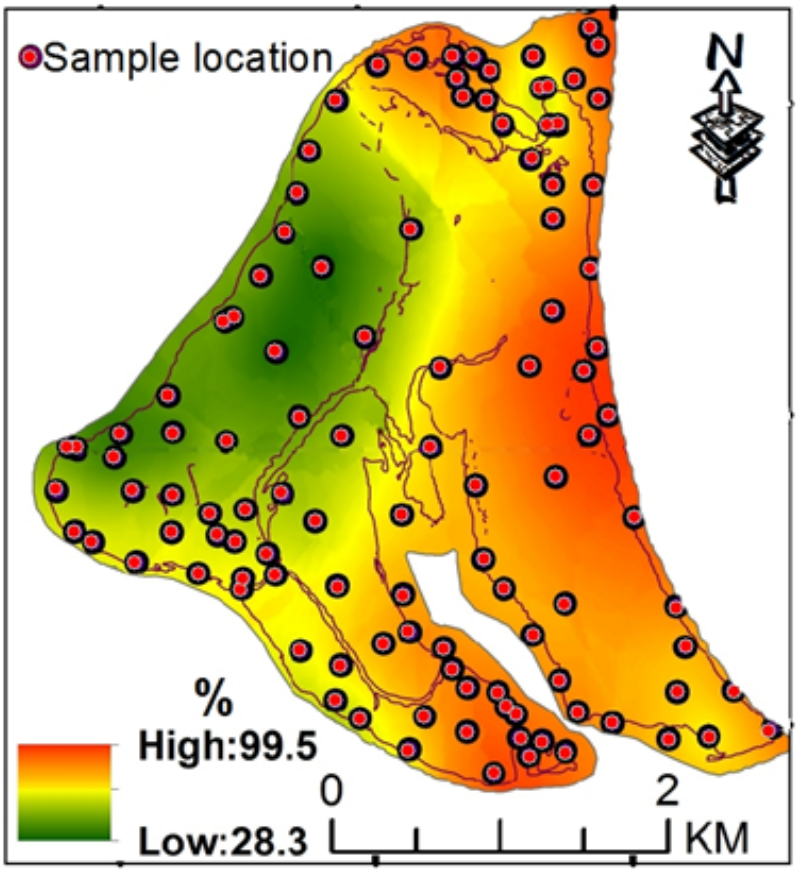

Figure 7-3. Sand content in sediment samples from grain size analysis, Comerong Island (after Al-Nasrawi *et al.*, 2016b).

The Towamba estuary is located on the southeast NSW coast to the south of Sydney by ~385 km near Victoria border, Australia (Fig. 7.1c). Main coastal ecosystem of Towamba estuary is located at the end of the Towamba River delta where the active tidal channel has an average depth of 1.14 metres. Towamba estuary is mostly surrounded by rock outcrops, resulting in restricted estuarine shape (Fig. 7.1c). According to the Roy *et al.* (2001) classification, it is a wave dominated estuary and estuarine barrier in mature stage of ecosystem development.

The Macquarie Rivulet delta and Mullet/Hooka Creek delta are part of Lake Illawarra system. They are river and wave-dominated deltas, respectively, located south of Sydney (~80 km; Fig. 7.1d). Lake Illawarra has about 35 km^2 total surface area but it is relatively shallow (~3.5 m maximum depth). Morphologically, it depends on approximately 235 km^2 of a catchment area with twelve waterways draining five sub-catchments, including Macquarie Rivulet (96.35 km^2) and Mullet Creek (75.2 km^2). The Macquarie Rivulet and Mullet/Hooka Creek deltas are actively prograding from the western margin of Lake Illawarra (Hopley *et al.*, 2007; Hopley, 2013).

7.3 Methodology

The geomorphic-hydrodynamic numerical model combines the geomorphological land datasets with the local sea level hydrodynamic data. The proposed method is based on LiDAR data point clouds that reflect the island surface elevation (ground level as a geomorphological landscape datasets) and incorporate the IPCC (2013, 2014) hydrodynamic variable scenarios that estimate the future position of sea level around the island. According to the IPCC (2013, 2014) sea level is estimated to rise by 26-82 cm by 2100 (Fig. 7.4 and Table 7.1), and this needs to be taken into account when assessing future sustainable approaches to wetland conservation that may be applicable to the eastern Australian coast and similar ecosystems worldwide.

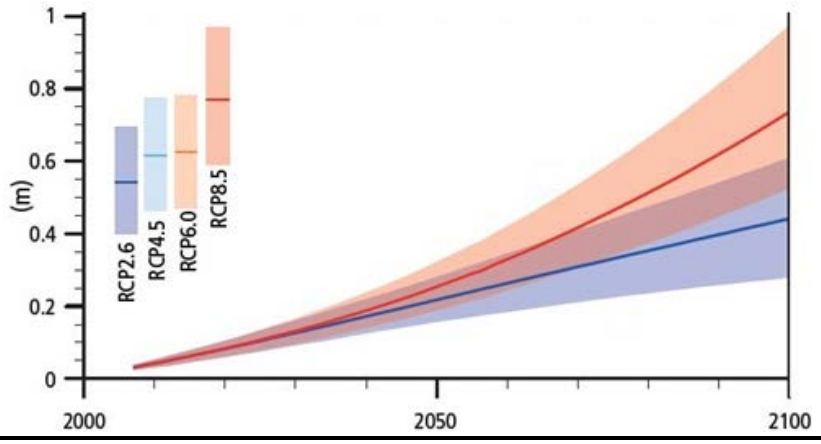

Figure 7-4. The scenarios of the sea level rises (the Global mean) from 2006 to 2100, which hve been generated according to a time-series dataset that been multi-modelled from 1986-2005. The red and blue lines are the mean estimates, and the red and blue bands are the estimated uncertainties of the scenarios that have a likely range of ~ ±7 cm for 2050 and ~±15 cm for 2100 (IPCC/2014-AR5/SYR/SPM; Table 7.1).

Table 7.1. Projected change of "Global Mean Sea Level Rise" (GMSLR) during this century (mid "2050" and end "2100" scenarios), by simulating the time series dataset from the 1986-2005 period (IPCC, 2014).

		2050		2100	
	Scenario	Mean	Likely range [a]	Mean	Likely range [a]
Global Mean Sea Level Rise (m) [b]	RCP2.6	0.24	0.17 to 0.32	0.40	0.26 to 0.55
	RCP4.5	0.24	0.17 to 0.32	0.40	0.26 to 0.55
	RCP6.0	0.26	0.19 to 0.33	0.47	0.32 to 0.63
	RCP8.5	0.30	0.22 to 0.38	0.63	0.45 to 0.82

[a]= "Calculated from projections of 5 to 95% model ranges. These ranges are then assessed to be likely ranges after accounting for additional uncertainties or different levels of confidence in the models. For projections of global mean sea level rise confidence is medium for both time horizons" (IPCC, 2014).

[b]= "Based on 21 CMIP5 models; changes are calculated with respect to the 1986-2005 period. Based on current understanding (from observations, physical understanding and modelling), only the collapse of marine-based sectors of the Antarctic ice sheet, if initiated, could cause global mean sea level to rise substantially above this likely range during the 21st Century. There is medium confidence that this additional contribution would not exceed several tenths of a metre of sea level rise during the 21st Century" (IPCC, 2014).

However, the mean and medium confidence scenarios (Table 7.1) show that, by 2050, the mean SLR will range from 24 cm to 30 cm above current SL and by 2100 will be increased to 40 cm to 63 cm. Whereas, the likely maximum estimates show up to 38 cm and 82 cm of GMSLR, respectively.

Based on IPCC (2013, 2014) projections, this study quantifies the local GMSLR (as a hydrological function), the island elevation and erosion rates (as geomorphological variables), and then applies these using GIS analysis tools. A detailed geomorphic assessment of erosion within the coastal zone of the study site has been done (Al-Nasrawi *et al.*, 2016b). It started by looking at historical mapping and aerial photographs to determine how the local area/shoreline has changed over time to see which areas are eroding and by how much per year, and then applying these rates to future long term scenarios.

The GIS analysis was accomplished by using ArcScene10.2 and its animation manager tools as follows. Firstly, use the generated DEM (as a raster) and add a simple polygon covering the study site (as the second layer), and then converting the area to 'ScenLayers'. Secondly, from the raster properties choose Display, Cubic Convolution (for continuous data) and then choose Base Heights, floating on a custom surface, change the custom default elevation (to 300 or whatever would make a logical 3D shape). After that go to the ScenLayers properties, and choose Calculate from Extent. Finally, open the Animation manager tool and create an Animation Key frame (for the polygon), then add a number of these keys and change their 'Z' value to the IPCC (2013, 2014) future scenarios, as decided above (24 cm, 62 cm and 82 cm). Then simply run and save the scenarios via the Animation control panel.

The available geomorphic data from Comerong Island are sufficiently accurate to model a range of scenarios covering the IPCC (2013, 2014) GMSLR predictions. This research has tested the extreme projections as well the predicted average GMSLR. Models have been produced to test the current distribution (2015) and the predictions for 2050 and 2100 for sea level rises of 26 cm, the 62 cm average value, and 82 cm, which is a reasonable approach within the Comerong Island area. Thus, this study has quantified the range of predictions for mean estimated levels for the 21st Century. Furthermore, the geomorphological datasets for the island and the hydrological dynamic factors affecting the shoreline changes and erosion rates have been applied independently to the existing wetland mapped for another study based on the historical and existing situation at the same study site (Al-Nasrawi *et al.*, 2016b). Sedimentation rates play an important component that depends on a number of external factors including catchment contributions. Therefore, addressing all relevant factors using empirical data is the safest approach to gain results that reflect the existing situation and any future predictions.

GIS and RS datasets (e.g. LiDAR data-cloud) have contributed important roles in representing and digitising the geomorphological surface covers to assess the influences of natural disasters and climate change patterns like GMSLR (Haq *et al.*, 2012; Arun, 2013; Mohamed *et al.*, 2013). This study is based on manipulation of the LiDAR data set (point cloud elevations and Digital Elevation Model – DEM; as Fig. 7.5 is showing) and comparison with measured tidal planes at the tidal monitoring station closest to the most affected parts of the island –the Greenwell Point station (Fig. 7.2) located at the middle of Crookhaven River on the southern side of Comerong Island.

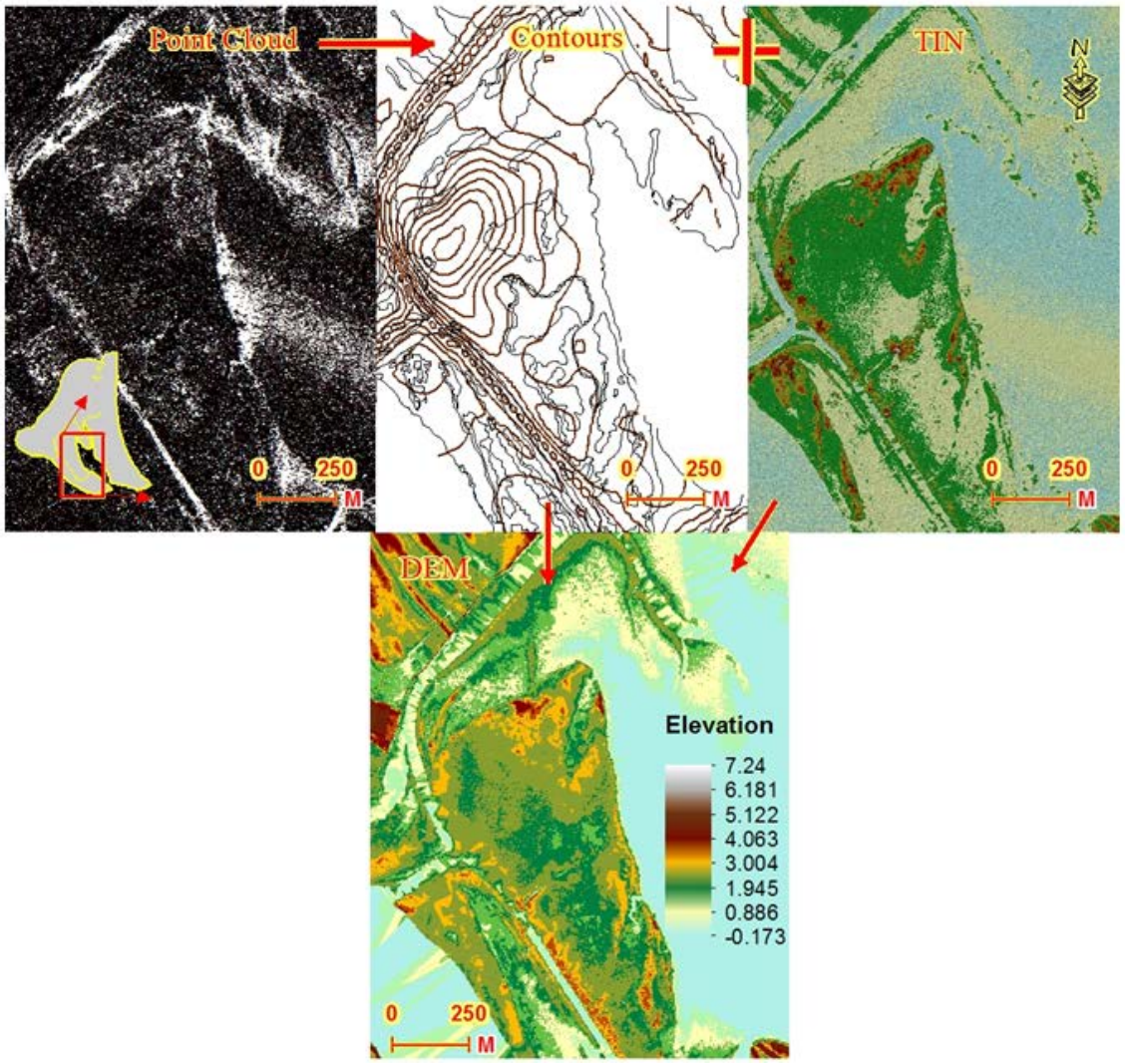

Figure 7-5. Methods applied to the LiDAR data of the southern part of Comerong Island. Starting with the point cloud data on the left side, it was converted to two data sets, the contours and TIN in the middle, and then the generated DEM is shown on the right side.

Figure 7.5 shows a new modelling method based on RS data and GIS has been used for the study site. It used a standard airborne LiDAR survey carried out by the NSW Government in 2010 using a Leica ALS50-II that was integrated with a RCD105 digital camera. The accuracy of these data are a minimum density of 1 point cloud per square metre (representing a minimum

1 m^2) for spatial resolution, and less than 30 cm for vertical accuracy to create a DEM with 95% confidence (LPI, 2010). This research focuses on the hydrodynamic and geomorphic processes, which can be influenced by SLR and cause considerable modification of the mean levels of the tides. These elevated tidal levels were then applied as the model boundaries and were related to the Comerong Island surface elevations. Such models are commonly used for modelling rivers, estuaries, coasts and flooding, using various aspects of the ArcGIS toolbox. They create contours that converted to the triangulated irregular networks (TINs) which can be built on to generate the digital elevation models (DEMs), as shown in Figure 7.6 below, using an example applied from the southern part of the study site.

7.4 Results and discussion

The Department of Land and Property Information (LPI) in NSW provided LiDAR survey data that covered Comerong Island. These data record the surface elevation as heights (Z values) relative to a local zero level datum. The data also incorporate the actual local mean sea level at the time of the survey according to the local ground base-stations for tidal/time dynamics, including the Crookhaven Heads, Shoalhaven Heads and Greenwell Point stations. The recorded surface elevations at Comerong Island ranged from -0.17 m to 9.75 m and a DEM was generated using a TIN and the contour spatial analyst tools in ArcGIS.

After creating the DEM a hydrodynamic numerical model has been used to simulate the future GMSLR influences. So, by increasing the water level by 26 cm to 82 cm, the island will show its new boundaries and shape. In other words, Z value manipulation of the LiDAR dataset has defined the increasing areas of inundation affected by a continuously rising sea level up to the maximum 0.82 m according to the IPCC (2013, 2014) scenarios.

The geomorphic-hydrodynamic numerical model, which combines the geomorphological land datasets with the local sea level hydrodynamic data, has simulated the future GMSLR scenarios technically to estimate and detect the areas that will be inundated during the 21st Century. Such assessments can be used to determine the sustainability of the ecosystems and for risk management studies.

Applying this methodology has resulted in the production of clear and significant future vulnerability maps that delineate the changes expected to affect Comerong Island starting with the current stage based on 2010 LiDAR data, and subsequent changes within the next 50 and 100 years. Results show that Comerong Island is currently under pressure in 2015 (as showing in red in b) compared with the LiDAR data obtained in 2010 (a), and about 18% of the island will be covered by sea water by 2050 (c). Greater influences become apparent at the study site

in 2100 when approximately 43% of the island will be lost if the 82 cm maximum average sea level rise scenarios is used (Fig. 7.6d). Ground losses will occur particularly within the low elevations of the island surface, which are currently covered by sensitive mangrove and saltmarsh habitats.

Figure 7.6d presents the IPCC-2100 scenario on Comerong Island but because of the ongoing hydraulic activity, especially wave action and tidal currents, this whole area will be more open to erosion and the entire southern portion (sandy substrates; see Fig. 7.3) would be reworked and rounded with most of the remaining beach ridges and sandspits, also being reworked and truncated. The mapped changes in Fig. 7.6d also illustrate that the only remaining areas are elevated beach ridges that may support *Casuarina,* but not saltmarsh or mangroves, resulting in an almost total loss of the coastal wetland habitat on the island.

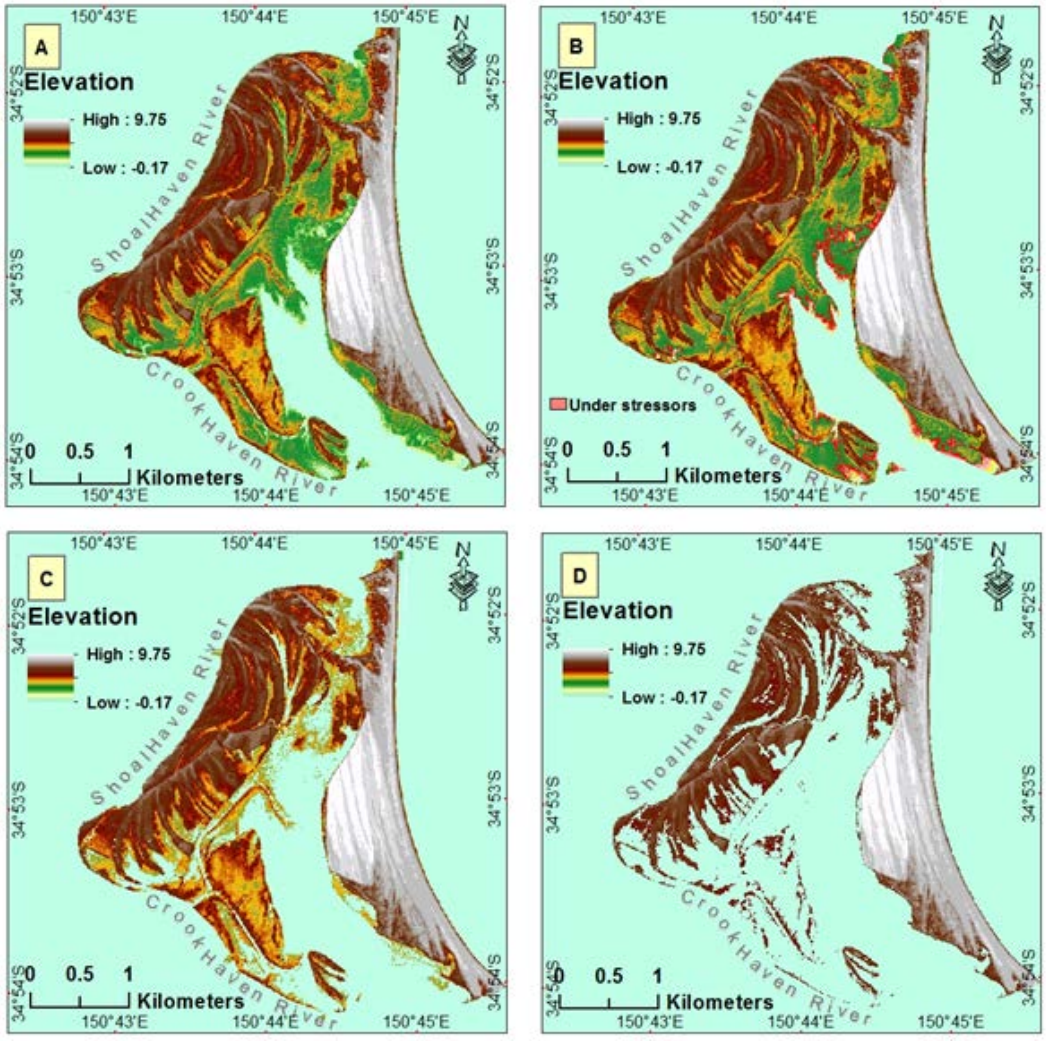

Figure 7-6. Applying the future GMSLR scenarios (IPCC-AR5/RCP8.5) to the study site: (a) = Comerong Island in 2010; (b) = the existing situation (2015 with threated shorelines in red highlighted); (c) = Comerong Island in 2050; and (d) = Comerong Island in 2100.

Similar losses of wetland habitat would also occur on most other southeastern Australian

lagoons and inlets as the sediment supply and lateral migration of wetlands is unlikely to be able to keep pace with the predicted GMSLR. To establish the degree of applicability of this modelling approach examples, from different locations along the southeastern Australian coast have been investigated using appropriate datasets/tools to yield similar results of future inundation estimates.

Wandandian Creek delta is located on the NSW south coast, about 30 km southwest of Comerong Island (Hopley & Jones, 2006; Fig. 7.1b). It drains a moderately altered catchment and extends out eastern toward to the west side of the basin of St Georges, a large lagoon that is subjected to moderate wave action during some weather events. Using equivalent LiDAR datasets from Wandandian Creek delta modelled with Arc Hydro 10.2 tools (an ESRI extension tool) the majority of the subaerial portions of the delta will be inundated by 2100 (Fig. 7.7). Again wave reworking of the thin levee sequences would occur as inundation proceeds removing still more of the protruding delta. Figure 7.7d, again, shows significant losses of the low-lying landforms at Wandandian delta, which would result in almost total loss of these coastal wetlands by the end of 2100 AD.

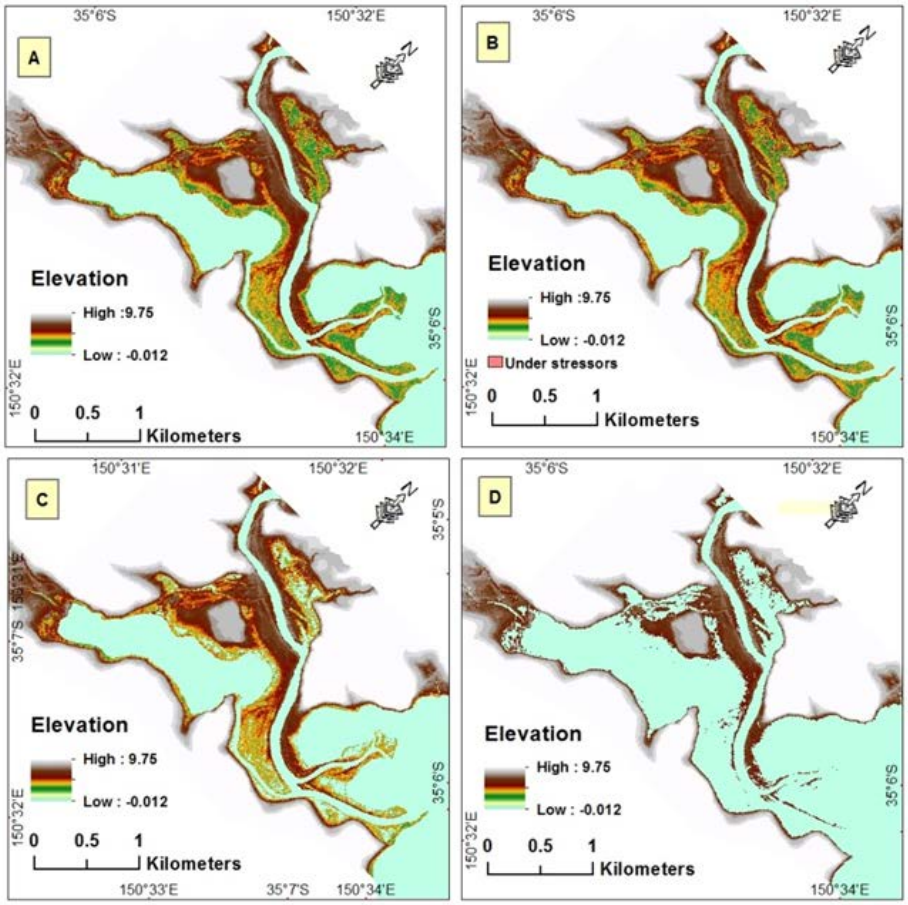

Figure 7-7. Applying the future GMSLR scenarios (IPCC-AR5/RCP8.5) to the Wandandian Creek delta site: (a) = current Wandandian delta (LiDAR data, 2016); (b) = the existing situation under stressors (2017 with threatened shorelines in red highlighted); (c) = Wandandian delta in 2050; and (d) = Wandandian delta in 2100.

The Towamba estuary is situated at the southern end of the NSW coast, ~255 km south of Comerong Island (Fig. 7.1c), and draining a predominantly forested catchment. This bedrock-enclosed estuary lies within Twofold Bay and is open to northeastern wave and wind activity. Like Comerong Island this estuary is protected by a coastal sand spit which, in this case, is much narrower than the equivalent geomorphic units at Comerong Island. The analysis used an equivalent LiDAR dataset but with 'Hydrologic Engineering Centre-River Analysis System tools' (HEC-RAS v5.0.3) including the Steady Flow Analysis and Sediment Analysis Tools (HEC, 2017), which represent totally different forecasting analysis tools. After modifying and presenting the results in the ArcGIS 10.2 format, it resulted in similar future predictions of inundation in the Towamba estuary (Fig. 7.8). Figure 7.8d shows clear losses of the low-lying geomorphological features in the Towamba estuary. However, in contrast to Wandandian Creek delta, the coastal spit at Towamba estuary remains intact with only a small estuary entrance even at 2100 AD. Therefore the flooded estuary would not be subjected to wave action but increased tidal flows may scour some of the partially flooded sandbanks. The net effect is the Towamba coastal wetlands may be lost completely by the end of this century.

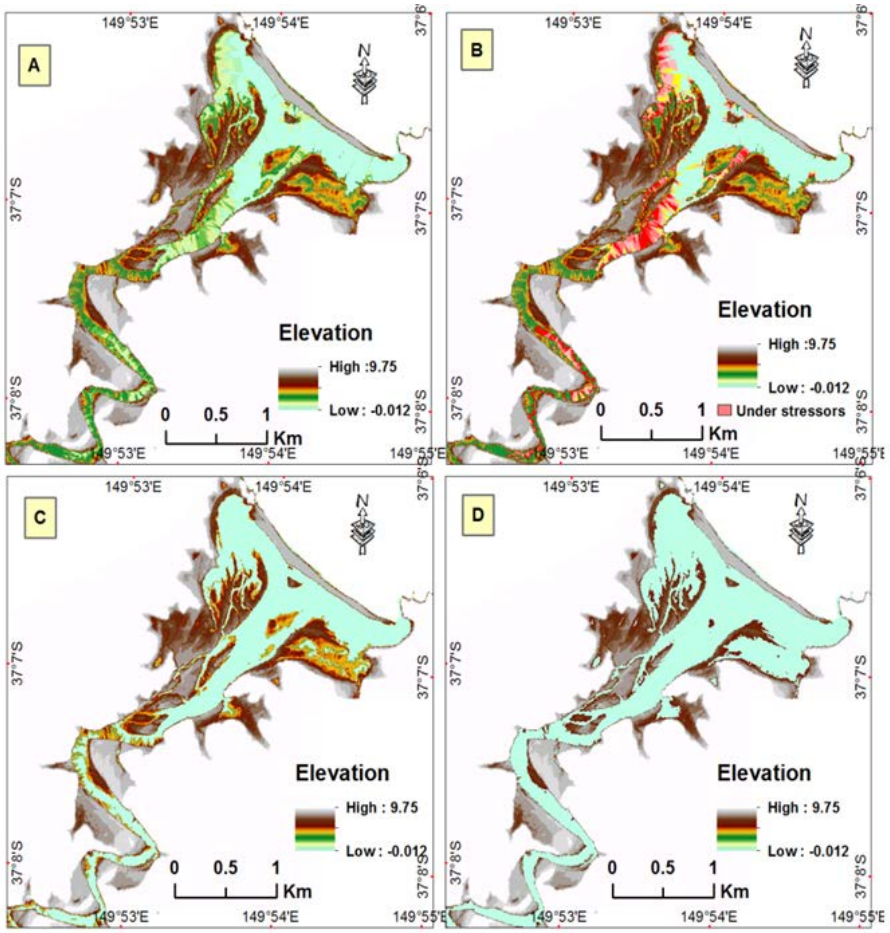

Figure 7-8. Applying the future GMSLR scenarios (IPCC-AR5/RCP8.5) to the Towamba estuary site: (a) = current Towamba estuary (LiDAR data 2016); (b) = the existing situation (2017 with threated shorelines in red highlighted); (c) = Towamba estuary in 2050; and (d) = Towamba estuary in 2100.

Hopley (2013) and Hopley & Jones (2017) have predicted the potential inundation extent, attributable to sea level rise, for the Macquarie Rivulet and Mullet Creek deltas, Lake Illawarra (35 km north of Comerong Island; see Fig. 7.1d). The predicted inundation extents were determined using a high resolution LiDAR dataset overlain with the NSW-Policy Statement of SLR (DECCW 2009) of 2050 (+0.4 m) and 2100 (+0.9 m) projected SLR scenarios as well as current water elevations relative to mean sea level. To illustrate the inundation extent, Hopley (2013) and Hopley & Jones (2017) adopted a simple approach where they modified the DEM scales and colour ramps to align with the nominated scenarios. Despite this simpler approach, Hopley's results show future estimates of inundation and wetland loss at the Macquarie Rivulet delta (Fig. 7.9a) and Mullet/Hooka Creek delta (Fig. 7.9b) similar to those identified in this study.

Although GMSLR has a greater effect on the Macquarie Rivulet delta than Mullet/Hooka Creek delta, due to the rapid progradation of Macquarie Rivulet delta limiting vertical accretion as mapped by Hopley *et al.* (2007). Irrespective, the models indicate that the existing coastal wetlands are likely to be lost by the end of 2100 AD. This is also supported by Hopley (2013) who noted that subsidence of the Macquarie Rivulet delta is already resulting in the loss of wetlands.

These examples are typical of most of the estuarine systems in southeastern Australia, and globally, where sediment supply is graded to current sea level and wetland ecosystems have become well established through the mid to late Holocene. The rate of infilling of these estuarine systems is dependent on the catchment's sediment supply rates. Comerong Island lies at the mouth of the extensively infilled Shoalhaven estuary (Umitsu *et al.*, 2001) where abundant sediment was supplied from a very large catchment. In contrast Wandandian Creek delta has only prograded a short distance into St Georges Basin since it is fed from a much smaller catchment. Human influence has also affected sediment supply whereby essentially natural catchments such as Towamba estuary have seen very little change in sediment supply whereas the Lake Illawarra catchment has experienced moderately significant changes in sediment supply caused by agricultural and urban development (Hopley *et al.*, 2007) and the Shoalhaven catchment has had both agricultural and urban development and has subsequently had a large reduction in sediment supply caused by the construction of Tallowa dam (Al-Nasrawi *et al.*, 2016a).

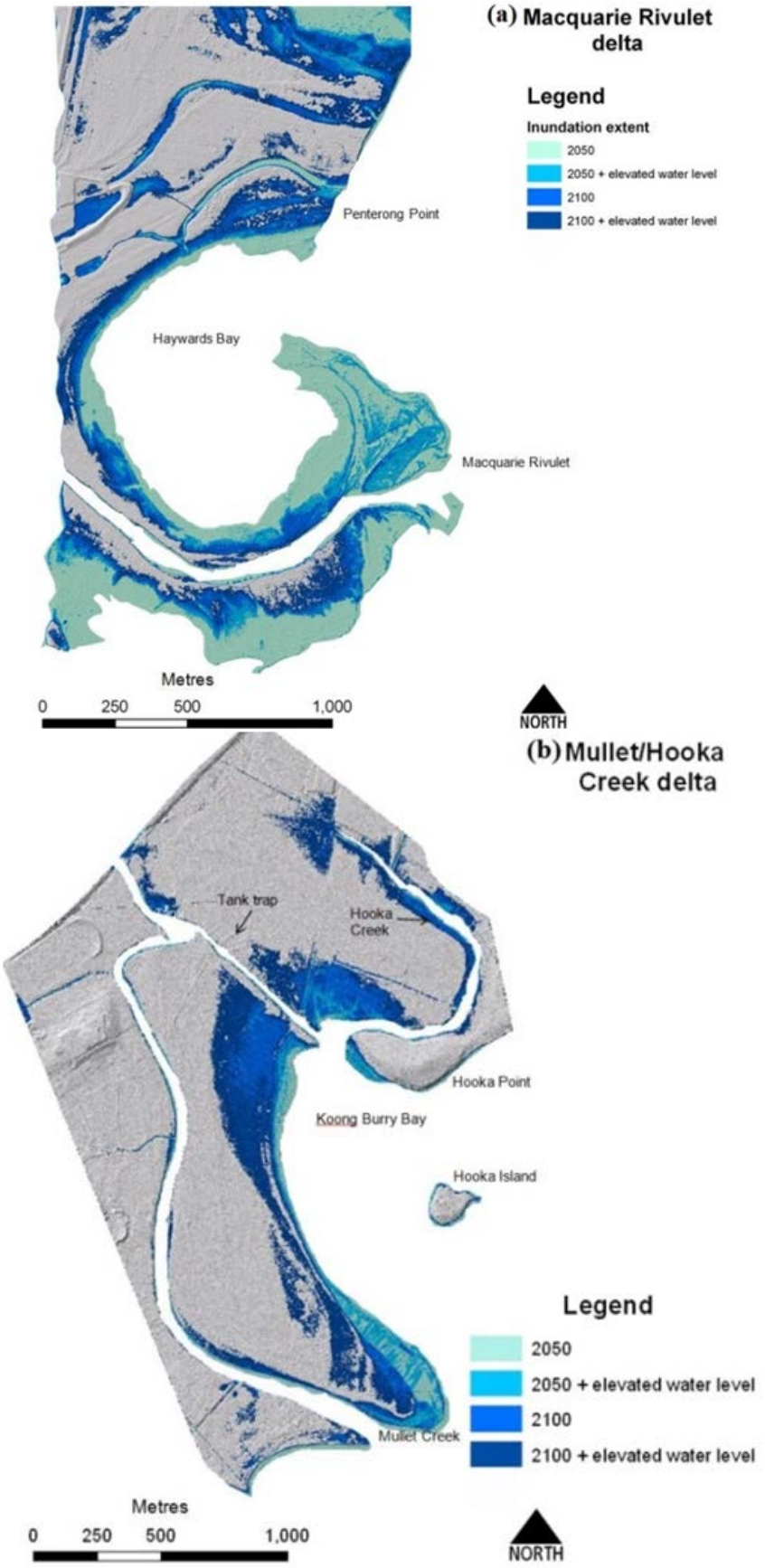

Figure 7-9. Potential inundation map of; (a) Macquarie Rivulet delta (Hopley, 2013; Hopley & Jones, 2018) and (b) Mullet/Hooka Creek delta (Hopley, 2013). Maps show 2050 and 2100 inundation extents plus the 2050 and 2100 inundation extents with an additional 0.25 m overlain to reflect the current elevated water level within the lagoon.

Thus SLR is going to show a significant impact on the coastal eco-geomorphic systems throughout southeastern Australia and equivalent systems overseas by the end of this century. This will particularly have huge influences on coastal wetland ecosystems as they are the most sensitive and responsive coastal ecosystems as clearly seen by the results from Comerong Island and other southeast Australian examples. These examples show predicted extensive to total losses of coastal wetlands locally, which can be extrapolated regionally and globally, unless they have a high enough sediment supply to maintain shallow subaqueous platforms suitable for wetland development. However, inland wetlands might also have the opportunity to grow and develop as the rising sea level may inundate low-lying coastal plains. That could occur where suitable low-sloped estuaries and catchments occur, such as west of Comerong Island where the Shoalhaven alluvial plain is not far above current sea level. To a lesser extent the floodplains behind the Macquarie Rivulet and Mullet/Hooka Creek deltas could be partly inundated to form wetlands. However, this would not be the case for higher sloped estuaries, including the Towamba estuary catchment, where low-lying floodplains are not present.

7.5 Conclusions

This research provides significant results from case studies about the future vulnerability of eastern Australian coastal ecosystems, in a geomorphological context, to IPCC (2013, 2014) GMSLR scenarios.

Assessing eco-geomorphic coastal systems for the future GMSLR predictions, using IPCC (2013, 2014) hydro-scenarios and the chosen geomorphological coastal datasets, has provided significant results that show the Comerong Island study site will lose about 18% of its wetlands and associated habitats by 2050, and approximately 43% of the island will lost by 2100, which represents an almost total wetland loss by the end of 21st Century. This study approach has resulted in similar outcomes for the other four chosen study sites on the southeastern coast of Australia, indicating that similar effects would accrue on the whole east Australian coastline and worldwide.

Greenhouse gas emissions is causing climate changes such as global warming, are likely to increase in the near future or even if it stays the same, will have a very negative effect on the Earth's ecosystems. It is clear that Comerong Island has already been affected by GMSLR leading to: (i) its low-lying wetlands becoming inundated by the rising sea level; (ii) increased erosion rates caused by higher sea level impacting on the vulnerable sandy sediments around the island; and (iii) a decrease in sediment delivery following catchment modifications and dam construction. The vulnerability of coastal ecosystems has also been affected by increased

human settlement and modification of the landscape that controls sediment resources in the catchment area. This has interrupted the balance of the natural eco-geomorphic processes of sediment weathering, transporting and even accumulation over thousands of years that established the equilibrium between SLR dynamics in conjunction with the coastal environments. Coastal eco-geomorphic systems loss, especially wetlands, has been confirmed by other examples on the NSW south coast in a variety of geomorphic settings. To assess the problems associated with rising sea level the use of advanced and suitable data and modern software in conjunction with recognised climate change scenarios is highly recommended. This will help us to understand well the impacts of the influences of GMSLR on coastal ecosystems.

GMSLR is virtually certain to continue after 2100 for hundreds years according to the current and likely future gas emissions. Highly confidant scenarios produced by the IPCC (2013) have estimated that sea level will rise by up to ~82 cm by 2100 (within upper end maximum scenario) of about 70% of the world, including southeastern Australia (Church *et al.*, 2013). However, based on the findings of AR5, sea level rise may be less than 82 cm by 2100.

The southeastern Australian coastal zone will face strong challenges from ecosystem stressors during the 21st Century. Most of the Earth's oceans will be very likely to rise, which means that we will have new shorelines leading to changes in the shape of the exposed continents as well. Moreover, depending on the future amount of gas emissions, the coming centuries could have continued sea level rise after 2100 AD.

LiDAR and other similar modern RS data incorporated with GIS software analysis will prove to be very effective tools to obtain accurate predictions that could be available to help manage the environmental conservation targets for ecosystem sustainability. This approach was shown to be very suitable for study sites. In addition, ecological responses to relative stressors could be evaluated using geoinformatics to classify any temporal-vegetation changes indicated by the normalised difference vegetation index (NDVI) and their effect on ecological successions.

Chapter VIII: CONCLUSIONS

8.1 General Conclusions

This study assesses the potential impacts of upstream anthropogenic modifications, climatic factors and sea level rise on the estuarine eco-geomorphic intertidal sedimentary landforms and their associated coastal wetlands in southeastern Australia. These case studies show that RS imagery and GIS analysis, in combination with sedimentological and morphological data, make a useful methodological framework for documenting the evolution of prograding estuarine land-cover dynamics. Understanding how an estuary has evolved in the past can be used to help establish the probable vulnerability and adaptability of the estuary into the future. This has potential application to assess similar estuaries worldwide.

This thesis presents an overview of estuarine formation, development stages and their inclusion in the classification schemes advanced by Roy *et al.* (2001) and Sloss *et al.* (2006). Case studies including mapped and monitored the chosen estuaries/coastal wetlands in southeastern NSW with their geomorphic features, using: satellite imagery and airborne LiDAR combined with fieldwork investigations and sampling. GIS modelling predicted the potential spatial distribution of future influences on intertidal sedimentary landforms under various environmental stressors, including the global warming scenarios, such as rising sea level and declining sediment yield, leading to higher erosion rates on Comerong Island, particularly within mangroves and saltmarsh areas. This thesis has modelled the possible effect of rising sea level on an eco-geomorphic estuarine regime and its coastal ecosystems by the end of this century, using IPCC-AR5 (2014) scenarios in ArcScene (ArcGIS) inundating simulation tools. A process-based modelling technique was used to estimate the shoreline position and rate of land-classes growth for the selected sites using an observed land cover using fuzzy membership function and vegetation dynamics. Furthermore, this thesis develops the possible mitigation and adaptation strategies and sustainable solutions, which can be utilized to curtail the indirect adverse effects of climatic and anthropogenic dynamisms, in general, with more attention focused and suggested on damming rivers, which cause direct sediment problems as implied by the Tallowa Dam case study.

This thesis has mapped, monitored and modelled the following intertidal sedimentary landform types: barrier-estuary, deltaic-estuary and an open estuary with a large island at its entrance (Comerong Island). All of these studies have included diverse coastal wetland including mangroves, saltmarshes, *Casuarina*, *Juncus*, as well as downstream water bodies, dense-vegetation-covered wetlands, dune wetlands and coastal swamps. It revealed significant

changes to the distribution of shorelines and land classes, estuarine extent and wetland vegetation dynamics.

The thesis combines the GIS analytic tools with RS data, climatic data and fieldwork sampling/surveys to show that degradation levels on estuarine platforms are dependent on catchment development, sediment characteristics, ecosystem stability and sea level rise inundations. During anticipated climate change and rising sea level conditions, estuaries depend on their sediment source areas, especially any modifications to the catchment basin. Catchments with high anthropogenic modification levels, like the dam infrastructure in the Shoalhaven River catchment, influence sediment availability, and transportation with clear impacts on eco-geomorphic coastal platform losses.

In contrast, mostly unmodified but high-sloped catchments, such as the Towamba example, may have other negative effects on the estuary since the sediments are poorly sorted coarser non-cohesive quartz-dominated particles that cause the geomorphic landforms and associated ecosystems to be more vulnerable to erosion. Whereas, regions with small moderately modified catchments, such as the Wandandian area, allow ideal geomorphic processes to occur whereby sediment is weathered slowly and moved downstream naturally to a secure inner estuarine deltaic setting where fine sandy/silty particles can accumulate providing more geomorphic stability to be inhabited and to build the prograding and steady growing deltaic eco-geomorphic system.

The thesis assessment shows the eco-geomorphic-dynamism of the Towamba estuary, which has a mostly unmodified catchment surface (only 14% anthropogenic modifications), has been growing by 2609 m^2/yr at a total of 0.17 km^2 since 1949 as well as its barrier island that has moved seaward by 0.52 m/yr (on average). These growing indicators have driven the estimated Towamba estuary future scenarios to be mostly filled by 2100. In comparison, the partially modified catchment (with only 22.1%) has prograded the Wandandian deltaic shorelines into a wave-dominated zone but with low impact from nearshore processes. This has resulted in the total area growth of 0.24 km^2 at an overall rate of 4168 m^2/yr, with an average of 1.451 m/yr shoreline movement during the study period (1949-2016). Whereas, results on Comerong Island show there are significant changes to the areal extents, elevation and shorelines in the wetlands on Comerong Island over the time period of analysis (1949-2014). Changes include northern accretion (0.4 km^2), and western, middle and southern erosion (-0.7 km^2) of the island, which resulted in the overall erosion of -0.3 km^2 and net erosion rated of -4615m^2/yr.

This thesis emphasises the dynamic character of the estuarine eco-geomorphic system, particularly using NDVI as a vegetation canopy assessment approach. This illustrates the relationship between the vegetation-NDVI and factors such as time, temperature, rainfall, sea level and sedimentation rates. This analysis shows that; (i) Towamba estuary has grown ecologically and geomorphologically since 1975, with the rate of geomorphic growth (sedimentary surfaces) being faster and wider than the plant communities. This confirms the eco-geomorphic assessment findings (chapter2), which suggested that the growth on Towamba estuary is a sedimentary characteristic, whereby mostly unmodified-high sloped catchment drove high sediment rates, poorly sorted sediment (which caused more and longer stabilisation of platform-dynamics), to infills the estuary providing a ground on which vegetation could become established. (ii) The eco-geomorphic system on the Wandandian site is growing ecologically and geomorphologically, but the ecological rate of growth is higher (7.3%) than the geomorphic growth of only 3.4%. This reflects the well stabilised and vegetated platform with less geodynamics modification resulting from the small related catchment with limited modifications and sea dynamic impacts. (iii) In comparison, the temporal NDVI trends of Comerong Island have slowly declined, which indicates that Comerong Island is deteriorating ecologically and geomorphologically but the rate of ecological decline is higher.

A linear regression model was used to tracks these changes and has attributed and linked them over time (year) to temperature, precipitation, rising sea level and sediment rates (erosion). For the Towamba vegetation canopy, the variables time (year), rising sea level and sedimentation rate have significant effects on NDVI values whereas temperature and rainfall have insignificant effects on increasing the NDVI values. At Wandandian delta all the variables have significant positive effects on the NDVI index, except rainfall. In contrast, at Comerong Island time, temperature and sea level rise have significant negative impacts on the NDVI, whereas rainfall has an insignificant effect on NDVI and sedimentation rate has a positive influence. Thus it can be concluded that the correlation between NDVI and climatic and geomorphic factors is very significant at Towamba, Wandandian and Comerong indicating that these factors (except the remaining R square of other non-regressed factors) are the main controllers that will disturb the NDVI at such intertidal sedimentary landforms during the 21st Century worldwide.

NDVI change-distribution maps (using the map-algebra expression) show the zonation and spatial distribution of NDVI changes. These, reflect the vegetation distribution dynamics at each study site, identifying the areas that need to be managed in relation to the causes and/or

drivers of change at the local scale. NDVI change maps have effectively analysed the NDVI datasets, to show a clear pattern of changes at particular areas over the study period. The zoning changes, that have been detected, have smoothly interpolated and mapped the dynamic changes of NDVI distributions over-time/study-sites. This has allowed these zoning changes to be related to the responsible factors, which included mainly high sedimentation rates and shoreline dynamics on the Towamba estuary, water shortage on some elevated parts of Wandandian delta, as well as such shoreline erosion rates around Comerong Island.

The LiDAR-DEMs-driven character of the existing situations and the influencing factors are controlling the estimated future-scenarios, and have illustrate clear inundatable landform zonations at all study sites by 2100, as well as the Lake Illawarra validation examples. However, there are variations in the future vulnerability since responses to rising sea level at the study sites depends on their elevation and sedimentary processes/character. Thus a huge eco-geomorphic loss (43%) on Comerong Island is predicted that represents an almost total wetland loss by 2100 since the island has mostly formed as low-lying platforms, which would be inundated due to surge of sea level, as well as the negative sedimentation rates. Loss at the Wandandian and Towamba sites is also estimated to occur causing total wetland loss by 2100, but it will affect less geomorphic area since they have higher elevated platforms and some rocky margins. Thus, sea level rise will have a significant influence on the coastal eco-geomorphic systems throughout southeastern Australia and equivalent systems overseas by 2100. This will particularly affect estuarine/coastal wetlands as they are the most sensitive and responsive coastal ecosystems as clearly seen by the results from Comerong Island and other southeast Australian examples.

8.2 Importance and significance

The thesis shows estuarine evolution is strongly reliant on human impacts which have negative effects on the sensitive ecosystems of such coastal wetlands. The thesis develops existing methods to investigate coastal landforms with GIS and remote sensing, which contribute to understanding their development. An understanding of the historical evolution of these landscapes can, in turn, contribute to the conservation of these sensitive ecosystems.

The thesis characterises the impact that rising sea levels will have on estuaries in the case study sites employed. As erosion rates will be increased as the SLR affects new shoreline levels. At the same time, anthropogenic impact levels are also predicted to increase, as the population is growing and is concentrated on the coastal zones. Together, the thesis establishes at specific locations that these factors will put a tremendous effect to coastal eco-

geomorphic systems and result in serious loss scenarios of its shorelines and associated wetlands habitats. I was able to show that relatively unmodified catchments will act differently, since higher sedimentation rates will continue to be transported downstream and accumulate in their respective estuaries, which may be able to grow or at least keep-pace up with SLR.

The thesis shows that intertidal sedimentary landforms will have a future negative or positive vegetarian response according to their evolving morphological character. Then, it was confirmed that, within a short-term timescale, the whole eco-geomorphic system will interact according to many environmental and anthropogenic variables (particularly the sedimentation rates) to evolve its own character in the long-term timescale.

The intertidal eco-geomorphic bodies of riverine estuaries have formed as unstable systems adjusting to environmental disturbances in the form of a dynamicity in shorelines, land cover and the associated habitat conditions, instigated post-1950 as a result of increased trends of global warming. This is particularly noticeable within high anthropogenic modification areas, which have affected the sedimentary process rates that have transported material from the catchments. Subsequently, the integration of these environmental together with human stressors has caused a significant control of the erosion/deposition processes on the estuarine banks due to increased fluvial and tidal influences. The riverine estuaries on the southeastern Australian coast are, therefore, still adjusting to a disturbance that was instigated and concentrated within the past a few decades when higher global warming and human settlement affected estuaries worldwide, including Australia. This adjustment has meant that the three investigated sites form part of a system experiencing dynamic equilibrium with erratic trends related to the gradual decrease in rates of sediment transported to the coastal area. This results from continued climatic and anthropogenic interactions, which control a decline in sediment sources from the catchments and result in increased erosion dynamics in the coastal zones. However, the decrease in sedimentation rates over the past 67 years at some sites has reacted differently where they still have a slight shoreline and vegetation growth, reflecting that such systems are approaching a new equilibrium state. Such riverine estuaries will, therefore, continue to grow at an erratic but declining rate focusing on where the inner secure geomorphic forms meet the stablising vegetation canopies and the associated habitats, as they have a significant eco-geomorphic reciprocal relationship. Erosion evidence presented on Comerong Island shorelines is focussed on the outer bend of the west, south and middle sides, and has involved eroding Comerong Island banks and mangrove areas. At the same time, eco-geomorphic growth is evidence format the Towamba and Wandandian sites,

but it occurs at a declining rate due to SLR that limits sediment deposition efficiently.

It is clear that these intertidal sedimentary landforms are adjusting their eco-geomorphic regimes to the whole eco-geomorphic controlling dynamics. Adjustment levels and character depend on the environmental/anthropogenic stressors on one side and the formation/vulnerability and characteristics of such transitional landforms on the other side. Past examples have shown the size of such eco-geomorphic regimes depends on the length of the adjustment period of the estuarine system (68 years in the studied cases), but it could be impacted by seasonal to millennial scale systems which will require continued adjustment for the next few decades or it may even take centuries to come.

Through understanding the driving forces and resistance variables influencing the geomorphology (and the ecological consequences) of such estuarine landforms, sedimentation factors, most likely due to anthropogenic modifications in the catchment with declined precipitation, are responsible for the general pattern of erosion along the estuarine shorelines. Variations in the rates of erosion reflect differential sediment characteristics (amount and sorting) that depend on the sources and the deposition conditions in conjunction with the hydraulic forces, tidal, high flow events and sea level dynamics that adjusting such systems. Thus, this short-term assessment would suggest that shoreline adjustment is a function of estuarine vulnerability and sediment characterisation and is most likely to correlate with greater anthropogenic impacts, especially global warming.

This project provides significant, detailed results of estuarine morphodynamics and their associated coastal wetland responses in an eco-geomorphic context for risk assessment, using modern modelling approaches. The results are very informative for government agencies to issue and revise their policies. The findings are also important for the general public and environmental scientists who are currently focusing their attention on the best way to preserve wetland ecosystems. For instance, accurate estimates of environmental change can help to manage the environmental conservation targets.

The goals of this research are novel. While much research has previously been conducted on coastal wetlands (including; Nicholls, 2004; Valiela & Fox, 2008; Saintilan & Williams, 2010; Oliver *et al.*, 2012), none of these studies have reported detailed changes of estuaries and their associated coastal wetlands in terms of shoreline, vegetation and sediment characteristics for the study sites investigated here. Neither has previous work focused on the relationships between different estuarine landforms (as natural processes) and development levels (as human-modifications).

Future projections indicate the importance of indirect anthropogenic-induced global warming

that is changing climates and leading to SLR and more extreme weather events like storms and floods (Michener *et al.*, 1997; Watson, 1999; Hofmeister *et al.*, 2010; Nguyen *et al.*, 2016). Additionally, direct human impacts on the estuaries and their catchments will have a greater effect on estuaries and coastal wetlands in the 21st Century (Oscar *et al.*, 2016). It is essential of get more understanding of how southeastern Australian estuarine/coastal wetlands behave in response to current global and local stressors through the available historical records (Hofmeister *et al.*, 2010). This research will also help to provide an important framework for quantifying the current and future stressors/responses during any intensification of natural and artificial coastal hazards. This approach is very important at the current stage of human settlements which control most of the eco-geomorphic processes.

Human activities have had the greatest impact on the destruction of the existing coastal wetlands in many regions around the world (Nicholls, 2004). Due to the importance of wetlands to the ecosystem in terms of the resources they provide, it remains crucial to ensure that human activities are controlled to prevent any devastating impacts. The alteration of hydrology through modification of landcover and associated dynamism could be minimised by assessing the land's suitability around various coastal wetlands using GIS technology (Malczewski, 2004). While the wetlands cannot be recreated, the loss can be restored through undertaking a hydrological analysis of an environment whose hydrology has been altered by human activity (Zedler, 2000). A wetland could be created that is self-sustaining when such considerations are made.

The growing population in many urban centres has necessitated the damming of many rivers to ensure water supply to the citizens. Damming, however, has significant effects on the geomorphic ecosystems downstream, especially within the wetlands in the coastal regions (e.g. Al-Nasrawi *et al.*, 2016a). While undertaking these developments to provide water resources for urban dwellers, it is critical to consider the impacts of the developments on the coastal wetlands as a way of ensuring their sustainability (Masselink & Heteren, 2014). According to Beluru & Hegde (2016), such constructions commonly make coastal wetlands highly vulnerable to the effects of natural phenomena like storms, as well as sea level rise (Al-Nasrawi *et al.*, 2018c). The sustainability of the ecosystems should be ensured through controlled development upstream to prevent negative effects like the loss of coastal wetlands.

In seeking to accurately assess coastal wetlands to determine their vulnerability and to develop sustainable solutions, a model needs to consider the most important elements, which are (mainly) shorelines and vegetation dynamics. Adoption of a broad-scale modelling of coastal environments presents the involved managers with the capability to assess a wide range of mechanisms that affect the behaviours of wetland ecosystems (McFadden *et al.*,

2007) in order to devise effective plans for ecosystem sustainability. This requires the application of a variety of modelling methods to overcome any weaknesses. A variety of methods can be applied in seeking to develop a sustainable ecosystem within the estuarine regimes and prevent the loss of the wetlands.

In conclusion, coastal wetlands play an important role in estuarine ecosystem dynamics. An assessment of the literature on the impacts of changes on coastal wetlands describes a range of elements that could have adverse environmental impacts. These need to be considered in the modelling process, including methods for measuring and monitoring changes, the effects of the change, and modelling the factors that develop sustainable coastal wetland ecosystems. A wide range of methods can be utilized in the measurement of the shoreline extent and vegetation dynamics but it remains critical to consider the timing, frequency and the aspects of assessment for the results to be meaningful. The degradation of wetlands through human and natural activities has led to a need to adopt modelling methods which seek to ensure sustainability of the wetland ecosystems.

8.3 Future research directions

The short-term GIS-modelling and assessment approach suggests that the short-term-estuarine dynamics is driving the long term existence and situation produced by the complex interactions between the variables. This should be used to direct the long term assessment approaches by having a better understanding of the existing situation and identifying the past drivers accurately. However, more tools and datasets need to be made publically available over time, such as more temporal-LiDAR data needed for better comparison of surface elevations over time. At the same time, the GIS modelling approach can provide a greater benefit and more accurate results by adopting the next-update of the Geocentric Datum of Australia (GDA2020). GDA2020 will express the new-dynamic Australian datum that incorporates the Australian continental movement of 2 cm/yr, which could influence the reference-point coordinates and the GIS and RS-short-term assessments, such as the orthorectification processes, and the use of drones to capture imagery for the short term dynamics that have better control over timing of surveys for monitoring dynamics.

At the landscape level, maybe more geoinformatics (GIS/RS) investigations need to be undertaken on the catchment surface and its runoff interactions, both spatially and temporally, with respect to the availability and reliability of remote sensing datasets.

REFERENCES

Aarts, B. G. W., and Nienhuis, P. H., 1999. Ecological sustainability and biodiversity. *International Journal of Sustainable Development and World Ecology*, 6, 89-102.

ABS, 2011. *Australian Bureau of Statistics, Australian Government* [Online]. Available: http://www.abs.gov.au/.

Adnan, F. A., Hamylton, S. M., & Woodroffe, C. D., 2016. A comparison of shoreline changes estimated using the base of beach and edge of vegetation line at North Keeling Island. *Journal of Coastal Research,* 75**,** 967-971.

Akumu, C. E., Pathirana, S., Baban, S. & Bucher, D. 2011. Examining the potential impacts of sea level rise on coastal wetlands in north-eastern NSW, Australia. *Journal of Coastal Conservation,* 15**,** 15-22.

Akumu, C. E., Pathirana, S., Baban, S., & Bucher, D., 2010. Monitoring coastal wetland communities in north-eastern NSW using ASTER and Landsat satellite data. *Wetlands Ecology and Management,* 18**,** 357-365.

Al-Fadhli, I. H. 2013. *Turbulance characteristics in unsteady and non-uniform flows and their impacts on the incipient motion of sediment transport-water resources-river mechanics.* PhD thesis, University of Wollongong.

Ali, M., Sterk, G., Seeger, M., Boersema, M., & Peters, P., 2011. Effect of hydraulic parameters on sediment transport capacity in overland flow over erodible beds. *Hydrology and Earth System* Sciences Discussions, 8, 6939-6965.

Al-Nasrawi, A. K. M., Al-Hamdany, U. A., Hamylton, S. M., Jones, B. G. & Alyazichi, Y. M. 2017a. Surface Elevation Dynamics Assessment Using Digital Elevation Models, Light Detection and Ranging, GPS and Geospatial Information Science Analysis: Ecosystem Modelling Approach. International Journal of Environmental, Chemical, Ecological, Geological and Geophysical Engineering, Vol: 11, No: 11, 2017, 918 - 923. Digital Article Identifier (DAI): urn:dai:10.1999/1307-6892/10008196. Available at: http://waset.org/publications/10008196.

Al-Nasrawi, A. K. M., Hamylton, S. M., & Jones, B. G., 2018a. An assessment of anthropogenic and climate stressors on estuaries using a spatio-temporal GIS-modelling approach for sustainability: Towamba estuary, southeastern Australia. *Environmental Monitoring and Assessment*, (in press). DOI: 10.1007/s10661-018-6720-5.

Al-Nasrawi, A. K. M., Hamylton, S. M., Jones, B. G. & Kadhim, A. A. 2018b. Geoinformatic analysis of vegetation and climate change on intertidal sedimentary landforms in southeastern Australian estuaries from 1975–2015. *AIMS Geosciences*, 4 (1): 36-65. doi: 10.3934/geosci.2018.1.36.

Al-Nasrawi, A. K. M., Hopley, C. A., Hamylton, S. M., Jones, B. G., 2017b. A spatio-temporal assessment of landcover and coastal changes at Wandandian delta system, southeastern Australia. *Journal of Marine Science and Engineering,* 5, 55; doi:10.3390/jmse5040055.

Al-Nasrawi, A. K. M., Jones, B. G., Alyazichi, Y. M. & Hamylton, S., 2015a. Modelling the future eco-geomorphological change scenarios of coastal ecosystems in southeastern Australia for sustainability assessment using GIS.

Al-Nasrawi, A. K. M., Jones, B. G., Alyazichi, Y. M., Hamylton, S. M., Jameel, M. T. and Hammadi, A. F., 2016a. Civil-GIS incorporated approach for water resource management in a developed catchment for urban-geomorphic sustainability: Tallowa Dam, southeastern Australia. *International Soil and Water Conservation Research*, 4, 303-313. doi.org/10.1016/j.iswcr.2016.11.001.

Al-Nasrawi, A. K., Jones, B. G. & Hamylton, S. 2015b. Modelling changes of coastal wetlands responding to disturbance regimes (Eastern Australia) Using GIS. Conference: Australian Mangrove and Saltmarsh Network - Working with Mangrove and Saltmarsh for Sustainable Outcomes, At the University of Wollongong. https://smah.uow.edu.au/content/groups/public/@web/@smah/@sees/documents/doc/uow188074.pdf

Al-Nasrawi, A. K., Jones, B. G. & Hamylton, S. M., 2016b. GIS-based modelling of vulnerability of coastal wetland ecosystems to environmental changes: Comerong Island, southeastern Australia. *Journal of Coastal Research*, 75, 33-37. doi.org/10.2112/SI75-007.1.

Al-Nasrawi, A. K., Sarah M. Hamylton, Brian G. Jones, Carl A. Hopley, Yasir M. Al Yazichi. 2018c. Geoinformatics vulnerability predictions of coastal ecosystems to sea level rise in southeastern Australia. Geomatics, Natural Hazards and Risk Journal (in press). https://doi.org/10.1080/19475705.2018.1470112.

ALUM (Australian Land Use and Management), 2010. Classification Version 7 (Geo-datasets), The Australian Land Use and Management, Geoscience Australia, Canberra.

Alyazichi, Y. M. M. 2015a. Trace element pollution in marine sediments from Botany Bay and Port Hacking estuary, NSW, Australia, PhD thesis, University of Wollongong, Wollongong, Australia.

Alyazichi, Y. M., Jones, B. G., Mclean, E., Altalyan, H. N. & Al-Nasrawi, A. K. M., 2015b. Risk Assessment of Trace Element Pollution in Gymea Bay, NSW, Australia. *International Science Index, Environmental and Ecological Engineering*, 9, 1286-1292.

ANZECC and NHMRC (2000). Australian and New Zealand guidelines for the assessment and management of contaminated sites.: Australian and New Zealand Environment Conservation Council and National Health and Medical Research Council, Canberra.

Arun, P. V., 2013. A comparative analysis of different DEM interpolation methods. *Egyptian Journal of Remote Sensing and Space Science*, 16, 133-139.

ASCPSS, 2009. Climate Change and Its Impact on Sydney's Water Supply – Technical Report: Authority, Sydney Catchment Planning, Strategic Supply.

Asrar, G., Fuchs, M., Kanemasu, E., & Hatfield, J., 1984. Estimating absorbed photosynthetic radiation and leaf area index from spectral reflectance in wheat. *Agronomy journal,* 76**,** 300-306.

ASTER GDEM, 2016. A product of METI and NASA. Available from http://earthexplorer.usgs.gov/.

Aziz, N. M., & Scott, D. E., 1989. Experiments on sediment transport in shallow flows in high gradient channels. *Hydrological Sciences Journal,* 34**,** 465-478.

Baban, S. M., 1997. Environmental monitoring of estuaries; estimating and mapping various environmental indicators in Breydon Water Estuary, UK, using Landsat TM imagery. *Estuarine, Coastal and Shelf Science,* 44**,** 589-598.

Ball, G. L., 1994. Ecosystem modeling with GIS. *Environmental Management,* 18**,** 345-349.

Barnett, T. P., 1983. Recent changes in sea level and their possible causes. *Climatic Change,* 5**,** 15-38.

Batzer, D. P., and Sharitz, R. R., 2014. *Ecology of Freshwater and Estuarine Wetlands*, University of California Press, Los Angeles.

Beluru, J. A., & Hegde, A. V., 2016. GIS Based Approach for Vulnerability Assessment of the Karnataka Coast, India. *Advances in Civil Engineering*, 2016. Article ID 5642523, 10 pages, 2016. doi:10.1155/2016/5642523.

Berry, S., Mackey, B., & Brown, T., 2007. Potential applications of remotely sensed vegetation greenness to habitat analysis and the conservation of dispersive fauna. *Pacific Conservation Biology,* 13**,** 120-127.

Bhattacharya J. P., & Walker, R. G., 1992. Deltas. In: Walker R. G., & James N. P., eds. *Facies Models: Response to Sea Level Change*, pp. 157 – 178. Geological Association of Canada, Toronto.

Bianchi, T. S., & Allison, M. A., 2009. Large-river delta-front estuaries as natural "recorders" of global environmental change. *Proceedings of the National Academy of Sciences,* 106**,** 8085-8092.

Blay, J., 1944. *On Track: Searching out the Bundian Way, Eden local history reference collection.*, NewSouth Publishing, . Sydney.

Blott, S. J., 2010. A package of grain size distribution and statistics for the analysis of unconsolidated sediments by sieving or Laser Granulometer-GRADISTAT V.8.0.

Blott, S. J., Pye, K., Van Der Wal, D., & Neal, A., 2006. Long-term morphological change and its causes in the Mersey Estuary, NW England. *Geomorphology,* 81**,** 185-206.

BOM, 2016. Climate classification of Australia [Online]. Australian Government, Bureau of Meteorology. Available: http://www.bom.gov.au.

BOM, 2017a. *NSW Weather* [Online]. Australian Governmet, Bureau of Meterology. Available: http://www.bom.gov.au.

BOM, 2017b. *Climate classification of Australia* [Online]. Australian Government, Bureau of Meteorology. Available: http://www.bom.gov.au/climate/.

BOM-NSW. 2017. *Tide Gauge Metadata and Observed Monthly Sea Levels and Statistics* [Online]. Bureau of Meteorology. Available: http://www.bom.gov.au/oceanography/projects/ntc/monthly/.

Bonetti, J., Klein, A. H. F., Muler, M., De Luca, C. B., Silva, G. V., Toldo, E. E., & González, M., 2012. Spatial and numerical methodologies on coastal erosion and flooding risk assessment. In: Finkl, C. (Ed.) Coastal Hazards. Chapter 16. Coastal Research Library Series. Springer, Dordrecht, p. 423-442. ISBN: 978-94-007-5233-7.

Borre, J. V., Paelinckx, D., Mücher, C. A., Kooistra, L., Haest, B., De Blust, G., & Schmidt, A. M., 2011. Integrating remote sensing in Natura 2000 habitat monitoring: Prospects on the way forward. *Journal for Nature Conservation,* 19**,** 116-125.

Borrell, A., 2013. The Effects of Catchment Land Cover Change on Sedimentation in Back Lake, Merimbula, NSW. Bachelor of Environmental Science (Honours) thesis, University of Wollongong, 2013.http://ro.uow.edu.au/thsci/71.

Boto, K. G., & Wellington, J. T., 1984. Soil characteristics and nutrient status in a northern Australian mangrove forest. *Estuaries*, 7, 61-69.

Boumans, R. M., & Day, J. W., 1993. High precision measurements of sediment elevation in shallow coastal areas using a sedimentation-erosion table. *Estuaries*, 16, 375-380.

Boyes, B., 2006. *Determining and Managing Environmental Flows for the Shoalhaven River: Report 1- Environmental Flows Knowledge Review*, Department of Natural Resources, Sydney.

Braatne, J. H., Rood, S. B., Goater, L. A., & Blair, C. L., 2008. Analysing the impacts of dams on riparian ecosystems: A review of research strategies and their relevance to the Snake River through Hells Canyon. *Environmental Management*, 41, 267-281.

Bradshaw, B. E., 1987. *St Georges Basin – Morphology and Late Quaternary Deposits.* BSc Honours thesis, University of Sydney, Sydney, (unpublished).

Bullock, A., & Acreman, M., 2003. The role of wetlands in the hydrological cycle. *Hydrology and Earth System Sciences Discussions*, 7, 358-389.

Cahoon, D. R., 2015. Estimating relative sea-level rise and submergence potential at a coastal wetland. *Estuaries and Coasts*, 38, 1077-1084.

Cahoon, D. R., Lynch, J. C., Hensel, P., Boumans, R., Perez, B. C., Segura, B., & Day, J. W., 2002. High-precision measurements of wetland sediment elevation: I. Recent improvements to the sedimentation-erosion table. *Journal of Sedimentary Research*, 72, 730-733.

Calzadilla P. A., Damen, M. C. J., Geneletti, D., and Hobma, T.W., 2002. Monitoring a recent delta formation in a tropical coastal wetland using remote sensing and GIS. Case study: Guapo River Delta, Laguna De Tacarigua, Venezuela. *Environment, Development and Sustainability*, 4, 201-219.

Carlson, A. E., Legrande, A. N., Oppo, D. W., Came, R. E., Schmidt, G. A., Anslow, F. S., Licciardi, J. M., & Obbink, E. A., 2008. Rapid early Holocene deglaciation of the Laurentide ice sheet. *Nature Geoscience,* 1**,** 620.

Carter, R. W. G. & Woodroffe, C. D. 1997. *Coastal evolution: Late Quaternary shoreline morphodynamics*, Cambridge University Press, Cambridge.

Carter, V., 1999. *Technical Aspects of Wetlands (Wetland Hydrology, Water Quality, and Associated Functions)* [Online]. Available: http://water.usgs.gov/nwsum/WSP2425/hydrology.html.

Carvalho, R. C., & Woodroffe, C., 2013. Shoalhaven River mouth: a retrospective analysis of breaching using aerial photography, landsatimagery and LiDAR. *In Proceedings of the 34th Asian Conference on Remote Sensing 2013* Indonesia: Indonesian Remote Sensing Society, SC03-592- pp.1-7.

Carvalho, R., & Woodroffe, C., 2014. The sediment budget as a management tool: the Shoalhaven coastal compartment, southeastern NSW, Australia. *23rd NSW Coastal Conference.* Ulladulla, NSW. pp. 1-12

Cazenave, A., Champollion, N., Paul, F. & Benveniste, J. 2017. *Integrative Study of the Mean Sea Level and Its Components*, Springer. Cham, Switzerland. DOI 10.1007/978-3-319-56490-6.

Çengel, Y. A., Cimbala, J. M., & Kanoglu, M., 2010. *Fluid mechanics : Fundamentals and Applications*, Boston, Mass: McGraw-Hill Higher Education. 2nd ed..

Chapin, F. S., Sturm, M., Serreze, M., Mcfadden, J., Key, J., Lloyd, A., Mcguire, A., Rupp, T., Lynch, A., & Schimel, J., 2005. Role of land-surface changes in Arctic summer warming. *Science,* 310**,** 657-660.

Chen, J., & Gong, P., 1998. *Practical GIS: building and maintaining a successful GIS*. Science Press, Beijing.

Cheng, N.-S., & Chen, X., 2014. Slope correction for calculation of bedload sediment transport rates in steep channels. *Journal of Hydraulic Engineering*, 140 (6), 04014018, 1-7.

Cherfas, J., 1990. The fringe of the ocean-under siege from land: the ecology of the ocean margins, crucial to human life, is being disrupted by our activities-and perhaps by global change. *Science (New York)*, 248 (4952), pp. 163-165.

Chien, N., & Wan, Z., 1999. *Mechanics of Sediment Transport*, ASCE, Reston, VA.

Cho, H.Y.; Lakshumanan, C.; Usha, N. Coastal wetland and shoreline change mapping of Pichavaram, south east coast of India using satellite data. In Proceedings of the Geospatial Application Papers, Map Asia Conference, Beijing, China, 26–29 August 2004.

Christian, A. T., & Hill, S. M., 2002. Regolith-landform mapping of the Shoalhaven River Delta and hinterland, NSW: towards a model for landscape change and management. *Regolith and Landscapes in Eastern Australia***,** 8-13.

Christiansen, T., Wiberg, P., & Milligan, T., 2000. Flow and sediment transport on a tidal salt marsh surface. *Estuarine, Coastal and Shelf Science,* 50**,** 315-331.

Church, J. A., Clark, P. U., Cazenave, A., Gregory, J. M., Jevrejeva, S., Levermann, A., Merrifield, M., Milne, G., Nerem, R., Nunn, P., Payne, A.J., Pfeffer, W.T., Stammer, D., & Unnikrishnan, A. S., 2013: Sea level change. In Stocker, T. F., Qin, D., Plattner, G.-K., Tignor, M., Allen, S. K., Boschung, J., Nauels, A., Xia, Y., Bex, V., & Midgley, P. M. (eds.), 2013. Projections of sea level rise IPCC AR5.*Climate Change 2013: The Physical Science Basis*. Contribution of Working Group I to the Fifth Assessment Report of the Intergovernmental Panel on Climate Change. Cambridge University Press, Cambridge. pp. 1137-1216.

Coleman, J. M., & Wright, L., 1975. Modern river deltas: variability of processes and sand bodies, Deltas. Models for Exploration, *Houston Geological Society*, USA, 99-149

Cooper, J. D., and Keller, M., 2001. Palaeokarst in the Ordovician of the southern Great Basin, USA: implications for sea-level history. *Sedimentology*, 48, 855-873.

Cordeiro, J. P. C., Câmara, G., Moura, U. F., Barbosa, C. C., & Almeida, F., 2005. Algebraic Formalism over Maps. *In Proceedings of the 7th Brazilian Symposium on GeoInformatics, GEOINFO 2005; Campos do Jordao, SP; Brazil; 20 November 2005 through 23 November 2005; Code 93474.*

Costanza, R., 1999. Ecological sustainability, indicators, and climate change. IPCC Expert Meeting on Development, Equity and Sustainability, Colombo, Sri Lanka, Citeseer, 27-29.

Costanza, R., Pérez-Maqueo, O., Martinez, M. L., Sutton, P., Anderson, S. J., & Mulder, K., 2008. The value of coastal wetlands for hurricane protection. *AMBIO: A Journal of the Human Environment,* 37**,** 241-248.

Cronk, J. K., & Fennessy, M. S., 2001. *Wetland Plants: Biology and Ecology,* Boca Raton, Fla, Lewis Publishers.

Crosset, K. M., Culliton, T. J., Wiley, P. C., & Goodspeed, T. R., 2004. *Population trends along the coastal United States: 1980-2008*: U.S. Department of Commerce National Oceanic and Atmospheric Administration National Ocean Service. Management and Budget Office, Special Projects, Coastal Trends Report Series. United States.

Crossland, C. J., Kremer, H. H., Lindeboom, H., Crossland, J. I. M., & Le Tissier, M. D., 2005. *Coastal fluxes in the Anthropocene: the land-ocean interactions in the coastal zone project of the International Geosphere-Biosphere Programme*, Germany, Springer Science & Business Media. ISBN 978-3-540-27851-1.

Cukic, E. Z., & Venter, P., 2012. Sediment removal and management. *Civil Engineering: Magazine of the South African Institution of Civil Engineering*, 20, 42-47.

Dalezios, N., Domenikiotis, C., Loukas, A., Tzortzios, S., & Kalaitzidis, C., 2001. Cotton yield estimation based on NOAA/AVHRR produced NDVI. *Physics and Chemistry of the Earth, Part B: Hydrology, Oceans and Atmosphere,* 26**,** 247-251.

Dall'osso, F., Dominey-Howes, D., Moore, C., Summerhayes, S., & Withycombe, G., 2014. The exposure of Sydney (Australia) to earthquake-generated tsunamis, storms and sea level rise: a probabilistic multi-hazard approach. *Scientific Reports 4-7401*; DOI:10.1038/srep07401.

Dalrymple, R. W., Zaitlin, B. A., & Boyd, R., 1992. Estuarine facies models: conceptual basis and stratigraphic implications: perspective. *Journal of Sedimentary Research,* 62, 1130-1146.

Daly, G., 1996. Some problems in the management of the green and golden bell frog Litoria aurea (Anura: Hylidae) at Coomonderry Swamp on the south coast of New South Wales. *Australian Zoologist,* 30**,** 233-236.

Damgaard, J. S., Whitehouse, R. J., & Soulsby, R. L., 1997. Bed-load sediment transport on steep longitudinal slopes. *Journal of Hydraulic Engineering*, 123, 1130-1138.

Dao, N., 2011. Damming rivers in Vietnam: a lesson learned in the Tay Bac region. *Journal of Vietnamese Studies*, 6, 106-140.

Davenport, J., & Davenport, J. L., 2006. The impact of tourism and personal leisure transport on coastal environments: a review. *Estuarine, Coastal and Shelf Science,* 67**,** 280-292.

Davies, J., 1974. The coastal sediment compartment. *Australian Geographical Studies,* 12**,** 139-151.

Davies, P. M., & Stewart, B. A., 2013. Aquatic biodiversity in the Mediterranean climate rivers of southwestern Australia. *Hydrobiologia,* 719**,** 215-235.

Day, J. W., Christian, R. R., Boesch, D. M., Yáñez-Arancibia, A., Morris, J., Twilley, R. R., Naylor, L., & Schaffner, L., 2008. Consequences of climate change on the ecogeomorphology of coastal wetlands. *Estuaries and Coasts,* 31**,** 477-491.

Dean, L., & De Deckker, P., 2013. Recent benthic foraminifera from Twofold Bay, Eden NSW: community structure, biotopes and distribution controls. *Australian Journal of Earth Sciences,* 60**,** 475-496.

Deconto, R. M., & Pollard, D., 2016. Contribution of Antarctica to past and future sea-level rise. *Nature,* 531**,** 591-597.

DEE, 2006. *Coasts and oceans: Ecosystem conditions* [Online]. Department of the Environment and Energy Available: https://www.environment.gov.au/node/21960.

Deeley, D. M., & Marine, E. P., 1999. Assessing the ecological health of estuaries in Australia. *LWRRDC Occasional Paper 17/99 (Urban Subprogram, Report No. 10).* Marine and Freshwater Research Laboratory, Institute for Environmental Science Murdoch University, Perth

Department of Environment Climate Change and Water (DECCW), 2009. *NSW Sea Level Rise Policy*

Statement, Sydney.

Department of Environment, Climate Change and Water, 2010. Riverine Ecosystems, Southern river Region. State of the Catchments, New South Wales Government, Sydney.

Deser, C., Phillips, A. S., & Hurrell, J. W., 2004. Pacific interdecadal climate variability: Linkages between the tropics and the North Pacific during boreal winter since 1900. *Journal of Climate,* 17**,** 3109-3124.

Despland, E., Rosenberg, J., & Simpson, S. J., 2004. Landscape structure and locust swarming: a satellite's eye view. *Ecography,* 27**,** 381-391.

Dittmer, D., 2010. *River Sediment Sampling Methods-Causeway Building and Removal.* Environmental Studies thesis, University of Nebraska, Lincoln.

Donohue, R. J., Mcvicar, T., & Roderick, M. L., 2009. Climate-related trends in Australian vegetation cover as inferred from satellite observations, 1981–2006. *Global Change Biology,* 15**,** 1025-1039.

DPI/OW, 2017. Towamba catchment [Online]. Department of Primary Industries / Office of Water. Available: http://www.water.nsw.gov.au/water-management/basins-and-catchments/towamba-catchment.

DSE, 2007. Index of Wetland Condition (Review of wetland assessment methods): Department of Sustainability and Environment, Melbourne, Victorian Government, Australia.

Duda, A., 2002. Monitoring and evaluation indicators for GEF international waters projects. Global Environment Facility Monitoring and Evaluation Working Paper, 10.

Edington, J. M., & Edington, M. A., 1986. *Ecology, recreation and tourism*, Cambridge University Press Archive, Cambridge.

Ehrenfeld, J. G., 2000. Evaluating wetlands within an urban context. *Ecological Engineering*, 15(3), 253-265.

El-Sayed, A., El-Sherbiny, M., Abo-El-Ezz, A., & Aggag, G., 1995. Friction and wear properties of polymeric composite materials for bearing applications. *Wear*, 184, 45-53.

Essington, T. E., & Carpenter, S. R., 2000. Mini-review: nutrient cycling in lakes and streams: insights from a comparative analysis. *Ecosystems*, 3, 131-143.

Fairbanks, R. G., 1989. A 17, 000-year glacio-eustatic sea level record: influence of glacial melting rates on the Younger Dryas event and deep-ocean circulation. *Nature,* 342**,** 637-642.

FAO, 2003. Status and trends in mangrove area extent worldwide. Wilkie, M.L. and Fortuna, S. (eds) Forest Resources Assessment Working Paper No. 63. *Forest Resources Division*. FAO, Rome.

Fensham, R., Fairfax, R., & Archer, S., 2005. Rainfall, land use and woody vegetation cover change in semi-arid Australian savanna. *Journal of Ecology,* 93**,** 596-606.

Fensholt, R., Rasmussen, K., Kaspersen, P., Huber, S., Horion, S., & Swinnen, E., 2013. Assessing land degradation/recovery in the African Sahel from long-term earth observation based primary productivity and precipitation relationships. *Remote Sensing,* 5**,** 664-686.

Fernandes, L., Nayak, G.N., Ilangovan, D., & Borole, D.V., 2011. Accumulation of sediment, organic matter and trace metals with space and time, in a creek along Mumbai coast, India. *Estuarine, Coast, and Shelf Science*, 91, 388-399.

Fernandez Luque, R., & Van Beek, R., 1976. Erosion and transport of bed-load sediment. *Journal of Hydraulic Research*, 14, 127-144.

Fernández, A., Illera, P., & Casanova, J. L., 1997. Automatic mapping of surfaces affected by forest fires in Spain using AVHRR NDVI composite image data. *Remote Sensing of the Environment,* 60**,** 153-162.

Finlayson, C., Storrs, M., & Lindner, G., 1997. Degradation and rehabilitation of wetlands in the Alligator Rivers Region of northern Australia. *Wetlands Ecology and Management,* 5**,** 19-36.

Firth, C., Stewart, I., Mcguire, W., Kershaw, S., & Vita-Finzi, C., 1996. Coastal elevation changes in eastern Sicily: implications for volcano instability at Mount Etna. *Geological Society, London, Special Publications,* 110**,** 153-167.

Fischlin, A., Midgley, G. F., Price, J. T., Leemans, R., Gopal, B., Turley, C., Rounsevell, M. D. A., Dube, O. P., Tarazona, J., & Velichko, A. A., 2007: Ecosystems, their properties, goods, and services. *Climate Change 2007: Impacts, Adaptation and Vulnerability. Contribution of Working Group II to the Fourth Assessment Report of the Intergovernmental Panel on Climate Change*, Parry, M. L., Canziani, O. F., Palutikof, J. P., van der Linden, P. J., & Hanson, C. E., Eds., Cambridge University Press, Cambridge, 211-272.

Franke, J., Keuck, V., & Siegert, F., 2012. Assessment of grassland use intensity by remote sensing to support conservation schemes. *Journal for Nature Conservation,* 20**,** 125-134.

Frey, P., 2014. Particle velocity and concentration profiles in bedload experiments on a steep slope. *Earth Surface Processes and Landforms*, 39, 646-655.

Fuller, D., 1998. Trends in NDVI time series and their relation to rangeland and crop production in Senegal, 1987-1993. *International Journal of Remote Sensing,* 19**,** 2013-2018.

Fuqua, M. A., Huo, S., & Ulven, C. A., 2012. Natural fiber reinforced composites. *Polymer Reviews,* 52**,** 259-320.

Gabler, C. A., Osland, M. J., Grace, J. B., Stagg, C. L., Day, R. H., Hartley, S. B., Enwright, N. M., From, A. S., Mccoy, M. L., & Mcleod, J. L., 2017. Macroclimatic change expected to transform coastal wetland ecosystems this century. *Nature Climate Change,* 7**,** 142-147.

Ganju, N. K., & Schoellhamer, D. H., 2010. Decadal-timescale estuarine geomorphic change under future scenarios of climate and sediment supply. *Estuaries and Coasts,* 33**,** 15-29.

Gedan, K. B., Kirwan, M. L., Wolanski, E., Barbier, E. B., & Silliman, B. R., 2011. The present and future role of coastal wetland vegetation in protecting shorelines: answering recent challenges to the paradigm. *Climatic Change,* 106**,** 7-29.

Geological Survey of New South Wales, 1975. Jervis bay and Currarong 1:50 000 geology map. Geological Survey of New South Wales, Sydney.

Geoscience Australia, 2017. *Applying geoscience to Australia's most important challenges "Australia's Coasts and Estuaries"* [Online]. Canberra: Australian Government. Available: http://www.ga.gov.au/scientific-topics/marine/coasts-estuaries.

Gillin, C. P., Bailey, S. W., Mcguire, K. J., & Prisleyt, S. P., 2015. Evaluation of LiDAR-derived DEMs through terrain analysis and field comparison. *Photogrammetric Engineering & Remote Sensing,* 81**,** 387-396.

Giri, C., Ochieng, E., Tieszen, L. L., Zhu, Z., Singh, A., Loveland, T., Masek, J., & Duke, N., 2011. Status and distribution of mangrove forests of the world using earth observation satellite data. *Global Ecology and Biogeography*, 20, 154-159.

Gleick, P. H., 2003. Global freshwater resources: soft-path solutions for the 21st century. *Science*, 302, 1524-1528.

Goetz, S. J., Bunn, A. G., Fiske, G. J., & Houghton, R., 2005. Satellite-observed photosynthetic trends across boreal North America associated with climate and fire disturbance. *Proceedings of the National Academy of Sciences of the United States of America,* 102**,** 13521-13525.

Goodbred, S. L., 2003. Response of the Ganges dispersal system to climate change: a source-to-sink view since the last interstade. *Sedimentary Geology*, 162, 83-104.

Goward, S. N., & Prince, S. D., 1995. Transient effects of climate on vegetation dynamics: satellite observations. *Journal of Biogeography***,** 549-564.

Growns, I., Reinfelds, I., Williams, S., & Coade, G., 2009. Longitudinal effects of a water supply reservoir (Tallowa Dam) on downstream water quality, substrate and riffle macroinvertebrate assemblages in the Shoalhaven River, Australia. *Marine and Freshwater Research*, 60, 594-606.

Haack, B. 1996. Monitoring wetland changes with remote sensing: an East African example. *Environmental Management*, 20(3), 411-419.

Hadadin, N., Qaqish, M., Akawwi, E., & Bdour, A., 2010. Water shortage in Jordan – sustainable solutions. *Desalination*, 250, 197-202.

Håkanson, L., Gyllenhammar, A. & Brolin, A. 2004. A dynamic compartment model to predict sedimentation and suspended particulate matter in coastal areas. *Ecological Modelling*, 175, 353-384.

Hamylton, S. M., 2017. *Spatial Analysis of Coastal Environments*. Cambridge University Press, Cambridge.

Hamylton, S. M., Carvalho, R. C., Duce, S., Roelfsema, C. M., & Vila-Concejo, A., 2016. Linking pattern to process in reef sediment dynamics at Lady Musgrave Island, southern Great Barrier Reef. *Sedimentology,* 63**,** 1634-1650.

Haq, M., Akhtar, M., Muhammad, S., Paras, S., & Rahmatullah, J., 2012. Techniques of remote sensing and GIS for flood monitoring and damage assessment: a case study of Sindh province, Pakistan. *Egyptian Journal of Remote Sensing and Space Science*, 15, 135-141.

Harji, R. R., Yvenat, A., & Bhosle, N. B., 2008. Sources of hydrocarbons in sediments of the Mandovi estuary and the Marmugoa harbour, west coast of India. *Environment International*, 34, 959-965.

Haslam, S. M., 2004. *Understanding wetlands: fen, bog and marsh*, Taylor and Francis e-Library, USA. ISBN 0-415-25794-8.

Haslett, S. K., Davies, P. & Curr, R. H. 2000. Geomorphologic and palaeoenvironmental development of Holocene perched coastal dune systems in Brittany, France. *Geografiska Annaler: Series A, Physical Geography,* 82**,** 79-88.

Haslett, S., 2008. *Coastal Systems*, second edition. Routledge, London.

HEC (Hydrologic Engineering Center), 2017. HEC-RAS v5.0.3. In: Http://Www.Hec.Usace.Army.Mil/Software/Hec-Ras/ (ed.).

Hegarat-Mascle, S. L., Bloch, I. & Vidal-Madjar, D. 1997. Application of Dempster-Shafer evidence theory to unsupervised classification in multisource remote sensing. *IEEE Transactions on Geoscience and Remote Sensing*, 35, 1018-1031.

Henley, B. J., Gergis, J., Karoly, D. J., Power, S., Kennedy, J., & Folland, C. K., 2015. A tripole index for the interdecadal Pacific oscillation. *Climate Dynamics,* 45**,** 3077-3090.

Herben, R., Khoury, M., Rolfe, D., Wilkie, S., Wynn, K., & Collins, R., 2012. Interpreting Estuary Health Data, EstuaryWatch Victoria: Corangamite Catchment Management Authority, Melbourne.

Hofmeister, E., Rogall, G. M., Wesenberg, K., Abbott, R., Work, T., Schuler, K., Sleeman, J., & Winton, J., 2010. Climate change and wildlife health: direct and indirect effects. USA: USGS- Geological Survey.

Hopley, C. A., & Jones, B. G., 2006. Holocene stratigraphic and morphological evolution of the Wandandian Creek delta, St Georges Basin, New South Wales. *Australian Journal of Earth Sciences,* 53**,** 991-1000.

Hopley, C. A., & Jones, B. G., 2018. The Holocene and future evolution of Macquarie Rivulet delta, Lake Illawarra, Australia. *Australian Journal of Earth Sciences* (in submission).

Hopley, C. A., 2004. *The Holocene and beyond: Evolution of Wandandian Creek delta, St Georges Basin, New South Wales.* B Sc (Hons) thesis, University of Wollongong, Wollongong.

Hopley, C. A., 2013. *Autocyclic, allocyclic and anthropogenic impacts on Holocene delta evolution and future management implications: Macquarie Rivulet and Mullet/Hooka Creek, Lake Illawarra, New South Wales.* PhD thesis, University of Wollongong, Wollongong.

Hopley, C. A., Jones, B. G., & Puotinen, M., 2007. Assessing the recent (1834–2002) morphological evolution of a rapidly prograding delta within a GIS framework: Macquarie Rivulet delta, Lake Illawarra, New South Wales. *Australian Journal of Earth Sciences,* 54**,** 1047-1056.

Hoque, M. E., Chowdhury, S. R., Uddin, M. M., Alam, M. S., & Monwar, M. M., 2013. Grain size analysis of a growing sand bar at Sonadia Island, Bangladesh. *Open Journal of Soil Science*, Vol.03 No.02, 10.

Horn, B. K., & Woodham, R. J., 1979. Destriping Landsat MSS images by histogram modification. *Computer Graphics and Image Processing,* 10**,** 69-83.

Hosier, P. E., & Cleary, W. J., 1977. Cyclic geomorphic patterns of washover on a barrier island in southeastern North Carolina. *Environmental Geology,* 2**,** 23-31.

Hu, L., Guo, Z., Feng, J., Yang, Z., & Fang, M., 2009. Distributions and sources of bulk organic matter and aliphatic hydrocarbons in surface sediments of the Bohai Sea, China. *Marine Chemistry*, 113, 197-211.

Hudson, J. P., 1991. *Late Quaternary Evolution of Twofold Bay, Southern New South Wales.* Unpublished MSc. Thesis, University of Sydney.

Huete, A. R., 1988. A soil-adjusted vegetation index (SAVI). *Remote sensing of environment,* 25**,** 295-309.

Huete, A., Didan, K., Miura, T., Rodriguez, E. P., Gao, X., & Ferreira, L. G., 2002. Overview of the radiometric and biophysical performance of the MODIS vegetation indices. *Remote Sensing of the Environment,* 83**,** 195-213.

Hughes, L., 2003. Climate change and Australia: trends, projections and impacts. *Austral Ecology,* 28**,** 423-443.

Hughes, M. L., McDowell, P. F., & Marcus, W. A., 2006. Accuracy assessment of georectified aerial photographs: implications for measuring lateral channel movement in a GIS. *Geomorphology*, 74, 1-16.

Ian, H., 2013. *Coast: A History of the New South Wales Edge*, University of New South Wales Press, Sydney.

IPCC, 2013. Summary for policymakers in climate change 2013: the physical science basis, contribution of working group I to the fifth assessment report of the intergovernmental panel on climate change, Stocker, T.F., Qin, D., Plattner, G. K., Tignor, M., Allen, S. K., and Boschung, J. (Eds). Cambridge University Press, Cambridge,.

IPCC, 2014. Climate Change 2014: Synthesis Report. Contribution of Working Groups I, II and III to the Fifth Assessment Report of the Intergovernmental Panel on Climate Change [Core Writing Team, R.K. Pachauri and L.A. Meyer (eds.)]. IPCC, Geneva, Switzerland, 1-151.

Jeong, S. G., Mo, Y., Kim, H. G., Park, C. H., & Lee, D. K., 2016. Mapping riparian habitat using a combination ofremote-sensing techniques. *International Journal of Remote Sensing,* 37**,** 1069-1088.

Jones, B. G., Killian, H. E., Chenhall, B. E., and Sloss, C. R., 2003a. Anthropogenic effects in a coastal lagoon: geochemical characterisation of Burrill Lake, NSW, Australia. *Journal of Coastal Research* 19, 621-632.

Jones, B. G., Martin, G. R., and Senapati, N., 1993. Riverine-tidal interactions in the monsoonal Gilbert River fandelta, northern Australia. *Sedimentary Geology,* 83, 319-337.

Jones, B. G., Woodroffe, C. D., & Martin, G. R., 2003b. Deltas in the Gulf of Carpentaria, Australia: forms, processes and products. *SEPM Society for Sedimentary Geology Special Publication*, 76, 21-43.

Jones, H., & Byrne, M., 2014, Changes in the distributions of freshwater mussels (Unionoida: Hyriidae) in coastal south-eastern Australia and implications for their conservation status. *Aquatic Conservation,* 24, 203.

Jones, P. D., New, M., Parker, D. E., Martin, S., & Rigor, I. G., 1999. Surface air temperature and its changes over the past 150 years. *Reviews of Geophysics,* 37**,** 173-199.

Julien, P. Y., 1998*. Erosion and Sedimentation.* Cambridge University Press: Cambridge*;* 280 pp.

Kamwi, J. M., Kaetsch, C., Graz, F. P., Chirwa, P., & Manda, S., 2017. Trends in land use and land cover change in the protected and communal areas of the Zambezi Region, Namibia. *Environmental Monitoring and Assessment,* 189**,** 242.

Kassakian, J., Jones, A., Martinich, J., & Hudgens, D., 2017. Managing for no net loss of ecological services: an approach for quantifying loss of coastal wetlands due to sea level rise. *Environmental Management,* 59**,** 736-751.

Keddy, P. A., 2010. *Wetland ecology: principles and conservation*, Cambridge University Press, New York, USA. ISBN 978-0-521-51940-3.

Kelleway, J. J., Cavanaugh, K., Rogers, K., Feller, I., Ens, E., Doughty, C., Saintilan, N.,2017. Review of the ecosystem service implications of mangrove encroachment into salt marshes. *Global Change Biology*. DOI: 10.1111/gcb.13727, 1-18.

Kench, P. S., 1999. Geomorphology of Australian estuaries: review and prospect. *Australian Journal of Ecology,* 24**,** 367-380.

Kench, P. S., Chan, J., Owen, S., & Mclean, R., 2014. The geomorphology, development and temporal dynamics of Tepuka Island, Funafuti atoll, Tuvalu. *Geomorphology,* 222**,** 46-58.

Kennish, M. J., 2002. Environmental threats and environmental future of estuaries. *Environmental Conservation,* 29**,** 78-107.

Kerr, J. T., & Ostrovsky, M., 2003. From space to species: ecological applications for remote sensing. *Trends in Ecology & Evolution,* 18**,** 299-305.

Kingsford, R. T., 1990. The effects of human activities on shorebirds, seabirds and waterbirds of Comerong Island, at the mouth of the Shoalhaven River. *Wetlands (Australia),* 9**,** 7-12.

Kingsford, R. T., 2000. Ecological impacts of dams, water diversions and river management on floodplain wetlands in Australia. *Austral Ecology*, 25, 109-127.

Kirkpatrick, S., 2012. The Economic Value of Natural and Built Coastal Assets: Part 2: Built Coastal Assets. *Australian Climate Change Adaptation Research Network for Settlements and Infrastructure. National Climate Change Adaptation Research Facility*.

KNMI, 2017. *Climate Explorer: Select a monthly time series* [Online]. Available: https://climexp.knmi.nl/selectstation.cgi?id=someone@somewhere.

Koltun, G., Landers, M., Nolan, K., & Parker, R., 1997. Sediment transport and geomorphology issues in the water resources division. Proceedings of the US Geological Survey (USGS) sediment workshop, WV. USA.

Krumbein, W., & Pettijohn, F., 1938. *Manual of Sedimentary Petrography*. Appleton-Century Co, New York, 549 pp.

Kumar, S. 2011. *Land use land cover change and atmospheric feedback: Impact on regional water resources.* Doctor of Philosophy, Purdue University.

Le Hegarat-Mascle, S., Bloch, I., & Vidal-Madjar, D., 1997. Application of Dempster-Shafer evidence theory to unsupervised classification in multisource remote sensing. *IEEE transactions on geoscience and remote sensing,* 35**,** 1018-1031.

Lee, S. Y., Dunn, R. J. K., Young, R. A., Connolly, R. M., Dale, P., Dehayr, R., Lemckert, C. J., Mckinnon, S., Powell, B., & Teasdale, P., 2006. Impact of urbanization on coastal wetland structure and function. *Austral Ecology,* 31**,** 149-163.

Li, G., Yin, H., & Kuret, J., 2004. Casein kinase 1 delta phosphorylates tau and disrupts its binding to microtubules. *Journal of Biological Chemistry*, 279, 15938-15945.

Li, J., & Heap, A. D., 2008. A review of spatial interpolation methods for environmental scientists. *In:* Geoscience Australia (ed.) *Record: 2008/23-GeoCat # 68229.* Canberra, Australia.

Li, Q., Unger, A., Sudicky, E., Kassenaar, D., Wexler, E., & Shikaze, S., 2008. Simulating the multi-seasonal response of a large-scale watershed with a 3D physically-based hydrologic model. *Journal of Hydrology*, 357, 317-336.

Ligon, F. K., Dietrich, W. E., & Trush, W. J., 1995. Downstream ecological effects of dams. *BioScience*, 45, 183-192.

Lim, K. J., Sagong, M., Engel, B. A., Tang, Z., Choi, J., & Kim, K. S., 2005. GIS-based sediment ass**s**essment tool. *Catena*, 64, 61-80.

Liu, Z., 2012. Dynamics of interdecadal climate variability: a historical perspective. *Journal of Climate*, 25, 1963-1995.

Lovelock, C. E., Bennion, V., Grinham, A., & Cahoon, D. R., 2011. The role of surface and subsurface processes in keeping pace with sea level rise in intertidal wetlands of Moreton Bay, Queensland, Australia. *Ecosystems,* 14**,** 745-757.

LP-DAAC (Land Processes-Distributed Active Archive Centre), 2017. *DEMs data sets, NASA Land Data Products and Services*; USGS [Online]. Available: https://lpdaac.usgs.gov/.

LPI (Land and Property Information), 1998. *Historical Data*. NSW Government, Sydney, Australia.

LPI (Land and Property Information), 2004 & 2010. LiDAR data, Geosciences, Australia.

LPI (Land and Property Information), 2017. Available: mapping and imagery, web services access, LPI services, Australia.

Lu, L., Kuenzer, C., Wang, C., Guo, H., & Li, Q., 2015. Evaluation of three MODIS-derived vegetation index time series for dryland vegetation dynamics monitoring. *Remote Sensing,* 7**,** 7597-7614.

Lynch, H. J., Campbell Grant, E. H., Muneepeerakul, R., Arunachalam, M., Rodriguez-Iturbe, I., & Fagan, W. F., 2011. How restructuring river connectivity changes freshwater fish biodiversity and biogeography. *Water Resources Research*, 47, W05531, DOI: 10.1029/2010WR010330.

Magilligan, F. J., Nislow, K. H., & Graber, B. E., 2003. Scale-independent assessment of discharge reduction and riparian disconnectivity following flow regulation by dams. *Geology*, 31, 569-572.

Malczewski, J., 2004. GIS-based land-use suitability analysis: a critical overview. *Progress in Planning,* 62**,** 3-65.

March, J. G., Benstead, J. P., Pringle, C. M., & Scatena, F. N., 2003. Damming tropical island streams: problems, solutions, and alternatives. *BioScience*, 53, 1069-1078.

Maselli, F., Romanelli, S., Bottai, L., & Zipoli, G., 2003. Use of NOAA-AVHRR NDVI images for the estimation of dynamic fire risk in Mediterranean areas. *Remote Sensing of Environment,* 86**,** 187-197.

Matheussen, B., Kirschbaum, R. L., Goodman, I. A., O'donnell, G. M., & Lettenmaier, D. P., 2000. Effects of land cover change on streamflow in the interior Columbia River Basin (USA and Canada). *Hydrological Processes,* 14**,** 867-885.

Matthews, G. V. T., 1993. *The Ramsar Convention on Wetlands: its history and development,* Switzerland, Ramsar convention bureau, 1-87.

McIvor, A. L., Spencer, T., Möller, I., & Spalding. M., 2013. The response of mangrove soil surface elevation to sea level rise. Natural Coastal Protection Series: Report 3. Cambridge Coastal Research Unit Working-Paper 42. *The Nature Conservancy and Wetlands International*. ISSN 2050-7941. 1-59.

Meng, W., & Liu, L., 2010. On approaches of estuarine ecosystems health studies. *Estuarine, Coastal and Shelf Science,* 86**,** 313-316.

Meyer-Peter, E., & Müller, R., 1948. Formulas for bed-load transport. IAHR (report). Zweite tagung – Second Meeting – Decxieme Reunion Stockholm 7-9, VI, 39-64.

Meynecke, J.-O., Lee, S. Y., & Duke, N., 2008. Linking spatial metrics and fish catch reveals the importance of coastal wetland connectivity to inshore fisheries in Queensland, Australia. *Biological Conservation,* 141**,** 981-996.

Meyssignac, B., & Cazenave, A., 2012. Sea level: a review of present-day and recent-past changes and variability. *Journal of Geodynamics,* 58**,** 96-109.

Michener, W. K., Blood, E. R., Bildstein, K. L., Brinson, M. M., & Gardner, L. R., 1997. Climate change, hurricanes and tropical storms, and rising sea level in coastal wetlands. *Ecological Applications,* 7**,** 770-801.

Miller, B. P., Sinclair, E. A., Menz, M. H., Elliott, C. P., Bunn, E., Commander, L. E., Dalziell, E., David, E., Davis, B., & Erickson, T. E., 2016. A framework for the practical science necessary to restore sustainable, resilient, and biodiverse ecosystems. *Restoration Ecology*, 25 (4), 605-617.

Mitsch, W., & Gosselink, J., 1993. *Wetlands (2nd edition)*, Van Nostrand Reinhold , New York.

Mkpenie, V. N., Ebong, G., & Abasiekong, B., 2007. Studies on the effect of temperature on the sedimentation of insoluble metal carbonates. *Journal of Applied Sciences and Environmental Management*, 11, 67-69.

Mohamed, E., Schütt, B., & Belal, A., 2013. Assessment of environmental hazards in the north western coast-Egypt using RS and GIS. *Egyptian Journal of Remote Sensing and Space Science*, 16, 219-229.

Morris, J. T., Sundareshwar, P., Nietch, C. T., Kjerfve, B., & Cahoon, D., 2002. Responses of coastal wetlands to rising sea level. *Ecology*, 83, 2869-2877.

Murray, C. G., Kasel, S., Loyn, R. H., Hepworth, G., & Hamilton, A. J., 2013. Waterbird use of artificial wetlands in an Australian urban landscape. *Hydrobiologia,* 716 (1)**,** 131-146.

Murray, E. J., Haese, R., Smith, C., & Heggie, D., 2005. Nutrient cycling in St Georges Basin, south coast NSW: report on field survey November 2003. Geoscience Australia, Record 2005/22, Canberra.

Murray-Wallace, C. V., & Woodroffe, C. D., 2014. *Quaternary Sea-Level Changes: a Global Perspective*, Cambridge University Press, Cambridge.

Myneni, R. B., Hall, F. G., Sellers, P. J., & Marshak, A. L., 1995. The interpretation of spectral vegetation indexes. *IEEE Transactions on Geoscience and Remote Sensing,* 33**,** 481-486.

Nanson, G. & Croke, J. 1992. A genetic classification of floodplains. *Geomorphology,* 4**,** 459-486.

Nanson, G. C. 1986. Episodes of vertical accretion and catastrophic stripping: a model of disequilibrium flood-plain development. *Geological Society of America Bulletin,* 97**,** 1467-1475.

Nemani, R. R., Keeling, C. D., Hashimoto, H., Jolly, W. M., Piper, S. C., Tucker, C. J., Myneni, R. B., & Running, S. W., 2003. Climate-driven increases in global terrestrial net primary production from 1982 to 1999. *Science,* 300**,** 1560-1563.

Neumann, B., Vafeidis, A. T., Zimmermann, J., & Nicholls, R. J., 2015. Future coastal population growth and exposure to sea-level rise and coastal flooding-a global assessment. *PloS one,* 10**,** e0118571.

Newton, P., Flood, J., Berry, M., Bhatia, K., Brown, S., Cabelli, A., Gomboso, J., Higgins, J., Richardson, T. & Ritchie, V. 1998. Environmental indicators for national state of the environment reporting: Human settlements, Australia: State of the Environment (Environmental Indicator Reports), Department of the Environment, Canberra.

Nguyen, T. T., Bonetti, J., Rogers, K., & Woodroffe, C. D., 2016. Indicator-based assessment of climate-change impacts on coasts: a review of concepts, methodological approaches and vulnerability indices. *Ocean & Coastal Management*, 123, 18-43.

Nguy-Robertson, A. L., & Gitelson, A. A., 2015. Algorithms for estimating green leaf area index in C3 and C4 crops for MODIS, Landsat TM/ETM+, MERIS, Sentinel MSI/OLCI, and Venμs sensors. *Remote Sensing Letters,* 6**,** 360-369.

Nicholls, R. J., 2004. Coastal flooding and wetland loss in the 21st century: changes under the SRES climate and socio-economic scenarios. *Global Environmental Change,* 14**,** 69-86.

Nicholls, R. J., Hoozemans, F. M., & Marchand, M., 1999. Increasing flood risk and wetland losses due to global sea-level rise: regional and global analyses. *Global Environmental Change,* 9**,** S69-S87.

Nielsen, D. L., & Brock, M. A., 2009. Modified water regime and salinity as a consequence of climate change: prospects for wetlands of Southern Australia. *Climatic Change,* 95**,** 523-533.

Ning, T., Liu, W., Lin, W., & Song, X., 2015. NDVI variation and its responses to climate change on the northern Loess Plateau of China from 1998 to 2012. *Advances in Meteorology,* 2015.

Norrish, K., & Chappell, B., 1977. X-ray fluorescence spectrometry. In *Physical Methods in Determinative Mineralogy*, Zussman, J. (ed.), Academic Press, London, pp. 201- 272.

North Central Catchment C.M.A., 1998. The role of wetlands. Department of catchment management authority, Victoria.

Notaro, M., Vavrus, S., & Liu, Z., 2007. Global Vegetation and Climate Change due to Future Increases in CO2 as Projected by a Fully Coupled Model with Dynamic Vegetation*. *Journal of Climate,* 20**,** 70-90.

Nott, J. F., & Price, D. M., 1991. Late Pleistocene to early Holocene aeolian activity in the upper and middle Shoalhaven catchment, New South Wales. *The Australian Geographer,* 22**,** 168-177.

Nott, J., Price, D., & Nanson, G., 2002. Stream response to Quaternary climate change: evidence from the Shoalhaven River catchment, southeastern highlands, temperate Australia. *Quaternary Science Reviews,* 21**,** 965-974.

NPWS, 1998. Seven Mile Beach National Park and Comerong Island Nature Reserve, plan of management. National Parks and Wildlife Service, Sydney

OEH, 2013. Assessing estuary ecosystem health: Sampling, data analysis and reporting protocols: NSW Natural Resources Monitoring, Evaluation and Reporting Program: State of NSW. Office of Environment and Heritage, NSW, Sydney.

Oliver, T. S. N., Rogers, K., Chafer, C. J., & Woodroffe, C. D., 2012. Measuring, mapping and modelling: an integrated approach to the management of mangrove and saltmarsh in the Minnamurra River estuary, southeast Australia. *Wetlands Ecology and Management,* 20**,** 353-371.

Oliver, T. S., Donaldson, P., Sharples, C., Roach, M., & Woodroffe, C. D., 2017b. Punctuated progradation of the Seven Mile Beach Holocene barrier system, southeastern Tasmania. *Marine Geology,* 386**,** 76-87.

Oliver, T., Tamura, T., Hudson, J., & Woodroffe, C. D., 2017a. Integrating millennial and interdecadal shoreline changes: Morpho-sedimentary investigation of two prograded barriers in southeastern Australia. *Geomorphology*, 288, 129-147.

Omran, E.-S. E., 2016. A stochastic simulation model to early predict susceptible areas to water table level fluctuations in North Sinai, Egypt. *Egyptian Journal of Remote Sensing and Space Science*, 19, 235-257.

OWA (OceanWatch Australia), 2010. The Shoalhaven River Catchment-CS1. Sydney, Australia: OceanWatch Australia. http://www.oceanwatch.org.au/wp-content/uploads/2010/02/CS1-Shoalhaven-Catchement.pdf.

Ozesmi, S. L. & Bauer, M. E. 2002. Satellite remote sensing of wetlands. *Wetlands Ecology and Management,* 10**,** 381-402.Pachauri, R. K., Allen, M., Barros, V., Broome, J., Cramer, W., Christ, R., Church, J., Clarke, L., Dahe, Q., & Dasgupta, P., 2014. Climate Change 2014: Synthesis Report. Contribution of Working Groups I, II and III to the Fifth Assessment Report of the Intergovernmental Panel on Climate Change, Geneva, Switzerland.

PACHAURI, R. K., ALLEN, M., BARROS, V., BROOME, J., CRAMER, W., CHRIST, R., CHURCH, J., CLARKE, L., DAHE, Q. & DASGUPTA, P. 2014. Climate Change 2014: Synthesis Report. Contribution of Working Groups I, II and III to the Fifth Assessment Report of the Intergovernmental Panel on Climate Change. Geneva, Switzerland.

Parcher, J., 2012. Landsat History And Legacy. Presented at the UNCOPUOS Special Panel for the 40th Anniversary of Landsat: International Coordination Land Remote Sensing Program United States Geological Survey.

Parker, G., 2007. Transport of gravel and sediment mixtures. *In* Garcia, M. H. (ed). *Sedimentation Engineering: Processes, Measurements, Modeling and Practice, Manual 110*, Sedimentation

Committee of the Environmental and Water Resources Institute, American Society of Civil Engineers: Reston, VA, 165-251.

Parmesan, C., & Yohe, G., 2003. A globally coherent fingerprint of climate change impacts across natural systems. *Nature,* 421**,** 37-42.

Patel, A., Katiyar, S., & Prasad, V., 2016. Performances evaluation of different open source DEM using Differential Global Positioning System (DGPS). *Egyptian Journal of Remote Sensing and Space Science*, 19, 7-16.

Pendleton, L. H., 2010. *The economic and market value of coasts and estuaries: what's at stake?* Restore America's Estuaries, Arlington, USA,1-175.

Pendón, J. G., Morales, J. A., Borrego, J., Jimenez, I., & Lopez, M., 1998. Evolution of estuarine facies in a tidal channel environment, SW Spain: evidence for a change from tide- to wave-domination. *Marine Geology*, 147, 43-62.

Peng, Y., Nguy-Robertson, A., Arkebauer, T., & Gitelson, A. A., 2017. Assessment of canopy chlorophyll content retrieval in maize and soybean: Implications of hysteresis on the development of generic algorithms. *Remote Sensing,* 9**,** 226.

Penland, S., Connor, P. F., Beall, A., Fearnley, S., & Williams, S. J., 2005. Changes in Louisiana's Shoreline: 1855–2002. *Journal of Coastal Research*, 21, 7-39.

Perillo, G. M. E., Wolanski, E., Choon, D. R., & Brinson, M. M., 2009. *Coastal wetlands: an integrated ecosystem approach.* Elsevier, Burlington, Vt.

Pettorelli, N., Vik, J. O., Mysterud, A., Gaillard, J.-M., Tucker, C. J., & Stenseth, N. C., 2005. Using the satellite-derived NDVI to assess ecological responses to environmental change. *Trends in Ecology & Evolution,* 20**,** 503-510.

Petts, G. E., & Gurnell, A. M., 2005. Dams and geomorphology: research progress and future directions. *Geomorphology*, 71, 27-47.

Phillips, J. D., 2017. Coastal wetlands, sea level, and the dimensions of geomorphic resilience. *Geomorphology,* (article in press), http://dx.doi.org/10.1016/j.geomorph.2017.03.022, 1-12.

Pijanowski, B. C., Brown, D. G., Shellito, B. A., & Manik, G. A., 2002. Using neural networks and GIS to forecast land use changes: a land transformation model. *Computers, Environment and Urban Systems,* 26**,** 553-575.

Pittock, A. B., 2003. *Climate change: an Australian guide to the science and potential impacts*, Australian Greenhouse Office Canberra.

Postel, S. L., Daily, G. C., & Ehrlich, P. R., 1996. Human appropriation of renewable fresh water. *Science-AAAS-Weekly Paper Edition*, 271, 785-787.

Postgate, N., 1992. Early Mesopotamia: Society and Economy at the Dawn of History (Book Review), *London, Oxford University Press*, 1-198.

Preston, C., & Schmidt, M., 2006. Black (pyrogenic) carbon in boreal forests: a synthesis of current knowledge and uncertainties. *Biogeosciences Discussions,* 3**,** 211-271.

Priestas, A. M., & Fagherazzi, S., 2010. Morphological barrier island changes and recovery of dunes after Hurricane Dennis, St George Island, Florida. *Geomorphology,* 114**,** 614-626.

Qi, J., Chehbouni, A., Huete, A., Kerr, Y., & Sorooshian, S., 1994. A modified soil adjusted vegetation index. *Remote sensing of environment,* 48**,** 119-126.

Raynolds, M., Magnússon, B., Metúsalemsson, S., & Magnússon, S. H., 2015. Warming, sheep and volcanoes: land cover changes in Iceland evident in satellite NDVI trends. *Remote Sensing,* 7**,** 9492-9506.

Rebelo, L.-M., Finlayson, C. M., & Nagabhatla, N., 2009. Remote sensing and GIS for wetland inventory, mapping and change analysis. *Journal of Environmental Management,* 90**,** 2144-2153.

Recking, A., Frey, P., Paquier, A., Belleudy, P., & Champagne, J.-Y., 2008. Bed-load transport flume experiments on steep slopes. *Journal of Hydraulic Engineering*, 134, 1302-1310.

Reeves, A., & Chudek, J., 1998. Application of nuclear magnetic resonance imaging (MRI) to migration studies of oil-related residues in estuarine sediments (Tay Estuary). *Water Science and Technology*, 38, 187-192.

Richter, B. D., Mathews, R., Harrison, D. L., & Wigington, R., (2003). Ecologically sustainable water management: managing river flows for ecological integrity. *Ecological Applications*, 13, 206-224.

Rogers, K., Lymburner, L., Salum, R., Brooke, B. P., & Woodroffe, C. D., 2017. Mapping of mangrove extent and zonation using high and low tide composites of Landsat data. *Hydrobiologia*, DOI 10.1007/s10750-017-3257-5, 1-20.

Rogers, K., Wilton, K. M., & Saintilan, N., 2006. Vegetation change and surface elevation dynamics in estuarine wetlands of southeast Australia. *Estuarine, Coastal and Shelf Science,* 66**,** 559-569.

Rohling, E. J., & Palike, H., 2005. Centennial-scale climate cooling with a sudden cold event around 8,200 years ago. *Nature*, 434, 975.

Rood, S. B., & Mahoney, J. M., 1993. River damming and riparian cottonwoods: management opportunities and problems. *General Technical Report RM* (USA).

Roper, T., Creese, B., Scanes, P., Stephens, K., Williams, R., Dela-Cruz, J., Coade, G., Coates, B., & Fraser, M., 2011. Assessing the condition of estuaries and coastal lake ecosystems in NSW, monitoring, evaluation and reporting program, Technical report series, Office of Environment and Heritage, Sydney.

Rose, H., Matt, K., Doug, R., Simone, W., Kate, W., & Rhys, C., 2012. Interpreting Estuary Health Data. EstuaryWatch Victoria -Turbidity: Corangamite Catchment Management Authority, Australia.

Roshier, D. A. & Rumbachs, R. M. 2004. Broad-scale mapping of temporary wetlands in arid Australia. *Journal of Arid Environments,* 56**,** 249-263.

Roy, P. S., & Cowell, P. J., 1994. Wave-dominated coasts. In: Carter, R.W.G., and Woodroffe, C. D., (eds). *Coastal Evolution: Late Quaternary Shoreline Morphodynamics*. Cambridge University Press, Cambridge.

Roy, P., & Crawford, E., 1977. Significance of sediment distribution in major coastal rivers, northern NSW. Third Australian Conference on Coastal and Ocean Engineering, 1977: The Coast, the Ocean and Man. Institution of Engineers, Australia, 173-180.

Roy, P., Williams, R., Jones, A., Yassini, I., Gibbs, P., Coates, B., West, R., Scanes, P., Hudson, J., & Nichol, S., 2001. Structure and function of south-east Australian estuaries. *Estuarine, Coastal and Shelf Science,* 53**,** 351-384.

Saeijs, H., & Van Berkel, M., 1995. Global water crisis: the major issue of the 21st century a growing and explosive problem. *European Water Pollution Control*, 5, 26-40.

Saintilan, N., & Imgraben, S., 2012. Principles for the monitoring and evaluation of wetland extent, condition and function in Australia. *Environmental Monitoring and Assessment*, 184, 595-606.

Saintilan, N., & Williams, R., 2010. Short note: the decline of saltmarsh in southeast Australia: results of recent surveys. *Wetlands (Australia),* 18**,** 49-54.

SCA, 2015. Tallowa Dam The Centrepiece of the Shoalhaven System (Facts and History) Sydney, Australia: Sydney Catchment Authority. http://www.sca.nsw.gov.au/water/visit/tallowa-dam.

SCA, 2016. Tallowa Dam - Facts & History [Online]. Sydney Catchment Authority Available at: http://www.sca.nsw.gov.au/water/visit/tallowa-dam.

Scavia, D., Field, J. C., Boesch, D. F., Buddemeier, R. W., Burkett, V., Cayan, D. R., Fogarty, M., Harwell, M. A., Howarth, R. W., & Mason, C., 2002. Climate change impacts on US coastal and marine ecosystems. *Estuaries,* 25**,** 149-164.

Semeniuk, C., & Semeniuk, V., 2013. The response of basin wetlands to climate changes: a review of case studies from the Swan Coastal Plain, south-western Australia. *Hydrobiologia,* 708**,** 45-67.

Shahbaz, K.; Mohsin, H.; Akhtar, A., & Aftab, A., 2009. Spatial assessment of water use in an environmentally sensitive wetland. *AMBIO*, 38, 157-165.

Shoalhaven City Council. 1998. *St Georges Basin Estuary Management Plan,* Shoalhaven City Council, Nowra.

Short, A., & Hesp, P., 1982. Wave, beach and dune interactions in southeastern Australia. *Marine Geology,* 48**,** 259-284.

Siddall, M., Rohling, E. J., Almogi-Labin, A., Hemleben, C., Meischner, D., Schmelzer, I., & Smeed, D., 2003. Sea-level fluctuations during the last glacial cycle. *Nature,* 423**,** 853-858.

Singh, K., Suman, A., Singh, P., & Srivastava, T., 2007. Improving quality of sugarcane-growing soils by organic amendments under subtropical climatic conditions of India. *Biology and Fertility of Soils*, 44, 367-376.

Skilbeck, C. G., Heap, A. D., & Woodroffe, C. D., 2017. Geology and sedimentary history of modern estuaries. *In:* Weckström, K., Saunders, K. M., Gell, P. A., & Skilbeck, C. G., (eds.) *Applications of Paleoenvironmental Techniques in Estuarine Studies.* Dordrecht: Springer Netherlands,. 45-74.

Sloss, C. R., Jones, B. G., McClennen, C. E., De Carli, J., & Price, D. M., 2006b. The geomorphological evolution of a wave-dominated barrier estuary: Burrill Lake, New South Wales, Australia. *Sedimentary Geology,* 187**,** 229-249.

Sloss, C. R., Jones, B. G., Switzer, A. D., Nichol, S., Clement, A. J. H., & Nicholas, A. W., 2010. The Holocene infill of Lake Conjola, a narrow incised valley system on the southeast coast of Australia. *Quaternary International*, 221, 23-35.

Sloss, C. R., Jones,, B. G., Murray-Wallace C. V., & McClennen, C. E., 2005. Holocene sea level fluctuations and the sedimentary evolution of a barrier estuary: Lake Illawarra, New South Wales, Australia. *Journal of Coastal Research*, 21, 943-959, 974-975.

Sloss, C. R., Murray-Wallace, C. V., & Jones, B. G., 2007. Holocene sea-level change on the southeast coast of Australia: a review. *The Holocene* 17, 999-1014.

Sloss, C. R., Murray-Wallace, C. V., Jones, B. G., & Wallin, T., 2004. Aspartic acid racemisation dating of mid-Holocene to recent estuarine sedimentation in New South Wales, Australia: a pilot study. *Marine Geology,* 212**,** 45-59.

Sloss, C. R.; Murray-Wallace, C. V., & Jones, B. G., 2006a. Aminostratigraphy of two Holocene wave-dominated barrier estuaries in southeastern Australia. *Journal of Coastal Research*, 22, 113-136.

Smart, G. M., 1984. Sediment transport formula for steep channels. *Journal of Hydraulic Engineering,* 110, 267-276.

SOC (State of the Catchments), 2010. Riverine ecosystems, southern river region. State of the Catchments, New South Wales Government, Sydney.

Sondi, I., Lojen, S., Juračić, M., & Prohić, E., 2008. Mechanisms of land-sea interactions – the distribution of metals and sedimentary organic matter in sediments of a river-dominated Mediterranean karstic estuary. *Estuarine, Coastal and Shelf Science*, 80, 12-20.

Steffen, W., Burbidge, A. A., Hughes, L., Kitching, R., Lindenmayer, D., Musgrave, W., Smith, M. S., & Werner, P. A., 2009. *Australia's Biodiversity and Climate Change*, CSIRO Publishing, Sydney.

Sutherland, R. A., 1998. Loss-on-ignition estimates of organic matter and relationships to organic carbon in fluvial bed sediments. *Hydrobiologia*, 389, 153-167.

Thieler, E. R., Himmelstoss, E. A., Zichichi, J. L., & Ergul, A., 2009. The Digital Shoreline Analysis System (DSAS) version 4.0-an ArcGIS extension for calculating shoreline change. *US Geological Survey, Open-File Report* 2008-1278.

Thom, B. G., 1967. Mangrove ecology and deltaic geomorphology: Tabasco, Mexico. *British Ecological Society, The Journal of Ecology,* 55**,** 301-343.

Thom, B. G., Wright, L., & Coleman, J. M., 1975. Mangrove ecology and deltaic-estuarine geomorphology: Cambridge Gulf-Ord River, Western Australia. *The Journal of Ecology*, 63, 203-232.

Thompson, C. M., 2012. *Recent Dynamic Channel Adjustments of Berrys Canal Shoalhaven Region, New South Wales Approach.* University of Wollongong, Wollongong.

Tian, F., Fensholt, R., Verbesselt, J., Grogan, K., Horion, S., & Wang, Y., 2015. Evaluating temporal consistency of long-term global NDVI datasets for trend analysis. *Remote Sensing of Environment,* 163**,** 326-340.

Tongway, D. J., & Ludwig, J. A., 1990. Vegetation and soil patterning in semi-arid mulga lands of eastern Australia. *Australian Journal of Ecology,* 15**,** 23-34.

Tran Thi, V., Tien Thi Xuan, A., Phan Nguyen, H., Dahdouh-Guebas, F., & Koedam, N., 2014. Application of remote sensing and GIS for detection of long-term mangrove shoreline changes in Mui Ca Mau, Vietnam. *Biogeosciences,* 11**,** 3781-3795.

Troedson, A., Hashimoto, T. R., Jaworska, J., Malloch, K., & Cain, L., 2004. *New South Wales Coastal Quaternary Geology (CCA 03)*, prepared for the Comprehensive Coastal Assessment (DoP), Department of Primary Industries (New South Wales), Mineral Resources. Sydney.

Tucker, C. J., Goff, T., & Townshend, J., 1985. African land-cover classification using satellite data. *Science,* 227**,** 369-375.

Tucker, C. J., Slayback, D. A., Pinzon, J. E., Los, S. O., Myneni, R. B., & Taylor, M. G., 2001. Higher northern latitude normalized difference vegetation index and growing season trends from 1982 to 1999. *International Journal of Biometeorology,* 45**,** 184-190.

Turner, W., Spector, S., Gardiner, N., Fladeland, M., Sterling, E., & Steininger, M., 2003. Remote sensing for biodiversity science and conservation. *Trends in Ecology and Evolution,* 18**,** 306-314.

Twilley, R., Chen, R., & Hargis, T., 1992. Carbon sinks in mangroves and their implications to carbon budget of tropical coastal ecosystems. *Water, Air and Soil Pollution,* 64**,** 265-288.

U.S. Fish and Wildlife Service, 2014. *Endangered Species: Habitat Conservation Plans* [Online]. Available: http://www.fws.gov/endangered/.

Uddin, N., ed. 2013. *Developments in Fiber-reinforc*ed *Polymer (FRP) Composites for Civil Engineering*. Elsevier, Amsterdam.

Umitsu, M., Buman, M., Kawase, K., & Woodroffe, C. D., 2001. Holocene palaeoecology and formation of the Shoalhaven River deltaic-estuarine plains, southeast Australia. *The Holocene,* 11**,** 407-418.

USAID, 2016. *U.S. Agency for International Development* [Online]. Available: https://www.usaid.gov/.

USEPA, 2001. Threats to wetlands. The United States Environmental Protection Agency, Office of Water, Office of Wetlands, Oceans and Watersheds (4502T).

USGS, 2017a. *USGS.gov | Science for a changing world* [Online]. Available: https://www.usgs.gov/.

USGS, 2017b. *EarthExplorer* [Online]. U.S. Geological Survey. Available: http://earthexplorer.usgs.gov/.

USGS-LANDSAT, 2016. *Landsat Collections* [Online]. Available: http://landsat.usgs.gov//landsatcollections.php.

Vail, P. R., Mitchum, R., & Thompson, S., 1977. Seismic stratigraphy and global changes of sea level: Part 3. Relative changes of sea level from coastal onlap: section 2. Application of seismic reflection configuration to stratigrapic interpretation. Exxon Production Research Co. Texas, USA. 51.

Valiela, I., & Fox, S. E., 2008. Managing coastal wetlands. *Science,* 319**,** 290-291.

Van Den Bergh, J. C., 2004. *Spatial Ecological-Economic Analysis for Wetland Management: Modelling and Scenario Evaluation of Land Use*. Cambridge University Press, Cambridge.

Venter, O., Sanderson, E. W., Magrach, A., Allan, J. R., Beher, J., Jones, K. R., Possingham, H. P., Laurance, W. F., Wood, P., and Fekete, B. M., 2016. Sixteen years of change in the global terrestrial human footprint and implications for biodiversity conservation. *Nature Communications*, 7, 12558, doi:

10.1038/ncomms12558, 1-11.

Vörösmarty, C. J., Mcintyre, P. B., Gessner, M. O., Dudgeon, D., Prusevich, A., Green, P., Glidden, S., Bunn, S. E., Sullivan, C. A., & Liermann, C. R., 2010. Global threats to human water security and river biodiversity. *Nature,* 467**,** 555-561.

Vourlitis, G. L., Verfaillie, J., Oechel, W. C., Hope, A., Stow, D., & Engstrom, R., 2003. Spatial variation in regional CO_2 exchange for the Kuparuk River Basin, Alaska over the summer growing season. *Global Change Biology,* 9**,** 930-941.

Wall, G., 1998. Implications of global climate change for tourism and recreation in wetland areas. *Climatic Change,* 40**,** 371-389.

Walters, D., Moore, L. J., Duran Vinent, O., Fagherazzi, S., & Mariotti, G., 2014. Interactions between barrier islands and backbarrier marshes affect island system response to sea level rise: Insights from a coupled model. *Journal of Geophysical Research: Earth Surface,* 119**,** 2013-2031.

Walther, G.-R., Post, E., Convey, P., Menzel, A., Parmesan, C., Beebee, T. J., Fromentin, J.-M., Hoegh-Guldberg, O., & Bairlein, F., 2002. Ecological responses to recent climate change. *Nature,* 416**,** 389-395.

Wang, Q., Watanabe, M., Hayashi, S., & Murakami, S., 2003. Using NOAA AVHRR data to assess flood damage in China. *Environmental monitoring and assessment,* 82**,** 119-148.

Ward, T. J., & Butler, A., 2006. Coasts and oceans: Theme commentary prepared for the 2006 Australia State of the Environment Committee, Department of Environment and Heritage. Canberra. <http://www.deh.gov.au/soe/2006/commentaries/ coasts/index.html >.

Watson, R. T., 1999. *Australasian impacts of climate change: an assessment of vulnerability : extracted from The regional impacts of climate change : an assessment of vulnerability*. Australian Greenhouse Office, Canberra.

Watson, R. T., Zinyowera, M. C. & Moss, R. H. 1998. *The regional impacts of climate change: an assessment of vulnerability*, Cambridge University Press, UK.

Webb, McKeown & Associates, 1993. *Stage 1 – Estuarine Processes St Georges Basin Management Study*. NSW Public Works and Shoalhaven City Council, Sydney.

Webb, McKeown & Associates, 2001. *St Georges Basin Flood Study.* Shoalhaven City Council, Nowra.

Wei, T., Chen, Z., Duan, L., Gu, J., Saito, Y., Zhang, W., Wang, Y., & Kanai, Y., 2007. Sedimentation rates in relation to sedimentary processes of the Yangtze Estuary, China. *Estuarine, Coastal and Shelf Science*, 71, 37-46.

Weier, J. & Herring, D., 2000. *Measuring Vegetation (NDVI & EVI)* [Online]. NASA, Earth Observatory Available: http://earthobservatory.nasa.gov/Features/MeasuringVegetation/.

Whelan, K. R., Smith, T. J., Cahoon, D. R., Lynch, J. C., & Anderson, G. H., 2005. Groundwater control of mangrove surface elevation: Shrink and swell varies with soil depth. *Estuaries*, 28, 833-843.

White, S. A., & Wang, Y., 2003. Utilizing DEMs derived from LIDAR data to analyze morphologic change in the North Carolina coastline. *Remote Sensing of Environment*, 85, 39-47.

Windley, B., 1986. Comparative tectonics of the western Grenville and the western Himalaya. *The Grenville Province: Geological Association of Canada Special Paper,* 31**,** 341-348.

Windley, V, 1986. *Wandrawandandian (home of lost lovers): A history of Wandandian*. Bay and Basin Printshop, Jervis Bay.

Wood, J., 1996. The geomorphological characterisation of digital elevation models. PhD thesis, University of Leicester, UK.

Woodroffe, C. D., 1990. The impact of sea-level rise on mangrove shorelines. *Progress in Physical Geography,* 14**,** 483-520.

Woodroffe, C. D., 2002. *Coasts: Form, Process and evolution*, Cambridge University Press, Cambridge.

Woodroffe, C. D., Buman, M., Kawase, K., & Umitsu, M., 2000. Estuarine infill and formation of deltaic plains, Shoalhaven River. *Wetlands (Australia)* 18 (2)**,** 72-84.

Woodroffe, C. D., Rogers, K., Mckee, K. L., Lovelock, C. E., Mendelssohn, I., & Saintilan, N., 2016. Mangrove sedimentation and response to relative sea-level rise. *Annual Review of Marine Science,* 8**,** 243-266.

Woodward, W. A., Parr, W. C., Schucany, W. R. & Lindsey, H. 1984. A comparison of minimum distance and maximum likelihood estimation of a mixture proportion. *Journal of the American Statistical Association*, 79 (387), 590-598.

Wookey, P. A., Aerts, R., Bardgett, R. D., Baptist, F., Bråthen, K. A., Cornelissen, J. H., Gough, L., Hartley, I. P., Hopkins, D. W., & Lavorel, S., 2009. Ecosystem feedbacks and cascade processes: understanding their role in the responses of Arctic and alpine ecosystems to environmental change. *Global Change Biology,* 15**,** 1153-1172.

WRC, 2012. Wetland Mapping: Exercises – Create the NDVI Layer ArcMap 10. Water Resources Center (WRC), University of Minnesota [Online]. Available: https://www.wrc.umn.edu/sites/ wrc.umn.edu/files/create_the_ndvi.pdf.

Wright, L., 1970. The influence of sediment availability on patterns of beach ridge development in the vicinity of the Shoalhaven River delta, NSW. *The Australian Geographer,* 11**,** 336-348.

Yang, C. T., Marsooli, R., & Aalami, M. T., 2009. Evaluation of total load sediment transport formulas using ANN. *International Journal of Sediment Research*, 24, 274-286.

Yassini, I., & Jones, B. G., 1995. *Foraminiferida and Ostracoda from Estuarine and Shelf Environments on the Southeastern Coast of Australia.* University of Wollongong Press, Wollongong, 484 pp.

Young, R. W., 2011, Reverend W. B. Clarke, 'the Father of Australian Geology', on the origin of valleys. *Australian Journal of Earth Sciences*, 54, 127-134.

Zedler, J. B., & Kercher, S., 2005. Wetland resources: status, trends, ecosystem services, and restorability. *Annual Review of Environmental Resources,* 30**,** 39-74.

Zhang, J., Zhang, Z., Liu, S., Wu, Y., Xiong, H., & Chen, H., 1999. Human impacts on the large world rivers: would the Changjiang (Yangtze River) be an illustration? *Global Biogeochemical Cycles,* 13**,** 1099-1105.

Zheng Niu, Huang, N., Niu, Z., Zhan, Y., Xu, S., Tappert, M. C., Wu, C., Huang, W., Gao, S., Hou, X. & Cai, D. 2012. "Relationships between soil respiration and photosynthesis-related spectral vegetation indices in two cropland ecosystems", *Agricultural and Forest Meteorology*.

Zhou, W., Xie, S., Meyers, P. A., & Zheng, Y., 2005. Reconstruction of late glacial and Holocene climate evolution in southern China from geolipids and pollen in the Dingnan peat sequence. *Organic Geochemistry*, 36, 1272-1284.

Zhu, L., Wu, J., Xu, Y., Hu, R., & Wang, N., 2010, Recent geomorphic changes in the Liaohe estuary. *Journal of Geographical Sciences*, 20, 31-48.

Zinnert, J. C., Shiflett, S. A., Vick, J. K., & Young, D. R., 2011. Woody vegetative cover dynamics in response to recent climate change on an Atlantic coast barrier island: a remote sensing approach. *Geocarto International,* 26**,** 595-612.

Zuo, P., Li, Y., Liu, C.-A., Zhao, S.-H., & Guan, D.-M., 2013. Coastal wetlands of China: changes from the 1970s to 2007 based on a new wetland classification system. *Estuaries and Coasts,* 36**,** 390-400.

Appendices

A.1 Appendix A

These appendixes attach copies of all the published and submitted papers that are included in this thesis.

**Note: all the additional RS, GIS and fieldwork datasets and most of the analysed details behind the resultant data in the chapters, which might be useful for any future work; are stored on SEES (UOW) drive system due to the data format and size.*

Peer-reviewed publications (listed below in order of their appearance in the thesis, except paper no. 4 for license requirements of the publisher that should be downloaded directory from their system):

1. GIS-based modelling of vulnerability of coastal wetland ecosystems to environmental changes: Comerong Island, southeastern Australia.
2. Civil-GIS incorporated approach for water resource management in a developed catchment for urban-geomorphic sustainability: Tallowa Dam, southeastern Australia.
3. A Spatio-Temporal Assessment of Landcover and Coastal Changes at Wandandian Delta System, Southeastern Australia.
4. An assessment of anthropogenic and climate stressors on estuaries using a spatio-temporal GIS-modelling approach for sustainability: Towamba estuary, southeastern Australia. DOI: 10.1007/s10661-018-6720-5.
5. Geoinformatic analysis of vegetation and climate change on intertidal sedimentary landforms in southeastern Australian estuaries from 1975–2015.
6. Geoinformatics vulnerability predictions of coastal ecosystems to sea level rise in southeastern Australia.

Conference proceedings, papers, and abstracts

1. Modelling changes of coastal wetlands responding to disturbance regimes (Eastern Australia) Using GIS.
2. Surface Elevation Dynamics Assessment Using Digital Elevation Models, Light Detection and Ranging, GPS and Geospatial Information Science Analysis: Ecosystem Modelling Approach. (Peer-reviewed though).
3. Using GIS-modelling to determine the hydrological factors that affect a catchment area: a practical experiment.
4. Risk assessment of trace element pollution in Gymea Bay, NSW, Australia.
5. Modelling the future eco-geomorphological change scenarios of coastal ecosystems in southeastern Australia for sustainability assessment using GIS.